

High Performance Materials Containing Nitrile Groups

Michael Jameson Sumner

Dissertation submitted to the Faculty of the Virginia Polytechnic Institute and State
University in partial fulfillment of the requirements for the degree of

DOCTOR OF PHILOSOPHY in CHEMISTRY

Approved by:

Judy S. Riffle, Chair

James E. McGrath

Alan Esker

Jack Lesko

Timothy Long

April, 2003

Blacksburg, VA

Keywords: phenolic networks, phthalonitrile, vinyl ester networks, polystyrene
copolymers, proton conducting membranes

High Performance Materials Containing Nitrile Groups

Michael Jameson Sumner

Department of Chemistry

Virginia Polytechnic Institute and State University

Abstract

The objective of the research described in this thesis has been to improve the toughness of phenolic networks while maintaining flame resistance. A four step synthetic scheme has been developed to prepare 4,4'-Bis(3,4-dicyanophenoxy)biphenyl(biphenoxyphtalonitrile). A 700 g mol^{-1} novolac oligomer was cured with relatively low concentrations of this reagent ($\sim 20 \text{ wt } \%$) into high T_g ($\sim 190 \text{ }^\circ\text{C}$) networks. The curing reaction was attributed to nucleophilic attack of the phenolic hydroxyl on the nitrile groups of the phthalonitrile resulting in the formation of heterocyclic rings. TGA and cone calorimetry demonstrated that these networks have excellent thermo-oxidative stability.

Further goals were to develop halogen-free, flame retardant monomers for improving the thermo-oxidative resistance of polystyrene and dimethylacrylate/styrene(vinyl ester) networks. 4-Vinylphenoxyphthalonitrile, a phthalonitrile derivative of styrene, was synthesized. FTIR has been utilized to demonstrate this new monomer co-cured into vinyl ester networks in free radical thermosetting polymerizations. Upon post-curing the networks between $200\text{-}260 \text{ }^\circ\text{C}$ for $\sim 1.5 \text{ h}$, the nitrile groups reacted to form heterocyclic crosslinks. TGA and cone

calorimetry demonstrated that the 4-vinylphenoxyphthalonitrile substantially improved the flame resistance of vinyl ester networks.

Copolymerizations of styrene and 4-vinylphenoxyphthalonitrile were conducted at 75 °C for 24 h using 0.5 wt % AIBN in chlorobenzene. Dynamic TGA at 10 °C min⁻¹ in air showed that copolymers containing 10 and 25 mole % of 4-vinylphenoxyphthalonitrile had increased initial weight loss temperatures in air by (~50 °C higher) and increased the char yield between 400-600 °C.

High molecular weight nitrile-functional, (hexafluoroisopropylidene)diphenol based aromatic poly(arylene ether)s with pendent sulfonic acid groups were prepared by nucleophilic step copolymerization of 4,4'-(hexafluoroisopropylidene)diphenol, 2,6-dichlorobenzonitrile, and 3,3'-disulfonate-4,4'-dichlorodiphenylsulfone under basic conditions in *N*-methyl-2-pyrrolidinone at 200 °C. A series of these materials with systematically varied concentrations of the sulfonic acid moieties showed increased glass transition temperatures, proton conductivities, and hydrophilicities as a function of disulfonation. Atomic force microscopy (AFM) demonstrated that the acidified copolymer with 35 mole % of disulfonated units was phase separated into a co-continuous morphology of hydrophobic and hydrophilic domains.

Acknowledgements

Firstly, I would like to thank Dr. Riffle for accepting me into her group as a Ph.D. candidate. Her guidance, encouragement, and sincerity were tremendous in helping me complete my work and accomplish my goals. I am truly grateful for the experiences I have had in her group as a graduate student. I also thank my committee members for their suggestions and advice.

To the members of the Riffle group, I thank you for helping me out whenever I needed it. I have truly enjoyed coming into work everyday and working with you. I especially thank Mark Flynn for his patience and persistence in fabricating my composites and Angie Flynn for all her insight on the *ins and outs* of Microsoft Word and for kindly making my travel arrangements. I also extend special gratitude to Usman Sorathia for cone calorimetry testing, Steve McCartney for his SEM and AFM work, Tom Glass for his expertise and advice regarding NMR, and John Bausano for kindly having my composites machined. Special thanks go out to Ryan Weyers for being a wonderful person to work with and going the extra mile whenever I asked him.

From day one my wonderful family has always been there to support me with their love and encouragement. For this I thank you because I am extremely blessed to have you in my life. Finally, I thank the Lord for the multitude of blessings that He has bestowed upon me and my family throughout our lives.

Table of Contents

Abstract	ii
Acknowledgements	iv
List of Figures.....	xi
List of Tables	xvii
Chapter 1: Dissertation Overview.....	1
Chapter 2: Literature Review.....	3
2.1 Phenolic Resin Chemistry	3
2.1.1 Introduction	3
2.1.2 Resole Chemistry and Network Formation	4
2.1.3 Novolac Chemistry and Network Formation	8
2.1.4 Phenolic Degradation and Flame Retardance	10
2.1.4.1 <i>Phenolic Degradation Mechanisms</i>	10
2.1.4.2 <i>Cross-Linking and Halogenation Effects</i>	24
2.1.4.3 <i>Kinetic Parameters for Thermal Decomposition</i>	29
2.1.4.4 <i>Pyrolysis Compositions</i>	31
2.2 Phenolic Epoxy Chemistry	37
2.2.1 Phenolic/Epoxy Network Formation.....	37
2.2.2 Epoxy Degradation.....	42
2.3 High Temperature Functional Groups	51
2.3.1 Phenylethynyl End Groups.....	51
2.3.2 Maleimide and Bismaleimide End Groups	60
2.3.3 Phthalonitrile Curing Reagents	68
2.4 Cone Calorimetry.....	76
2.4.1 Introduction	76
2.4.2 Flame Properties of Aliphatic Polymeric Matrices	77

2.4.3 Flame Properties of Aromatic Polymeric Matrices	79
Chapter 3: Synthesis of 4,4'-Bis(3,4-dicyanophenoxy)biphenyl (biphenoxyphthalonitrile)	87
3.1 Introduction.....	87
3.2 Experimental	91
3.2.1 Materials.....	91
3.2.2 Synthesis of 4-Nitrophthalimide	91
3.2.3 Synthesis of 4-Nitrophthalamide.....	91
3.2.4 Synthesis of 4-Nitrophthalonitrile	92
3.2.5 Synthesis of 4,4'-Bis(3,4-dicyanophenoxy)biphenyl (biphenoxyphthalonitrile).....	92
3.3 Measurements	93
3.3.1 Differential Scanning Calorimetry (DSC).....	93
3.3.2 Proton Nuclear Magnetic Resonance (¹ H NMR)	93
3.3.3 Fourier Transform Infrared Spectroscopy (FTIR)	93
3.4 Results and Discussion.....	94
3.4.1 Synthesis of 4-Nitrophthalimide	94
3.4.2 Synthesis of 4-Nitrophthalamide.....	96
3.4.3 Synthesis of 4-Nitrophthalonitrile	101
3.4.4 Synthesis of 4,4'-Bis(3,4-dicyanophenoxy)biphenyl (biphenoxyphthalonitrile).....	104
3.5 Conclusions.....	107
Chapter 4: Flame Retardant Novolac-Bisphthalonitrile Structural Thermosets	110
4.1 Introduction.....	110
4.2 Experimental	114
4.2.1 Materials.....	114
4.2.2 Network Formation from the Novolac Resin and 4,4'-Bis-(3,4- dicyanophenoxy)biphenyl (BPh).....	115
4.2.3 Melt Reaction Between 2-Hydroxydiphenylmethane and BPh	115

4.3 Measurements	117
4.3.1 Dynamic Mechanical Analysis (DMA).....	117
4.3.2 Scanning Electron Microscopy (SEM)	118
4.3.3 Stress Intensity Factor (K_{IC})	118
4.3.4 Sol-Fractions	118
4.3.5 Fourier Transform Infrared Spectroscopy (FTIR)	119
4.3.6 Proton Nuclear Magnetic Resonance (^1H NMR)	119
4.3.7 Cone Calorimetry and Thermogravimetric Analysis (TGA)	119
4.4 Results and Discussion.....	120
4.4.1 Network Synthesis.....	120
4.4.2 Model Study -- Melt Reaction of 2-Hydroxydiphenylmethane and BPh	120
4.4.3 Network Properties.....	126
4.4.4 Network Thermo-Oxidative Stability Characterization	133
4.4.5 Network Fracture Toughness	138
4.5 Conclusions	138
 Chapter 5: Novolac/Biphenoxyphthalonitrile Carbon Fiber Reinforced Composites	 141
5.1 Introduction.....	141
5.2 Experimental	144
5.2.1 Materials.....	144
5.2.2 Preparation of Fracture Toughness Bars Using Novolac and Biphenoxyphthalonitrile at 85:15 Wt:Wt Ratio	144
5.2.3 Hot-Melt/Powder Prepregging and Composite Fabrication of Carbon Fiber Reinforced Composites Containing Novolac/Biphenoxyphthalonitrile (85:15 Wt:Wt) Matrix Material	145
5.3 Measurements	147
5.3.1 Dynamic Mechanical Analysis (DMA).....	147
5.3.2 Scanning Electron Microscopy (SEM)	147
5.3.3 Melt Rheometry.....	148
5.3.4 Cone Calorimetry	148

5.4 Results and Discussion.....	148
5.5 Conclusions.....	153
Chapter 6: Synthesis and Characterization of Vinyl Ester/Phthalonitrile Networks and Styrene/Vinyl Phthalonitrile Copolymers	156
6.1 Introduction.....	156
6.2 Experimental	163
6.2.1 Materials.....	163
6.2.2 Synthesis of 4-Vinylphenoxyphthalonitrile (VinylPh)	163
6.2.3 Synthesis of Vinyl Ester/Styrene/4-Vinylphenoxyphthalonitrile Networks	164
6.2.4 Synthesis of Styrene/4-Vinylphenoxyphthalonitrile Copolymers.....	165
6.3 Measurements	166
6.3.1 Dynamic Mechanical Analysis (DMA).....	166
6.3.2 Differential Scanning Calorimetry (DSC).....	166
6.3.3 Thermogravimetric Analysis (TGA) and Cone Calorimetry.....	167
6.3.4 Gel Permeation Chromatography (GPC)	167
6.3.5 Proton Nuclear Magnetic Resonance (¹ H NMR)	167
6.3.6 Fourier Transform Infrared Spectroscopy (FTIR) Monitoring of the Conversion of Styrenic, Methacrylate, and Nitrile Groups in Vinyl Ester/Styrene/4-Vinylphenoxyphthalonitrile Resins.....	168
6.3.7 Melt Rheometry.....	169
6.4 Results and Discussion.....	169
6.4.1 Synthesis of 4-Vinylphenoxyphthalonitrile	169
6.4.2 Synthesis and Characterization of Vinyl Ester/Styrene/4- Vinylphenoxyphthalonitrile Networks.....	171
6.4.3 Synthesis and Characterization of Styrene/4- Vinylphenoxyphthalonitrile Copolymers	187
6.5 Conclusions.....	199
Chapter 7: Novel Proton Conducting Disulfonated Poly(Arylene Ether) Copolymers Containing Aromatic Nitriles	202

7.1 Introduction.....	202
7.2 Experimental	207
7.2.1. Materials.....	207
7.2.2 Synthesis of 3,3'-Disulfonate-4,4'-dichlorodiphenylsulfone (SDCDPS)	208
7.2.3 Synthesis of Poly(Arylene Ether) Copolymers Containing Disulfonated Repeat Units	209
7.2.4 Membrane Preparation	210
7.3 Measurements	211
7.3.1 Proton Nuclear Magnetic Resonance (¹ H NMR).	211
7.3.2 Differential Scanning Calorimetry (DSC) and Thermogravimetric Analysis (TGA)	211
7.3.3 Intrinsic Viscosities	212
7.3.4 Gel Permeation Chromatography (GPC)	212
7.3.5 Water Absorption.	212
7.3.6 Atomic Force Microscopy	213
7.3.7 Conductivity	213
7.3.8 Methanol Permeability	215
7.4 Results and Discussion.....	217
7.4.1 Synthesis of the Disulfonated Monomer (3,3'-Disulfonate-4,4'-Dichlorodiphenylsulfone), and Copolymers Containing Nitrile Moieties.....	217
7.4.2. Thermal Properties of the Disulfonated Copolymers.....	228
7.4.3 Water Uptake, Methanol Permeability, and Morphology	232
7.4.4 Conductivity	239
7.5 Conclusions.....	245
Chapter 8: Summary and Conclusions.....	247
Chapter 9: Suggested Research	249
9.1 Phenolic/Biphenoxyphthalonitrile Matrix Materials.....	249

9.2 Fabrication of Vinyl Ester/4-Vinylphenoxyphthalonitrile Fiber Reinforced Composites.....	249
9.3 Free Radical Synthesis of 4-Vinylphenoxyphthalonitrile Copolymers	250
9.4 Further Evaluation of Sulfonated Poly(Arylene Ether Nitrile) Proton Conducting Membranes	250
Vita	252

List of Figures

Figure 2.1: Reaction of phenol with formaldehyde under basic conditions generating mono, di, and trihydroxymethylphenols.....	5
Figure 2.2: Resol prepolymer formation	6
Figure 2.3: Formation of diphenylmethane prepolymers from methylolphenols.....	7
Figure 2.4: Novolac prepolymer formation	9
Figure 2.5: Intermediates formed during HMTA catalyzed novolac network formation	11
Figure 2.6: Low temperature degradation of phenolic networks.....	13
Figure 2.7: Proposed high temperature oxidative degradation of phenolic resins.....	15
Figure 2.8: Char formation in phenolic networks	16
Figure 2.9: In vacuo low temperature (360 °C) cleavage of methylene units	20
Figure 2.10: Phenolic resin degradation involving the reaction of a phenolic hydroxyl group and methylene bridge.....	21
Figure 2.11: Low temperature oxidative degradation of novolac networks.....	23
Figure 2.12: Main chain and catalyst decomposition for triphenylphosphine catalyzed epoxy-phenol reaction.....	40
Figure 2.13: Proposed mechanism for the tertiary amine catalyzed phenol-epoxy polymerization.....	41
Figure 2.14: Proposed degradation pathways of bisphenol A epoxy networks	44
Figure 2.15: Cis-elimination of ester linkages in anhydride cured epoxy networks.....	46
Figure 2.16: Proposed mechanisms for epoxized novolac degradation	47
Figure 2.17: Proposed degradation mechanism of an amine-cured epoxy resin via a Cope reaction	50
Figure 2.18: Synthesis of hexafluorinated polyimide oligomer end-capped with PEPA.....	54

Figure 2.19: Polyimides endcapped with electron-withdrawing substituted PEPA	57
Figure 2.20: p-Ethynyl-terminated rigid-rod monomers	59
Figure 2.21: β - β' -Dichloroterephthalyl dimalonitrile synthesis and imidization	62
Figure 2.22: Proposed curing mechanisms for BMI/DABPA resin	66
Figure 2.23: Additional reaction pathways during the curing of BMI/DABPA resin	67
Figure 2.24: Phthalonitrile polymerization via indole formation.....	69
Figure 2.25: Phthalonitrile monomer and aromatic diamine curing agents	71
Figure 2.26: Phthalonitrile monomers and curing agent	73
Figure 2.27: Phthalonitrile functional benzoxazine monomers.....	75
Figure 2.28: Cone calorimeter	78
Figure 2.29: Flame properties from cone calorimetry (measured at an incident heat flux of 40 kW/m ²) of halogenated vs. non-halogenated aliphatic polymers.....	80
Figure 2.30: Cone calorimetry data for flame retardant polyimides and poly(arylene ether)s	81
Figure 2.31: Flame properties of thermoset polymer matrices for composites measured by cone calorimetry with an incident heat flux of 50 kW/m ² (PHHR is peak heat release rate)	83
Figure 3.1: Synthesis of biphenoxyphthalonitrile	89
Figure 3.2: Four step synthetic scheme for biphenoxyphthalonitrile	90
Figure 3.3: ¹ H NMR of 4-nitrophthalimide	95
Figure 3.4: Melting point range of 4-nitrophthalimide determined by DSC at 0.5 °C/min	97
Figure 3.5: ¹ H NMR of 4-nitrophthalamide	99
Figure 3.6: Melting point range of 4-nitrophthalamide determined by DSC at 0.5 °C/min	100
Figure 3.7: ¹ H NMR of 4-nitrophthalonitrile	102

Figure 3.8: FTIR of 4-nitrophthalonitrile.....	103
Figure 3.9: Melting point range of 4-nitrophthalonitrile determined by DSC at 0.5 °C/min.....	105
Figure 3.10: ¹ H NMR of biphenoxyphthalonitrile	106
Figure 3.11: FTIR of biphenoxyphthalonitrile.....	108
Figure 3.12: Melting point of biphenoxyphthalonitrile determined by DSC at 0.5 °C/min	109
Figure 4.1: Proposed bisphthalonitrile oligomer reaction with a minor amount of an aromatic amine to form a “B-staged resin”, and subsequent network formation	113
Figure 4.2: Molecular structure of 4,4'-bis-(3,4-dicyanophenoxy)biphenyl.....	116
Figure 4.3: FTIR spectra of a 90:10 weight percent novolac:BPh network cured for 1 h at 200 °C, then 1 h at 220 °C	121
Figure 4.4: Possible reaction products of the model melt reaction between 2-hydroxydiphenylmethane and a bisphthalonitrile.....	123
Figure 4.5: ¹ H NMR of the product isolated from the 2-hydroxydiphenylmethane-BPh model reaction.....	124
Figure 4.6: FTIR Spectrum <i>A</i> —25:1 molar ratio (6.1:1 eq ratio) of a melt mixture of 2-hydroxydiphenylmethane and BPh before reaction. FTIR Spectrum <i>B</i> —Product generated after 3 h at 200 °C	125
Figure 4.7: Gel-fractions versus novolac-BPh composition	128
Figure 4.8. SEMs at 500X of 85:15 and 80:20 wt:wt ratios of novolac-BPh networks.....	129
Figure 4.9: <i>M_c</i> versus novolac-BPh composition (wt%).....	130
Figure 4.10: <i>T_g</i> versus novolac-BPh composition.....	132
Figure 4.11: Residual weight of Nov-BPh networks by TGA in air	135
Figure 4.12: <i>K_{1c}</i> versus novolac-BPh composition	139
Figure 5.1: The hot-melt prepregging process	146
Figure 5.2: Shear viscosity versus time at 170 °C and 190 °C for novolac/BPh (85:15 wt:wt) and novolac/biphenol A diepoxide (65:35 wt:wt) resins	150

Figure 5.3: DMA analysis at 1 Hz of a novolac/BPh (85:15 wt:wt) neat network and a novolac/BPh (85:15 wt:wt) carbon fiber reinforced composite	152
Figure 5.4: A) SEM of a cross-section of a novolac/BPh (85:15) cross ply (0/90 °) composite at 50X magnification B) SEM of 90 ° layer of cross-ply composite at 5,000X magnification.....	154
Figure 6.1: Free radical synthesis of the vinyl ester/styrene/4-vinylphenoxyphthalonitrile networks and the formation of heterocyclic crosslinks within the network via post-curing between 200-300 °C for 4 h	162
Figure 6.2: Two step synthetic scheme for the synthesis of 4-vinylphenoxyphthalonitrile	170
Figure 6.3: ¹H NMR of 4-vinylphenol	172
Figure 6.4: ¹H NMR of 4-vinylphenoxyphthalonitrile.....	173
Figure 6.5: FTIR spectra of Derakane 441-400 resin and a blend of 80 wt % Derakane 441-400 with 20 wt % 4-vinylphenoxyphthalonitrile	174
Figure 6.6: Conversion of methacrylate and styrenic groups with Derakane 441-400 and Derakane 441-400/4-vinylphenoxyphthalonitrile resins mixtures versus time	176
Figure 6.7: Conversion of nitrile groups versus time for Derakane 441-400/4-vinylphenoxyphthalonitrile networks containing 20, 30, and 40 weight% of the vinyl phthalonitrile monomer.....	178
Figure 6.8: DMA analyses of Derakane 441-400/VinylPh networks as a function of the wt % 4-vinylphenoxyphthalonitrile.....	180
Figure 6.9: DMA analyses of Derakane/4-VinylPh networks that had been post-cured for 4 hours at 220 °C, 240 °C, or 260 °C.....	181
Figure 6.10: TGA analyses of Derakane 441-400/VinylPh networks in air.....	183
Figure 6.11: TGA analyses of Derakane 441-400/VinylPh (40 wt %) networks in air after post-curing for 4 hours at 220 °C, 240 °C or 260 °C	184
Figure 6.12: Shear viscosity versus temperature for the vinyl ester control (Derakane 441-400) and Derakane 441-400/VinylPh (30 wt %) resins	188
Figure 6.13: Synthetic scheme for styrene/4-vinylphenoxyphthalonitrile random copolymers	189
Figure 6.14: ¹H NMR monitoring the conversion of styrene versus time for the (75:25 mol:mol) styrene/VinylPh copolymer	191

Figure 6.15: ^1H NMR of styrene/VinylPh (90:10) and (75:25) copolymers	192
Figure 6.16: DSC analysis of styrene/VinylPh (90:10) and (75:25) copolymers versus polystyrene	195
Figure 6.17: DSC analysis of the styrene/VinylPh (90:10) copolymer cured for either 4 hours at 220 °C or 4 hours at 240 °C	196
Figure 6.18: DSC analysis of the styrene/VinylPh (75:25) copolymer cured for 4 hours at 220 °C or 4 hours at 240 °C	197
Figure 6.19: TGA analysis in air of styrene/VinylPh (90:10) and (75:25) copolymers	198
Figure 6.20: TGA analysis in air of the styrene/VinylPh (75:25) copolymer uncured, cured for 4 hours at 220 °C, and cured for 4 hours at 240 °C	201
Figure 7.1: Post-sulfonation of a poly(arylene ether sulfone)	204
Figure 7.2: Synthesis of disulfonated poly(arylene ether sulfone)s and disulfonated hexafluoroisopropylidene poly(arylene ether sulfone)s	206
Figure 7.3: Conductivity cell with labeled components	214
Figure 7.4: Parr reactor assembly for high temperature fuel cell measurements	216
Figure 7.5: ^1H NMR at 80 °C of SDCDPS after recrystallization	218
Figure 7.6: ^1H NMR of SDCDPS after stirring for 12 hours in a 3:1 wt:wt isopropanol:water solution	220
Figure 7.7: Isothermal (200 °C) TGA measurements of moisture content in SDCDPS versus time exposed to the atmosphere	222
Figure 7.8: Synthesis of disulfonated hexafluoroisopropylidene poly(arylene ether nitrile)	223
Figure 7.9: ^1H NMR of disulfonated hexafluoroisopropylidene poly(arylene ether nitrile) copolymers	225
Figure 7.10: Glass transition temperatures of disulfonated hexafluoroisopropylidene poly(arylene ether nitrile) copolymers (in the acidified form) containing 5 up to 55 mole % disulfonation	229
Figure 7.11: TGA curves in air at 10 °C min ⁻¹ of disulfonated hexafluoroisopropylidene poly(arylene ether nitrile) copolymers containing 0, 10, 20, 35, and 45 mole % disulfonation	231

Figure 7.12: Water uptake (wt%) versus time for disulfonated hexafluoroisopropylidene poly(arylene ether nitrile) copolymers containing 0 up to 55 mole % disulfonation	233
Figure 7.13: AFM images using a scan size of 1μm for: A) disulfonated biphenol poly(arylene ether sulfone) at 40 mole % disulfonation, B) disulfonated hexafluoroisopropylidene poly(arylene ether nitrile) at 35 mole % disulfonation	236
Figure 7.14: Water uptake (wt%) versus mole % disulfonation for disulfonated hexafluoroisopropylidene poly(arylene ether nitrile) copolymers	238
Figure 7.15: Mole % disulfonation versus proton conductivity for disulfonated hexafluoroisopropylidene poly(arylene ether nitrile) copolymers	241
Figure 7.16: Proton conductivity versus calculated IEC values for three different disulfonated poly(arylene ether) copolymers	243
Figure 7.17: Proton conductivity versus temperature for the 35 mole % disulfonated hexafluoroisopropylidene poly(arylene ether nitrile) copolymer	244
Figure 7.18: Proton conductivity versus % relative humidity for the 20, 30, 35, and 45 mole % - disulfonated hexafluoroisopropylidene poly(arylene ether nitrile) copolymers	246

List of Tables

Table 2.1: List of gases evolved during the phenolic resin TG-MS experiment	35
Table 2.2: Current applications of moderate and high glass transition thermosetting polymer matrix systems	85
Table 4.1: Cone calorimetry results measured at an incident heat flux of 50kW/m² for 90:10 and 80:20 wt:wt novolac-BPh networks as compared to selected aromatic linear polymers	137
Table 5.1: Cone calorimetry testing results at a heat flux of 75 kW/m² for novolac/BPh(85:15 wt:wt) and novolac/bisphenol A diepoxide composites	155
Table 6.1: Cone calorimetry data at an incident heat flux of 50 kW•m⁻² for the vinyl ester control (Derakane 441-400), the brominated vinyl ester (Derakane 510A-40), and Derakane 441-400/VinylPh (30 wt %) networks.....	186
Table 6.2: GPC analysis of polystyrene, a styrene/VinylPh (90:10) copolymer and a styrene/VinylPh (75:25) copolymer in chloroform.....	193
Table 7.1: Theoretical versus experimental ¹H NMR integration ratios of protons”a” to “i” for disulfonated hexafluoroisopropylidene poly(arylene ether nitrile) copolymers containing 5 up to 50 mole % disulfonation.....	226
Table 7.2: Intrinsic viscosity (NMP, 25 °C) and weight average molecular weights of disulfonated hexafluoroisopropylidene poly(arylene ether nitrile) copolymers containing 20, 30, 35, and 50 mole % disulfonation.....	227
Table 7.3: Water uptake (wt%) and calculated IEC values for Nafion 117[®] and three different disulfonated poly(arylene ether)s at 20, 30, and 35 mole % disulfonation	234
Table 7.4: Methanol permeability values at 25 °C for Nafion 117[®] and three different disulfonated poly(arylene ether) copolymers	240

Chapter 1: Dissertation Overview

This dissertation is comprised of five areas of research focused on the synthesis and study of high performance polymeric networks, as well as materials suitable for proton conducting membranes, which contain aromatic nitrile groups. Chapter 2 is a literature overview concerning syntheses and thermal properties of high performance networks and linear polymers. Cone calorimetry is also introduced in this chapter and a summary of the thermo-oxidative stabilities of high performance materials using this instrument is also provided.

Chapter 3 describes a new, four-step synthesis for preparing biphenoxyphthalonitrile in good yield. The synthesis and physical property characterization of high performance novolac networks crosslinked with biphenoxyphthalonitrile is presented in chapter 4, and the processing of these network materials into carbon fiber composites is described in chapter 5.

Flame retardant vinyl ester composites are currently used in many civilian and military applications. The current standard is a brominated vinyl ester with lower peak heat release rates upon burning relative to non-brominated materials, but the smoke and carbon monoxide generation are high. Therefore it is of great interest to find suitable non-halogenated alternatives. Chapter 6 describes the synthesis of a novel vinyl-functional phthalonitrile monomer, the cure of this monomer into vinyl ester networks, and effects of this monomer on physical and thermo-oxidative properties. The copolymerization of this monomer with styrene and its effects on the thermo-oxidative properties of the resultant copolymers is also presented in this chapter.

Currently there is great demand for polymeric proton-conducting membranes with low water uptake and low methanol permeability. Chapter 7 demonstrates the synthesis and characterization of new disulfonated poly(arylene ether nitrile) copolymers that have comparable proton conductivities and lower water uptakes when compared to analogous disulfonated poly(arylene ether sulfone) copolymers.

The research is summarized and concluded in chapter 7 and suggestions for future work are provided in the final chapter.

Chapter 2: Literature Review

2.1 Phenolic Resin Chemistry

2.1.1 Introduction

Polymeric phenolic compounds have a wide range of applications, including fields such as aerospace, construction, and electronics.¹ There are three core reasons for the broad application range of these materials. One, the synthesis of phenolic prepolymers by electrophilic aromatic substitution is relatively simple and inexpensive. Two, methods for their conversion into thermoset networks are well established. Three, these networks are highly aromatic and thus, they are resistant to thermal oxidation.

The most common types of phenolic-based prepolymers are resoles and novolacs.¹ Syntheses of resole and novolac prepolymers are carried out using phenol or derivatives and formaldehyde under acidic or basic conditions. Novolacs are formed under highly acidic conditions with an excess of phenol. Resoles are synthesized under basic conditions with an excess of formaldehyde. The conversion of novolacs into insoluble and infusible networks requires catalysts, whereas resoles only require heating over a certain period.

¹ A. Knop and W. Scheib, Chemistry and Applications of Phenolic Resins, Springer-Verlag, New York, 1979.

2.1.2 Resole Chemistry and Network Formation

The synthesis of resole prepolymers requires the initial synthesis of certain hydroxymethylphenol precursors. These are prepared by electrophilic aromatic substitution, carried out under basic conditions with phenol and formaldehyde (Figure 2.1). The ratio of phenol to formaldehyde ranges from about 1:1 to 1:3.1. Depending on the ratio of phenol to formaldehyde, a mixture of mono, di, and trihydroxymethylphenols is produced. The hydroxymethylphenols form prepolymers via two different reaction pathways (Figure 2.2). Due to their thermal stability, the hydroxydiphenylmethane prepolymers are by far the most important of the two.

The hydroxydibenzyl ether is prevalent when such materials are prepared under weakly acidic or neutral conditions at temperatures less than 130 °C (Figure 2.2).¹ However, at temperatures between 130 and 150 °C, formation of methylene bridges dominates, which leads to hydroxydiphenylmethanes. Also, hydroxydiphenylmethanes are produced under strong alkaline conditions at temperatures between 130 °C and 150 °C (Figure 2.2).¹ The prepolymer forms as a result of two possible condensation reactions between methylolphenols (Figure 2.3).¹ These reactions are strongly activated by the methylol groups. After formation, both types of prepolymers can be stored under cool conditions to prevent premature gelation.

The two types of resole prepolymers or resins can be cross-linked through heating at temperatures between 130 and 180 °C, under basic conditions (pH of 9 or greater). Water and formaldehyde can be eliminated during cure. Both water and formaldehyde vaporize at the reaction temperatures employed, and this usually results in voids within

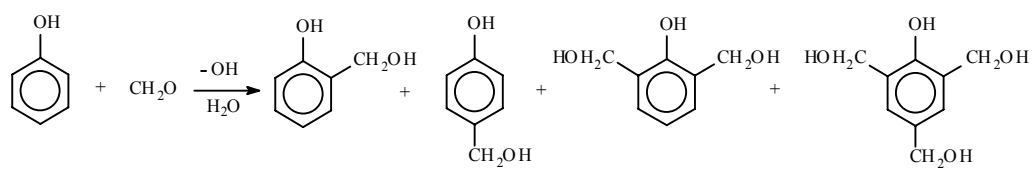


Figure 2.1: Reaction of phenol with formaldehyde under basic conditions generating mono, di, and trihydroxymethylphenols

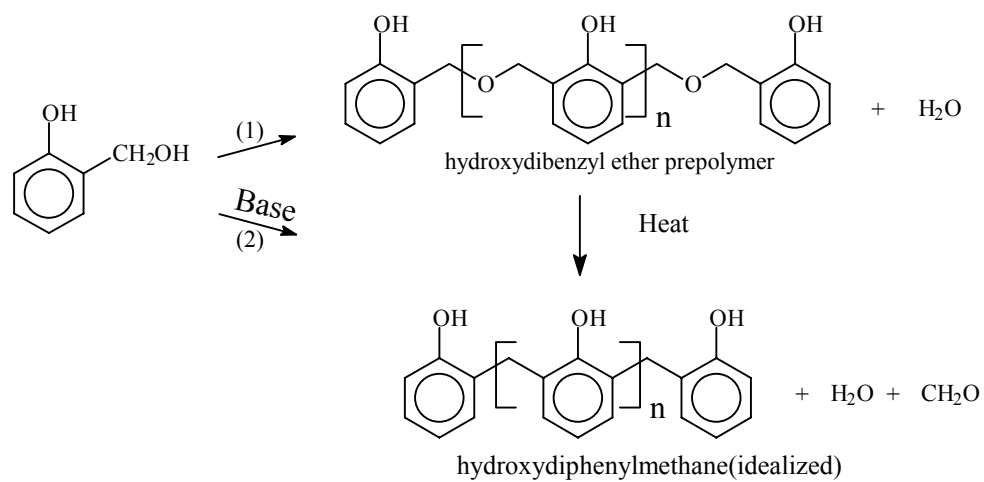


Figure 2.2: Resol prepolymer formation

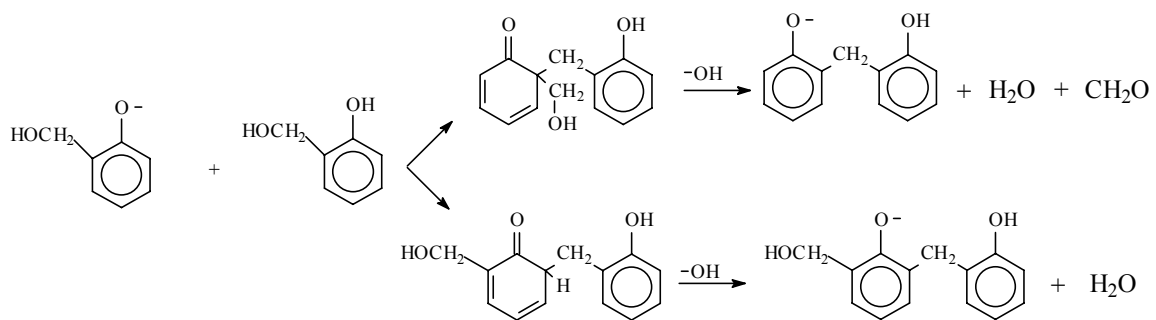


Figure 2.3: Formation of diphenylmethane prepolymers from methyllolphenols

the network. Network voids reduce the mechanical properties of these materials and limit their structural applications.

2.1.3 Novolac Chemistry and Network Formation

Novolac prepolymers are synthesized by electrophilic aromatic substitutions, which involve reactions of an excess of phenol with formaldehyde under mildly acidic conditions, pH 4 to 6 (Figure 2.4).² Oxalic acid is the preferred acid catalyst for this reaction for two reasons. One, it produces colorless resins and two it decomposes to form CO₂ and CO at high temperatures(>180 °C).³ Thermal decomposition allows easy removal of the catalyst from the solution. Usually, oxalic acid is used at 1 to 6 weight %.

Metal hydroxides of first and second group elements can enhance ortho substitution. The degree of ortho substitution depends on the strength of metal chelating effects linking the phenolic oxygen with the formaldehyde as it approaches the ortho position. Transition metal ions of elements such as Fe, Cu, Cr, Ni, Co, Mn and Zn as well as boric acid direct ortho substitutions via a chelating effect. This approach produces “high-ortho” novolacs because of the dominating ortho-ortho linkage.¹ Typically, novolac prepolymers have average molecular weights between 500 and 1000 g/mol. These prepolymers require an external curing agent to form networks.

The most common curing agent for novolac prepolymers is hexamethylenetetramine (HMTA). HMTA serves as a source of the required

² A. Hale and C. W. Macosko, "DSC and ¹³C NMR Studies of the Imidazole-Accelerated Reaction Between Epoxides and Phenols," *Journal of Applied Polymer Science*, 1989, **38**, 1253.

³ S. R. Sandler and W. Karo, *Polymer Synthesis, Vol. 2*, 2 ed., Academic Press, Boston, 1992.

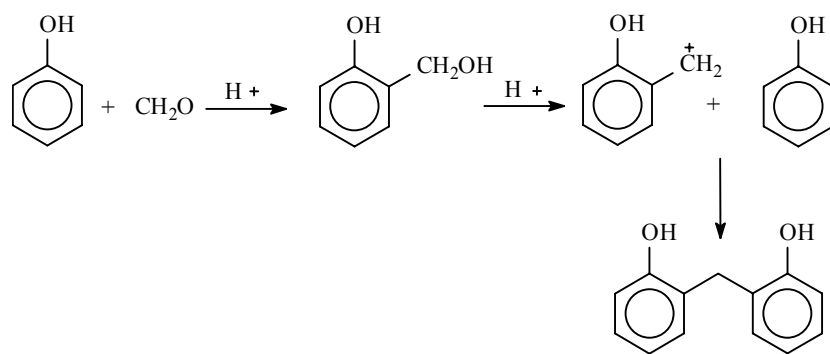


Figure 2.4: Novolac prepolymer formation

formaldehyde needed to react with the vacant ortho or para positions on the novolac prepolymer. High “ortho” novolacs react more rapidly with HMTA because the reactivity of the free para positions is higher than the reactivity of sterically hindered free ortho positions.¹ Typical HMTA concentrations range between 5 and 15% by weight. The curing reaction with HMTA is complete and generates hydroxylbenzylamine and benzoxazine intermediates (Figure 2.5). Upon thermal decomposition significant amounts of formaldehyde and ammonia are produced. This leads to a network primarily comprised of methylene linkages between rings, but which may contain about 6% bound nitrogen.¹ The gas contains approximately 95 weight % ammonia. Similar to resoles, the volatilization of significant levels of gas forms networks with high levels of voids, which detract from mechanical properties.

Maximizing the mechanical properties of novolac networks requires the absence of volatile by-products during cure, which leads to a void-free network. Novolacs can be chemically modified with epoxy functionality using epichlorohydrin in the presence of base.¹ The methods for curing epoxidized novolacs are similar to those for curing other epoxy resins. Epoxidized novolac networks demonstrate improved properties relative to HMTA cured novolacs such as higher strength and stronger adhesion. However, the aliphatic character of the epoxy linkages leads to a network with reduced thermal resistance.¹

2.1.4 Phenolic Degradation and Flame Retardance

2.1.4.1 Phenolic Degradation Mechanisms

The high thermal stability of phenolic networks has led to their incorporation into

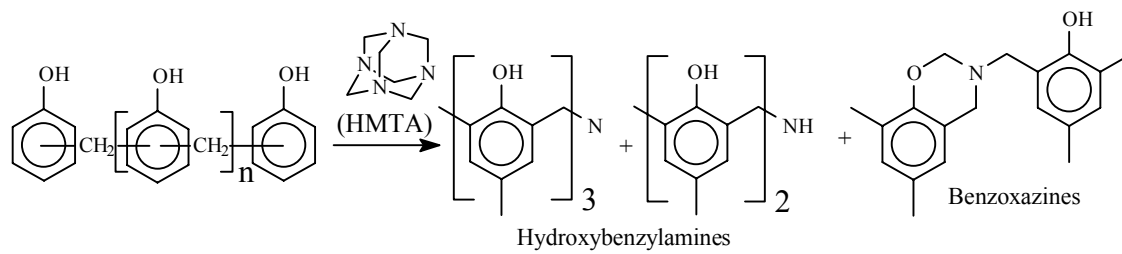


Figure 2.5: Intermediates formed during HMTA catalyzed novolac network formation

many commercial products. The unique thermal characteristics of phenolic networks have fostered much interest in determining their mechanisms of degradation in both oxidative and inert atmospheres. Some of the earliest and most significant work in determining phenolic network degradation mechanisms was completed by Conley and coworkers between 1963 and 1965.

Initially, Conley and Bieron⁴ investigated the low temperature (100 °C-200 °C) thermal degradation of phenol-formaldehyde networks using infrared spectroscopy. Upon heating the networks up to 200 °C for 50 hours, under vacuum or nitrogen, no observable changes in the infrared spectra occurred. In contrast, when the experiments were conducted under atmospheric conditions several changes in the infrared spectra were observed.⁴ Conley concluded that degradation of phenolic networks was initiated by the presence of oxygen. It was also observed that the rate of degradation of phenolic networks increases with the temperature within the temperature range of 100 to 200 °C. Using infrared spectroscopy to monitor changes in functional groups and chemical analyses, Conley and Bieron proposed a mechanism for the low temperature thermal degradation of phenolic networks (Figure 2.6).⁵

As a follow-up to the low temperature degradation study, Jackson and Conley⁶ completed a high temperature (greater than 200 °C) degradation study on phenolic networks. The degradation of phenolic networks was monitored using infrared spectroscopy, vapor phase chromatography, and thermogravimetric analysis (TGA). It

⁴ R. T. Conley and J. F. Bieron, "A Study of the Oxidative Degradation of Phenol-Formaldehyde Polycondensates Using Infrared Spectroscopy," *Journal of Applied Polymer Science*, 1963, 7, 103.

⁵ R. T. Conley, *Thermal Stability of Polymers*, Marcel Dekker Inc., New York, 1970.

⁶ W. M. Jackson and R. T. Conley, "High Temperature Oxidative Degradation of Phenol-Formaldehyde Polycondensates," *Journal of Applied Polymer Science*, 1964, 8, 2163.

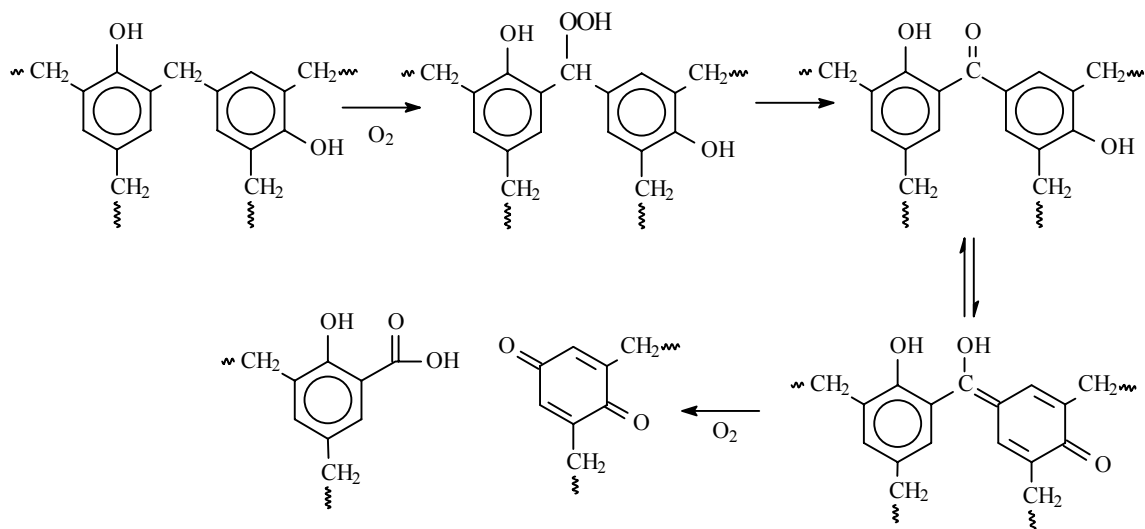
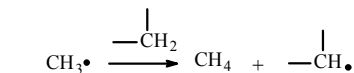


Figure 2.6: Low temperature degradation of phenolic networks

was observed that temperatures under 400 °C produced carbon dioxide, carbon monoxide, water, paraformaldehyde, methane, and a variety of aromatic products. Above 400 °C water and paraformaldehyde were the major volatile products. Jackson and Conley suggested this was the result of a high temperature curing reaction.⁶ Three degradation pathways were proposed based upon observation of all the products generated during the high temperature degradation (Figure 2.7). Pathway 1 is an oxidative degradation pathway, which accounts for the formation of carbon monoxide and carbon dioxide. Pathway 2 is a radical fragmentation, which projects a route for the formation of methane, phenol, cresol, and a variety of other methyl substituted species. The final pathway is an extension of both pathways 1 and 2. It accounts for the formation of benzene, toluene, and benzaldehyde as a result of hydroxyl radical rupture of the phenol species formed from both pathways 1 and 2. Jackson and Conley concluded that the predominant route of phenolic degradation is oxidative degradation.

Jackson and Conley also analyzed the char formed during these reactions using infrared spectroscopy. At 450 °C or greater, elemental analysis indicated a drastic loss of oxygen and IR analysis of the char at 700 °C revealed the presence of hydroxyl and carbonyl groups. Gas chromatograms of the volatile components demonstrated that carbon monoxide was generated simultaneously with char formation. These three analytical observations support the proposed mechanism for char formation by Jackson and Conley (Figure 2.8).



15

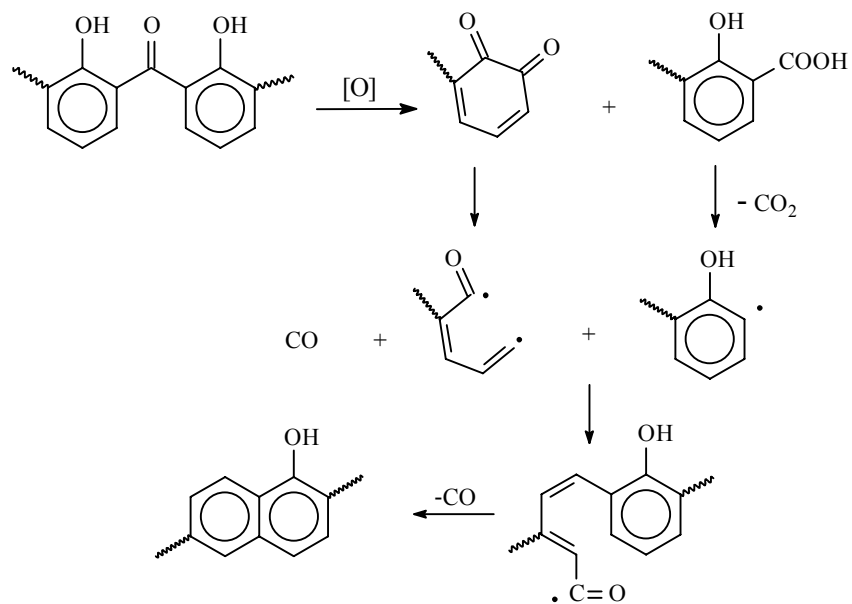


Figure 2.8: Char formation in phenolic networks

In a similar study, Lochte et al.⁷ analyzed the mechanisms of phenolic network degradation under atmospheric conditions. Five different prepolymers, with phenol-formaldehyde ratios ranging from 0.50 to 0.36, were thermally cured. The prepolymers were cured according to the following cycle: 72 hours at 74 °C, 2.5 hours increasing from 74 to 108 °C, 2 hours 108 °C, and finally 19 hours at 127 °C. Using TGA, the networks were heated from 25 °C to 800 °C with the residual char being subjected to elemental analysis. The group observed very similar weight loss curves between 400 and 700 °C for all of the networks. Also, elemental analysis on the char of the various networks at temperatures above 300 °C was almost identical. Between 425 and 530 °C a sharp rise in the level of oxygen was observed for all the networks. The group suggested the sharp rise in oxygen was the result of CO and CO₂ being the major degradation products. Above 530 °C, elemental analysis determined methane to be one of the major degradation products along with CO and CO₂. In order to explain the formation of carbon monoxide and methane as the main degradation products at higher temperatures, Madorsky⁸ proposed a mechanism which included the complete free radical breakdown of benzene rings. The logic behind this mechanism was that the breakdown of benzene rings could lead to free radical species capable of stripping hydrogen and oxygen leading to a highly carbonized char. Analysis of the char supported Madorsky's proposed mechanism because the char contained 99.2% carbon after pyrolysis at 1200 °C. Furthermore, molecular weight analysis of the volatile fragments at the pyrolysis

⁷ H. W. Lochte, E. L. Strauss, and R. T. Conley, "The Thermo-Oxidative Degradation of Phenol-Formaldehyde Plycondensates: Thermogravimetric and Elemental Composition Studies on Char Formation," *Journal of Applied Polymer Science*, 1965, **9**, 2799.

⁸ S. L. Madorsky, *Thermal Degradation of Organic Polymers*, Chapter XVI Phenolic Resins, Interscience Publishers, New York, 1964.

temperature suggested the existence of 3 to 4 benzene rings between cross-links. Based on the char and fragmentation analysis, Madorsky concluded the first step in thermal degradation for phenolics was scission between the methylene and the phenolic ring.⁸

In order to eliminate some of the uncertainty and disagreement concerning the degradation pathways of phenol-formaldehyde networks, recent work has been completed using several analytical techniques. Using IR, Moreterra and Low^{9, 10} studied the pyrolyzed chars produced in vacuo, oxygen, and nitrogen by phenol-formaldehyde networks after pyrolysis. Under nitrogen, pyrolysis at 350 °C produced very few spectral changes suggesting that structural changes did not occur. Surprisingly, it was observed that pyrolysis under vacuum at 360 °C produced many significant spectral changes. The O-H stretching band became narrower, decreased in intensity, and shifted from 3340 to 3530 cm^{-1} . Also, a sharp peak at 1260 cm^{-1} , which corresponds to an arylether stretching mode, was observed. These spectral changes were also correlated with significant water evolution.⁹ The above observations were associated with branching or cross-linking of the polymer. At 360 °C several other spectral changes were noticed. Most significantly, below 3000 cm^{-1} the aliphatic component appeared to be shifted with an increase in intensity, which was paralleled by an increase in intensity of a band near 1470 cm^{-1} .⁹ The change in the band near 1470 cm^{-1} was associated with CH_n deformation. These observations coupled with several other spectral transformations lead to a proposed

⁹ C. Moreterra and M. J. D. Low, "I.R. Studies of Carbons-VII. The Pyrolysis of a Phenol-Formaldehyde Resin," *Carbon*, 1985, **23**, 525.

¹⁰ C. Moreterra and M. J. D. Low, "Infrared Studies of Carbons. 8. The Oxidation of Phenol-Formaldehyde Chars," *Langmuir*, 1985, **1**, 320.

mechanism significantly different from previously suggested mechanisms (Figure 2.9). The mechanism infers that cleavage of the methylene units leads to an elimination reaction, which competes with cross-linking.

At higher pyrolysis temperatures, 500 to 520 °C, under both nitrogen and vacuum the same spectral changes observed at 360 °C occurred to a larger extent.⁹ The OH band continued to decrease and the diaryl ether CO stretch intensified. As well, the 1220 cm⁻¹ band associated with phenolic groups decreased. This information led to the conclusion that degradation at this temperature followed the mechanism originally proposed by Ouchi (Figure 2.10).¹¹ Also, the spectra from this pyrolysis indicated the absorption band for carbonyls at 1650 cm⁻¹ was very weak. The lack of an intense absorption from a carbonyl group suggested the primary autooxidative degradation routes proposed by Conley et al. were not significant for novolac networks.⁹

For pyrolysis temperatures greater than 560 °C, large changes in the IR spectra of the chars became apparent. Multiple bands between 1630 and 1580 cm⁻¹ transformed into a singlet that appeared around 1600 cm⁻¹. The 1600 cm⁻¹ band was assigned to C=C stretching within a polyaromatic system.⁹ The 1520 to 1000 cm⁻¹ region, corresponding to aliphatic CH stretching, converted into a single broad band at 1435 cm⁻¹. This band was not associated with the aliphatic CH stretching indicating the disappearance of methylene linkages within the novolac network. Bands between 900 and 750 cm⁻¹,

¹¹ K. Ouchi, "Infra-Red Study of Structural Changes During the Pyrolysis of a Phenol-Formaldehyde Resin," *Carbon*, 1966, **4**, 59.

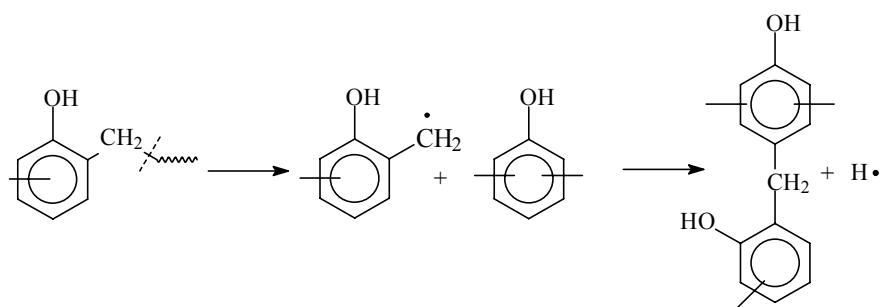


Figure 2.9: In vacuo low temperature (360 °C) cleavage of methylene units

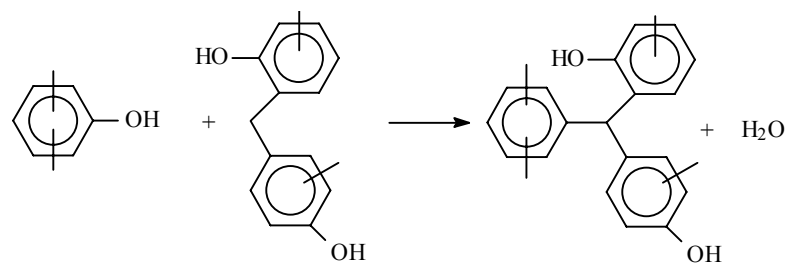


Figure 2.10: Phenolic resin degradation involving the reaction of a phenolic hydroxyl group and methylene bridge

associated with aromatic CH stretching, were observed.⁹ The lack of absorbance in the aliphatic region of the IR spectrum and the aromatic C=C stretching indicated that pyrolysis at temperatures greater than 560 °C lead to carbonization of the char.

Under oxygen, most significant changes in the spectra were observed at low and intermediate degradation temperatures, between 350 and 500 °C. The OH band broadened and the aliphatic CH band decreased upon heating from 350 °C to 500 °C. This suggested that methylene bridges were the most vulnerable parts of the network. Their oxidative destruction lead to the formation of H-bonded, OH containing structures, which are eliminated at higher temperatures.⁹ The low and intermediate temperature spectral changes were suggested to be the result of cross-linking and the low temperature oxidation mechanism shown in Figure 2.11. Interestingly, the TGA and IR analysis of pyrolyzed novolac networks completed by Jha et al. supported this mechanism.¹² Upon oxidizing at temperatures greater than 500 °C, Moreterra and Low observed that all of the double bonded structures previously observed, benzophenone and carboxylic acids, disappeared. This indicated destruction of the oxidized components and carbonization as the predominate mechanism of degradation at temperatures greater than 500 °C.⁹ In fact, the spectra were very similar to those produced when the novolac network was heated at 600 °C in vacuo and under nitrogen. The above observations led Moreterra and Low to conclude that novolac degradation, whether it be under oxygen, nitrogen, or in vacuo was

¹² V. Jha, A. K. Banthia, and A. Paul, "Thermal Analysis of Phenolic Resin Based Pyropolymers," *Journal of Thermal Analysis*, 1989, **35**, 1229.

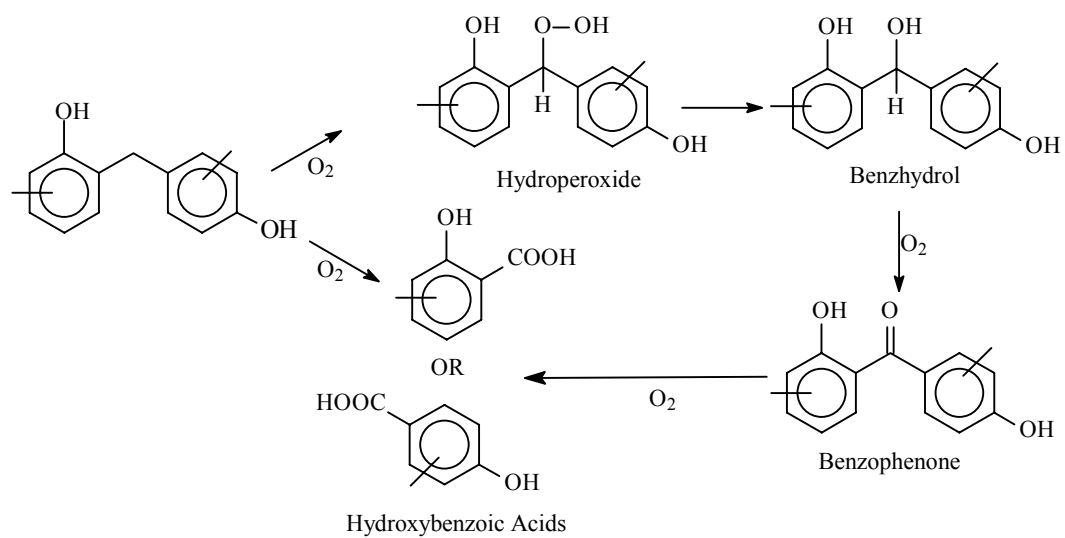


Figure 2.11: Low temperature oxidative degradation of novolac networks

essentially the same, without oxidative degradation being an important pathway.

Over the past fifty years much work has been completed in terms of synthesizing novolac and resole prepolymers, curing them and understanding their network thermal stability. Novolac and resole prepolymers can be synthesized using a variety of phenolic based compounds under acidic, basic, or neutral conditions. These prepolymers can then be converted into thermally stable networks using certain catalysts. The thermal characteristics of these networks have been well studied and some degradation mechanisms have been proposed. Although there is some disagreement concerning the mechanisms of phenolic network degradation, most groups have come to two basic conclusions. One, between 300 and 500 °C phenolic networks begin to degrade thermally as a result of methylene unit cleavage within the network. Two, heating phenolic networks above 500 °C eventually leads to pyrolysis of these networks which generates a carbonized char.

2.1.4.2 Cross-Linking and Halogenation Effects

Considering the wide range of applications for phenolic networks, improving certain physical properties of these materials, in particular flame retardance, is of high interest. Two approaches to improving the flame retardance of phenolics have been halogenation and cross-linking. The effects of these modifications have been studied extensively by several research groups.

Pearce et al.¹³ synthesized three phenol-formaldehyde resins, phenol-formaldehyde (PH-F), m-cresol-formaldehyde (MC-F), and p-cresol formaldehyde (PC-

¹³ L. Costa, L. R. d. Montelera, G. Camino, E. D. Weil, and E. M. Pearce, "Structure-Charring Relationship in Phenol-Formaldehyde Type Resins," *Polymer Degradation and Stability*, 1997, **56**, 23.

F), using a 0.95:1 molar ratio of formaldehyde to phenol. These resins were then cured into networks and compared in terms of thermal stability using TGA, to a less cross-linked commercially available material. Under nitrogen, the higher cross-linked material displayed a lower temperature of initial thermal degradation, but led to higher char levels after heating to 800 °C. Char yields of 50, 40, and 10% were produced by the networks synthesized from PH-F(branched), MC-F, and PC-F resins, respectively. The commercial PH-F network produced a char yield of 10%. However, it was the only commercial material to do so. The improved flame retardance of the “in house” synthesized material was attributed to the higher levels of cross-linking. In air, the opposite trend in thermal stability was observed. The higher cross-linked novolacs were shown to be less stable throughout the whole temperature range up to 800 °C. L. Costa et al. concluded that the added stability of the commercial networks in air was due to higher permeability. Higher permeability allows for added oxygen flow, which generates stable structures within the network that will only collapse at higher temperatures.¹³

Rao et al.¹⁴ completed a similar study where two different phenol-formaldehyde resins were cured and the networks were evaluated through analysis of volatiles and char using TGA, ¹H NMR, IR, and pyrolysis-GC. One of the two resole resins cured, contained a P/F (phenolic to formaldehyde) ratio of 1.0 (series I) and the other contained a P/F ratio of 1.5 (series II). The P/F ratios of the resins were determined using ¹H NMR. Based on ¹H NMR spectroscopy of series I, percent mass composition calculations of formal linkages and phenol linkages were completed. The formal linkages comprised approximately 36% and the phenol component comprised approximately 64%.¹⁴ Upon

curing and then pyrolysis at 800 °C, series I generated a higher percentage of char, 63-67%, compared to 45-58%, for series II. The excellent agreement between the experimental char yield and the calculated mass percent of the phenol linkages for series I suggested the formal linkages are thermally labile.¹⁴ Based on the TGA data, Rao et al. concluded the degradation of the phenolic networks occurred in two stages. Stage one correlates to a 11-14% mass loss, which was proposed to be the cleavage of the formal linkages.¹⁴ This value agreed well with the calculated mass of the formal linkages in series I being 15.5%. Stage two is represented by an additional 20% mass loss of methylene and water fragments which leaves a graphitized char.

Further analysis of the TGA data was completed in order to determine the kinetic parameters for the thermal degradation of phenolic networks. The two methods used were those of Ozawa and Chatterjee-Conrad. Treating the mass loss data by either of the two methods showed the activation energy of the decomposition of phenolic networks was dependent upon the extent of cross-linking. Plotting the activation energy versus the P/F ratio of the phenolic network showed the activation energy of decomposition increased with an increase in the P/F ratio of the resin.

The pyrolysis-GC data indicated the main products of degradation at 750 °C were phenol, formaldehyde, benzene, and toluene. The phenol to formaldehyde ratio in the products of degradation varied considerably for series I and II. This demonstrated that pyrolyzate compositions varied with the extent of the curing reaction.¹⁴ Therefore the pyrolysis-GC data was consistent with the TGA evaluations.

¹⁴ M. R. Rao, S. Alwan, K. J. Scariah, and K. S. Sastri, "Thermochemical Characterization of Phenolic Resins Thermogravimetric and Pyrolysis-GC Studies," *Journal of Thermal Analysis*, 1997, **49**, 261.

In summary, Rao et al. suggested that the thermal decomposition of phenolics was a two-stage process. First, the formal linkages cleave and second, the remaining network undergoes a series of reactions that leads to graphitization. Secondly, it was concluded that the activation energy for thermal decomposition of phenolic networks was proportional to the extent of cross-linking.¹⁴

Pearce et al.¹⁵ studied the flame-retardant properties of nonhalogenated and halogenated phenol-formaldehyde networks. In order to determine the relationship between the type of phenolic network and flammability, the group attempted to develop a correlation between char formation and oxygen index (OI). Oxygen index is a relative measurement that estimates the level of oxygen required to ignite a sample. Similar studies have measured OI values for phenolic networks under inert (nitrogen) and reactive atmospheres (air). Typical OI values for phenolic networks range between 45 and 60.¹⁶ A linear relationship between char yields and oxygen indices was developed by van Krevelan¹⁷ for halogen-free polymers (Equation 2.1) however, a correlation has not been developed for halogenated polymers. Pearce et al. attempted to develop a similar correlation for halogenated phenolic networks.

In terms of the nonhalogenated networks, Pearce et al. determined that for meta- and para-cresol phenol-formaldehyde networks the OI was lower than the unsubstituted-phenolics. In general, it was observed that halogenated phenolics generated a higher OI

¹⁵ Y. Zaks, J. Lo, D. Raucher, and E. M. Pearce, "Some Structure-Property Relationships in Polymer Flammability: Studies of Phenolic-Derived Polymers," *Journal of Applied Polymer Science*, 1982, **27**, 913.

¹⁶ R. M. Morchar and J. A. Hiltz, "A TGA Study Correlating Polymer Characteristics with Smoke and Flammability Properties of Polyester and Phenolic Resins," *Thermochimica Acta*, 1991, **192**, 221.

¹⁷ D. W. V. Krevelan, "Some Basic Aspects of Flame Resistance of Polymeric Materials," *Polymer*, 1975, **16**, 615.

and lower char yield than the nonhalogenated phenolics. Based on the data, the group was able to develop a correlation between char yield and oxygen index for the nonhalogenated phenolic networks (Equation 2.1).

$$\%OI = 2.4 + 0.57(\%CY) \quad \%OI = \text{oxygen index} \quad \%CY = \text{Char Yield}$$

Equation 2.1: Correlation between OI and CY for nonhalogenated phenolic resins¹⁵

The type of cross-linking agent was found to be the greatest influencing factor on the flammability of halogenated phenolic networks.¹⁵ The halogenated phenolic resin cross-linked with formaldehyde to give methylene units as cross-linking sites generated the highest OI values. The terephthaloyl chloride and s-trioxane[(CH₂O)₃] crosslinked phenolic resins generated the lowest OI values. This data suggests s-trioxane creates the most thermally unstable halogenated phenolic network.¹⁵ This lack of stability is believed to be due to the ether and ester linkages that s-trioxane and terephthaloyl chloride generate upon cross-linking.

The second part of the thermal study Pearce et al. completed involved synthesizing phenolic copolymers with 0 to 100 percent of halogenated phenol and then curing these materials. It was determined that OI values increased for networks comprised of resole copolymers with higher contents of halogenation.¹⁵ In contrast, for networks with halogenated novolac copolymer content of 0 to 80% the OI values showed only a slight increase and then plateaued. The group stated the reason for the lower OI values, or lower thermal stability, for networks comprised of significant levels of novolac copolymers is the presence of paraformaldehyde linkages. In conclusion, it was stated

that the resole copolymerization process generated network materials with better flame resistance.

These studies evaluated phenolic degradation using different types of instrumentation to determine the characteristics and nature of phenolic degradation. However, these studies did not focus extensively on determining the kinetic parameters for thermal degradation. A better understanding of the kinetic model for thermal degradation is an important factor in elucidating unknown facts about phenolic network degradation. As a result, kinetic parameters for phenolic network degradation have been the subject of several studies.^{18, 19, 20}

2.1.4.3 Kinetic Parameters for Thermal Decomposition

Many research groups have used TGA at multiple heating rates to better determine the kinetic parameters for phenolic decomposition. Moore, Tant, and Henderson²¹ applied multiple heating rate TGA techniques to phenolic ablative materials. The phenolic materials were heated under nitrogen at six different heating rates: 10, 20, 40, 80, 100, and 160 °C/min. The change in the weight loss versus the change in time and temperature was measured. It was determined that the thermal decomposition of the phenolic materials occurs in two stages. Using the method of Flynn and Wall, the average kinetic parameters for the degradation of these materials were calculated.²¹ The

¹⁸ B. Henderson, M. R. Tant, and G. R. Moore, "Determination of Kinetic Parameters for the Thermal Decomposition of Phenolic Ablative Materials by a Multiple Heating Rate Method," *Thermochimica Acta*, 1981, **44**, 253.

¹⁹ K. N. Ninan, "Effect of Heating Rate on Thermal Decomposition Kinetics of Fiberglass Phenolic," *Journal of Spacecraft and Rockets*, 1983, **23**, 347.

²⁰ I. Pektas, "High-Temperature Degradation of Reinforced Phenolic Insulator," *Journal of Applied Polymer Science*, 1998, **68**, 1337.

²¹ B. Henderson, M. R. Tant, and G. R. Moore, "Determination of Kinetic Parameters for the Thermal Decomposition of Phenolic Ablative Materials by a Multiple Heating Rate Method," *Thermochimica Acta*, 1981, **44**, 253.

average activation energy for the overall thermal decomposition was determined to be 269 kJ g/mole.

Ninan²² completed a similar kinetic study using TGA data. The thermal degradation of phenolic ablative networks was evaluated at heating rates of 1, 2, 5, 10, 20, 50, and 100 °C/min. However, in this study the samples were under an atmosphere of air instead of nitrogen. Also, the kinetic parameters were calculated using the following three integral equations: Coats-Redfern, MacCallum-Tanner, and Horowitz-Metzger. The study determined that as the heating rate increased the reaction inception temperature increased only slightly, 310 to 340 °C, while the percent mass loss remained virtually constant at 33%.²² In contrast, the reaction completion temperature increased dramatically, 495 to 900 °C, in going from a heating rate of 1 to 100 °C/min.²² At a heating rate of 1 °C/min, the Coats-Redfern, MacCallum-Tanner, and Horowitz-Metzger integral equations each determined the average activation energy for decomposition to be 77.72, 81.17, and 102.8 kJ/mole, respectively.²² Upon increasing the heating rate to 100 °C/min, all three integral equations showed the average activation energy for decomposition to decrease by half.²²

Multiple heating rate TGA and DSC were used by Pektas²³ to develop a better understanding of the kinetic parameters involved in phenolic ablative network degradation. Also, the half-life (service life) of phenolic networks at elevated temperatures was measured. The TGA data of the phenolic network in heating from 25

²² K. N. Ninan, "Effect of Heating Rate on Thermal Decomposition Kinetics of Fiberglass Phenolic," *Journal of Spacecraft and Rockets*, 1983, **23**, 347.

²³ I. Pektas, "High-Temperature Degradation of Reinforced Phenolic Insulator," *Journal of Applied Polymer Science*, 1998, **68**, 1337.

to 250 °C indicated a mass loss of 2.85% and 21.78% upon heating between 450 and 900 °C.²³ For the phenolic network, it was determined that T_{\max} , the degradation temperature, was dependent upon the heating rate.²³ Upon increasing the heating rate from 5 to 5000 °C/min, the degradation temperature increased from approximately 350 to 600 °C. Interestingly, the half-life of the phenolic network only changed slightly as a function of temperature in the temperature range of 1000 to 3500 °C. In going from 1000 to 3500 °C, the half-life decreased from 118.8 to 116.2 seconds.²³ Further analysis of the TGA data using the Ozawa method, determined the activation energy of thermal degradation to be 356 kJ/mol.²³ Finally, using DSC under inert conditions(nitrogen), enthalpy values were determined for two different temperatures, 207 °C and 540 °C. At 207 °C ΔH equaled 15 J/g; however, upon heating to 540 °C ΔH increased significantly to 301 J/g.²³

2.1.4.4 Pyrolysis Compositions

In past pyrolysis studies, there was not significant concern for determining compositional ratios of phenolic network pyrolysis products. In order to have a better understanding of phenolic degradation mechanisms, a greater knowledge base of pyrolysis product compositions is required. Several studies have focused on determining the compositions of pyrolysis products as a function of temperature through the use of several analytical techniques. These techniques include Pyrolysis-GC, IR, TGA, and TGA-mass spectroscopy (TGA-MS).

One of the earliest studies into identifying phenolic network degradation products was completed by Martinez and Guichon.²⁴ The purpose of the study was to synthesize

²⁴ J. Martinez and G. Guiochon, "Identification of Phenol-Formaldehyde Polycondensates by Pyrolysis Gas Chromatography," *Journal of Gas Chromatography*, 1967, **5**, 146.

and utilize seven different networks, containing varying mole percent levels of phenol, 3-methylphenol, and 3,5-dimethylphenol, to determine whether a relationship existed between the pyrolysis products and compositions of the networks. The mole percent ratio for each of the three components in the different networks varied from 100 to 0. The seven different networks were heated to a pyrolysis temperature of 750 °C and the corresponding pyrolysis products were analyzed using GC.

The results of the study show that total phenol/phenol derivative yield during pyrolysis is 13% for networks synthesized from pure phenol resins and 22 to 29% for all other networks.²⁴ The remaining part of the pyrolysis products was comprised of light gases, water, formaldehyde, aromatic hydrocarbons, and heavier compounds including tar. The other volatile phenolic components were phenol derivatives with methyl substituents only at the *p*- and *o*- positions. In a similar fashion, the pyrolysis of a network composed mainly of 3-methylphenol resin predominantly produced *m*-substituted derivatives. The *p*-methyl substituted phenols were detected in only trace amounts. Similar observations were made when the pure resin from 3,5-dimethylphenol was pyrolyzed. The predominant phenolic volatiles were 3,5-substituted. The results from the pyrolysis of pure networks indicate that scission between the methylene bridges was the predominant pathway for the beginning stages of degradation. For the networks from three different phenolic resins, a quantitative relationship was observed between the compositions of the phenolic resins used to make the network and the pyrolysis products.

In a similar fashion, pyrolysis-GC was used by Hetper and Sobera²⁵, however the GC was modified for the efficient collection of high boiling pyrolysates. High boiling pyrolysates allow for a more detailed determination of the pyrolysis compositions. After one second at 770 °C, pyrolysis of novolac networks, produced condensed ring aromatics which served only to confirm previous work. Surprisingly, two other types of components were also detected, unsubstituted and substituted bisphenols and trisphenols, which previous work had not detected.²⁶ The substituted bis and trisphenols were concluded to be pyrolysis products. However, the origin of the substituted compounds was uncertain. In order to explain the appearance of previously undetected pyrolysis products, a two-part pyrolysis-GC experiment was completed. The results of this experiment showed substituted bis and trisphenols to be evaporation and not pyrolysis products.²⁶ In conclusion, it was suggested that the study supported previous work in that decomposition of phenol-formaldehyde networks is the result of bond breaking between methylene bridges. Also, the group stated the formation of condensed aromatic rings was the result of cyclization with hydroxyl or methyl groups in an ortho position to methylene bridges.²⁵

Cascaval and Rosu²⁷, using IR and pyrolysis-GC, were able to determine a variety of phenolic pyrolysis products, suggesting a complicated degradation mechanism. Also, semi-quantitative estimations were established between the different products. It was

²⁵ J. Hetper and M. Sobera, "Thermal Degradation of Novolac Resins by Pyrolysis-Gas Chromatography with a Movable Reaction Zone," *Journal of Chromatography A*, 1999, **833**, 277.

²⁶ C. A. Lytle, W. Bertsch, and M. McKinley, "Determination of Novolac Resin Thermal Decomposition Products by Pyrolysis-Gas Chromatography-Mass Spectrometry," *Journal of Analytical and Applied Pyrolysis*, 1998, **45**, 121.

²⁷ C. N. Cascaval and D. Rosu, "Thermal Characterization by Pyrolysis-Gas Chromatography," *Revue Roumaine de Chimie*, 1991, **36**, 1331.

determined that phenolic networks begin to degrade at temperatures above 300 °C, which is accompanied with the generation of water, carbon monoxide, carbon dioxide, methane, phenol, cresols, and xylenols.²⁷ As the temperature elevates above 400 °C, the previously mentioned compounds are formed in conjunction with aromatic hydrocarbons. At 720 °C the main products formed during pyrolysis were highly volatile hydrocarbons (C1-C5), phenol, benzene, toluene, isopropylbenzene, m-cresol, and alkyl-phenols.²⁷

Using mass spectroscopy in conjunction with several other analytical techniques, Chang and Tackett²⁸ produced additional insight into the compositional nature of phenolic pyrolyzates. The TGA-MS data from this study showed that phenolic networks display weight loss over several regions (Table 2.1). The first region where significant weight loss was detected was between 20 and 180 °C. The major component generated during this stage was water.²⁸ The second region of detected weight loss occurred between 210 and 270 °C. The gases detected and attributed to the weight loss were water, phenol, carbon dioxide, ammonia, and methanol. The water and methanol generated during this stage was believed to result from condensation reactions between phenols and methylols.²⁸ The carbon dioxide and ammonia were suggested to be the result of additives in the network. The third region of significant weight loss occurs between 420 and 650 °C. Carbon dioxide and water are continually produced over this region. Between 650 and 720 °C, the next weight loss region, methane was the predominant gas detected accompanied by benzene, toluene, xylene, and

²⁸ C. Chang and J. R. Tackett, "Characterization of Phenolic Resins with Thermogravimetry-Mass Spectrometry," *Thermochimica Acta*, 1991, **192**, 181.

Table 2.1: List of gases evolved during the phenolic resin TG-MS experiment

Peak Temperature (°C)	Gas	Estimated Weight Loss (%)
120	Water	.8
145	Phenol	.3
210	Water	4.4
	Phenol	1.8
	Methanol	1.2
	Carbon dioxide	.4
270	Ammonia	2.7
370	Unidentified	.3
420	Water	5.0
	Carbon dioxide	.7
580	Water	5.7
	Carbon dioxide	1.3
650	Methane	3.8
	Benzene	3.4
	Toluene	2.7
	Xylene	1.3
	Trimethylbenzene	.2
720	Phenol	4.1
	Cresol	2.6
	Dimethylphenol	1.1
	Trimethylphenol	.1
	Carbon Monoxide	6.1

trimethylbenzene. The final region of degradation occurred at 750 °C. At this temperature carbon monoxide was the major component with phenol, cresol, dimethylphenol, and trimethylphenol comprising the rest of the evolved gases.

Interestingly, the results of this study compare well to the work completed by Jackson and Conley⁶ and, in general, support the mechanism proposed in 1965.²⁸ However, there are two areas of disagreement between the two studies. The largest disagreement is in the yield of carbon dioxide and possible mechanism for carbon dioxide formation. The yield of carbon dioxide was much higher in the earlier work⁶ and in this work the mass spectroscopy ion curve for water follows closely to that of carbon dioxide. This would indicate that any plausible mechanism proposed for phenolic network degradation would have to account for formation of water and carbon dioxide concurrently.²⁸ The substantial difference in yield was suggested to be the result of different heating rates, 5 versus 310 °C/min. Secondly, the earlier work⁶ showed the majority of phenol, cresols, and higher phenolic species were formed at 500 °C, which is considerably lower than what the current study demonstrated. The current study showed the initial formation of the same phenolic species at 600 °C and continual formation of the compounds until the heating process was complete. In addition, Chang and Tackett also completed elemental analysis on the char formed during the heating process. The percent elemental composition values for this work agreed well with earlier work completed by Lochte, Strauss, and Conley⁷, indicating the same decomposition process was present.

In order to validate the TGA-MS study, Chang and Tackett also completed Pyrolysis-GC-MS and direct insertion probe-MS. In the pyrolysis-GC-MS study, the

phenolic network was heated to 750 °C for 10 seconds at a heating rate of 1000 °C/s. The gases that were detected include water, benzene, toluene, xylene, phenol, cresols, and xylenol.²⁸ The same gases were detected in the TGA-MS study. During the direct insertion probe-MS analysis, the phenolic network was heated from 30 to 280 °C at a heating rate of 5 °C min⁻¹. The detected species included ammonia, water, methanol, benzene, toluene, xylene, phenol, cresol, and xylenol. Once again, these compounds were also detected during the TGA-MS analysis.

2.2 Phenolic Epoxy Chemistry

2.2.1 Phenolic/Epoxy Network Formation

The use of epoxy resins is wide ranging. These materials can be cured into a variety of aerospace materials or adhesives using amine curing agents. Epoxy materials can also be cured with phenolic compounds, into materials which have many potential applications. This potential has fostered much interest into understanding phenolic/epoxy reactions. Therefore, the chemical mechanisms of phenolic/epoxy reactions have been of significant literature study.

Schechter and Wynstra^{29, 30, 31} completed some of the earliest and most significant work in this area. Their work suggested an ionic reaction mechanism between a phenol and epoxide with competition between a main chain reaction and secondary alcohols

²⁹ L. Shechter and J. Wynstra, "Glycidyl Ether Reactions with Alcohols, Phenols, Carboxylic Acids, and Acid Anhydrides," *Industrial and Engineering Chemistry*, 1956, **48**, 86.

³⁰ L. Shechter, J. Wynstra, and R. P. Kurkijy, "Glycidyl Ether Reactions with Amines," *Industrial and Engineering Chemistry*, 1956, **48**.

³¹ L. Shechter, J. Wynstra, and R. P. Kurkijy, "Chemistry of Styrene Oxide Comparison with Phenyl Glycidyl Ether in Model Compound Reactions," *Industrial and Engineering Chemistry*, 1957, **49**, 1107.

formed during the reaction. It was also determined that catalysis for this reaction decreases in the following order:

Quaternary ammonium > Tertiary amine > Alkaline base > > Metal chloride

Banthia and McGrath³² studied the effect of catalyst and solvent on the low temperature (80-100 °C) polymerization of low molecular weight (5,000 – 10,000 g mol⁻¹) polyhydroxyethers using bisphenol A epoxy and bisphenol A. Two types of catalysts considered during this study were ammonium salts and trialkyl/triaryl nucleophiles of group V(A) elements. The ammonium salts were benzyltrimethylammonium hydroxide and tetramethylammonium hydroxide while the trialkyl/triaryl nucleophiles were triethanolamine and triphenylphosphine. It was determined that these catalysts were the more selective of the reaction between a phenoxide ion pair and epoxy which supported the conclusions of Schechter and Wynstra. It was suggested that ammonium salts promote the chain extending reaction because of the formation of highly basic phenoxide ions. The highly basic nature of phenoxide ions promotes the direct reaction with epoxy groups.³² It has been proposed that triaryl and trialkyl nucleophiles of group V(A) elements promote the primary reaction due to steric hindrance between the bulky catalysts and the secondary alcohol.³²

³² A. K. Banthia and J. E. McGrath, "Catalysts of Bisphenol-Diglycidyl Ether Linear Step-Growth Polymerization," *Polymer Preprints*, 1979, **20**, 629.

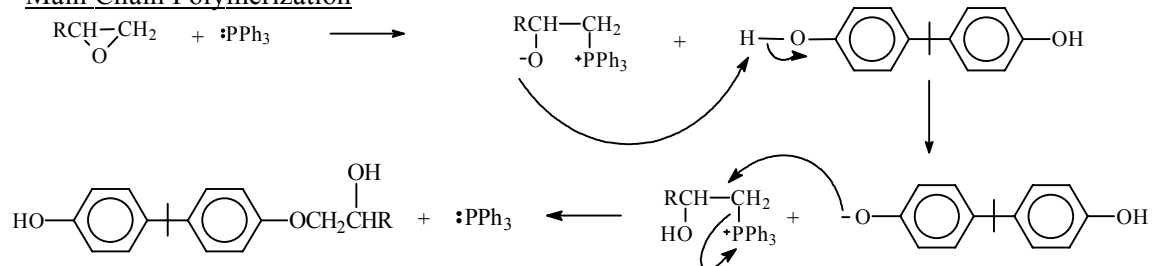
More recently, similar studies have investigated the epoxy-phenolic reaction mechanism in the melt phase. Romanchick et al.³³ evaluated the polymerization of phenol and epoxy in the presence of triphenylphosphine catalyst. Supported by experimental rate data, the group made two proposals concerning triphenylphosphine catalysis of phenol-epoxy polymerizations. They suggested using triphenylphosphine as a catalyst minimizes branching via the secondary alcohol and they also proposed a mechanism for the triphenylphosphine catalysis of phenol-epoxy polymerizations (Figure 2.12). The first step of the mechanism is the nucleophilic attack of triphenylphosphine on an epoxide ring, which generates a betaine.³³ The second step is the proton abstraction from bisphenol A generating a phenoxide ion. The third step is the attack of the phenoxide on a carbon bearing the positively charged phosphorous, which regenerates the catalyst. After all of the phenolic hydroxides are reacted the catalyst breaks down via a Wittig reaction.³³

Melt phase aliphatic tertiary amine catalysis of phenol-epoxy polymerization was also studied.³⁴ A main-chain mechanism for the tertiary amine catalysis of phenol-epoxy polymerization was proposed (Figure 2.13). The first step in the reaction is reaction of the tertiary amine with phenol forming an ion pair. The second step is an ion pair quadrupolar interaction with the epoxy ring, which rapidly disassociates generating the β -hydroxy ether. Three-side chain reactions were also proposed. One the homopolymerization of the epoxy groups. A second was a branching reaction where free

³³ W. A. Romanchick, J. E. Sohn, and J. F. Geibel, in *ACS Symposium Series 221-Epoxy Resin Chemistry II* (Ed.: R. S. Bauer), American Chemical Society, Washington D.C., 1982, pp. 85.

³⁴ D. Gagnebien, P. J. Madec, and E. Marechal, "Synthesis of Poly(sulfone-b-siloxanes)-I Model Study of the Epoxy Phenol Reaction in the Melt," *European Polymer Journal*, 1985, **21**, 273.

Main Chain Polymerization



Wittig Catalyst Decomposition

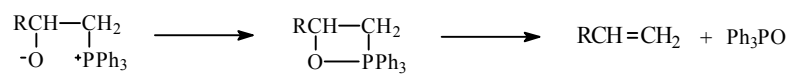


Figure 2.12: Main chain and catalyst decomposition for triphenylphosphine catalyzed epoxy-phenol reaction

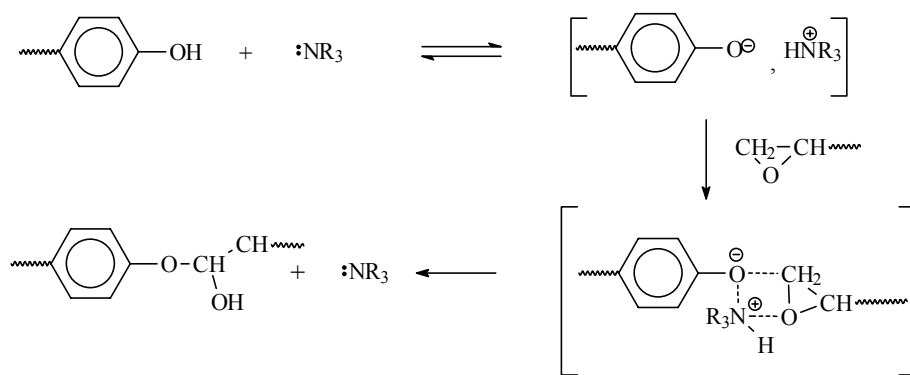


Figure 2.13: Proposed mechanism for the tertiary amine catalyzed phenol-epoxy polymerization

amine associated with secondary alcohols forming activated complexes and the activated complex leads to branched species. This branching reaction was supported by GPC data showing increasing the amine concentration lead to lower molecular weights and increased branching. Another branching reaction was a result of the zwitterion formed during the epoxy homopolymerization reacting with phenols forming activated secondary hydroxyl species.

2.2.2 Epoxy Degradation

Epoxy networks have a wide range of industrial applications. Many of these applications require epoxy networks to have considerable thermal stability for long periods of time. Therefore, many studies have focused on various aspects of epoxy degradation, such as degradation mechanisms, cross-linking effects, and halogenation to aid in the design of epoxy networks with higher thermal stability.

Some of the early work in determining epoxy degradation parameters focused on the kinetic parameters of epoxy thermal degradation. Neiman et al.³⁵ determined a low activation energy for thermal degradation, 146 kJ/mole. The group also found the activation energy for thermal degradation changes depending on the extent of cure and curing agent. The group suggested the low activation energy for thermal degradation indicated the oxidative degradation process of epoxies is a complex free radical process. However, no detailed degradation mechanisms were mentioned.

³⁵ M. B. Neiman, B. M. Kovarskaya, L. I. Golubenkova, A. S. Strizhkova, I. I. Levantovskaya, and M. S. Akutin, "The Thermal Degradation of Some Epoxy Resins," *Journal of Polymer Science*, 1962, **56**, 383.

Some of the most significant work in determining plausible epoxy degradation mechanisms was completed by Lee.³⁶ The thermal degradation products of cured and uncured epoxy resins were studied using TGA in conjunction with mass spectrometry. One part of the study focused on determining thermal stability correlations between epoxy networks and curing agents. The two types of epoxy networks evaluated were based on bisphenol A and an epoxidized phenol. The two types of curing agents used were methylenedianiline (MDA) and methyl nadic anhydride (MNA). Through analysis of TGA data, it was determined that phenolic based epoxy networks had a lower total weight loss than bisphenol A epoxy networks when either curing agent was used. Of the epoxidized novolac networks, the network cured with MDA generated the lowest total weight loss upon thermal exposure.

The pyrolysis compositions of the networks were also determined. The epoxidized-phenolic and bisphenol A networks cured with MDA generated water as the major boiling component at 350 °C. In contrast, at 450 °C the pyrolysis composition changed drastically. The main degradation product generated was carbon monoxide. Lee suggested the high concentration of carbon monoxide was most likely consistent with the degradation mechanism in Figure 2.14 for the networks. The epoxy networks cured with MNA yielded significant pyrolysis products between 350 and 450 °C. Higher concentrations of water, carbon dioxide, and methylcyclopentadiene were produced at

³⁶ L. Lee, "Mechanisms of Thermal Degradation of Phenolic Condensation Polymers. II. Thermal Stability and Degradation Schemes of Epoxy Resins," *Journal of Polymer Science*, 1965, **3**, 859.

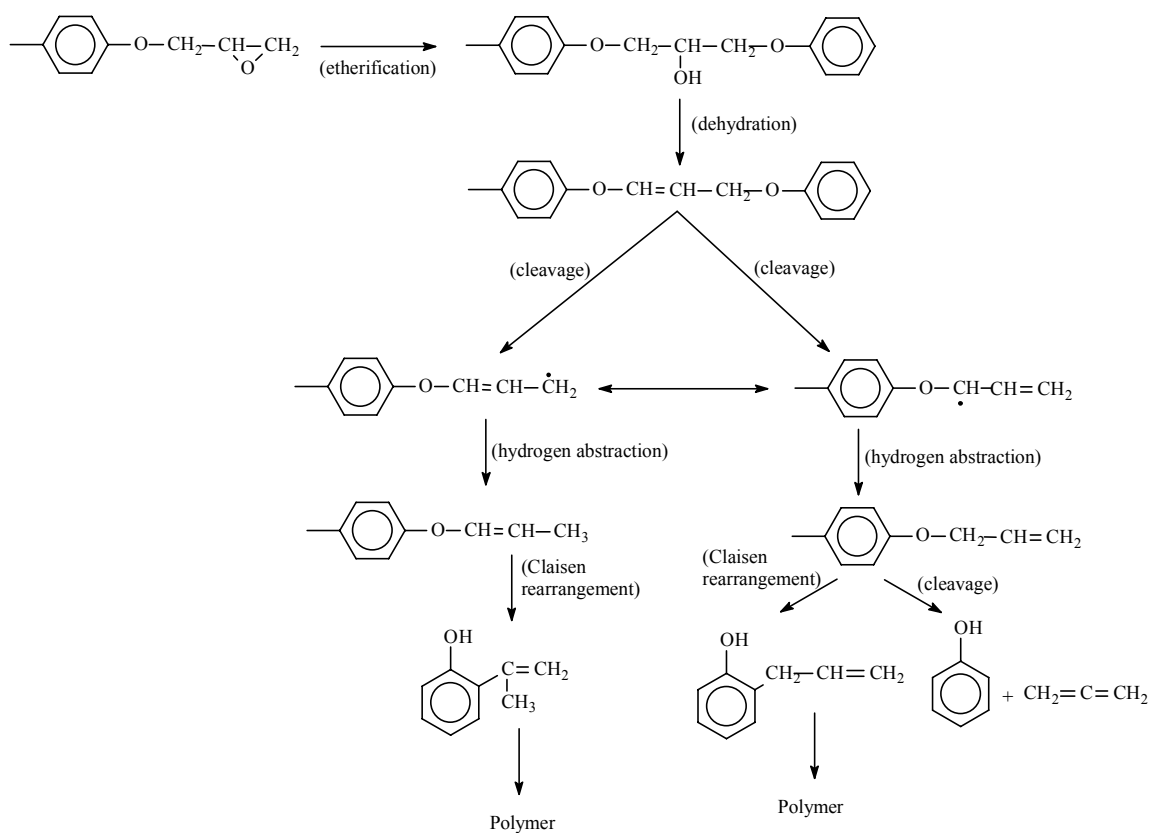


Figure 2.14: Proposed degradation pathways of bisphenol A epoxy networks

350 °C. Most significantly, H₂ and CO gases were detected at similar molar ratios. These results support a mechanism of degradation originally proposed by Anderson involving the cis-elimination of ester linkages (Figure 2.15).³⁷

The second part of the study was designed for determining high temperature uncured epoxy resin reactions. The pyrolysis compositions of three different epoxy resins based on bisphenol A, chain-extended bisphenol A, and an epoxidized phenolic were evaluated. The pyrolysis temperatures ranged from 350 °C to 475 °C. For the epoxidized-phenolic resins, toluene and ethane were the major pyrolysis products (68.30 mole %) at temperatures between 350 and 450 °C.³⁶ At 475 °C, a mixture of phenolic-based compounds comprised the largest percentage of compounds generated. Considering that ethane was detected in considerable amounts, 13.40 mole %, during pyrolysis at 450 °C, Lee indicated that the data was not fully supportive of the original mechanism proposed by Anderson (Figure 2.16).³⁷ Therefore, an alternative degradation scheme was suggested (Figure 2.16). The pyrolysis products of the bisphenol A epoxy resin were similar to those from epoxidized phenolic resin with toluene being the major component. However, the lack of carbon monoxide and carbon dioxide generation at temperatures between 350 and 450 °C gave more credence to Lee's proposed mechanism in Figure 2.16. For the chain-extended bisphenol A epoxy resin, the low temperature degradation products were significantly different. At 350°C, water and toluene were produced at almost equivalent levels, 40 and 38 mole % respectively.

³⁷ H. C. Anderson, "Thermal Degradation of Epoxide Polymers," *Journal of Applied Polymer Science*, 1962, **6**, 484.

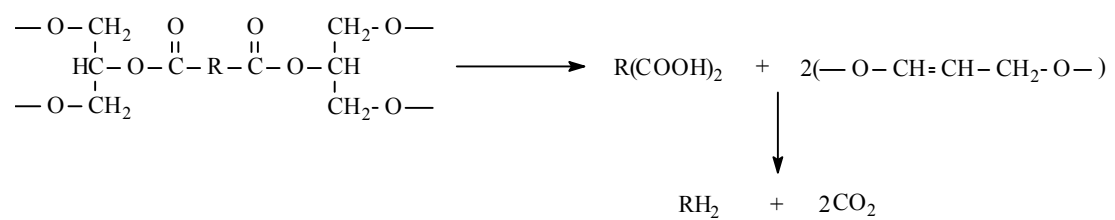


Figure 2.15: Cis-elimination of ester linkages in anhydride cured epoxy networks



Figure 2.16: Proposed mechanisms for epoxized novolac degradation

The higher concentration of water was attributed to the chain-extended bisphenol A epoxy resin having a larger percentage of free hydroxy groups when compared to other diglycidyl ethers. The degradation products at 450 °C were quite similar to the other two epoxy resins except higher concentrations of acetaldehyde were generated. After considering the increased acetaldehyde production, Lee suggested the degradation mechanism in Figure 2.16 as being most likely for the chain-extended bisphenol A epoxy resin. Interestingly, latter work concerning the oxidative degradation of bisphenol A epoxy resins completed by Leisgang et al.³⁸ supported many aspects of the degradation proposed by Lee.

Recently, studies have been focused on determining the degradation pathways of epoxy networks in the presence of oxygen and the effects that degradation has on certain physical properties. Past work³⁹ focused on the degradation of epoxy networks at low temperatures under a nitrogen atmosphere. However, the degradation of such networks under reactive atmospheres had not been extensively studied. Burton⁴⁰ studied the effects of various curing agents and antioxidants on the oxidative degradation of bisphenol A epoxy networks. Also, the effects of low temperature, 125 °C, oxidative degradation on the physical properties of bisphenol A epoxy networks were evaluated.

Using DSC and IR, Burton demonstrated that at low temperatures, 100-200 °C, antioxidants did not deter the degradation of cured bisphenol A epoxy networks. The type of curing agent significantly affected the oxidative resistance of bisphenol A epoxy

³⁸ E. C. Leisgang and A. M. Stephen, "The Thermal Degradation In Vacuo of an Amine-Cured Epoxide Resin," *Journal of Applied Polymer Science*, 1970, **14**, 1961.

³⁹ B. D. Gesner and P. G. Kelleher, "Oxidation of Bisphenol A Polymers," *Journal of Applied Polymer Science*, 1969, **13**, 2183.

networks. Based on flexural property measurements and IR, a correlation was established between the nucleophilicity of curing agents and oxidative resistance. The higher the nucleophilicity of the curing agent the lower the oxidative resistance of the network. Consequently, benzenesulfonamide, pKa of 10, produced an epoxy network which had higher thermal resistance and physical properties than aliphatic amines, pKa of 35. The lack of improvement by antioxidants and the reduction of thermal resistance as the basicity of the curing agent was increased suggested the degradation of epoxy networks at low temperatures was not free radical in nature.⁴⁰ To account for these observations Burton suggested alternate steps to the mechanism in Figure 2.17(lower right hand corner).^{40, 41}

This work clarified some of the issues concerning epoxy network degradation under different conditions (i.e. different curing agents, antioxidants, and temperature). However, the low temperature degradation of epoxy networks was not related to glass transition temperature, T_g . Gilham et al.⁴² monitored the effects of time and temperature on epoxy-phenolic networks. The networks were produced using a solution of bisphenol A epoxy and phenolic resin. Using TGA under a helium atmosphere, the group determined that macroscopic gelation occurred at 230 °C due to evaporation of the solvent. At prolonged times at this temperature minimal weight loss and vitrification were observed.⁴²

⁴⁰ B. L. Burton, "The Thermoxidative Study of Cured Epoxy Resins. I," *Journal of Applied Polymer Science*, 1993, **47**, 1821.

⁴¹ M. F. Dante and R. T. Conley, "The Oxidative Degradation of Epoxy Resins," *Polymer Preprints*, 1964, **24**, 135.

⁴² S. Gan and J. K. Gillham, "A Methodology for Characterizing Reactive Coatings: Time-Temperature-Transformation(TTT) Analysis of the Competition between Cure, Evaporation, and Thermal Degradation for an Epoxy-Phenolic System," *Journal of Applied Polymer Science*, 1989, **37**, 803.

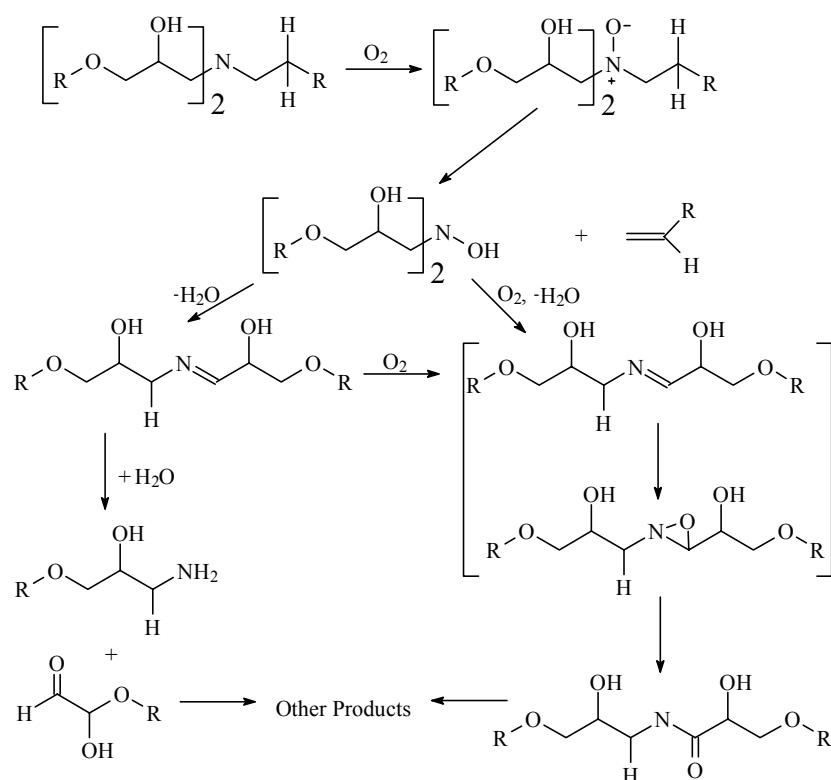


Figure 2.17: Proposed degradation mechanism of an amine-cured epoxy resin via a Cope reaction

The networks were heated from 135 to 240 °C and maintained at 240 °C over the same time frame. Glass transition temperature versus log time was plotted to determine whether a linear relationship between the two variables existed. For curing temperatures between 135 and 195 °C, the T_g increased linearly with respect to log time with the maximum T_g observed being 147 °C. Above 195 °C, T_g initially reached a plateau and then decreased significantly as a function of log time. The decrease in T_g was associated with the thermal degradation of the networks. These observations suggested that curing was the predominant chemical process at temperatures below 195 °C. Above 195 °C, a more complicated process for the increase in T_g was involved.⁴² T_g versus temperature of cure plots demonstrated a maximum T_g of 147 °C at a cure temperature of 155 °C. Above a cure temperature of 155 °C, the T_g decreased substantially. After considering that previous work had shown that increasing the cure temperature increased the cross-link density and T_g for phenolic-epoxy networks,^{43, 44} the group concluded that the decrease in T_g was the result of thermal degradation.⁴²

2.3 High Temperature Functional Groups

2.3.1 Phenylethynyl End Groups

Over the past twenty years there has been much interest in improving the mechanical properties, solvent resistance, and thermo-oxidative stability of certain rigid rod and thermoplastic polymers.⁴⁵ The approach has been to end-cap these polymers

⁴³ M. Ogata, N. Kinjo, and T. Kawata, "Effects of Crosslinking on Physical Properties of Phenol-Formaldehyde Novolac Cured Epoxy Resins," *Journal of Applied Polymer Science*, 1993, **48**, 583.

⁴⁴ D. Chinn, S. Shim, and J. C. Seferis, "Thermal and Mechanical Characterization of High Performance Epoxy Systems with Extended Cure Times," *Journal of Thermal Analysis*, 1996, **46**, 1511.

⁴⁵ Y. N. Lin, S. Joardar, and J. E. McGrath, "Synthesis of Triphenyl Phosphine Oxide Dianhydride Monomer and High T_g Soluble Polyimides," *Polymer Preprints*, 1993, **34**, 515.

with functional groups that cure into highly crosslinked, high T_g networks at temperatures greater than 200 °C. Increasing the polymeric crosslink density has been shown to improve thermo-oxidative resistance. The use of high temperature functional groups allows for retaining the processability of these polymers, while producing a highly crosslinked network. The end-capping of rigid rod polymers with phenylethynyl groups has received much attention because phenylethynyl groups have been shown to cure at temperatures in excess of 300 °C, while producing a highly thermally stable network.^{46,}

47, 48, 49, 50, 51

McGrath et al. completed much substantial work in this area. Initially, their work focused on improving the thermal stability of polyimides through end-capping with *m*-aminophenyl acetylene.⁵² This approach produced highly crosslinked networks with excellent thermo-oxidative stability. However, the curing exotherm for the end-capping agent was observed at approximately 220 °C. This relatively low exotherm temperature limits the applicability of polyimide oligomers end-capped with *m*-aminophenyl acetylene. Using phenylethynyl aniline as an end-capping reagent, the curing exotherm

⁴⁶ R. G. Bryant, B. J. Jensen, and P. M. Hergenrother, "Synthesis and Properties of Phenylethynyl-Terminated Polyimides," *Polymer Preprints*, 1993, **34**, 566.

⁴⁷ P. M. Hergenrother, R. G. Bryant, B. J. Jensen, and S. J. Havens, "Phenylethynyl-Terminated Imide Oligomers and Polymers Therefrom," *Journal of Polymer Science Part A: Polymer Chemistry*, 1994, **32**, 3061.

⁴⁸ J. W. Connell, J. G. Smith, and P. M. Hergenrother, "Properties of Imide Oligomers Containing Pendent Phenylethynyl Groups," *High Performance Polymers*, 1997, **9**, 250.

⁴⁹ J. W. Connell, J. G. Smith, and P. M. Hergenrother, "Imide Oligomers Containing Pendent and Terminal Phenylethynyl Groups II," *High Performance Polymers*, 1998, **10**, 273.

⁵⁰ P. M. Hergenrother, J. W. Connell, and J. G. Smith, "Phenylethynyl Containing Imide Oligomers," *Polymer*, 2000, **41**, 5073.

⁵¹ I. H. Ooi, P. M. Hergenrother, and F. W. Harris, "Synthesis and Properties of Phenylethynyl. Star-Branched, Phenylquinoxaline Oligomers," *Polymer*, 2000, **41**, 5095.

⁵² T. M. Moy, C. D. DePorter, and J. E. McGrath, "Synthesis of Soluble Polyimides and Functionalized Imide Oligomers Via Solution Imidization of Aromatic Diester-Diacids and Aromatic Diamines," *Polymer (London)*, 1993, **34**, 819.

for polyimide oligomers was increased to approximately 380-450 °C.^{53, 54, 55} This enabled these oligomers to be melt processed and still produce highly crosslinked networks with high thermal stability. However, one possible issue was the toxic nature of the amine endcapping reagent. Therefore, much emphasis was also devoted to using phenylethynyl end-capping agents with reduced toxicity along with a relatively wide processing window.⁵⁶

In an effort to find a low toxicity phenylethynyl end-capping reagent, McGrath et al.^{57, 58, 59, 60} synthesized phenylethynylphthalic anhydride. Polyimide oligomers with molecular weights between 3000 and 15000 g/mole were end-capped with this reagent. An exemplary synthesis is provided in Figure 2.18. These oligomers had T_g values ranging between 258 and 340 °C before curing, and after curing, the T_g range increased to 310-362 °C. After curing the various oligomers for 90 minutes at 380 °C, all of the resulting networks displayed gel fractions between 95 and 98%. Finally, thermal stability measurements were conducted on the networks under an air purge using TGA. The 5%

⁵³ G. W. Meyer, S. Jayaraman, and J. E. McGrath, "Synthesis and Characterization of Soluble High Temperature 3-Phenylethynyl Functionalized Polyimides via the Ester-Acid Route," *Polymer Preprints*, 1993, **34**, 540.

⁵⁴ G. W. Meyer, S. J. Pak, Y. J. Lee, and J. E. McGrath, "New High-Performance Thermosetting Polymer Matrix Material Systems," *Polymer*, 1995, **36**, 2303.

⁵⁵ S. Jayaraman, G. W. Meyer, T. M. Moy, R. Srinivasan, and J. E. McGrath, "Synthesis and Characterization of 3-Phenylethynyl Endcapped Matrix Resins," *Polymer Preprints*, 1993, **34**, 513.

⁵⁶ S. Jayaraman, R. Srinivasan, and J. E. McGrath, "Synthesis of 3-Phenylethynyl Phenol," *Polymer Preprints*, 1993, **34**, 511.

⁵⁷ G. W. Meyer, T. E. Glass, H. J. Grubbs, and J. E. McGrath, "Synthesis and Characterization of Polyimides Endcapped with a Novel Phenylethynyl Endcapping Agent," *Polymer Preprints*, 1994, **35**, 549.

⁵⁸ S. J. Mecham, PhD Thesis, Virginia Tech, 1997.

⁵⁹ B. Tan, PhD Thesis, Virginia Tech, 1997.

⁶⁰ G. W. Meyer, J. Saikumar, and J. E. McGrath, "Synthesis and Characterization of Polyimides Endcapped with Phenylethynylphthalic Anhydride," *Journal of Polymer Science: Part A: Polymer Chemistry*, 1995, **33**, 2141.

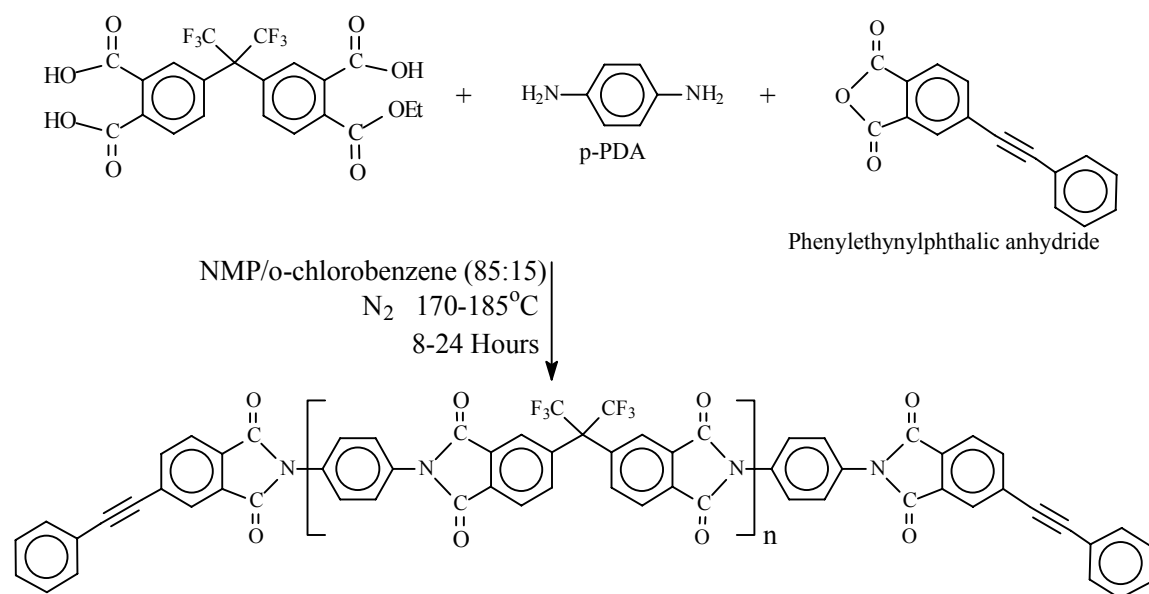


Figure 2.18: Synthesis of hexafluorinated polyimide oligomer end-capped with PEPA

weight loss at 10 °C/minute did not occur until a temperature range of 537-555 °C was reached.

In addition, poly(arylene ether phosphine oxide) copolymers were synthesized with phenylethynyl groups in pendant positions along the polymeric chain.⁵⁴ These copolymers had molecular weights between 7000 and 10000 g/mol. Upon curing at 350 °C for 30 minutes, these copolymers formed networks with T_g values between 200 and 220 °C. The gel fractions were in excess of 90 percent and the networks had good solvent resistance.

In summary, McGrath et al. were able to successfully synthesize 4-phenylethynylphthalic anhydride end-capped with pendant oligomers. This approach imparted a wide processing window which enabled the materials to be cured into highly crosslinked networks with high solvent resistance and thermo-oxidative stability.

In a similar study, Smith and Hergenrother⁶¹ synthesized polyimides with M_n values between 5000 and 9000 g/mole. These oligomers were end-capped with 4-phenylethynylphthalic anhydride (PEPA). According to DSC, the PEPA end-capped oligomers displayed curing exotherms between 382 and 390 °C.⁶¹ Films of the various oligomers were cast from solutions of NMP, were cured, and mechanical properties were measured. The average tensile strength, modulus, and elongation to break for all samples, were approximately 18.0 ksi, 430 ksi, and 45% at 23°C respectively.⁶² After exposure to water boil for 72 hours, the films were heated to 177 °C for 1 hour. Only

⁶¹ J. G. Smith and P. M. Hergenrother, "Chemistry and Properties of Phenylethynyl Phthalic Anhydride Imide Oligomers," *Polymer Preprints*, 1994, **35**, 353.

⁶² A. P. Melissaris, J. K. Sutter, M. H. Litt, D. A. Scheiman, and M. A. Shuerman, "High Modulus and High T_g Thermally Stable Polymers from *p*-Ethynyl Terminated Rigid-Rod Monomers. 2," *Macromolecules*, 1995, **28**, 860.

slight changes in mechanical properties were observed indicating good thermal stability. The average tensile strength and modulus values for the oligomers did not vary as a function of oligomer molecular weight and these values were comparable to other oligomers studied using different phenylethynyl end-capping agents. Smith and Hergenrother concluded the study by indicating that imide oligomers end-capped with 4-phenylethynyl anhydride are processable and produce tough thin films with high elongations at break.

Johnston et al.⁶³ synthesized PEPA end-capped polyimides of 3200 g/mole, 4200 g/mole and 7000 g/mole with different electron-withdrawing groups attached to the phenyl ring of PEPA. The study attempted to determine the effects of different electron-withdrawing groups bonded to the phenyl ring of PEPA on the thermo-oxidative stability and curing of the corresponding networks (Figure 2.19). Lower cure temperatures were observed using DSC for the 3200 and 7000 g/mole oligomers with electron-withdrawing groups attached to the phenyl ring of PEPA. For both oligomers, the electron-drawing groups attached to PEPA decreased the cure onset temperature by about 40 °C. After heating the different oligomers for 1 hour at 370 °C, 400 °C, and 420 °C, respectively, faster rates of increasing T_g were measured for oligomers end-capped with electron-withdrawing substituents. In particular, the nitrile-PEPA (CPEPA) and fluoro-PEPA (FPEPA) end-capped oligomers displayed the fastest rates of increasing T_g . The weight loss temperatures of the networks were measured using TGA to provide some indication of thermo-oxidative stability. No discernible difference was detected when PEPA

⁶³ J. A. Johnston, F. M. Li, and F. W. Harris, "Synthesis Characterization of Imide Oligomers End-Capped with 4-(phenylethynyl)phthalic Anhydrides," *Polymer*, 1994, **35**, 4865.

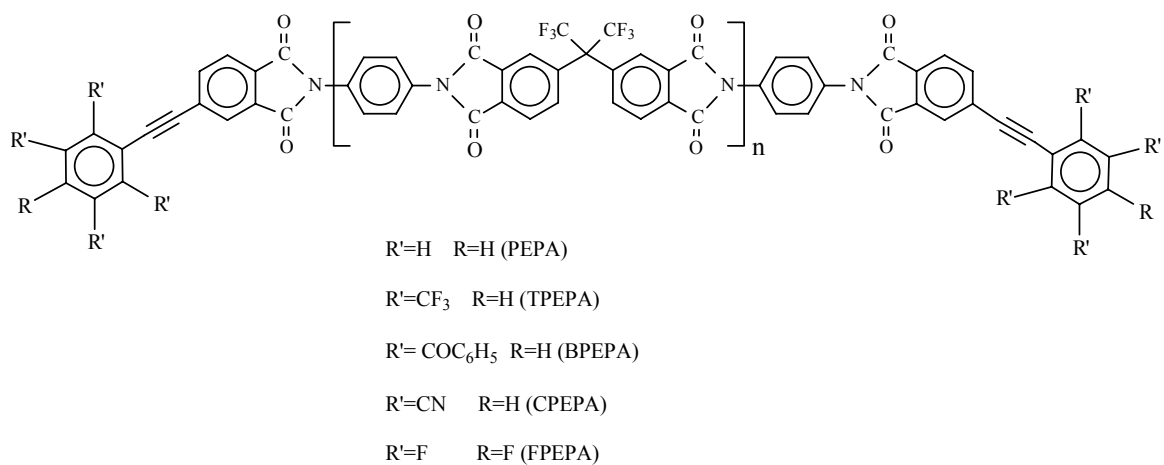


Figure 2.19: Polyimides endcapped with electron-withdrawing substituted PEPA

endcapping reagents containing electron-withdrawing substituents were used as compared to standard PEPA. 5% weight loss was shown to occur at approximately 470 °C in air and 495 °C in nitrogen for all of the networks.⁶³ The above results suggest the curing reaction of the phenylethynyl groups is enhanced by the presence of electron-withdrawing groups. However, the thermal stability of the corresponding networks remained unchanged. Other polymers in addition to polyimides have been end-capped with phenylethynyl groups to create networks with high thermo-oxidative stability and mechanical properties. Another approach to generating such networks has been to substitute rigid rod monomers with phenylethynyl groups (Figure 2.20).⁶⁴ Their curing behavior and thermo-oxidative stability was investigated using DSC, TGA, isothermal gravimetric analysis (ITGA), and TGA-IR. DSC evaluations of the curing behavior of monomers in air and nitrogen showed curing exotherms between 212 and 261 °C in nitrogen and 220 and 276 °C in air. The similarity between the curing temperatures in air and nitrogen suggests that oxygen plays little role in the curing of these monomers.⁶⁴ This was in contrast to other model studies which have shown that the rate of curing slows in the presence of oxygen.^{65, 66} The T_g values for the various networks were determined with monomer 1 (Figure 2.20) generating the highest T_g , 422 °C. The other two networks, corresponding to cured monomer 1 and 2, displayed T_g values of 329 and 380 °C. All of the networks were post-cured for 2 hours at 315 °C, however T_g values

⁶⁴ A. P. Melissaris, J. K. Sutter, M. H. Litt, D. A. Scheiman, and M. A. Shuerman, "High Modulus and High T_g Thermally Stable Polymers from *p*-Ethynyl Terminated Rigid-Rod Monomers. 2," *Macromolecules*, 1995, **28**, 860.

⁶⁵ T. V. Holland, T. E. Glass, and J. E. McGrath, "Investigation of the Thermal Curing Chemistry of the Phenylethynyl Group Using a Model Aryl Ether Imide," *Polymer*, 2000, **41**, 4965.

⁶⁶ C. C. Kuo, Y. C. Lee, and I. J. Goldfarb, "Effects of Air and Nitrogen Environment on Cure of Acetylene Terminated Resins," *Polymer Preprints*, 1982, **47**, 595.

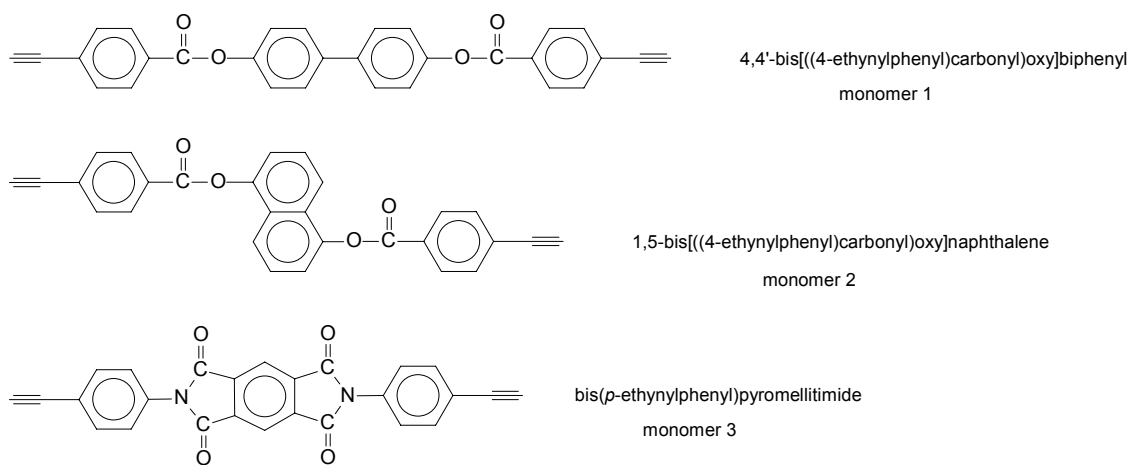


Figure 2.20: p-Ethynyl-terminated rigid-rod monomers

did not increase substantially. Surprisingly, the networks cured under nitrogen showed increases in T_g values of approximately 100 °C. TGA-IR analysis of monomers 1 and 2 determined that both monomers deteriorated in very similar fashions. 5% weight loss occurred between 500 and 630 °C for both monomers with CO₂ being the primary degradation product. The maximum degradation rate occurred at 640 °C where water and CO₂ were the main degradation products. Monomer 3 degraded somewhat differently than the other two monomers. 5% weight loss occurred at temperatures approximately 15 to 30 °C higher with small amounts of phenyl isocyanate being detected as a degradation product.

Isothermal analysis of the nitrogen post-cured networks showed that the networks from monomer 3 were the most thermally stable. These networks only lost 3% by weight after being heated for 500 hours at 288 °C. Finally, shear moduli measurements were made on the networks showed only slight decreases in moduli after being heated from 23 to 450 °C in air.⁶⁴ The group concluded that the three monomers synthesized are potential candidates for the fabrication of high strength and high thermal stability composites through solid state polymerization.

2.3.2 Maleimide and Bismaleimide End Groups

Several studies have demonstrated that phenylethynyl end groups^{46, 54, 55, 60, 61, 63, 67, 68} as end-capping agents, can produce networks with desirable thermo-oxidative stability and mechanical characteristics. One of the major drawbacks with using

⁶⁷ G. W. Meyer, T. E. Glass, H. J. Grubbs, and J. E. McGrath, "Synthesis and Characterization of Polyimides Endcapped with a Novel Phenylethynyl Endcapping Agent," *Polymer Preprints*, 1994, **35**, 549.

⁶⁸ G. W. Meyer, J. L. Heidbrink, J. G. Franchina, R. M. Davis, S. Gardner, V. Vasudevan, T. E. Glass, and J. E. McGrath, "Phenylmaleimide Endcapped Arylene Ether Imide Oligomers," *Polymer*, 1996, **22**.

phenylethynyl groups as end-cappers has been the cost associated with starting materials and catalysts. Recently, the focus has been on finding cross-linkable end-capping reagents which have comparable curing characteristics to phenylethynyl groups, but are relatively inexpensive. Maleimides, bismaleimides, and nadimides as end-capping reagents, have been of current interest because it has been shown that they have desirable curing characteristics, processability, mechanical properties, and low cost.^{69, 70, 71, 72, 73}

One focus has been on developing maleimide cross-linkable resins which have improved heat and fire resistant characteristics.⁷⁴ Bismaleamic acids of β,β' -dichloroterephthalyl dimalonitrile (DTD) were synthesized, thermally dehydrated to the corresponding imide and then cross-linked through the olefinic linkage of the maleimide (Figure 2.21). All the resins formed insoluble networks upon heating at 300 °C for 15 hours. The networks were evaluated using DTA, TGA and isothermal gravimetric analysis (ITGA). According to TGA, the various networks did not show weight loss of 5% until a temperature range of 355-389 °C was reached in either nitrogen or in air. In nitrogen, the networks generated a char yield of approximately 57-66% at 800 °C.

⁶⁹ G. D. Lyle, J. S. Senger, D. H. Chen, S. Kilic, S. D. Wu, D. K. Mohanty, and J. E. McGrath, "Synthesis, Curing and Physical Behavior of Maleimide-Terminated Poly(ether ketones)," *Polymer*, 1989, **30**, 978.

⁷⁰ A. Mathur and I. K. Varma, "Studies on Simultaneous Curing of Nadimides and Allyl Nadic-Imides and Thermal Behavior of Cured Resins," *Die Angewandte Makromolekulare Chemie*, 1993, **206**, 53.

⁷¹ K. C. Chuang, R. D. Vannucci, I. Ansari, L. L. Cerny, and D. A. Scheiman, "High Flow Addition Curing Polyimides," *Journal of Polymer Science: Part A: Polymer Chemistry*, 1994, **32**, 1341.

⁷² T. T. Serafini, P. Delvigs, and G. R. Lightsey, "Thermally Stable Polyimides from Solutions of Monomeric Reactants," *Journal of Applied Polymer Science*, 1972, **16**, 905.

⁷³ S. Alam, L. D. Kandpal, and I. K. Varma, "Co-Curing Studies of Ethynyl Terminated Oligoimide and (Methyl) Nadicimide Resins," *Journal of Thermal Analysis*, 1996, **47**, 685.

⁷⁴ J. A. Mikroyannidis, "High-Temperature Resins Obtained from Bismaleamic Acids of β,β' -Dichloroterephthalyl Dimalonitrile," *Journal of Macromolecular Science-Pure and Applied Chemistry*, 1992, **A29**, 137.

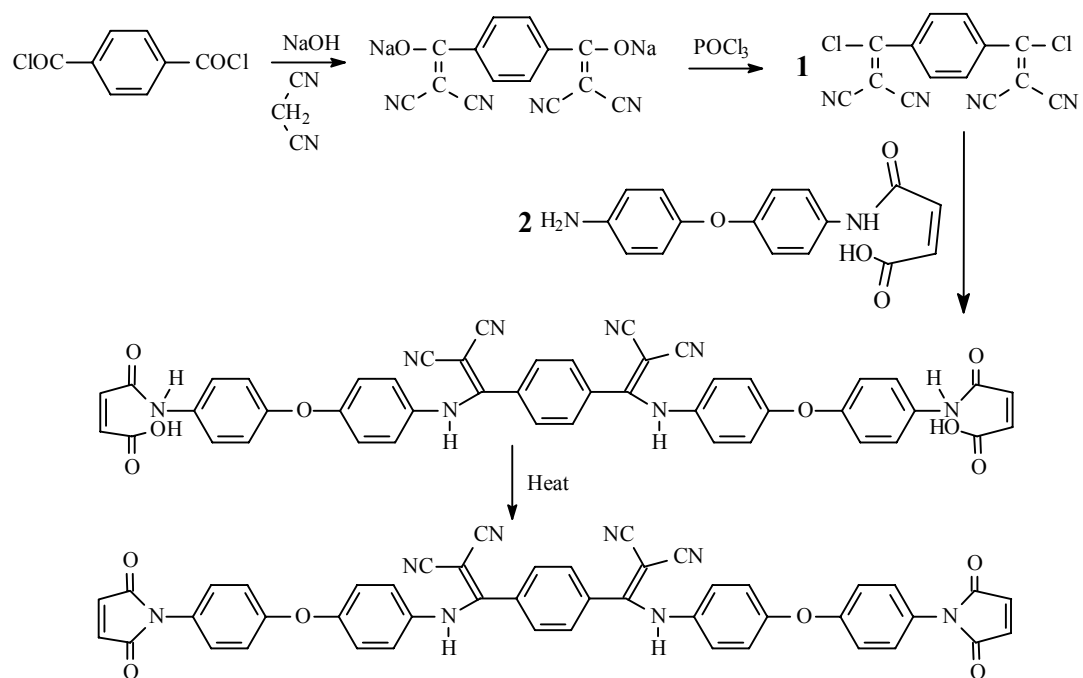


Figure 2.21: β - β' -Dichloroterephthalyl dimalonitrile synthesis and imidization

However, in air all networks were completely pyrolyzed at temperatures above 600 °C in air.

Maleimide derivatives have also been studied as end-capping reagents for arylene ether imide as well as polyimide oligomers. One of the maleimide derivatives of current interest is phenyl maleimide. It has been shown that this compound has improved thermal oxidative resistance and increased curing temperatures over maleimides. McGrath et al.⁷⁵ end-capped polyimides with phenylmaleimide and demonstrated that the curing temperature was indeed higher, 350 and 360 °C as compared to 220 °C, and thermo-oxidative resistance was improved as a result of insoluble high T_g network formation. In a similar study, synthesized poly(arylene ether imide oligomers) end-capped with the same maleimide derivative were synthesized.⁶⁸ Several oligomers with molecular weights of 2,000 and 15,000 g/mole were synthesized. An approximate 200 °C processing window between oligomer T_g and the curing exotherm was demonstrated for all of the oligomers studied. The networks were insoluble with gel contents of approximately 85% and showed an increase in T_g of 50 °C over the corresponding oligomer. Networks based on hexafluorinated dianhydride (FDA) displayed T_g values of approximately 300 °C after curing. Thermal analysis of the various FDA based networks in air did not display 5% weight loss until temperatures greater than 550 °C were reached.⁶⁸ Arylene poly(ether imide oligomers) networks from bisphenol A dianhydride and *m*-phenylene diamine displayed T_g values ranging from 215 to 230 °C. The 5% weight loss temperatures in air were not observed until temperatures greater than 500 °C

⁷⁵ T. M. Moy, M. Konas, J. E. McGrath, and E. K. Fields, "Synthesis of Soluble, Thermosetting Polyimides Derived from 1,4-Phenylenebis(phenylmaleic anhydride) and Aromatic Diamines," *Journal of Polymer Science: Part A: Polymer Chemistry*, 1994, **32**, 2377

were reached.⁶⁸ The group concluded the work by indicating that the wide processing window and good thermo-oxidative stability indicated that endcapped poly(arylene ether oligomers) were viable candidates for high performance thermosetting resins.

Curing maleimide or bismaleimide functionalized oligomers by means other than homopolymerization has been of interest^{76, 77, 78} Although many of these approaches have been successful, they have had the disadvantage of lowering the T_g values and the high temperature characteristics of the corresponding networks. Various bismaleimide (BMI) oligomers cured with allylamines were investigated.⁷⁹ 4,4'-bismaleimidodiphenylmethane (BDM), 4,4'-bismaleimidodiphenylether, 3,3'-bismaleimidodiphenylsulfone (3-BDS), and 4,4'-bismaleimidodiphenylsulfone (4-BDS) network properties were evaluated after curing with 10, 50, and 200 mole % allylamine. Of the various BMI/allylamine combinations evaluated, the 50 mole % BDM allylamine networks were observed to be the most promising because T_g values and thermo-oxidative stability were optimized.⁷⁹ This BDM/allylamine network had a T_g of 335 °C and 5% weight loss was not observed until 471 °C. The other BMI/allylamine networks with 200 mole % and 10 mole % allylamine all displayed lower T_g and flexural strength values due to a lack of curing.⁷⁹

Although bismaleimides have excellent processability and cure to form insoluble networks with high T_g values, one of the major drawbacks has been the brittle nature of

⁷⁶ M. Chaudhari, T. Galvin, and J. King, "Characterization of Bismaleimide System, XU 292," *SAMPE Journal*, 1985, **21**, 17.

⁷⁷ C. Maes, J. Devaux, R. Legras, and I. W. Parsons, "Curing of a Maleimide Model Compound," *Journal of Polymer Science: Part A: Polymer Chemistry*, 1995, **33**.

⁷⁸ H. D. Stenzenberger, "Recent Advances in Thermosetting Polyimides," *British Polymer Journal*, 1988, **20**, 383.

⁷⁹ K. Lin, J. Lin, and C.-H. Cheng, "High Temperature Resins Based on Allylamine/Bismaleimides," *Polymer*, 1996, **37**, 4729.

maleimide or bismaleimide cured networks. Therefore, some focus has been on increasing the toughness of these networks, through chain-extension of bismaleimides, without sacrificing thermo-oxidative resistance. Some of the most successful work in improving the toughness of bismaleimide networks has involved the use of diallylbisphenol A and its isomers.^{80, 81, 82} The chain-extension of bismaleimides by diallylbisphenol A has been studied fairly extensively. The chain-extension reaction is believed to result from a “ene” type reaction followed by a Diels-Alder reaction (Figure 2.22). It has also been suggested the curing reaction is the result of a series of reactions, namely homopolymerization, rearomatization, and alternating copolymerization (Figure 2.22 and Figure 2.23).^{83, 84, 85, 86, 87, 88, 89, 90, 91}

Another approach to improving the flexural strength of bismaleimide networks

⁸⁰ S. A. Zahir and A. Renner, U.S. 4,100,140 1978

⁸¹ J. J. King, M. A. Chaudari, and S. Zahir, "A New Bismaleimide System for High Performance Applications," *SAMPE Symposium*, 1984, **29**, 394.

⁸² Q. Yuan, F. Huang, and Y. Jiao, "Characterization of Modified Bismaleimide Resin," *Journal of Applied Polymer Science*, 1996, **62**, 459.

⁸³ J. C. Song and C. S. P. Sung, "Fluorescence Studies of Diaminodiphenyl Sulfone Curing Agent for Epoxy Cure Characterization," *Macromolecules*, 1993, **26**, 4818.

⁸⁴ H. J. Paik and N. H. Sung, "In-Situ Characterization of Tetrafunctional Epoxy and Composites via Fiberoptic Fluorescence," *Polymeric Materials: Science and Engineering*, 1994, **71**, 342.

⁸⁵ H. J. Paik, N. H. Sung, and C. S. P. Sung, "In-Situ Cure Monitoring of Aromatic Diamine-Epoxy System by Fiber Optic Fluorescence," *Polymer Preprints (A.C.S. Div. Poly. Chem.)*, 1991, **32**, 669.

⁸⁶ J. W. Yu and C. S. P. Sung, "Cure Characterization in Diamine-Cured Epoxy and Polyimide by UV Reflection Spectroscopy," *Macromolecules*, 1995, **28**, 2506.

⁸⁷ Y. S. Kim and C. S. P. Sung, "UV and Fluorescence Characterization of Styrene and Methyl Methacrylate Polymerization," *Journal of Applied Polymer Science*, 1995, **57**, 363.

⁸⁸ X. D. Sun and C. S. P. Sung, "Cure Characterization in Polyurethane and Model Urethane Reactions by an Intrinsic Fluorescence Technique," *Macromolecules*, 1996, **29**, 3198.

⁸⁹ K. R. Carduner and M. S. Chattha, "Carbon-13 NMR Investigation of the Oligomerization of Bismaleimidodiphenyl Methane with Diallyl Bisphenol A," *ACS Symposium Series*, 1987, **367**, 379.

⁹⁰ S. Zahir, M. A. Chaudhari, and J. King, "Novel High Temperature Resins Based on Bis(4-maleimido-phenyl)methane," *Die Makromolekulare Chemie. Macromolecular Symposia*, 1989, **25**, 141.

⁹¹ J. C. Phelan and C. S. P. Sung, "Cure Characterization in Bis(maleimide)/Diallylbisphenol A Resin By Fluorescence, FT-IR, and UV-Reflection Spectroscopy," *Macromolecules*, 1997, **30**, 6845.

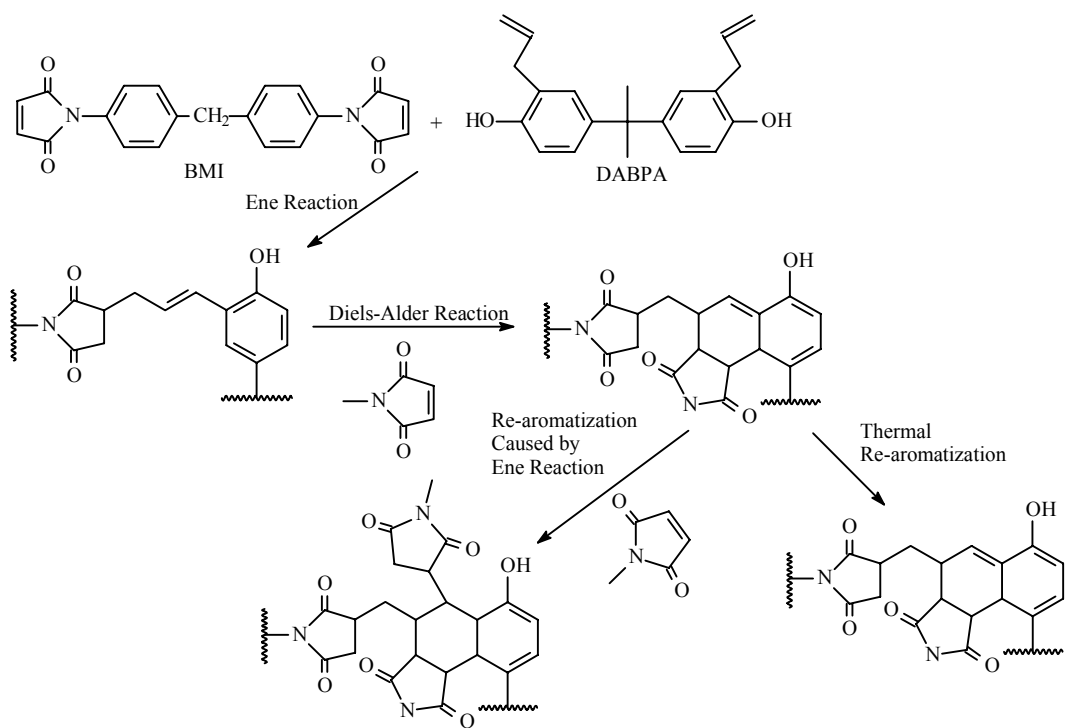


Figure 2.22: Proposed curing mechanisms for BMI/DABPA resin

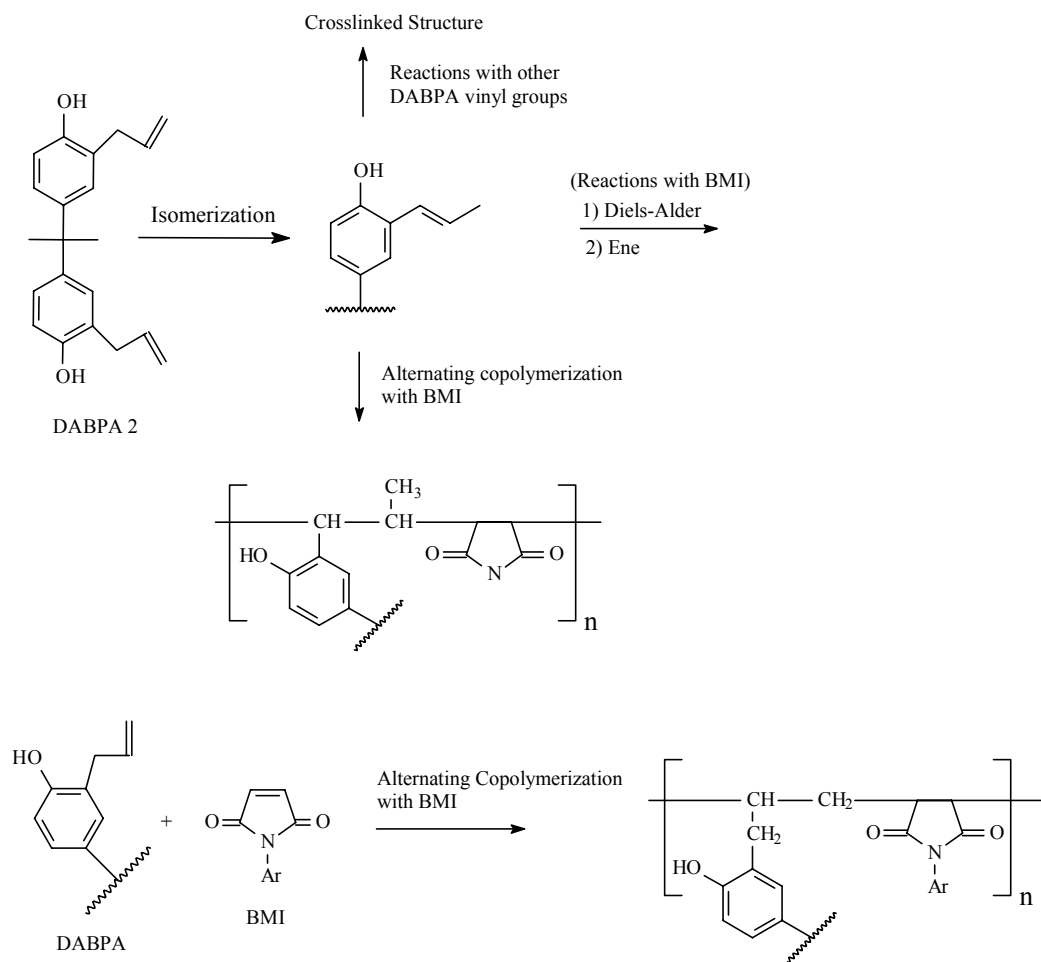


Figure 2.23: Additional reaction pathways during the curing of BMI/DABPA resin

has been to use primary amines as curing agents. It has been shown that primary amines attack maleimide double bonds in a nucleophilic fashion at low temperatures^{92, 93, 94} The nucleophilic addition of the primary amine has the effect of increasing the molecular weight between cross-links in the network, thus improving network flexural strength.⁹⁵

2.3.3 Phthalonitrile Curing Reagents

Polymeric materials with good mechanical and thermo-oxidative properties along with relative ease of processability are in high demand for use as advanced composite materials. It is well established that in order for network materials to retain high thermal stability it is necessary for these materials to have high levels of aromatic and heterocyclic ring structures within the network. The downside with incorporating such characteristics within the network has been brittleness. One approach to solving this problem has been to end-cap high temperature polymers with the curing groups mentioned above. This approach has been proven to produce networks with the desired physical properties as well as good processability. Another technique has been the use of phthalonitrile curing reagents. These reagents are of current interest because it has been demonstrated that phthalonitrile reagents cure thermally, via triazine ring formation,^{96, 97,}⁹⁸ in the presence of small amounts of curing agents (Figure 2.24).

⁹² P. Kovacic and R. W. Hein, "Cross-Linking of Polymers with Dimaleimides," *Journal of the American Chemical Society*, 1959, **81**, 1187.

⁹³ P. Kovacic and R. W. Hein, "Cross-linking of Unsaturated Polymers with Dimaleimides," *Journal of the American Chemical Society*, 1959, **81**, 1190.

⁹⁴ M. A. J. Mallet, "Polyaminobismaleimide Resins," *Modern Plastics*, 1973, **50**, 78.

⁹⁵ A. V. Tungare and G. C. Martin, "Analysis of the Curing Behavior of Bismaleimide Resins," *Journal of Polymer Science*, 1992, **46**, 1125.

⁹⁶ S. B. Sastri, J. P. Armistead, T. M. Keller, and U. Sorathia, "Flammability Characteristics of Phthalonitrile Composites," *SAMPE Symposium*, 1997, **42**, 1032.

⁹⁷ T. M. Keller, "Synthesis and Polymerization of Multiple Aromatic Ether Phthalonitriles," *Chemistry and Materials*, 1994, **6**, 302.

⁹⁸ T. M. Keller and T. R. Price, "Amine-Cured Bisphenol-Linked Phthalonitrile Resins," *Journal of Macromolecular Science-Chemistry*, 1982, **A18**, 931.

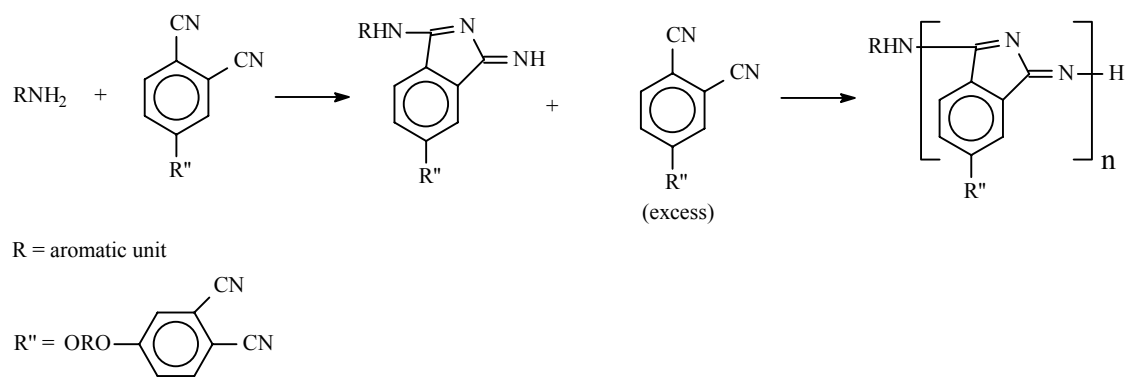


Figure 2.24: Phthalonitrile polymerization via indole formation

The networks formed are thermo-oxidatively stable with good mechanical properties and processability.^{99, 100, 101, 102}

High performance composites can be produced using phthalonitrile polymers and 1,3-bis(3-aminophenoxy)benzene (m-APB) as the curing agent. However, a significant level of volatiles has been observed during the process as a result of (m-APB) volatilization.^{103, 104, 105, 106} Also, the relatively low boiling temperature, 260-265 °C, and high reactivity of m-APB reduces the processing window for these resins due to higher processing viscosities. Recently, Keller et al.¹⁰⁷ have focused upon improving the processability of phthalonitrile polymer resins through the use of less reactive aromatic diamines which have higher boiling temperatures (in excess of 300 °C). The group evaluated the effects of three different aromatic diamines on processability and glass transition temperatures of 4,4'-bis(3,4-dicyanophenoxy)biphenyl (BPh) networks (Figure 2.25).

p-BAPS proved to be the most promising of the amines evaluated for three

⁹⁹ B. N. Achar, G. M. Fohlen, and J. A. Parker, "Synthesis and Characterization of the Novel Type of Polymerizable Bisphthalonitrile Monomers," *Journal of Polymer Science: Part A: Polymer Chemistry*, 1986, **24**, 1997.

¹⁰⁰ T. M. Keller, "Stable Polymeric Conductor," *SAMPE Symposium*, 1986, **31**, 528.

¹⁰¹ T. M. Keller and J. R. Griffith, "The Synthesis of a New Class of Polyphthalocyanine Resins," *ACS Symposium Series*, 1980, **132**, 25.

¹⁰² T. M. Keller, "Phthalonitrile-Based High Temperature Resin," *Journal of Polymer Science: Part A: Polymer Chemistry*, 1988, **26**, 3199. T. M. Keller and D. J. Moonay, "Phthalonitrile Resin for High Temperature Composite Applications," *SAMPE Symposium*, 1989, **34**, 941.

¹⁰³ S. B. Sastri, J. P. Armistead, and T. M. Keller, "Phthalonitrile-Carbon Fiber Composites," *Polymer Composites*, 1996, **17**, 816.

¹⁰⁴ T. M. Keller and C. M. Rolland, U.S. 5,242,755 1993

¹⁰⁵ S. B. Sastri, J. P. Armistead, T. M. Keller, and U. Sorathia, "Phthalonitrile-Glass Fabric Composites," *Polymer Composites*, 1997, **18**, 48.

¹⁰⁶ T. M. Keller and R. F. Katz, "High Temperature Intrinsically Conductive Polymers," *Polymer Communications*, 1987, **28**, 334.

¹⁰⁷ S. B. Sastri and T. M. Keller, "Phthalonitrile Cure Reaction with Aromatic Diamines," *Journal of Polymer Science: Part A: Polymer Chemistry*, 1998, **36**, 1885.

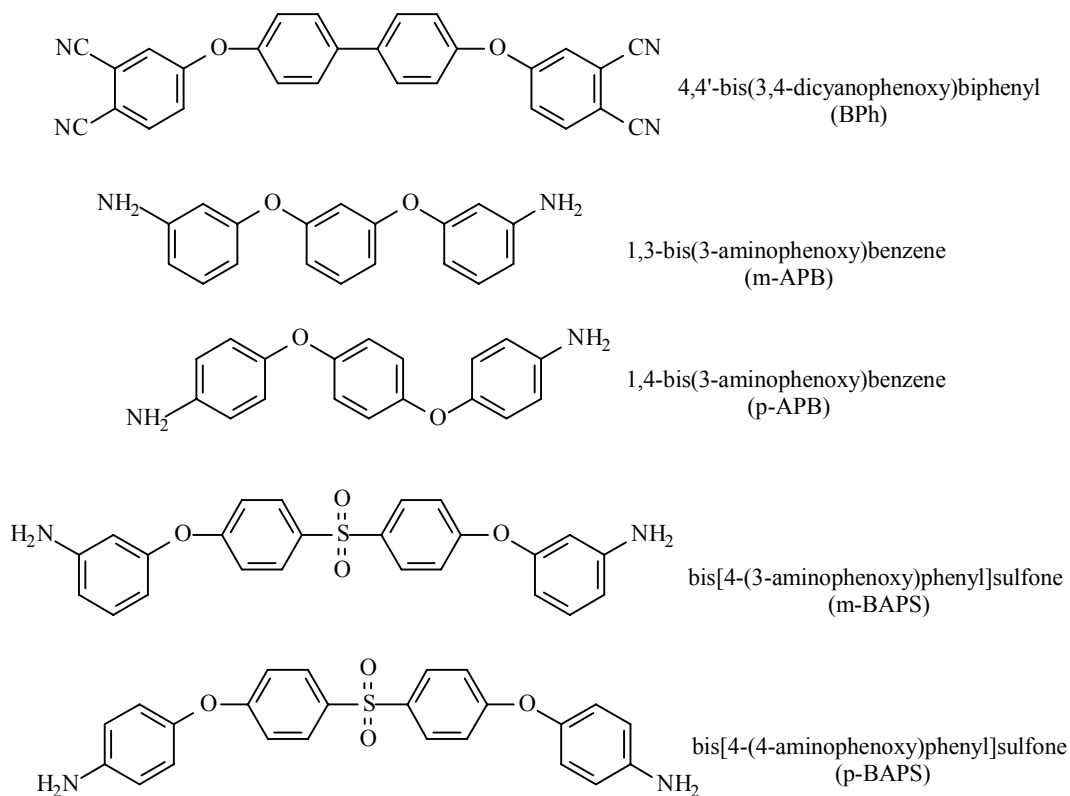


Figure 2.25: Phthalonitrile monomer and aromatic diamine curing agents

reasons. One, at temperatures of 300 °C or greater no significant volatilization of the amine was observed and two, the *p*-BAPS resins showed the widest processing window in terms of viscosity. Finally, according to $\tan \delta$ versus temperature plots *p*-BAPS resins demonstrated comparable network T_g values when compared to *m*-APB resins after being subjected to the same post-curing procedure.

A second approach employed by Keller et al. to improve the mechanical properties of phthalonitrile networks has been the evaluation of different phthalonitrile monomers.¹⁰⁸ In addition to the phthalonitrile monomer mentioned in the above study, BPh, the group evaluated two different phthalonitrile monomers, BAPh and 6FPh (Figure 2.26). The monomers were cured using the same aromatic diamine, *m*-APB. At 260 °C, the group determined the rate of viscosity increase or polymerization was dependent upon amine concentration with BAPh having the widest processing window. All of the monomers demonstrated T_g values in excess of 300 °C after being post-cured for 8 hours at 325, 350, and 375 °C. According to TGA measurements, all three networks had 5% weight loss at 450 °C in nitrogen with char yields being between 50 and 60%. In air, no char yields were observed upon heating to 800 °C with 5% weight loss values were between 500 and 600 °C. Differences between the monomers were observed upon completion of microscale calorimetric measurements. The 6FPh networks showed the lowest peak heat and total heat release rates, 7.2 J g⁻¹ K⁻¹ and 1.5 KJ g⁻¹ respectively. The group suggested the low heat release rates for 6FPh were the result of fluorocarbons

¹⁰⁸ S. B. Sastri and T. M. Keller, "Phthalonitrile Polymers: Cure Behavior and Properties," *Journal of Polymer Science: Part A: Polymer Chemistry*, 1999, **37**, 2105.

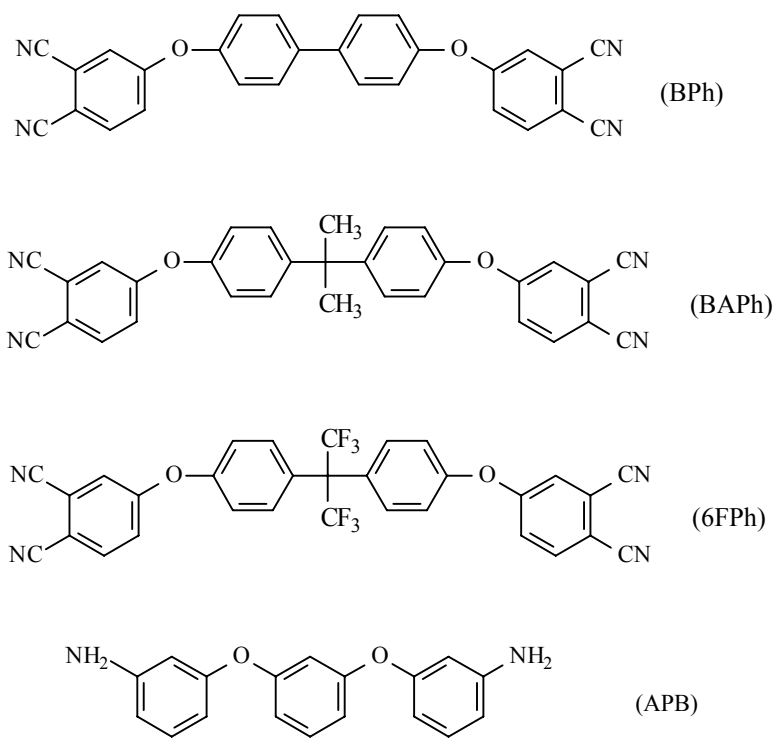


Figure 2.26: Phthalonitrile monomers and curing agent

being produced at elevated temperatures. In summary, the group pinpointed two resins that offer unique performance advantages over the previously studied resin, BPh. The BAPh resin offers a considerably wider processing window and the 6FPh resin has improved thermal characteristics in terms of energy release during burning.

One of the major drawbacks in using phthalonitrile monomers to form high temperature networks has been the extensive high temperature curing cycles these compounds require. Therefore, recent interest has been in studying nitrile functional compounds which cure at lower temperatures and still form high T_g and thermo-oxidative resistant networks. One study involved the curing and mechanical characteristics of networks derived from phthalonitrile functional polybenzoxazines.¹⁰⁹ Three different phthalonitrile functional benzoxazines were investigated in terms of curing temperature, thermal properties, and T_g (Figure 2.27). According to DSC, compounds III and IV had lower cure temperatures for the ring opening polymerization of the benzoxazines, 227-234 °C, and phthalonitrile groups, 240-250 °C than compounds I or II. The phthalonitrile curing temperatures were significantly lower than previously reported curing temperatures for phthalonitrile prepolymers.¹¹⁰ The T_g values for these networks were reported to be between 275-300 °C. This indicated a highly cross-linked network did form at the lower curing temperatures. Compound III displayed the highest level of thermal stability under nitrogen and air. Under nitrogen the char yield was 80% at 850 °C with the 5% weight loss being observed between 450 and 550 °C. Under atmospheric

¹⁰⁹ Z. Brunovska, R. Lyon, and H. Ishida, "Thermal Properties of Phthalonitrile Functional Polybenzoxazines," *Thermochimica Acta*, 2000, **357**, 195.

¹¹⁰ T. M. Keller, "Fluorinated High Temperature Phthalonitrile Resin," *Polymer Communications*, 1987, **28**, 337

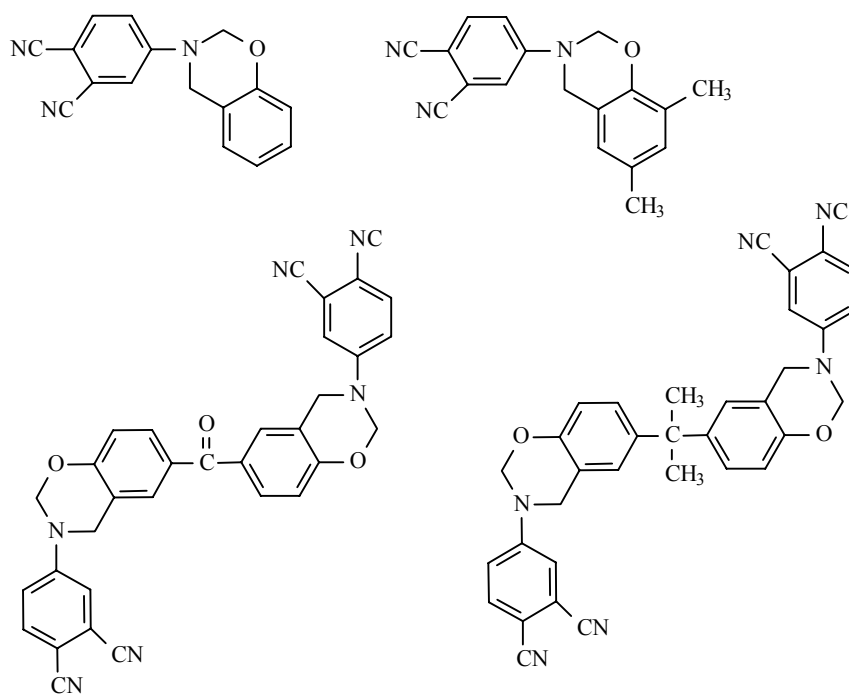


Figure 2.27: Phthalonitrile functional benzoxazine monomers

conditions 5% weight loss occurred at 500 °C with 70% residual char yield at 600 °C.

Based on TGA-FTIR analysis the high char yields for compound III were theorized to be the result of unreacted nitrile groups polymerizing at the thermal degradation temperatures. The T_g data coupled with thermal degradation characteristics indicated that high T_g and highly thermo-oxidative resistant networks can be formed using phthalonitrile functional polymers at significantly lower curing temperatures.

Over the past thirty years, network materials have been developed which have high T_g values and are thermo-oxidatively resistant. These networks form as the result of phenylethynyl, maleimide, and phthalonitrile endcapped oligomers being cured. Typically the T_g values exceed 200 °C and thermal degradation is not observed until temperatures of 400 to 500 °C are reached. These physical characteristics make these networks well suited for high temperature applications. However, the prolonged cure times and high curing temperatures many of these networks require to achieve sufficient gelation, coupled with brittleness, limits their applicability. Currently a demand exists for a network material that cures at temperatures below 250 °C to produce a high T_g material with good thermo-oxidative stability and toughness.

2.4 Cone Calorimetry

2.4.1 Introduction

Fiber-reinforced polymer composite materials (FRP) are gaining acceptance in civil and building infrastructure applications worldwide. Most FRP implementations in building structures are experimental and compliance with fire codes has either not been the focus, or this has been dealt with through application of protective coatings.

Recognizing that this is not a long term solution, this review seeks to summarize the general state of knowledge in the area of FRP composites and their response to fire conditions. With the polymer as the primary concern, there is a clear correlation between the matrix material and the resistance and response to damaging heat flux. Glass transition temperatures for commercially available matrix materials are typically 120-400 °C; no match for the higher temperatures observed in realistic fire situations. In order to simulate realistic fire situations matrix materials are evaluated using the cone calorimeter. (Figure 2.28) The cone calorimeter applies a constant heat flux to the surface of a 4 in by 4 in by 0.25 in sample and constantly sparks until the sample ignites. Once ignited the instrument then measures the amount of char, CO:CO₂ evolution, heat released, and various gases generated by the sample. Based on these measurements fire resistance is designed into these materials through one of two methods: (1) A gas phase mechanism whereby gaseous decomposition products inhibit approach of oxygen to the flame, and (2) Via char formation.

2.4.2 Flame Properties of Aliphatic Polymeric Matrices

Cone calorimetry can provide information on burning rate (indicated by the peak in the heat release rate and the average heat release rate) and char formation.^{111, 112, 113, 114}

While there is limited experience from which to specify polymer matrix composites in

¹¹¹ J. H. Koo, S. Venumbaka, P. E. Cassidy, J. W. Fitch, and A. F. Grand, "Flammability Studies of Thermally Resistant Polymers Using Cone Calorimetry," *Journal of Fire and Materials*, 2000, **24**, 209.

¹¹² F. Y. Hsieh, and R. R. Buch, "Controlled-atmosphere Cone Calorimeter Studies of Silicones," *Fire and Materials*, 1997, **21**, 265.

¹¹³ Commission on Engineering and Technical Systems, National Materials Advisory Board, Fire and Smoke-Resistant Interior Materials for Commercial Aircraft Interiors, Vol.NMAB-477-1 National Academy Press, Washington, D.C., **1995**.

¹¹⁴ U. Sorathia, R. Lyon, T. Ohlemiller, and A. Grenier, "A Review of Fire Test Methods and Criteria for Composites," *SAMPE Journal*, 1997, **33**, 23.

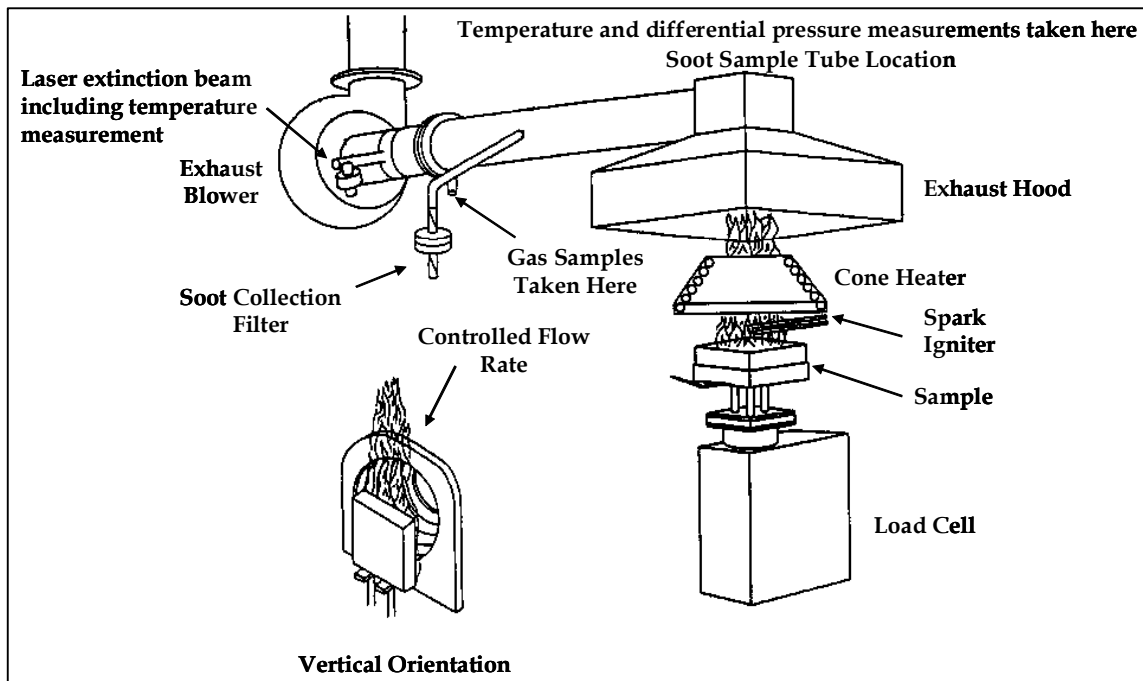


Figure 2.28: Cone calorimeter

fire critical areas¹¹⁴, the performance of various classes of fiber/polymer composites have been studied or at least screened.^{115, 116} Halogenated polymers burn relatively slowly due to the gas phase mechanism (Figure 2.29 and Figure 2.30), but such materials do not necessarily form high char yields. One major detraction when considering halogenated materials, however, is that dense smoke usually results upon burning, and in at least several cases, the concentrations of toxic carbon monoxide are unusually high. One can note at least an order of magnitude improvement in burning rates (i.e., lower PHHR) for all of the halogenated polymers vs. non-halogenated materials. For example, oligomers from tetrabromobisphenol A and epichlorohydrin provide the base materials for commercial flame retardant vinyl esters and epoxies. Flame retardant vinyl ester resins are typically blends of brominated with non-brominated oligomers diluted with styrene. Networks from such compositions have relatively slow burning rates but they typically only exhibit about 9 weight percent char^{117, 118, 119} Brominated epoxies or vinyl esters upon burning evolve high concentrations of toxic carbon monoxide.

2.4.3 Flame Properties of Aromatic Polymeric Matrices

Polymers with highly aromatic chemical structures in their backbones are flame

¹¹⁵ U. Sorathia, and C. Beck, Fire-Screening Results of Polymers and Composites, Vol.NMAB-477-2 National Academy Press, Washington, D.C., **1995**.

¹¹⁶ U. Sorathia, and T. Dapp, "Structural Performance of Glass/Vinyl Ester Composites at Elevated Temperatures," *SAMPE Journal*, 1997, **33**, 53.

¹¹⁷ J. S. Riffle Unpublished Results, **2002**.

¹¹⁸ M. M. Hirschler, "How to Measure Smoke Obscuration in a Manner Relevant to Fire Hazard Assessment: Use of Heat Release Calorimetry Test Equipment," *Journal of Fire Science*, 1991, **9**, 183.

¹¹⁹ F. Y. Hsieh, and H. D. Beeson, "Flammability Testing of Flame-retarded Epoxy Composites and Phenolic Composites," *Fire and Materials*, 1997, **21**, 41.

Polymer	Flame Performance	
	Time to Ignition	PHHR
Polytetrafluoroethylene	No ignition	13 kW/m²
Poly(vinyl chloride)	85 sec.	183 kW/m²
Polystyrene	97 sec.	1101 kW/m²
Nylon 6,6	65 sec.	1313 kW/m²

Figure 2.29: Flame properties from cone calorimetry (measured at an incident heat flux of 40 kW/m²) of halogenated vs. non-halogenated aliphatic polymers.

Polymer	Flame Performance			
	Incident Heat Flux	Time to Ignition	PHHR	Char
Ultem polyetherimide	50 kW/m²	160 sec.	128 kW/m²	79%
Poly(dimethylsiloxane-b-etherimide)	50 kW/m²	97 sec.	210 kW/m²	32%
Fluorine-containing PEEK	50 kW/m²	138 sec.	87 kW/m²	25%
Polysulfone (UDEL)	40 kW/m²		170 kW/m²	
	50 kW/m²	126 sec.	431 kW/m²	56%
	70 kW/m²		310 kW/m²	

Figure 2.30: Cone calorimetry data for flame retardant polyimides and poly(arylene ether)s

resistant due to formation of substantial char upon pyrolysis (Figure 2.31).^{111, 120, 121}

Polymers with aromatic backbones comprised of “ladder” structures, exemplified by the aromatic polyimides, also exhibit these properties. This is undoubtedly related to the fact that these materials lack thermally labile, aliphatic C-H bonds in the polymer backbones, and are thus inherently more thermally stable. Moreover, the aromatic rings lead to char, which may be important for forming protective surface layers during the pyrolysis process. Quantification of this aspect will require a better understanding of the behavior of these materials during pyrolysis.

Although it is known that aromatic polymers such as those described in Figure 2.31 have good flame retardance, these materials can be expensive, and this detracts from their desirability for composite components in construction and infrastructure. The military and civilian aircraft communities have developed methods to functionalize aromatic polyimides and poly(arylene ether)s with thermally stable, crosslinkable terminal groups (e.g., phenylethynyl functional oligomers)^{58, 67, 56, 122}, which could provide processible, corrosion resistant, flame resistant, polymer composite matrices. Such materials have not really been considered as construction materials due to their potential costs, but this may be attractive for flame resistant components.

Structural polymer matrix composites are typically comprised of about 60 volume

¹²⁰ Y. Liu, A. Bhatnagar, Q. Ji, J. S. Riffle, J. E. McGrath, J. F. Geibel, and T. Kashiwagi, "Influence of polymerization conditions on the molecular structure, stability, and physical behavior of poly(phenylene sulfide sulfone) homopolymers," *Polymer*, 2000, **41**, 5137.

¹²¹ D. J. Riley, A. Gungor, S. A. Srinivasan, M. Sankarapandian, C. Tchatchoua, M. W. Muggli, T. C. Ward, and J. E. McGrath, "Synthesis and Characterization of Flame Resistant Poly(Arylene Ether)s," *Polymer Engineering and Science*, 1997, **37**, 1501.

¹²² G. W. Meyer, B. Tan, and J. E. McGrath, "Solvent-resistant Polyetherimide Network Systems via Phenylethynylphthalic Anhydride Endcapping," *High Performance Polymers*, 1994, **6**, 423.

Matrix Materials for Construction and Infrastructure Resin Flame Performance

	Time to Ignition	PHHR	CO/CO ₂	Char
Unsaturated polyester-styrene	53 sec.	710 kW/m ²	0.025	13%
Vinyl ester-styrene	69 sec.	619 kW/m ²	0.028	11%
Epoxy-DDS		1230 kW/m ²	0.04	5%
Phenolic	272 sec.	124 kW/m ²	0.02	54%
Phenolic Resole		116 kW/m ²	0.01	65%
Phenolic-epoxy (65:35 wt:wt)	75 sec.	263 kW/m ²	0.02	26%
Phenolic-phthalonitrile (85:15 wt:wt)	102 sec.	137 kW/m ²	0.02	54%
Polysiloxane network	45 sec.	80 kW/m ²	0.02	

Figure 2.31: Flame properties of thermoset polymer matrices for composites measured by cone calorimetry with an incident heat flux of 50 kW/m² (PHHR is peak heat release rate)

percent fiber and 40 volume percent of the polymer matrix. Fibers utilized in applications requiring flame resistance are limited to carbon and glass, both of which exhibit excellent performance in a fire.¹²³

Thermosetting polymer matrix materials suitable for structural applications can be classified in terms of their thermal performance (Table 2.2), which often parallels their applications (and price). The vinyl ester and unsaturated polyester matrix materials are utilized to produce rapidly manufactured parts for construction and infrastructure. Their free radical curing mechanism and low viscosities make them ideal for pultrusion or low temperature VARTM processing. The resultant networks are highly crosslinked which leads to good environmental and corrosion resistance, and the materials are inexpensive. Unfortunately, unless they are halogenated, they lack flame resistance and residual integrity, and pose a health threat in enclosed spaces. It is clear from the flammability tests that these materials are not the most desirable systems in that regard (Figure 2.31). Phenolic novolac or resole networks have inherently low flame-spread, slow burning rates, and the materials are cost-effective.¹²⁴ They are highly aromatic and also have hindered phenol units along the backbones, which may effectively protect the materials through oxygen scavenging. The viscosities and curing chemistries for undiluted phenolic resins, however, do not allow fabrication of void-free composites by methods typically used for manufacturing construction components (i.e., pultrusion or VARTM).

¹²³ J. R. Brown, and Z. Mathys, "Reinforcement and matrix effects on the combustion properties of glass reinforced polymer composites," *Composites, Part. A*, 1997, **28A**, 675.

¹²⁴ U. Sorathia, T. Ohlemiller, R. Lyon, J. S. Riffle, and N. Schultz (2001). Effects of Fire, Chapter 9 in Gap Analysis for Durability of Fiber Reinforced Polymer Composites in Civil Infrastructure, Civil Engineering Research Foundation: 100.

Table 2.2: Current applications of moderate and high glass transition thermosetting polymer matrix systems

System	T_g (°C)	Current Applications
Vinyl esters-styrene Unsaturated polyesters-styrene Low temperature epoxies Phenolics	120 – 160	Civil engineering (e.g. construction, infrastructure, automotive, ships)
Cyanates	260	Electronic materials, adhesives and matrices, civilian aircraft
High modulus epoxies	240	Military
Functionalized poly(arylene ether)s	200-280	Tougheners, military
Functionalized polyimides Phthalonitriles	200-400	Aerospace, electronic

Conventional thermal curing of resole oligomers evolves water and produces voids in the composites which detract from structural properties. One approach to overcome some of these issues is to cure novolac resins with epoxy or even phthalonitrile crosslinking reagents.^{125, 126, 127, 128, 129} Some of these matrices have excellent structural properties combined with good fire resistance.

Finally, several extremely fire resistant thermosetting resins have been developed and studied by the Navy, including bis-phthalonitrile matrices.¹³⁰ These materials must be cured slowly at elevated temperatures, but indeed have extremely good flame properties. However, these materials currently have limited commercial utility due to their high cost.

¹²⁵ C. S. Tyberg, Ph.D. Thesis, Virginia Tech, **1999**.

¹²⁶ C. S. Tyberg, K. Bergeron, M. Sankarapandian, P. Shih, A. C. Loos, J. E. McGrath, D. A. Dillard, and J. S. Riffle, "Structure-Property Relationships of Void-Free Phenolic-Epoxy Matrix Materials," *Polymer*, 2000, **41**, 5053.

¹²⁷ C. S. Tyberg, M. Sankarapandian, K. Bears, P. Shih, A. C. Loos, D. Dillard, J. E. McGrath, J. S. Riffle, and U. Sorathia, "Tough, Void-Free, Flame Retardant Phenolic Matrix Materials," *Construction and Building Materials*, 1999, **13**, 343.

¹²⁸ C. S. Tyberg, P. Shih, K. N. E. Verghese, A. C. Loos, J. J. Lesko, and J. S. Riffle, "Latent Nucleophilic Initiators for Melt Processing Phenolic-Epoxy Matrix Composites," *Polymer*, 2000, **41**, 9111.

¹²⁹ M. J. Sumner, M. Sankarapandian, J. E. McGrath, J. S. Riffle, and U. Sorathia, "Synthesis and Physical Property Characterization of Novolac/Biphenoxyphtalonitrile Networks," *SAMPE Journal*, 2001, **33**, 1509.

¹³⁰ T. M. Keller, and T. R. Price, "Amine-Cured Bisphenol-Linked Phthalonitrile Resins," *Journal of Macromolecular Science - Chemistry*, 1982, **A18**, 931.

Chapter 3: Synthesis of 4,4'-Bis(3,4-dicyanophenoxy)biphenyl (biphenoxyphtalonitrile)

3.1 Introduction

Polymer matrix composites are envisioned to be effective alternatives to concrete and steel in many civil structures due to their high strength to weight ratio and environmental stability. In fact, due to these attractive properties, polymeric graphite reinforced composites have become the dominant material in many of today's high performance missile and aircraft structures.¹³¹ However, in the construction and aerospace industries the primary factors limiting further applications of polymeric composites are cost, high combustibility and limited high temperature application (application window < 200 °C)

Keller et al. have demonstrated that neat phthalonitrile networks can be synthesized via curing with a small amount (1 to 3 mole %) of an aromatic diamine or phenolic. These networks have very high T_g values ($\geq 300^\circ\text{C}$) and excellent thermooxidative stability.^{131, 132, 133, 134, 135, 136, 137, 138, 139, 140, 141, 142, 143, 144} Fire testing has also demonstrated their outstanding characteristics in composites.¹⁴⁵

¹³¹ S. B. Sastri, T. M. Keller, "Phthalonitrile Polymers: Cure Behavior and Properties," *Journal of Polymer Science: Part A: Polymer Chemistry*, **37**, 1999, 2105.

¹³² T. M. Keller, "Stable Polymeric Conductor," *SAMPE Symposium*, **31**, 1986, 528.

¹³³ T. M. Keller, "Fluorinated High Temperature Phthalonitrile Resin," *Polymer Communications*, **28**, 1987, 337.

¹³⁴ T. M. Keller, "Phthalonitrile-Based High Temperature Resin," *Journal of Polymer Science: Part A: Polymer Chemistry*, **26**, 1988, 3199.

¹³⁵ T. M. Keller, "Synthesis and Polymerization of Multiple Aromatic Ether Phthalonitriles," *Chemistry and Materials*, **6**, 1994, 302.

¹³⁶ T. M. Keller, J. R. Griffith, "The Synthesis of a New Class of Polyphthalocyanine Resins," *ACS Symposium Series*, **132**, 1980, 25.

¹³⁷ T. M. Keller, D. J. Moonay, "Phthalonitrile Resin for High Temperature Composite Applications," *SAMPE Symposium*, **34**, 1989, 941.

¹³⁸ T. M. Keller, T. R. Price, "Amine-Cured Bisphenol-Linked Phthalonitrile Resins," *Journal of Macromolecular Science-Chemistry*, **A18**, 1982, 931.

The attractive physical characteristics of the phthalonitrile crosslinked networks are sometimes overshadowed by the high cost of phthalonitrile reagents. Currently, phthalonitrile reagents are not commercially available which makes the supply of these materials virtually nonexistent. The lack of supply drives the cost of these reagents to levels that are not economically feasible (Figure 3.1). The laboratory price for phthalonitrile reagents is approximately 1\$ per gram which is far too high for the composites industry. This lack of cost effectiveness has prevented the rapid development of these materials as matrix components in carbon-fiber composites.

A new four step synthetic scheme has been developed for biphenoxyphthalonitrile to potentially reduce the cost of phthalonitrile reagents (Figure 3.2). Each step utilized inexpensive reagents to produce the desired intermediates and ultimately biphenoxyphthalonitrile in good yield. The products formed from each step were of high enough purity that purification was minimal. Demonstrating that biphenoxyphthalonitrile can be synthesized inexpensively may potentially reduce the economic penalties associated with these materials.

¹³⁹ S. B. Sastri, T. M. Keller, "Phthalonitrile Cure Reaction with Aromatic Diamines," *Journal of Polymer Science: Part A: Polymer Chemistry*, **36**, 1998, 1885.

¹⁴⁰ T. M. Keller, R. F. Katz, "High Temperature Intrinsically Conductive Polymers," *Polymer Communications*, **28**, 1987, 334.

¹⁴¹ T. M. Keller, C. M. Rolland, U.S. Patent 5,242,755 (1993).

¹⁴² S. B. Sastri, J. P. Armistead, T. M. Keller, "Phthalonitrile-Carbon Fiber Composites," *Polymer Composites*, **17**, 1996, 816.

¹⁴³ S. B. Sastri, J. P. Armistead, T. M. Keller, U. Sorathia, "Phthalonitrile-Glass Fabric Composites," *Polymer Composites*, **18**, 1997, 48.

¹⁴⁴ S. B. Sastri, J. P. Armistead, T. M. Keller, U. Sorathia, "Flammability Characteristics of Phthalonitrile Composites," *SAMPE Symposium*, **42**, 1997, 1032.

¹⁴⁵ I. Caplan, U. Sorathia, C. Rollhauser, "US Navy R&D Programs in Fire Performance of Materials," *SAMPE Journal*, **32**, 1996, 21.

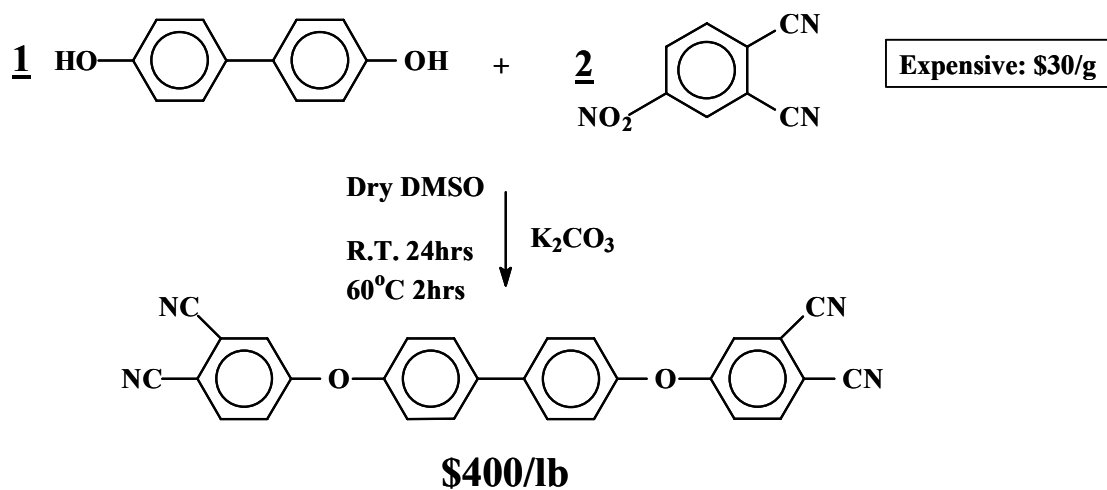


Figure 3.1: Synthesis of biphenoxyphthalonitrile

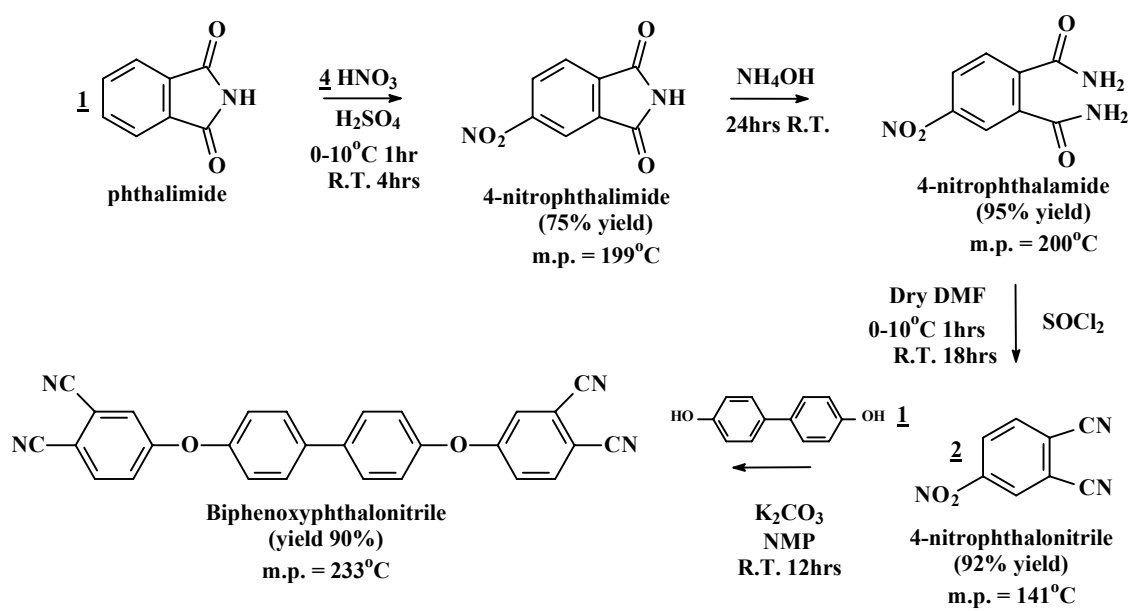


Figure 3.2: Four step synthetic scheme for biphenoxyphthalonitrile

3.2 Experimental

3.2.1 Materials

The following materials were purchased from Aldrich and used as received: formamide(98%), thionyl chloride, dimethyl formamide(99%), phthalimide, K_2CO_3 , and 4,4'-biphenol. The following materials were purchased from Fischer Scientific and used as received: HNO_3 (70%), H_2SO_4 (98%), NH_4OH . NMP was purchased from Fisher-Scientific and dried for 24 h over CaH_2 , distilled under vacuum, and collected over molecular sieves.

3.2.2 Synthesis of 4-Nitrophthalimide

Phthalimide (30 g, 0.204 mol) was added to a 320 mL mixture of concentrated H_2SO_4 and 70% HNO_3 (6:1 v/v) at 0-10 °C. The solution was allowed to slowly warm to room temperature and held for 4 h. The solution was added to ice water and stirred. The 4-nitrophthalonitrile crystallized and precipitated out of the ice water. The product was collected by vacuum filtration, washed with ice cold water, and air dried overnight; yield: 31.5 g (80%) m.p.: 199 °C (det. by DSC)

1H NMR($(CD_3)_2SO$): 8.05 (dd, 1H), 8.40 (d, 1H), 8.60 (dd, 1H), 11.80 (s, 1H)

3.2.3 Synthesis of 4-Nitrophthalamide

4-Nitrophthalonitrile (57.9 g, 0.300 mol) was added to NH_4OH (33%) (200 mL) with stirring to form a yellow suspension. The suspension was allowed to react for 24 h at room temperature. A yellow precipitate, 4-nitrophthalamide, was collected using vacuum filtration, washed with ice cold water, and air dried overnight; yield: 60.1 g (95%); m.p.: 199 °C (det. by DSC)

^1H NMR($(\text{CD}_3)_2\text{SO}$): 7.60 (s, 2H), 7.68 (dd, 1H), 7.98 (s, 1H), 8.04 (s, 1H), 8.26 (dd, 1H), 8.30 (dd, 1H)

3.2.4 Synthesis of 4-Nitrophthalonitrile

SOCl_2 (83.5 mL, 1.144 mol) was added dropwise under nitrogen purge to dry DMF (200 mL) which had been cooled to 0-5 °C. The solution was allowed to stir for 15 min at 0-5 °C. The 4-nitrophthalamide (60.1 g, 0.286 mol) was then added and the solution was allowed to slowly warm to room temperature and react for 18 h under nitrogen purge. The solution was then slowly added to ice water to crystallize and precipitate the product. The 4-nitrophthalonitrile was collected using vacuum filtration, washed with ice cold water, and allowed to air dry overnight; yield: 45.2 g (92%); m.p.: 141 °C (det. by DSC)

^1H NMR($(\text{CD}_3)_2\text{SO}$): 8.41 (dd, 1H), 8.67 (dd, 1H), 9.03 (dd, 1H)

FTIR: 3091 (m, aromatic C-H stretch), 2242 (d, CN stretch), 1534 (s, asymmetric N=O stretch), 1349 (s, symmetric N=O stretch), 853 (s, C-N stretch)

3.2.5 Synthesis of 4,4'-Bis(3,4-dicyanophenoxy)biphenyl (biphenoxypthalonitrile)

4,4'-Biphenol(**5**) (20 g, 0.107 mol), 4-nitrophthalonitrile (37.2 g, 0.215 mol), and K_2CO_3 (35.49 g, 0.257 mol) were charged to a one neck round bottom flask. Approximately 50 mL of dry NMP was added to the reagents while stirring. The reagents were allowed to react for 24 h at 27 °C. The biphenoxypthalonitrile was precipitated by adding the NMP solution to ice cold H_2O forming a cloudy orange solution. Sodium chloride was added until biphenoxypthalonitrile precipitated out of

solution. The biphenoxyphthalonitrile was collected via vacuum filtration and air dried overnight; yield: 0.90 g (90%); m.p.: 234 °C (det. by DSC)

^1H NMR($(\text{CD}_3)_2\text{SO}$): 7.30 (dd, 4H), 7.45 (dd, 2H), 7.80 (dd, 4H), 7.85 (dd, 4H), 8.10 (dd, 2H)

FTIR: 3104 (m, aromatic C-H stretch), 2232 (s, CN stretch), 1251 (s, C-O-C asymmetric stretch), 1008 (s, C-O-C symmetric stretch), 1598 and 1490 (s, C=C stretch)

3.3 Measurements

3.3.1 Differential Scanning Calorimetry (DSC)

Differential scanning calorimetry (DSC) was used to determine the melting points of the compound synthesized in this study. These measurements were performed using a TA differential scanning calorimetry, model Q1000. Approximately 2 to 3 milligrams of each sample were heated over an approximate temperature of 100 to 250 °C at a heating rate of 0.5 °C per minute. TA Universal Analysis software was used to calculate the melting points of the samples.

3.3.2 Proton Nuclear Magnetic Resonance (^1H NMR)

^1H NMR was collected on a Varian Unity 400 MHz instrument with a frequency of 399.954 MHz. A 22° pulse angle was used with an acquisition time of 3.7s and a recycle delay of 1s. d_6 -DMSO was used as the NMR solvent.

3.3.3 Fourier Transform Infrared Spectroscopy (FTIR)

The FTIR spectra of 4-nitrophthalonitrile and biphenoxyphthaonitrile were collected by first dissolving the compounds in acetone then adding a few drops of each solution to the surface of a NaCl plate. The acetone was allowed to evaporate leaving

small crystals of each compound on the surface of the NaCl plate. The FTIR spectra of the two compounds were then collected using a Nicolet Impact 400 spectrometer. The various stretches relating to the structures of 4-nitrophthalonitrile and biphenoxyphthalonitrile were determined using Omnic FTIR software.

3.4 Results and Discussion

3.4.1 Synthesis of 4-Nitrophthalimide

Step 1 in Figure 3.2 involved the electrophilic aromatic nitration of phthalimide using a $\text{H}_2\text{SO}_4/\text{HNO}_3$ solution at 6 to 1 volumetric ratio of sulfuric acid to nitric acid.¹⁴⁶
¹⁴⁷ The solution was formed by cooling the H_2SO_4 to ice bath temperatures and then adding the appropriate amount of HNO_3 . The solution was cooled to avoid any delayed exotherm. Upon adding the phthalimide the solution was allowed to warm to room temperature and react for 4 hours. During this time the solution turned an orangish-yellow color and increased in temperature to $\sim 50^\circ\text{C}$. The solution remained at $\sim 50^\circ\text{C}$ for ~ 1 h before cooling to room temperature. After reacting for 4 h at room temperature, the solution was added slowly to ice water and stirred. Upon stirring, the product, 4-nitrophthalimide, crystallized and precipitated out of solution. The compound was collected by vacuum filtration, washed with ice water, and allowed to air dry overnight. The desired product was synthesized in good yield $\sim 80\%$.

The ^1H NMR spectrum of the compound displayed 4 proton signals (Figure 3.3).

¹⁴⁶ F. J. Williams, P. E. Donahue, "Nitration of N-alkylphthalimides," *Journal of Organic Chemistry*, **43**, 1978, 1608.

¹⁴⁷ J. G. Young, W. Onyebuagu, "Synthesis and Characterization of Di-disubstituted Phthalocyanines," *Journal of Organic Chemistry*, **22**, 1990, 2155.

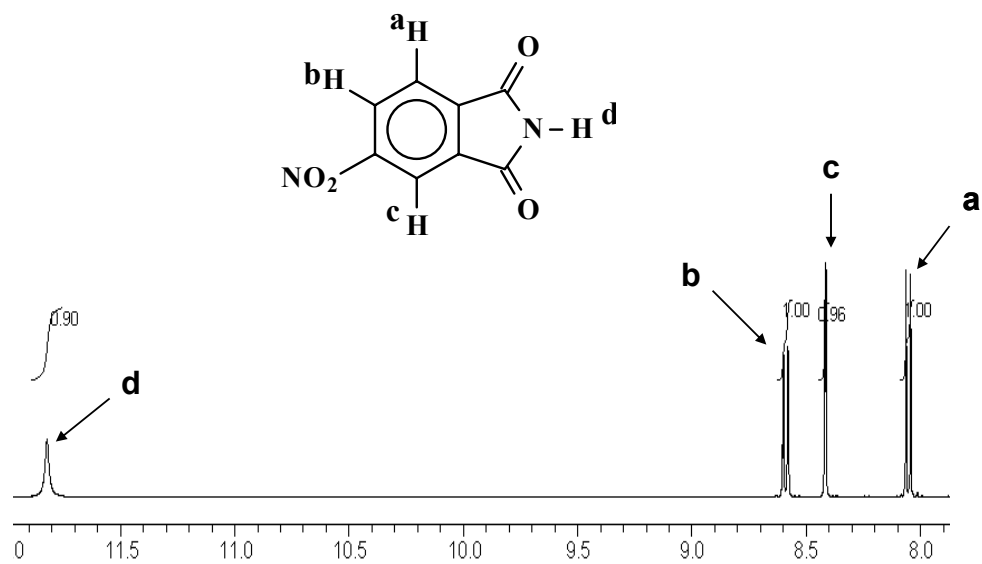


Figure 3.3: ^1H NMR of 4-nitrophthalimide

At 8.05 ppm, proton a, a doublet of doublets was observed which upon integration was equal to 1. Being the furthest upfield indicates that proton a is meta to the strong electron withdrawing nitro group. Therefore, proton a is located in the 6-position on the aromatic ring of 4-nitrophthalimide. Proton c appears at 8.4 ppm as a doublet and integrates to a value of ~1. The very small splitting which results in the doublet indicates that the proton related to this signal does not have protons located in either of its ortho positions. Therefore, it was concluded that the nitration occurred in the 4 position and proton c is located in the 3 position.¹⁴⁸

Proton b appears as a doublet of doublets with the largest splitting and chemical shift values of the 3 protons on the aromatic ring. The chemical shift and splitting values for proton b indicate that this proton is located ortho to the nitro group and has a proton in the meta and ortho positions relative to its location. Proton d appears as a broad singlet at 11.8 ppm with an integration value of ~1. The position of this proton has shifted slightly downfield by ~0.5 ppm indicating that this proton has been deshielded by the presence of an electron withdrawing group. Finally, the ratio of protons a:b:c:d is equal to 1:1:1:4 which is consistent with the molecular structure of 4-nitrophthalimide.

DSC indicated that 4-nitrophthalimide was indeed synthesized as evidenced by its melting point (Figure 3.4). Its melting point was determined to be 199 °C which is very close to the literature melting point value of 195 °C.¹⁴⁷

3.4.2 Synthesis of 4-Nitrophthalimide

4-nitrophthalimide was synthesized with high efficiency, 95% yield, by creating a

¹⁴⁸ R. D. George, A. W. Snow, "Synthesis of 3-nitrophthalonitrile and Tetra-alpha-substituted Phthalocyanines," *Journal of Heterocyclic Chemistry*, **32**, 1995, 495.

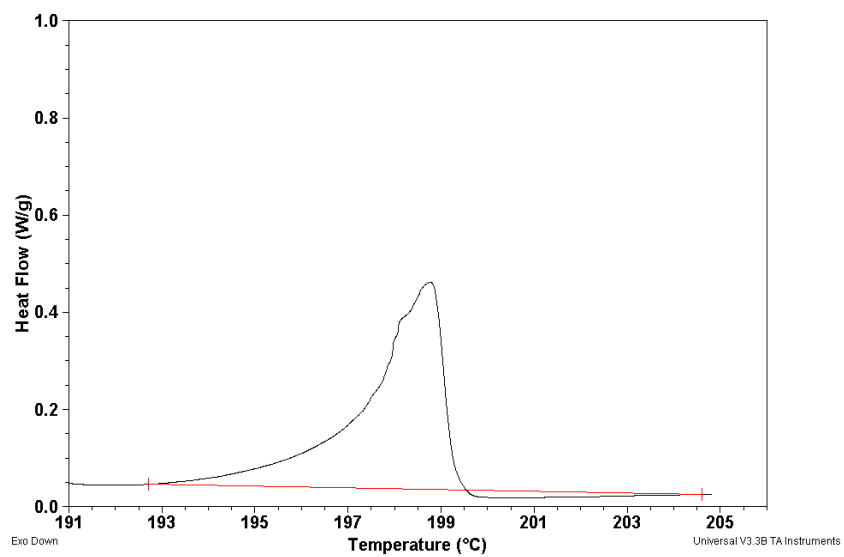


Figure 3.4: Melting point range of 4-nitrophthalimide determined by DSC at 0.5 °C/min

highly concentrated yellow slurry of 4-nitrophthalimide in concentrated ammonium hydroxide. After 5 hours at room temperature the reaction was vacuum filtered and washed with ice cold water. No further purification was completed.

In order to confirm the formation of the amide, a ^1H NMR spectrum of the 4-nitrophthalimide was compared to that of the product collected (Figure 3.5). Protons a, b, and c of the imide all shifted upfield with a shifting by ~ 0.37 ppm, b shifting by 0.30 ppm, and c shifting by 0.24 ppm. The nonequivalent shift of protons b and c resulted in both protons being overlapped. All three protons became more shielded due to the opening of the five membered heterocycle. The imide proton completely disappeared and three new proton sets appeared. Proton sets d, e, and f appeared at 7.06, 7.98, and 8.04 ppm, however protons e and f are exchangeable in terms of their ppm values due to resonance. All three protons were broad singlets, an indication that these protons are rapidly exchanging in solution, with d integrating to a value of 2. Protons e and f each integrated to a value of 1. The fact that e and f have different chemical shifts which are too large for splitting indicated that these protons are chemically different. This observed ^1H NMR spectral pattern is typical for nitrated aromatic amides.¹⁴⁸ The integration ratio of protons a, b, c, d, e, and f was equal to 1:1:1:2:1:1 which is appropriate for the molecular structure of 4-nitrophthalamide.

After completion of DSC two distinct narrow peaks were observed (Figure 3.6). The first peak at 199 °C was the melting point of 4-nitrophthalamide which is within two degrees of the literature melting point of 197 °C.¹⁴⁷ The second peak at ~ 202 °C occurred

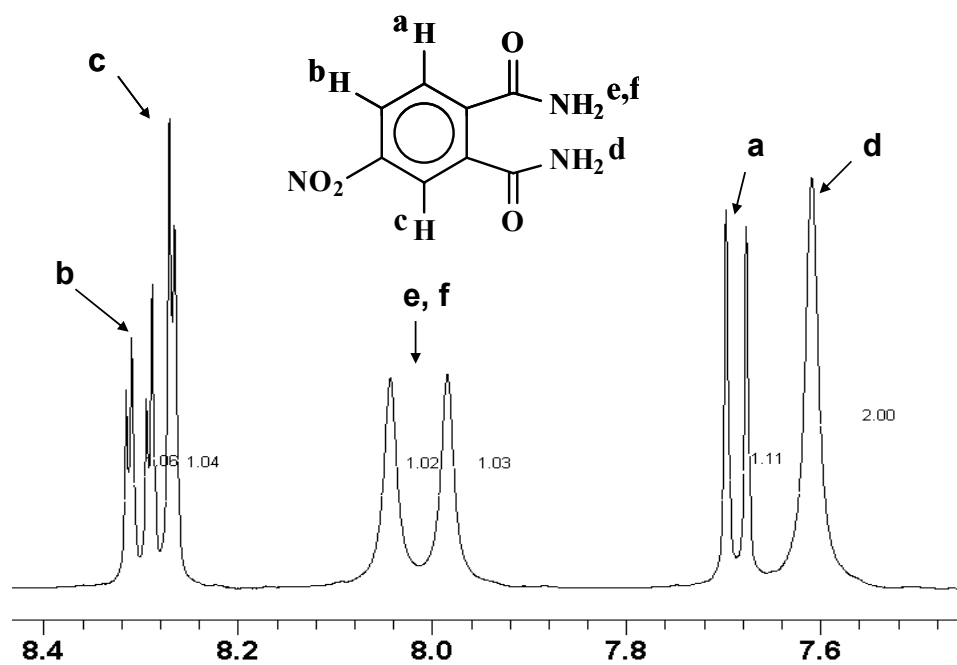


Figure 3.5: ^1H NMR of 4-nitrophthalamide

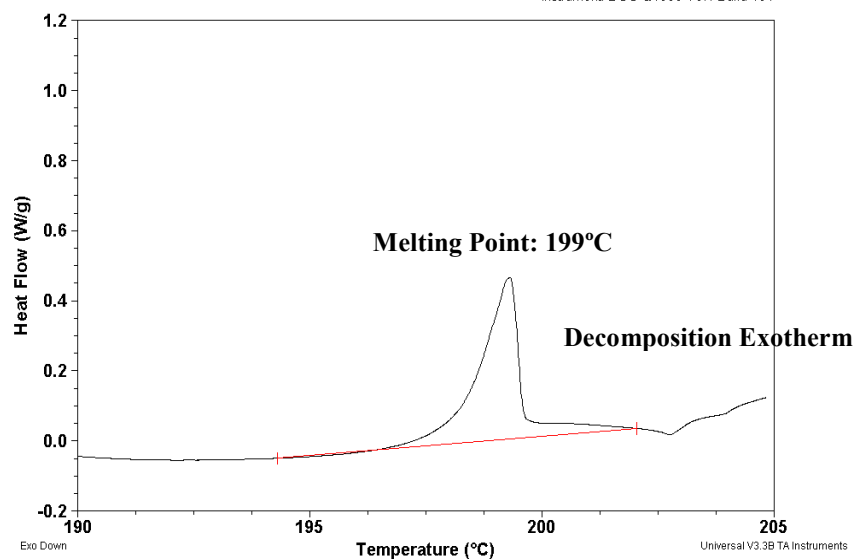


Figure 3.6: Melting point range of 4-nitrophthalamide determined by DSC at 0.5 °C/min

as an exotherm probably associated with the beginning stages of thermal decomposition.¹⁴⁸

3.4.3 Synthesis of 4-Nitrophthalonitrile

4-nitrophthalamide was converted to 4-nitrophthalonitrile via a dehydration of the amide by utilizing thionyl chloride and dry DMF as the solvent. Upon completion of the reaction the solution was slowly added to ice water where upon stirring the product crystallized out of solution. The crystallized product was collected in high yield, 84%.

A ^1H NMR spectrum of the compound displayed three aromatic proton signals (Figure 3.7). All three protons shifted considerably downfield upon conversion of the amide to the nitrile. Proton c became the most deshielded proton having a chemical shift value of 9.03 ppm. The shift of 0.77 ppm further downfield for proton c was large enough to offset the order of appearance for the aromatic protons when compared to the ^1H NMR spectrum of the amide precursor. Proton c appears further downfield than proton b when compared to the amide precursor. The amide protons associated with the precursor completely disappeared indicating that the amide groups converted to the nitrile.

Analysis of the FTIR spectrum determined the appropriate stretches associated with 4-nitrophthalonitrile were present (Figure 3.8).¹⁴⁷ At $\sim 3091\text{ cm}^{-1}$ the aromatic C-H stretches were observed and at 2242 cm^{-1} the nitrile stretch appeared. The nitro group had three stretches associated with its structure. One an asymmetric stretch at 1534 cm^{-1} and two a symmetric stretch at 1349 cm^{-1} . Finally, the last stretch for the nitro group was observed at 852 cm^{-1} which was a result of single bond stretching between the nitrogen

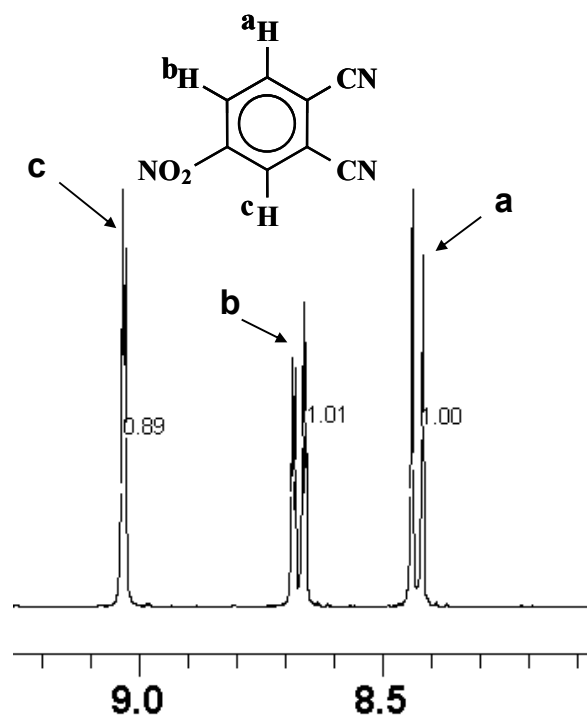


Figure 3.7: ^1H NMR of 4-nitrophthalonitrile

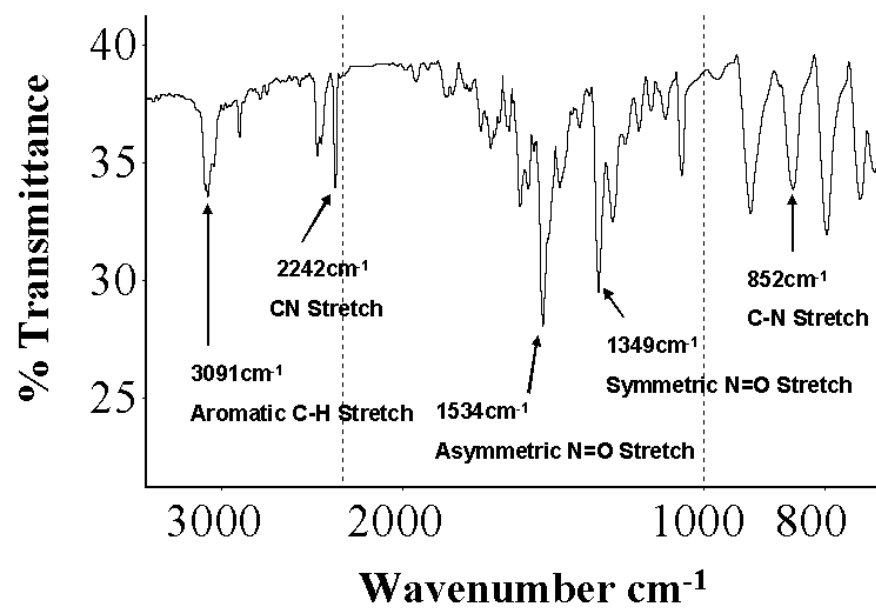


Figure 3.8: FTIR of 4-nitrophthalonitrile

and aromatic carbon.

The DSC scan of 4-nitrophthalonitrile showed a narrow melting range of 2 °C between 140 and 142 °C (Figure 3.9). The TA thermal analysis software calculated the melting point to be 141 °C which is equivalent to the literature melting point.¹⁴⁸

3.4.4 Synthesis of 4,4'-Bis(3,4-dicyanophenoxy)biphenyl (biphenoxypthalonitrile)

Biphenoxypthalonitrile was synthesized utilizing a nitro displacement reaction between 4-nitrophthalonitrile and 4,4'-biphenol. After ~24 h the reaction solution was added to ice water forming a cloudy orange solution. Sodium chloride was then added until the desired product precipitated out of solution. Upon collection and drying of the product the yield was calculated to be ~90%.

The ¹H NMR spectra of the compound displayed 5 distinct aromatic proton signals all were doublets of doublets (Figure 3.10). Proton sets a and c appeared at 7.30 and 7.80 ppm with both proton sets having an integration value of 4. Proton sets b, d, and e had chemical shift values of 7.45, 7.85, and 8.10 ppm respectively. All three protons shifted downfield when compared to the spectra of the starting material and each proton integrated to a value of 2. Protons b and d (protons b and c in the 4-nitrophthalonitrile spectrum) had the largest upfield shift of ~1.2 ppm which is to be expected because the electron withdrawing nitro group, ortho to their position in the starting material, is exchanged for an electron donating oxygen. The electron donation by the oxygen leads to more shielded protons with lower chemical shift values. Finally, the integration ratio of protons a, b, c, d, and e is 4:2:4:2:2 which is correct for the molecular structure of

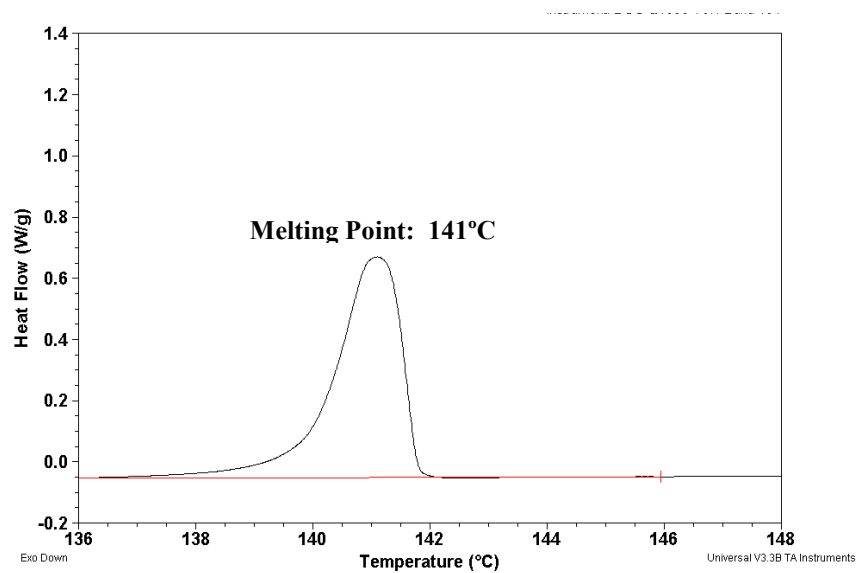


Figure 3.9: Melting point range of 4-nitrophthalonitrile determined by DSC at 0.5 °C/min

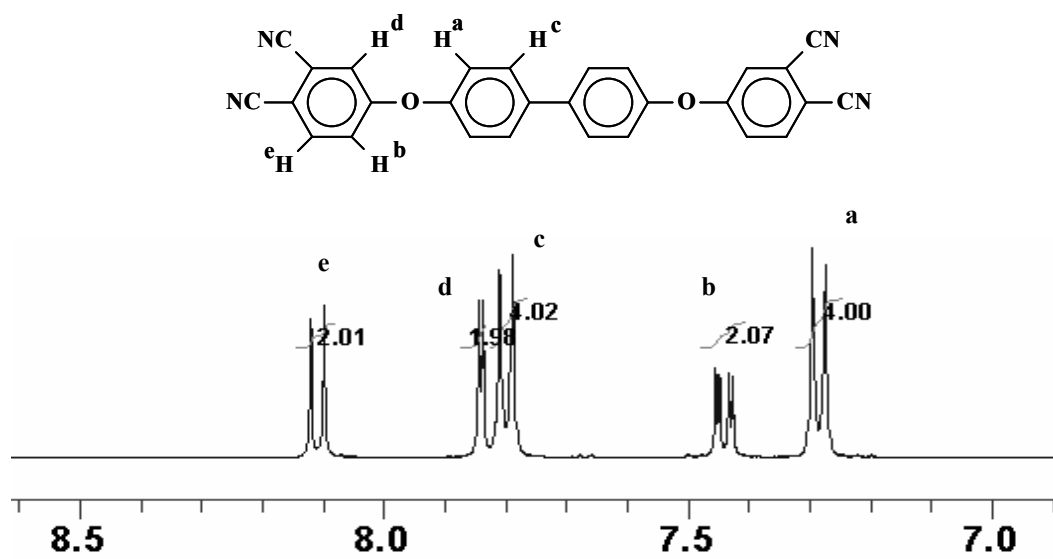


Figure 3.10: ^1H NMR of biphenoxyphthalonitrile

biphenoxyphthalonitrile.

The FTIR spectrum and melting point (determined by DSC) of the product were collected (Figures 3.11 and 3.12). The FTIR spectrum of the product displayed all of the appropriate structures associated with biphenoxyphthalonitrile. Aromatic C-H stretching was observed at 3104 cm^{-1} and the nitrile stretch appeared at 2232 cm^{-1} . Two stretches were associated with the C-O-C bonds that are within the molecular structure. An asymmetric stretch was observed at 1251 cm^{-1} and a symmetric stretch was observed at 1008 cm^{-1} . Also two stretches were observed for the C=C bonds within the aromatic rings, one at 1598 cm^{-1} and the other at 1490 cm^{-1} . The melting point of the product was determined to be $234\text{ }^{\circ}\text{C}$ using DSC. This value falls within the literature melting point of biphenoxyphthalonitrile, which is reported to be between $232\text{-}234\text{ }^{\circ}\text{C}$.¹³⁴

3.5 Conclusions

A new potentially inexpensive synthetic scheme has been developed for the production of biphenoxyphthalonitrile. It has been demonstrated that all of the desired intermediates and final product can be successfully synthesized in high yield with minimal purification.

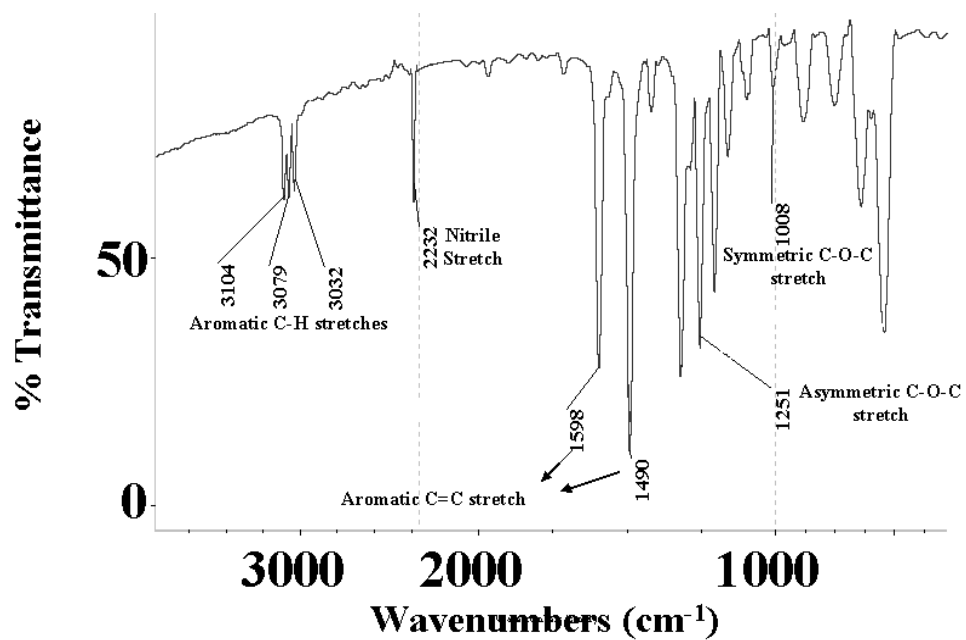


Figure 3.11: FTIR of biphenoxyphthalonitrile

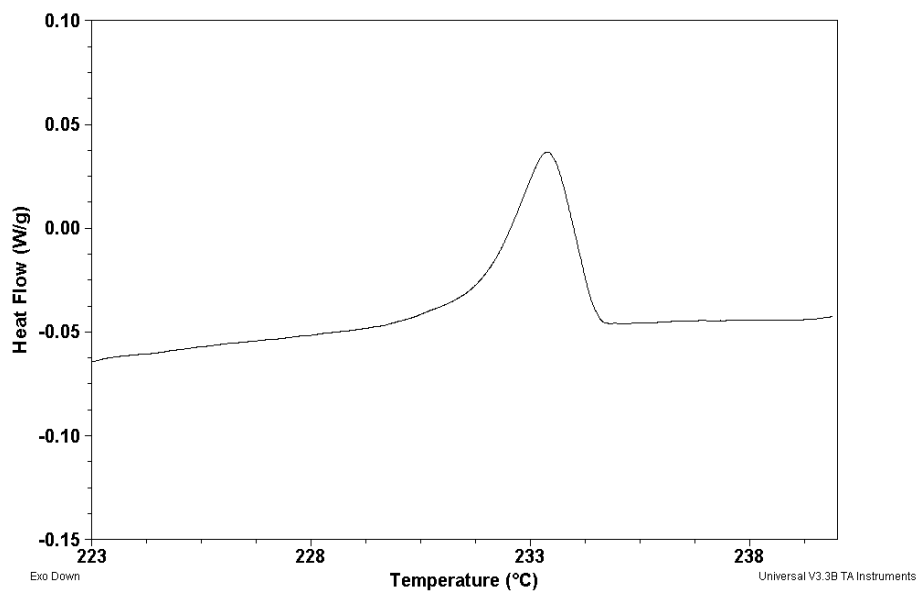


Figure 3.12: Melting point of biphenoxyphthalonitrile determined by DSC at 0.5 °C/min

Chapter 4: Flame Retardant Novolac-Bisphthalonitrile Structural Thermosets

4.1 Introduction

Phenolic networks have found many industrial applications ranging from aerospace and electronics to consumer goods since Baekeland patented the first processing technique for the production of phenol-formaldehyde resins in 1907.¹⁴⁹ These materials have as their principal attributes the combination of good flame performance and low cost. The flame resistance of these networks is attributed to their highly aromatic character, and possibly also to the inhibiting effect of the phenol groups against oxidative degradation.^{150, 151} They form large amounts of char upon burning, which causes slow burning rates and incomplete combustion. These performance characteristics make phenolic networks good matrix candidates for lightweight composites used in civil structures and transportation vehicles. In the interest of public safety, materials used in enclosed civil structures must have low combustibility and smoke toxicity. The limiting factor for most organic matrix composites is their lack of thermo-oxidative stability under intense heat such as in a fire.

Conventional curing reactions for novolac resins require a formaldehyde source, which is often hexamethylenetetramine (HMTA).^{151, 152} These curing reactions, however, generate volatile side products such as formaldehyde, ammonia and organic amines,¹⁵⁰ which in turn lead to voids in the networks or composites, and which compromise the

¹⁴⁹ L. H. Baekeland, U. S. Patent (1907).

¹⁵⁰ A. Knop, W. Scheib, "Chemistry and Applications of Phenolic Resins," Springer-Verlag, New York, 1979.

¹⁵¹ H. F. Mark, N. M. Bikales, C. G. Overberger, G. Menges, J. I. Kroschwitz (Ed.) (Eds.), "Encyclopedia of Polymer Science and Engineering," Wiley, New York, 1988.

¹⁵² X. Zhang, M. G. Looney, D. H. Solomon, A. K. Whitaker, "The Chemistry of Novolac Resins: 3. 13C and 15N NMR Studies of Curing with Hexamethylenetetramine," Polymer, 38, 1997, 5835.

strengths of the materials. Resoles can cure thermally without added crosslinking reagents, but these reactions also eliminate volatiles (e.g., water, formaldehyde) which cause voids. Therefore, most current phenolic resole or novolac networks have limited utility in structural applications due to poor mechanical properties.

Recent research has focused on curing novolac resins with reagents that do not generate volatiles upon cure to improve the toughness of phenolic networks. Indeed important products exist based on epoxy-cured phenolics where the epoxy reagent is the major component.¹⁵³ In some cases these materials comprise the base resins for semiconductor packaging because they have better hydrophobicity when compared to amine cured epoxies. These materials display good toughness but the high epoxy concentration undesirably increases their flammability.¹⁵³

More recently, workers in our laboratories have studied novolac-epoxy compositions with high novolac weight fractions and high phenol:epoxy offset stoichiometries.^{154, 155, 156} These networks had greatly improved combinations of mechanical and flame properties. For example, K_{Ic} toughness values of $>1 \text{ MPa}\cdot\text{m}^{1/2}$ were obtained with this approach as opposed to $K_{Ic}\approx 0.16$ for a conventional resole network. The flame properties of the neat networks (i.e., no reinforcing fiber) measured by cone calorimetry at 50 kW/m^2 incident heat flux indicated peak heat release rates of about $250\text{-}300 \text{ kW/m}^2$. This result was far better than analogous values for epoxy

¹⁵³ A. Hale, C. W. Macosko, "DSC and ^{13}C NMR Studies of the Imidazole-Accelerated Reaction Between Epoxides and Phenols," *Journal of Applied Polymer Science*, 38, 1989, 1253.

¹⁵⁴ C. S. Tyberg, P. Shih, K. N. Verghese, A. C. Loos, J. J. Lesko, J. S. Riffle, "Latent Nucleophilic Initiators for Melt Processing Phenolic-Epoxy Matrix Composites," *Polymer*, 41, 2000, 9033.

¹⁵⁵ C. S. Tyberg, M. Sankarapandian, K. Bears, P. Shih, A. C. Loos, D. Dillard, J. E. McGrath, J. S. Riffle, U. Sorathia, "Tough, Void-Free, Flame Retardant Phenolic Matrix Materials," *Construction and Building Materials*, 13, 1999, 343.

networks ($\sim 1250 \text{ kW/m}^2$) but not as low as those measured for neat (but brittle) resole networks ($\sim 100 \text{ kW/m}^2$).

There is continuing interest in high temperature thermosetting matrix resins for advanced composites. Keller et al. demonstrated that networks from bisphthalonitrile reagents cured with small amounts (1 to 3 mole %) of an aromatic diamine (Figure 4.1) were highly resistant to thermo-oxidative degradation, and some that were postcured at 375°C had T_g 's in excess of 450°C .^{157, 158, 159, 160, 161, 162, 163, 164, 165, 166, 167, 168, 169} Fire testing demonstrated their outstanding characteristics in composites.¹⁷⁰ The thermo-oxidative resistance of these networks was attributed to a high level of aromaticity and

¹⁵⁶ C. S. Tyberg, K. Bergeron, M. Sankarapandian, P. Shih, A. C. Loos, D. A. Dillard, J. E. McGrath, J. S. Riffle, U. Sorathia, "Structure-Property Relationships of Void-Free Phenolic-Epoxy Matrix Materials," *Polymer*, **41**, 2000, 5053.

¹⁵⁷ T. M. Keller, "Phthalonitrile-Based High Temperature Resin," *Journal of Polymer Science: Part A: Polymer Chemistry*, **26**, 1988, 3199.

¹⁵⁸ T. M. Keller, "Fluorinated High Temperature Phthalonitrile Resin," *Polymer Communications*, **28**, 1987, 337.

¹⁵⁹ T. M. Keller, "Synthesis and Polymerization of Multiple Aromatic Ether Phthalonitriles," *Chemistry and Materials*, **6**, 1994, 302.

¹⁶⁰ T. M. Keller, J. R. Griffith, "The Synthesis of a New Class of Polyphthalocyanine Resins," *ACS Symposium Series*, **132**, 1980, 25.

¹⁶¹ T. M. Keller, R. F. Katz, "High Temperature Intrinsically Conductive Polymers," *Polymer Communications*, **28**, 1987, 334.

¹⁶² T. M. Keller, T. R. Price, "Amine-Cured Bisphenol-Linked Phthalonitrile Resins," *Journal of Macromolecular Science-Chemistry*, **A18**, 1982, 931.

¹⁶³ T. M. Keller, D. J. Moonay, "Phthalonitrile Resin for High Temperature Composite Applications," *SAMPE Symposium*, **34**, 1989, 941.

¹⁶⁴ S. B. Sastri, T. M. Keller, "Phthalonitrile Polymers: Cure Behavior and Properties," *Journal of Polymer Science: Part A: Polymer Chemistry*, **37**, 1999, 2105.

¹⁶⁵ S. B. Sastri, T. M. Keller, "Phthalonitrile Cure Reaction with Aromatic Diamines," *Journal of Polymer Science: Part A: Polymer Chemistry*, **36**, 1998, 1885.

¹⁶⁶ S. B. Sastri, J. P. Armistead, T. M. Keller, "Phthalonitrile-Carbon Fiber Composites," *Polymer Composites*, **17**, 1996, 816.

¹⁶⁷ S. B. Sastri, J. P. Armistead, T. M. Keller, U. Sorathia, "Phthalonitrile-Glass Fabric Composites," *Polymer Composites*, **18**, 1997, 48.

¹⁶⁸ S. B. Sastri, J. P. Armistead, T. M. Keller, U. Sorathia, "Flammability Characteristics of Phthalonitrile Composites," *SAMPE Symposium*, **42**, 1997, 1032.

¹⁶⁹ T. M. Keller, C. M. Rolland, U.S. Patent 5,242,755 (1993).

¹⁷⁰ I. Caplan, U. Sorathia, C. Rollhauser, "US Navy R&D Programs in Fire Performance of Materials," *SAMPE Journal*, **32**, 1996, 21.

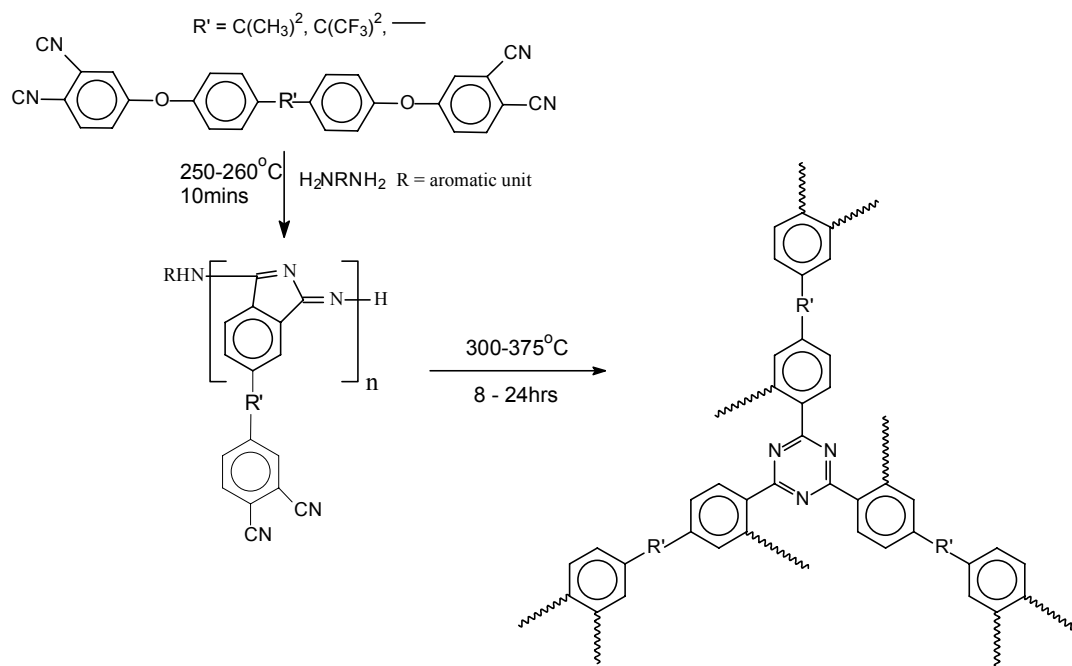


Figure 4.1: Proposed bisphthalonitrile oligomer reaction with a minor amount of an aromatic amine to form a “B-staged resin”, and subsequent network formation

the proposed formation of heterocyclic crosslinks in the networks (Figure 4.1). Networks from reactive oligomers with phenylethynyl, maleimide, or nitrile functionalities cured at elevated temperatures ($>200\text{ }^{\circ}\text{C}$) have also been shown to have good thermo-oxidative stability.^{163, 171, 172, 173}

The focus of this research has been to cure phenolic novolac resins with reagents that produce non-flammable crosslinked structures. We have discovered that phenolic novolac resins react with bisphthalonitrile reagents to produce void-free networks with attractive structural and fire characteristics. Importantly, the major components of these resins are the economical and commercially available novolacs. It has been demonstrated that nucleophilic phenol groups readily react with the nitrile groups of phthalonitriles.

The molecular structure of the novolac-BPh crosslink has been studied in model reactions in an effort to better understand the chemical nature of novolac-BPh networks. An excess of a monofunctional phenol and BPh were reacted to form a soluble model material, which was characterized using ^1H NMR and FTIR. Results suggest that the molecular structure of the novolac-BPh crosslink is heterocyclic, which helps to explain the excellent flame retardance of the networks.

4.2 Experimental

4.2.1 Materials

The commercial phenol-formaldehyde novolac resin with an average phenol functionality of 7.1 (GP-2073) was kindly provided by Georgia-Pacific. 4,4'-Bis-(3,4-

¹⁷¹ S. Alam, L. D. Kandpal, I. K. Varma, "Co-Curing Studies of Ethynyl Terminated Oligoimide and (Methyl) Nadicimide Resins," *Journal of Thermal Analysis*, **47**, 1996, 685.

¹⁷² S. Jayaraman, G. W. Meyer, T. M. Moy, R. Srinivasan, J. E. McGrath, "Synthesis and Characterization of 3-Phenylethynyl Endcapped Matrix Resins," *Polymer Preprints*, **34**, 1993, 513.

dicyanophenoxy)biphenyl (BPh) was generously provided by Eikos Incorporated. General aspects of its molecular structure were reported previously (Figure 4.2).¹⁷⁴ Both reagents were used as received. 2-hydroxydiphenylmethane was purchased from Aldrich and used as received.

4.2.2 Network Formation from the Novolac Resin and 4,4'-Bis-(3,4-dicyanophenoxy)biphenyl (BPh)

Systematically varied amounts of BPh and the novolac resin were charged to a three-neck, round bottom flask equipped with a vacuum tight mechanical stirrer and vacuum adapter. The novolac was melted at approximately 200 °C, was degassed for 10 to 15 min at 2-5torr, then the required amount of BPh was added resulting in a liquid blended composition. The solution turned black when the BPh diffused into the novolac melt. The solution was stirred and further degassed for approximately 5 min, then poured into a preheated polysiloxane mold. Each molded sample was cured for 1 h at 200 °C and 3 h at 220 °C in air, then cooled to room temperature.

4.2.3 Melt Reaction Between 2-Hydroxydiphenylmethane and BPh

2-Hydroxydiphenylmethane (10 g) was charged to a one-neck round bottom flask equipped with a reflux condenser and magnetic stir bar. The reagent was heated to 200 °C and maintained at this temperature for approximately 30 min. BPh (0.97 g) was blended into the melt to establish a 25:1 molar ratio (6.1:1 OH:CN eq. ratio) between 2-hydroxydiphenylmethane and BPh (Note: The 6.1:1 equivalence ratio was the same as

¹⁷³ J. J. King, M. A. Chaudari, S. Zahir, "A New Bismaleimide System for High Performance Applications," *SAMPE Symposium*, **29**, 1984, 394.

¹⁷⁴ M. Sankarapandian, T. E. Glass, J. E. McGrath, P. Mack, M. Smith, P. Glatkowski, J. Conroy, J. Piche, *SAMPE Proceedings*, **45**, 2000, 1214.

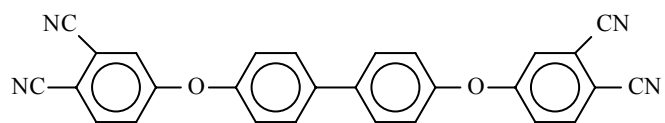


Figure 4.2: Molecular structure of 4,4'-bis-(3,4-dicyanophenoxy)biphenyl

that used to prepare the 85:15 wt:wt novolac-BPh networks.). The melt mixture was reacted for 3 h at 200 °C at which point the mixture turned dark green. The product from the reaction was isolated by precipitation in dichloromethane, then decantation of the dichloromethane. The product was purified by dissolving it in THF and reprecipitating it into dichloromethane. The THF/dichloromethane mixture was decanted and the product was air dried for 12 h, then vacuum dried at 40 °C overnight.

4.3 Measurements

4.3.1 Dynamic Mechanical Analysis (DMA)

Dynamic mechanical analysis (DMA) in a three-point-bend mode was used to determine the T_g 's and force versus displacement curves in the rubbery regions. These measurements were performed using a Perkin-Elmer dynamic mechanical analyzer, Model DMA-7. The samples were heated from 25 °C to 220 °C at 5 °C/min with the peak in the tan delta curve signifying the T_g . To measure force versus displacement in the rubbery regions, each sample was heated to approximately 60 °C above its T_g and was deformed at a rate of 20mN/min until 250mN was reached. The slopes of the force versus displacement curves were used in Eq. (1) to determine the rubbery moduli, E , for the samples. P/Δ is the slope of the force versus displacement curve,

$$E = p(P/\Delta)(L^3/48I) \quad (1)$$

L is the instrument span (20mm), p is gravitational acceleration (9.81m/s^2), and I is $(1/12)wb^3$, w is the width of the sample (6.35mm) and b is the height of the sample (2.00mm). The values of “ E ” from equation 1 were used with the theory of rubber elasticity to calculate the molecular weights between crosslinks (M_c) for the networks

(Eq. 2). M_c is molecular weight between crosslinks, E is the rubbery modulus, R is the gas constant, E is the rubbery modulus, R is the gas constant ($8.314\text{JK}^{-1}\text{mole}^{-1}$), T is the temperature in Kelvin at 60° above the T_g of the sample, and ρ is the density of the sample 60° above its T_g .

$$M_c = 3RT\rho/E \quad (2)$$

4.3.2 Scanning Electron Microscopy (SEM)

Scanning electron microscopy (SEM) was used at 500X magnification to view fractured surfaces of the thermosets, to confirm that voids were not being produced in the networks.

4.3.3 Stress Intensity Factor (K_{Ic})

The stress intensity factors (K_{Ic}) or fracture toughness values were measured using an Instron in the three-point-bend mode using a modified form of ASTM standard D 5045-91. The specimens were 3.12mm thick by 6.28mm wide by 38.1mm long. A small crack was initiated in each sample using a liquid nitrogen cooled razor blade. The crack spanned approximately 30 to 70% of the sample thickness. The crosshead speed was applied at 1.27mm/min and the stress at break was recorded. It should be noted these thermosets were “dark greenish-black” and it was not possible to measure the crack lengths before breaking the samples. Thus, the crack length was measured after the samples were broken by observing the “pre-cracked” as opposed to the fractured region.

4.3.4 Sol-Fractions

Sol-fractions of the networks were measured by placing 30 to 50mg of each sample into 20mL of tetrahydrofuran (THF). The samples were extracted in THF for 72

h, then the solvent was removed by air drying for 24 h and vacuum drying at ~ 40 °C for 24 h. The remaining mass was weighed as the sol. The sol-fractions and gel-fractions were calculated by dividing the weights of the sols by the initial sample weights. Three measurements were made on each network and an average was taken.

4.3.5 Fourier Transform Infrared Spectroscopy (FTIR)

Network formation was monitored by FTIR using a Nicolet Impact 400 spectrometer coupled with a thermostatically controlled IR cell. The percent conversion of the nitrile groups was monitored by measuring the disappearance of the nitrile peak at approximately 2200 cm^{-1} . FTIR was also used to help determine the structure of the product isolated from the model melt reaction by monitoring characteristic stretches in the 3000 to 3300 cm^{-1} region and the 1600 to 1700 cm^{-1} region.

4.3.6 Proton Nuclear Magnetic Resonance (^1H NMR)

^1H NMR was collected on a Varian Unity 400 MHz instrument with a frequency of 399.954 MHz. A 22° pulse angle was used with an acquisition time of 3.7s and a recycle delay of 1s. d_6 -DMSO was used as the NMR solvent.

4.3.7 Cone Calorimetry and Thermogravimetric Analysis (TGA)

Flame and thermal properties were measured using cone calorimetry and TGA. The cone calorimetry samples were 4" in length by 4" wide and 0.25" thick. The samples were heated in a horizontal orientation in a cone calorimeter at 50 kW/m^2 incident heat flux. Char yields, smoke toxicity, peak heat release rates, total heat released, and times to ignition were measured. Using a Perkin-Elmer model TGA 7 thermogravimetric analyzer, 8 to 12 mg of small solid samples were heated from 25°C to 900°C at a

heating rate of 10 °C/min. The final char yields, and the temperatures at which 5% weight loss occurred were recorded for each sample under inert (N₂) and atmospheric conditions.

4.4 Results and Discussion

4.4.1 Network Synthesis

A ~700g/mole novolac oligomer from phenol and formaldehyde with an average functionality of 7.1 was cured for 1 hour at 200 °C and 3 h at 220 °C with 5, 10, 15, 20 and 25 weight percent BPh. Although the curing reaction is not well understood, it is hypothesized that the nucleophilic phenol can attack the electrophilic carbon of a nitrile to form a phenoxy substituted imine. The imine may then propagate further by attacking another nitrile, either intramolecularly in the ortho position to form an isoindoline type structure or intermolecularly to form a diimine containing conjugated structure. The rate of disappearance of the nitrile infrared absorbance at 2200 cm⁻¹ was one metric used to monitor progress in these reactions. It must be noted, however, that since the fully cured network structure is not yet well understood, disappearance of the nitrile starting material may not signify full cure. The areas under the nitrile FTIR peaks for mixtures of 90:10 and 80:20 wt:wt ratios of novolac to BPh decreased by 90% upon curing for 1 hour at 200 °C and 1 h at 220 °C (Figure 4.3). Curing beyond this time or temperature did not reduce these areas further in either case.

4.4.2 Model Study -- Melt Reaction of 2-Hydroxydiphenylmethane and BPh

The chemical structures of the novolac-BPh networks synthesized with high

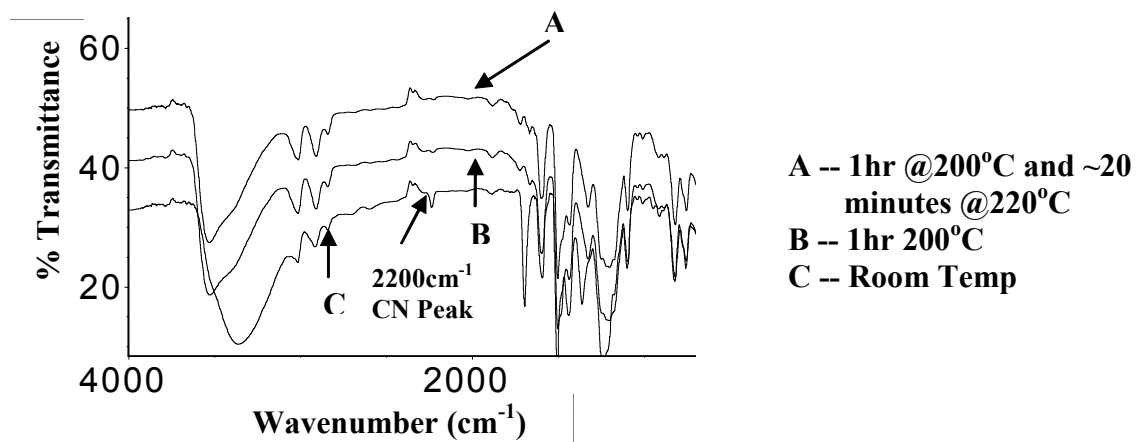


Figure 4.3: FTIR spectra of a 90:10 weight percent novolac:BPh network cured for 1 h at 200 °C, then 1 h at 220 °C

concentrations of phenol relative to phthalonitrile are not clear. In this study we attempted to clarify the molecular structure of the novolac-BPh networks by characterizing the product(s) formed from the melt reaction of a monofunctional phenol (which had a similar chemical structure to the novolac) with BPh. 2-Hydroxydiphenylmethane was reacted with BPh using the same OH:CN equivalence ratio used to synthesize the 85 weight percent novolac-15 weight percent BPh networks (Figure 4.4). This corresponded to a 25:1 molar ratio of 2-hydroxydiphenylmethane to BPh (6.1 hydroxyls per nitrile). The reaction was conducted in the melt at 200 °C for 3 h which was similar to the curing cycle for the novolac-BPh networks. The green crude mixture formed as a result of the reaction was added slowly to dichloromethane to remove unreacted phenols and to precipitate the product(s) generated from the reaction. After purifying the product(s), their molecular structure was characterized using ^1H NMR and FTIR (Figures 4.5 and 4.6).

The ^1H NMR spectra of the compound isolated and purified from the melt reaction of 2-hydroxydiphenylmethane with BPh showed three broad proton signals at 3.9 – 4.1, 6.5 – 8, and 9 – 9.3 ppm (Figure 4.5). The proton signals between 3.9 – 4.1 correspond to the methylene protons of 2-hydroxydiphenylmethane. These C-H methylene absorptions also appear in the FTIR spectra as a doublet stretch at $\sim 3000\text{ cm}^{-1}$. The proton signals between 6.5 – 8 ppm correspond to the aromatic protons of both 2-hydroxydiphenylmethane and BPh. The protons resonating between 9 – 9.3 ppm are characteristic of N-H protons. These can be attributed to isoindoline type protons formed from intramolecular imine attack on a nitrile, or also to diimine structures resulting from

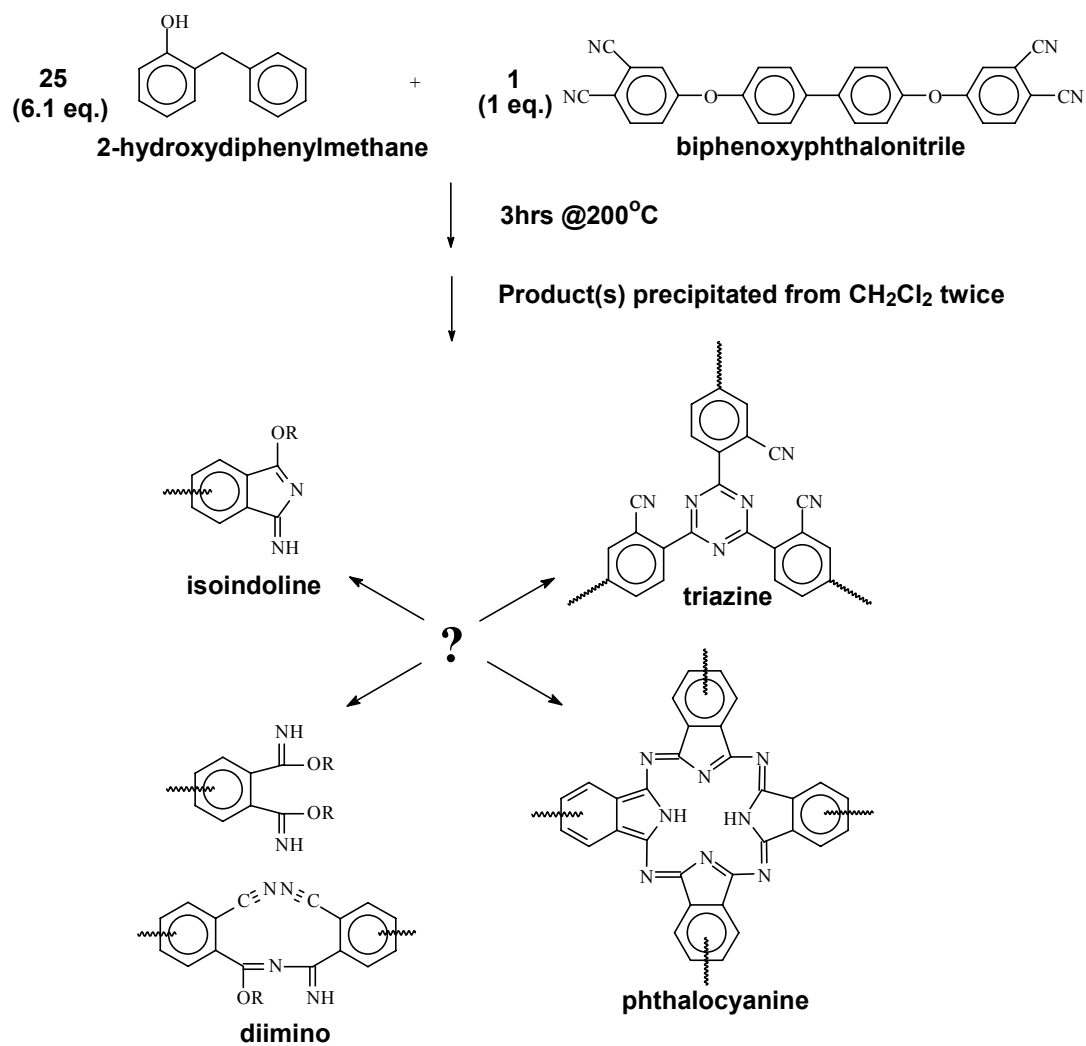


Figure 4.4: Possible reaction products of the model melt reaction between 2-hydroxydiphenylmethane and a bisphthalonitrile

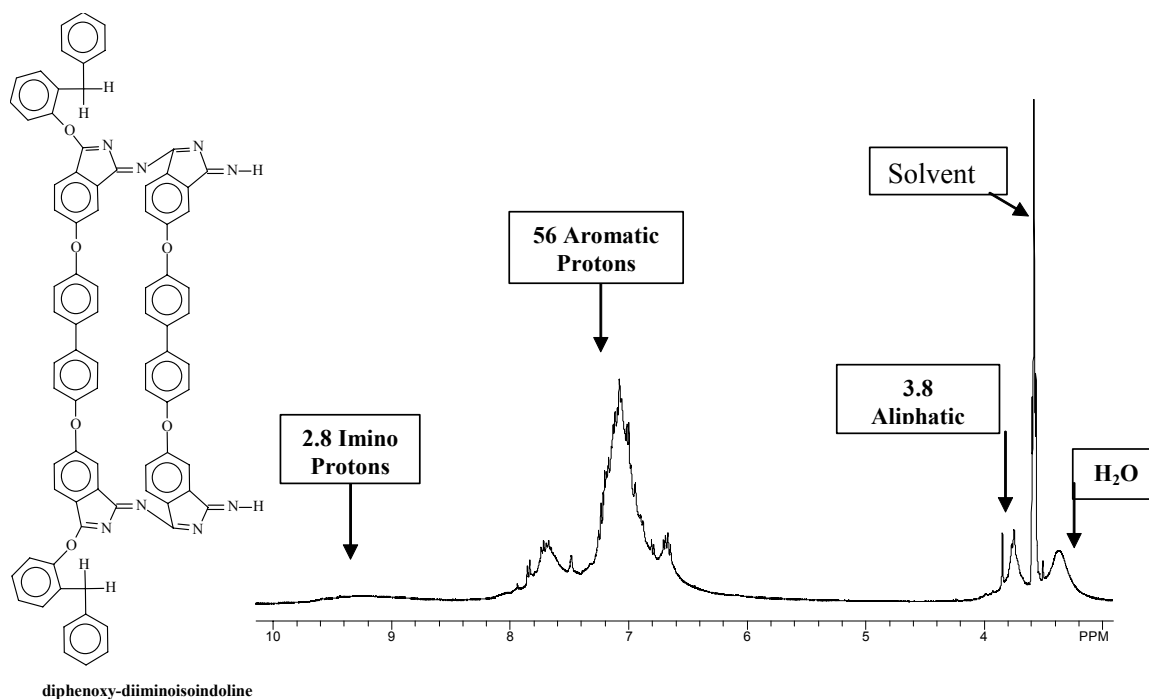


Figure 4.5: ¹H NMR of the product isolated from the 2-hydroxydiphenylmethane-BPh model reaction

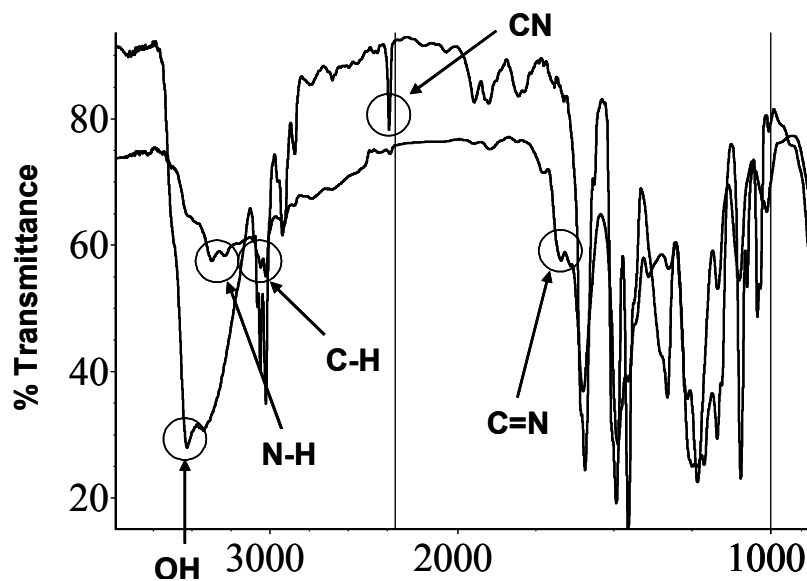


Figure 4.6: FTIR Spectrum *A*—25:1 molar ratio (6.1:1 eq ratio) of a melt mixture of 2-hydroxydiphenylmethane and BPh before reaction. FTIR Spectrum *B*—Product generated after 3 h at 200 °C

intermolecular imine attack on a nitrile. It is expected that intramolecular reactions would be favored due to the formation of the 5-membered heterocyclic ring. Unfortunately, these imine resonances are broad which makes quantification very difficult. The absorption bands in the FTIR spectra occurring at 1600 cm^{-1} (C=N) and 3300 cm^{-1} (N-H) provide support for these structures within its molecular framework (Figure 4.6).^{175, 176} Peaks at upfield chemical shifts between -8 to -9 ppm indicative of phthalocyanines were not observed. Also, a sharp doublet at ≈ 9 ppm characteristic of triazine rings was not observed.¹⁷⁷ Integration of the three groups of proton resonances in the ^1H NMR spectra yields a ratio of 3.8:56:2.8 of aliphatic to aromatic to N-H protons on isoindoles and diimines (Figure 4.5). This ratio along with FTIR data suggests that the product has approximately one phenol fragment per 4 nitriles (Figure 4.6).

It is important to point out that the molecular structures of the novolac-BPh crosslinks may differ with higher concentrations of BPh relative to nucleophilic phenols in the networks. Determining the molecular structure of the crosslinks in other compositions of novolac-BPh networks is currently under investigation.

4.4.3 Network Properties

Gel-fraction measurements were completed to investigate the level of cure in the novolac-BPh network materials. Networks with 15, 20 and 25 weight percent BPh had

¹⁷⁵ T. P. Forsyth, D. Bradley, G. Williams, A. G. Montalban, C. L. Stern, G. M. Barnett, B. M. Hoffman, "A Facile and Regioselective Synthesis of Trans-Heterofunctionalized Porphyrazine Derivatives," *Journal of Organic Chemistry*, **63**, 1998, 331.

¹⁷⁶ K. Abdur-Rashid, A. J. Lough, R. H. Morris, "RuHCl(diphosphine)(diamine): Catalyst Precursors for the Stereoselective Hydrogenation of Ketones and Imines," *Organometallics*, **20**, 2001, 1047.

¹⁷⁷ A. W. Snow, J. R. Griffith, N. P. Marullo, "Synthesis and Characterization of Heteroatom-Bridged Metal-Free Phthalocyanine Network Polymers and Model Compounds," *Macromolecules*, **17**, 1984, 1614.

gel-fractions greater than 0.9 (Figure 4.7). The gel-fractions, coupled with the FTIR data, suggest the novolac-BPh resins undergo high levels of crosslinking during the designated cure procedure.

We analyzed fracture surfaces of the networks with SEM to ensure that no volatiles were generated during the curing cycle. Network compositions with 85:15 and 80:20 wt:wt novolac to BPh were analyzed at 500X magnification (Figure 4.8), and no voids, which would appear as large dark craters, were observed. Voids promote crack propagation, which reduces the fracture toughness of glassy network materials. Thus, the absence of voids in the novolac-BPh networks helps to explain the good toughness of these materials ($K_{Ic} \approx 0.8 \text{ MPa}\cdot\text{m}^{1/2}$) as discussed later in this paper.

Rubbery moduli were measured on the novolac-BPh networks and used to estimate M_c (Figure 4.9). The equivalence ratio of phenol to nitrile (i.e. OH:CN) in the initial thermosetting mixtures decreased from 19.6:1 at 5 weight percent BPh to 3.1:1 at 25 weight percent BPh. Thus, it was expected that more crosslinks would result as the level of BPh was increased along this series (i.e., more phenol groups would react). Consistent with this premise, the rubbery moduli increased significantly as the concentration of BPh in the networks was increased, suggesting that BPh efficiently cures the novolac resin. Corresponding substantial decreases in calculated M_c values followed from this data (Figure 4.9).

The 85:15 wt:wt novolac-BPh network had calculated M_c values similar to a 65:35 wt:wt novolac-diepoxide network (control). The 65:35 wt:wt novolac-diepoxide network was elected as the control in this experiment because it had been previously

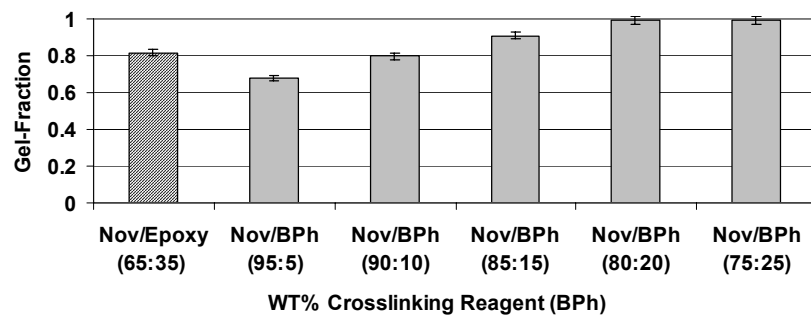


Figure 4.7: Gel-fractions versus novolac-BPh composition

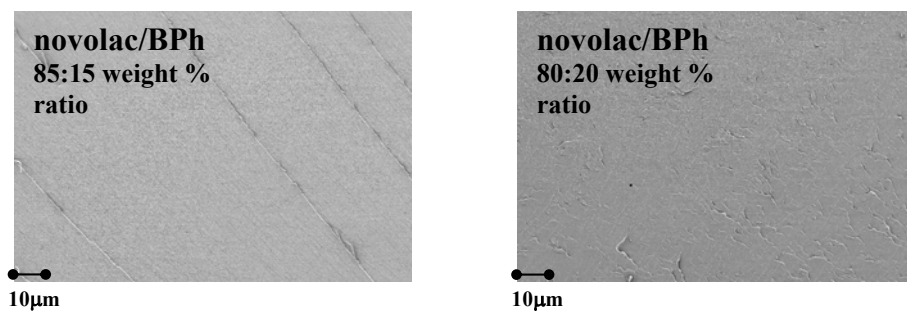


Figure 4.8. SEMs at 500X of 85:15 and 80:20 wt:wt ratios of novolac-BPh networks

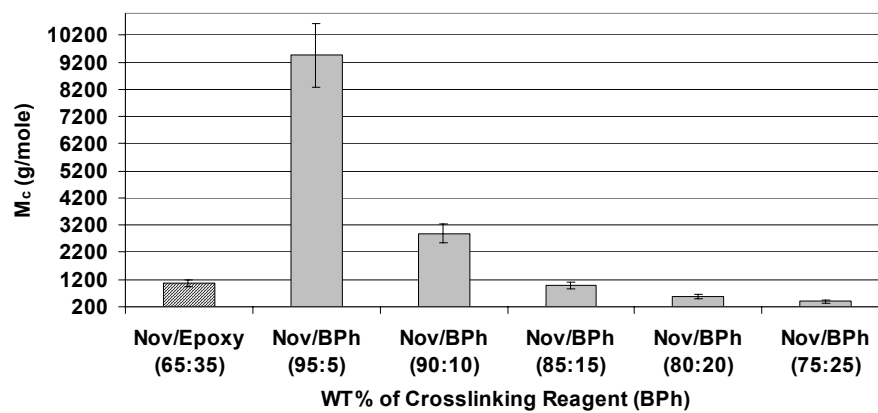


Figure 4.9: M_c versus novolac-BPh composition (wt%)

demonstrated in our labs that this network had a high T_g , good toughness, and good flame retardance.^{155, 156} Therefore this material served as an excellent benchmark for any new network materials prepared from high compositions of novolacs crosslinked with minor compositions of different crosslinking reagents. Increasing the BPh concentration in the networks beyond 15 weight percent resulted in significantly higher rubbery moduli and correspondingly lower M_c values (Figure 4.9). Based on a rubbery modulus of the 25 weight percent BPh-75 weight percent novolac network, the M_c was calculated to be approximately 400g/mole. The low M_c value (high rubbery modulus) suggests that the reaction between BPh and the novolac resin produced a highly crosslinked network. The high level of crosslinking helps to explain the good toughness observed in these materials using considerably less crosslinking reagent as compared to novolacs crosslinked with epoxy components.^{155, 156, 178} Also, the low M_c values for the novolac-BPh networks correlate well with the high percent conversion of nitrile groups determined by FTIR and the high gel-fractions measured for these materials.

Novolac oligomers cured with 15, 20, and 25 weight percent BPh had T_g 's in excess of 180 °C (as demonstrated with DMA), which is well into the range desirable for electronic applications (and maybe even aerospace) (Figure 4.10). This is significantly higher than T_g 's observed for networks prepared with the same novolac resin cured with diepoxides (from bisphenol-A and epichlorohydrin).^{155, 156, 178} For example, a 65:35 wt:wt novolac-bisphenol-A diepoxide network (which had the most desirable mechanical properties of this compositional series) prepared from the same novolac oligomer had a

¹⁷⁸ C. S. Tyberg, Ph.D. Thesis, Virginia Tech, **2000**.

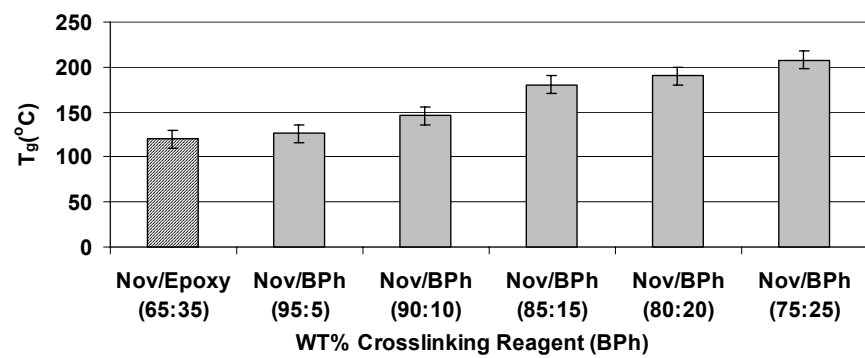


Figure 4.10: T_g versus novolac-BPh composition

T_g of ≈ 120 °C. Novolac oligomers cured with only 5 weight percent BPh had a T_g of ≈ 120 °C, whereas the neat novolac oligomer had a T_g of 90 °C. The elevation of the glass transition temperature to 120 °C indicated that even low levels of BPh significantly cure the novolac oligomer. The decreases in M_c values with increasing concentration of BPh correlated well with the increases in T_g .

4.4.4 Network Thermo-Oxidative Stability Characterization

The thermo-oxidative characteristics of the novolac-BPh networks were excellent, as measured by both TGA and cone calorimetry. The weight loss profiles of the materials were analyzed as a function of temperature by TGA in both inert (nitrogen) and air (20% oxygen) environments at a heating rate of 10 °C/min. All of the networks yielded approximately 50 wt. % char after burning in the cone calorimeter (under atmospheric conditions), and between 60 and 80 wt. % char at 700 °C by TGA (in both air and nitrogen). Polyarylene ethers as well as polyimides, which are noted for their thermo-oxidative resistance, show little or no char yields at this temperature in air and about 20-50wt. % in nitrogen.^{179, 180, 181, 182, 183, 184, 185, 186, 187, 188} As would be expected

¹⁷⁹ A. Bhatnagar, Y. N. Liu, J. F. Geibel, J. E. McGrath, "Synthesis and Characterization of Advanced Fire-Resistant Thermoplastics," *Polymer Preprints*, **38**, 1997, 227.

¹⁸⁰ Y. Liu, A. Bhatnagar, Q. Ji, J. S. Riffle, J. E. McGrath, J. F. Geibel, T. Kashiwagi, "Influence of Polymerization Conditions on the Molecular Structure, Stability, and Physical Behavior of Poly(Phenylene Sulfide Sulfone) Homopolymers," *Polymer*, **41**, 2000, 5137.

¹⁸¹ S. Matsuo, "Synthesis and Properties of Poly(Arylene Ether Phenyl-s-Triazine)s," *Journal of Polymer Science Part A: Polymer Chemistry*, **32**, 1994, 2093.

¹⁸² Y. Ding, A. R. Hlil, A. S. Hay, "Poly(Arylene Ether)s and Poly(Arylene Thioether)s Containing the 1,2-Dihydro-4-Phenyl(2H)Phthalazinone Moiety," *Journal of Polymer Science Part A: Polymer Chemistry*, **36**, 1998, 455.

¹⁸³ S. Banerjee, G. Maier, M. Burger, "Novel Poly(Arylene Ether)s with Pendent Trifluoromethyl Groups," *Macromolecules*, **32**, 1999, 4279.

¹⁸⁴ D. J. Riley, A. Gungor, S. A. Srinivasan, M. Sankarapandian, C. Tchatchoua, M. W. Muggli, T. C. Ward, J. E. McGrath, "Synthesis and Characterization of Flame Resistant Poly(Arylene Ether)s," *Polymer Engineering and Science*, **37**, 1997, 1501.

¹⁸⁵ K. U. Jeong, J.-J. Kim, T.-H. Yoon, "Synthesis and Characterization of Novel Polyimides Containing Fluorine and Phosphine Oxide Moieties," *Polymer*, **42**, 2001, 6019.

based on the higher crosslink densities of the higher composition BPh networks, the TGA study indicated that networks cured with higher compositions of the BPh reagent had higher char yields (Figure 4.11). The weight loss measurements also showed that under atmospheric conditions the 5% weight loss temperature for each novolac-BPh network did not occur until 480 to 500 °C, which is comparable to polyimides and polyarylene ethers.^{179, 180, 181, 182, 183, 184, 185, 186} Under nitrogen, the 5% weight loss temperatures and char yields for the novolac-BPh networks were approximately equivalent to those observed under atmospheric conditions. This observation suggests that oxygen does not play a significant role in the thermal degradation of novolac-BPh networks.

The primary interest for material applications of bisphthalonitrile resins has been in the fields of marine and aerospace applications. The marine industry depends on glass or carbon fiber reinforced polymer composites to provide good mechanical properties at significantly reduced weight when compared to certain metals. Typical polymers used for these applications are unsaturated polyesters, vinyl esters, and epoxy resins. However, these materials are highly flammable and do not pass the U.S. Navy's extremely stringent MIL-STD-2031. The MIL-STD-2031 is a flammability specification issued by the Navy in 1991 concerning materials to be used aboard submarines.¹⁸⁹ This specification contains test methods and requirements for cone calorimeter flammability

¹⁸⁶ A. K. Salunke, M. K. Madhra, M. Sharma, S. Banerjee, "Synthesis and Characterization of Poly(Arylene Ether)s Derived from 4,4'-Bishydroxybiphenyl and 4,4'-Bishydroxyterphenyl," *Journal of Polymer Science Part A: Polymer Chemistry*, **40**, 2002, 55.

¹⁸⁷ J. H. Koo, S. Venumbaka, P. E. Cassidy, J. W. Fitch, A. F. Grand, "Flammability Studies of Thermally Resistant Polymers Using Cone Calorimetry," *Journal of Fire and Materials*, **24**, 2000, 209.

¹⁸⁸ G. W. Meyer, S. J. Pak, Y. J. Lee, J. E. McGrath, "New High-Performance Thermosetting Polymer Matrix Material Systems," *Polymer*, **36**, 1995, 2303.

¹⁸⁹ MIL-STD-2031(SH), "Fire and Toxicity Test Methods and Qualification Procedure for Composite Material Systems Used in Hull, Machinery, and Structural Applications Inside Naval Submarines," **1991**.

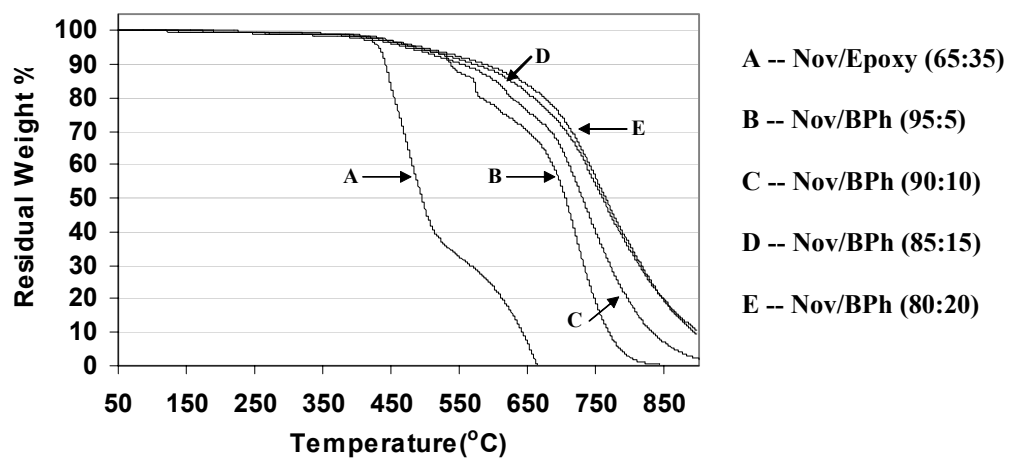


Figure 4.11: Residual weight of Nov-BPh networks by TGA in air

performance such as peak heat release rates, ignitability, and combustion gas generation. The cone calorimeter is an instrument which applies a given radiant heat flux, such as 50 kW/m², to the surface of a 4" x 4" sample. The surface of the sample is continually sparked until it ignites, then the sample is allowed to burn. The cone calorimeter records such flammability characteristics as peak heat release rates, total heat released, and char yield following the burning process.

The MIL-STD-2031 specification has been in place for the last decade, however the bisphtalonitrile composites are one class of only a few organic materials which has met the specifications without surface treatment.^{166, 167, 168} Therefore these materials have been of significant interest to the Navy for materials aboard submarines as well as naval vessels. However, the greatest drawbacks against these materials have been their high cost and lack of availability.

Our approach, which has involved curing the low cost novolac with relatively low weight percentages of BPh, has enabled us to produce materials with the combined properties of superior flame resistance and ductile, structural mechanical properties. Cone calorimetry results demonstrated that the rates of burning for the novolac-BPh networks were slow as compared to almost any other flame retardant networks or linear polymers (Table 4.1).^{179, 184, 187} The peak heat release rate represents the maximum burning rate during the experiment. For example, at an incident heat flux of 50 kW/m², the peak heat release rate of an 80wt. percent novolac-20wt. percent bisphtalonitrile neat network (i.e., no reinforcing fibers) was 137 kW/m², almost as low as the resole control material with a value of 116 kW/m² (recall that the resoles are known to be flame resistant but are quite brittle).

Table 4.1: Cone calorimetry results measured at an incident heat flux of 50kW/m² for 90:10 and 80:20 wt:wt novolac-BPh networks as compared to selected aromatic linear polymers

Material	Time to Ignition (s)	Total Heat Release (MJ/m²)	Peak Heat Release Rate (kW/m²)	CO/CO₂ (kg/kg)	% Char Yield
Novolac/BisA Epoxy (65:35)	74	156	263	.02	26
Commercial Resol Network (Control)	-	-	116	.011	65
Polyetherimide*	70	128	128	.08	79
Polysulfone*	67	297	431	.06	56
Fluorine and Phosphorus containing Polyether*	91	87	120	5.0	19
Novolac/BPh (90:10)	73	85	212	.015	53
Novolac/BPh (80:20)	102	49	137	.019	54

* Koo JH, Venumbaka S, Cassidy PE, Fitch JW, Grand AF, Bundick J. Fire and Mater 2000; 24: 209-18.

This can be compared to a typical peak heat release rate of 1250 kW/m^2 for aromatic epoxy networks measured under the same conditions.¹⁵⁵ Upon increasing the network concentration of BPh from 10 to 20 weight percent, the total heat released and peak heat release rate decreased while the time to ignition increased. This is most likely a result of a higher level of crosslinking in the 80:20 network which improved the thermo-oxidative resistance. The char yields for both networks after burning (from the cone calorimetry measurements – Table 4.1) were similar.

4.4.5 Network Fracture Toughness

Critical stress intensity factors (K_{Ic}) were measured to determine toughness and relate this to the chemical compositions. The 85:15, 80:20, and 75:25 novolac-BPh wt:wt networks all had good toughness ranging from 0.8 to $>1 \text{ MPa}\cdot\text{m}^{1/2}$ (Figure 4.12). Such values mean that these materials fall into the range of epoxy networks, and are a tremendous improvement over the analogous K_{Ic} value of $0.16 \text{ MPa}\cdot\text{m}^{1/2}$ recorded for the resole control network. It is also significant that although the novolac-BPh networks had much higher levels of crosslinking as related to the phenolic-epoxy networks previously evaluated in our laboratories^{154, 155, 156} this did not diminish their toughness.

4.5 Conclusions

We have discovered that high compositions of phenolic novolac oligomers can be readily cured with 15-20 weight percent of bisphthalonitriles to form tough, high T_g , extremely flame resistant thermosets. Studies of soluble model compounds suggest that the molecular structures of the novolac-BPh crosslinks are isoindole and diimine

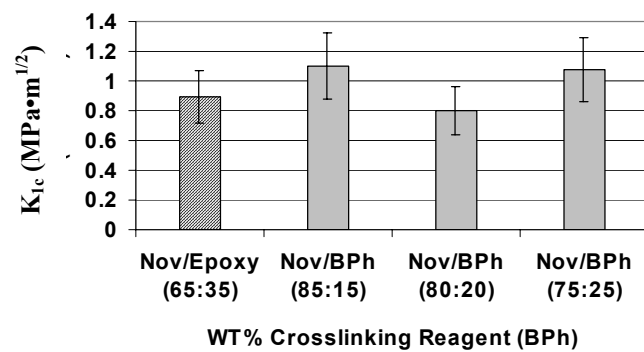


Figure 4.12: K_{Ic} versus novolac-BPh composition

structures. Current focus is on elucidating the molecular structures of other novolac-BPh compositions and understanding the evolution of such structures during burning.

Chapter 5: Novolac/Biphenoxyphthalonitrile Carbon Fiber Reinforced Composites

5.1 Introduction

Currently there is a great demand for a new class of high performance composite materials which bridge the gap between organic, metal, and ceramic based materials. The requirements for this new class of composite material are that it must have good processability, show good mechanical performance characteristics and long term, high service temperature capabilities.¹⁹⁰ Other requirements include good dimensional stability, excellent thermo-oxidative stability, moisture resistance and insulating properties. Over the past 50 years research in this area has been mainly stimulated by the performance demands of the aerospace industry. Initially, epoxy matrix composites were developed with great success for specialty aerospace applications.

Today epoxy based resins are widely used in the aerospace industry to fabricate composite materials which are used as structural materials for aircraft and cruise missiles. However these materials can not be used at temperatures above 200 °C due to the material passing through its glass transition temperature. This results in a catastrophic loss in mechanical properties for the composite. Another major limitation for the epoxy based composites is their thermo-oxidative resistance. These materials begin to degrade rapidly at temperatures well below 400 °C and once the degradation begins these materials sustain ignition. Although the epoxy composites have excellent mechanical properties the lack of thermo-oxidative stability at elevated temperatures has eliminated these materials as high performance candidates particularly for marine applications. The

¹⁹⁰ S. B. Sastri, J. P. Armistead, T. M. Keller, "Phthalonitrile-Carbon Fiber Composites," *Polymer Composites*, **17**, 1996, 816.

lack of high performance capabilities of the epoxy materials has led to intensive research over the past several years to develop materials with the desired high temperature performance characteristics.

Polyimide composites have been shown to have upper limit temperature performance and thermo-oxidative performance superior to that of epoxy matrix based composites. Polyimide systems have been demonstrated to retain useful mechanical properties up to 250 °C and good thermo-oxidative stability approaching 500 °C.¹⁹⁰ In fact, the polyimide matrix materials such as PMR-15 have become the most widely used high performance matrix material.^{191, 192, 193, 194, 195, 196} However, the polyimide matrix materials have been limited in terms of high performance applications due to difficulty in processing. A major problem is in processing blister and void-free components using these matrix resins due to the volatilization of a low boiling component that is generated during the step growth synthesis of polyimides.¹⁹⁷ These flaws compromise the mechanical properties of the final composite material which limits the application scope of these materials.

Phthalonitrile based composites have been developed by Keller et al. of Naval research which have high temperature mechanical and thermo-oxidative properties

¹⁹¹ J. G. Smith, P. M. Hergenrother, "Chemistry and Properties of Phenylethynyl Phthalic Anhydride Imide Oligomers," *Polymer Preprints*, **35**, 1994, 353.

¹⁹² J. G. Smith, J. W. Connell, P. M. Hergenrother, J. M. Criss, "Resin Transfer Moldable Phenylethynyl Containing Imide Oligomers," *Journal of Composite Materials*, **36**, 2002, 2255.

¹⁹³ P. M. Hergenrother, "Encyclopedia of Polymer Science and Engineering," John Wiley and Sons, Inc., New York, **1985**.

¹⁹⁴ P. M. Hergenrother, R. G. Bryant, B. J. Jensen, S. J. Havens, "Phenylethynyl-Terminated Imide Oligomers and Polymers Therefrom," *Journal of Polymer Science Part A: Polymer Chemistry*, **32**, 1994, 3061.

¹⁹⁵ P. M. Hergenrother, J. W. Connell, J. G. Smith, "Phenylethynyl Containing Imide Oligomers," *Polymer*, **41**, 2000, 5073.

¹⁹⁶ P. M. Hergenrother, J. G. Smith, "Chemistry and Properties of Imide Oligomers End-Capped with Phenylethynylphthalic Anhydrides," *Polymer*, **35**, 1994, 4857.

superior to that of the polyimide base composites.^{190, 197, 198, 199, 200, 201, 202, 203, 204, 205, 206, 207,}

²⁰⁸ It has been shown that these materials have degradation temperatures in air of ~500 °C and useful long term mechanical properties at 371 °C. It has also been demonstrated that phthalonitrile resins have low enough viscosity to be processed using the economical vacuum assisted resin transfer and molding technology (VARTM). Although the phthalonitrile resins have excellent processability and the resultant composites have good high performance characteristics there are two major factors which limit the applications of these materials. The phthalonitrile resins are highly expensive(~\$400 per pound) and curing these materials into composites requires temperature in excess of 300 °C for 24 to 72 h. The high cost and impractical cure cycles severely limits the potential for these materials as high performance candidates for aerospace and marine structural materials.

Recently in our labs it has been demonstrated that novolac/biphenoxyphtalonitrile networks can be cured into void-free materials using

¹⁹⁷ T. M. Keller, D. J. Moonay, "Phthalonitrile Resin for High Temperature Composite Applications," *SAMPE Symposium*, **34**, 1989, 941.

¹⁹⁸ T. M. Keller, "Fluorinated High Temperature Phthalonitrile Resin," *Polymer Communications*, **28**, 1987, 337.

¹⁹⁹ T. M. Keller, "Phthalonitrile-Based High Temperature Resin," *Journal of Polymer Science: Part A: Polymer Chemistry*, **26**, 1988, 3199.

²⁰⁰ T. M. Keller, "Synthesis and Polymerization of Multiple Aromatic Ether Phthalonitriles," *Chemistry and Materials*, **6**, 1994, 302.

²⁰¹ T. M. Keller, J. R. Griffith, "The Synthesis of a New Class of Polyphthalocyanine Resins," *ACS Symposium Series*, **132**, 1980, 25

²⁰² T. M. Keller, R. F. Katz, "High Temperature Intrinsically Conductive Polymers," *Polymer Communications*, **28**, 1987, 334.

²⁰³ T. M. Keller, T. R. Price, "Amine-Cured Bisphenol-Linked Phthalonitrile Resins," *Journal of Macromolecular Science-Chemistry*, **A18**, 1982, 931.

²⁰⁴ T. M. Keller, C. M. Rolland, U.S. Patent 5,242,755 (1993).

²⁰⁵ S. B. Sastri, J. P. Armistead, T. M. Keller, U. Sorathia, "Phthalonitrile-Glass Fabric Composites," *Polymer Composites*, **18**, 1997, 48.

²⁰⁶ S. B. Sastri, J. P. Armistead, T. M. Keller, U. Sorathia, "Flammability Characteristics of Phthalonitrile Composites," *SAMPE Symposium*, **42**, 1997, 1032.

²⁰⁷ S. B. Sastri, T. M. Keller, "Phthalonitrile Cure Reaction with Aromatic Diamines," *Journal of Polymer Science: Part A: Polymer Chemistry*, **36**, 1998, 1885.

²⁰⁸ S. B. Sastri, T. M. Keller, "Phthalonitrile Polymers: Cure Behavior and Properties," *Journal of Polymer Science: Part A: Polymer Chemistry*, **37**, 1999, 2105.

relatively low curing temperatures (1 h 200 °C and 3 h 220 °C).²⁰⁹ These network materials have good toughness ($\sim 0.8 \text{ MPa}\cdot\text{m}^{1/2}$), high T_g 's (~ 200 °C) and excellent thermo-oxidative resistance ($\sim 50\%$ char yield at 50 kW/m² heat flux). The novolac/biphenoxyphtlaonitrile networks also have reduced cost when compared to neat phthalonitrile networks due to the primary component being the inexpensive novolac. The primary goal of this research was to demonstrate the feasibility of processing these materials into void-free carbon fiber reinforced composites as potential alternatives to polyimide and neat phthalonitrile networks for certain high performance marine and aerospace applications.

5.2 Experimental

5.2.1 Materials

The commercial novolac resin was provided by Georgia-Pacific (Product no. GP-2073). The novolac resin was 7 functional with an average molecular weight of $\sim 700 \text{ g/mole}$. 4,4'-Bis-(3,4-dicyanophenoxy)biphenyl (biphenoxyphtalonitrile) (BPh) was generously provided by Eikos Incorporated. The two reagents were used as received. The 36K sized AS4 carbon fiber tow was purchased from Hexel Incorporated and used as received.

5.2.2 Preparation of Fracture Toughness Bars Using Novolac and Biphenoxyphtalonitrile at 85:15 Wt:Wt Ratio

Approximately 85g of novolac resin was charged to a three-neck, round bottom flask equipped with a vacuum tight mechanical stirrer and vacuum adapter. The novolac

²⁰⁹ M. J. Sumner, M. Sankarapandian, J. E. McGrath, J. S. Riffle, U. Sorathia, "Synthesis and Physical Property Characterization of Novolac/Biphenoxyphtalonitrile Networks," *Polymer*, **43**, 2002, 5069.

was melted at approximately 200 °C, was degassed for 10 to 15 min at 2-5torr, then the required amount of BPh(15g) was added resulting in a liquid blended composition. The solution turned black when the BPh diffused into the novolac melt. The solution was stirred and further degassed for approximately 5 min, then poured into a preheated polysiloxane mold. Each molded sample was cured for 1 h at 200 °C and 3 h at 220 °C in air, then cooled to room temperature. The dimensions of the cured samples were 3.18 mm in thickness, 6.35 mm in height, and 38.1 mm in length.

5.2.3 Hot-Melt/Powder Prepregging and Composite Fabrication of Carbon Fiber Reinforced Composites Containing Novolac/Biphenoxyphthalonitrile (85:15 Wt:Wt) Matrix Material

A model 30 prepegger manufactured by Research Tool Corporation, Ovid, MI, USA was used in composite preparation (Figure 5.1). Using this apparatus, a 36K sized AS4 carbon fiber tow was passed through a wedge-slit die at the bottom of heated resin pot containing the melted novolac. The wetted tow was then passed between a pair of flattening pins and around a guide roller before being wound on a drum. The flattening pin, guide rollers, and resin bath were independently heated. The resin bath was heated to ~200 °C while the guide rollers and flattening pin were heated to ~180 °C. These high temperatures were necessary to give a low enough melt viscosity to adequately process these materials. The low melt viscosity was necessary to permit to good wet-out of the reinforcing fiber tows and yield uniform resin content.

The novolac coated tows were then cut into 7 6" X 6" plies for cross directional composites and 10 6" X 6" plies for unidirectional composites. Each ply was then placed in a 6" X 6" stainless steel mold and coated with a predetermined amount of powder form

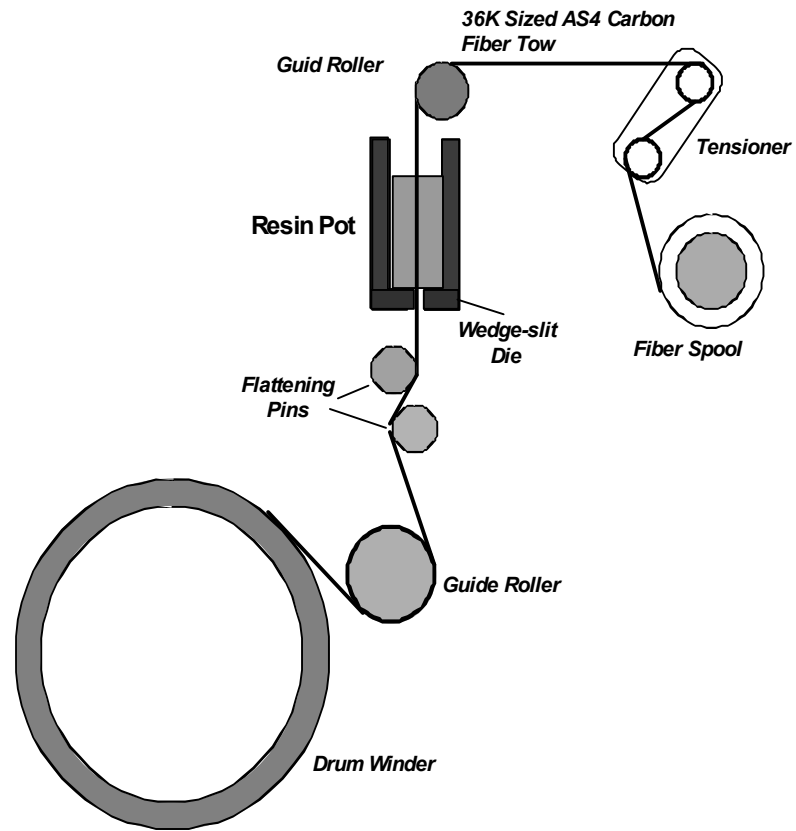


Figure 5.1: The hot-melt prepregging process

biphenoxyphthalonitrile. The amount of biphenoxyphthalonitrile used was such that the weight ratio in the final composite of novolac to biphenoxyphthalonitrile was 85:15. The metal mold was then heated to 200 °C under touch pressure ~50 lbs then the pressure was slowly ramped to 10 tons. Finally, the metal was mold was heated to 200 °C for 1.5 h, 240 °C for 1.5 h, and then allowed to slowly cool to room temperature. The volume fraction of fibers in the composites were determined to be ~60% based on calculations using the densities of the fiber and resin.

5.3 Measurements

5.3.1 Dynamic Mechanical Analysis (DMA)

A TA dynamic mechanical analyzer model Q800 equipped with a three-point-bend clamp was used to determine the T_g 's of the neat novolac/BPh networks(85:15 wt:wt) and carbon fiber reinforced novolac/BPh(85:15 wt:wt) composites. The sample dimensions for the neat novolac/biphenoxyphthalonitrile networks were ~3 mm in thickness, ~6 mm in width, and ~20 mm in length. The dimensions for the composite materials were ~3 mm in thickness, 6~mm in width, and 20 mm in length. At a frequency of 1Hz and an amplitude setting of 20 μ m, the neat network samples were heated from 25 °C to 280 °C at 5 °C/min with the abrupt loss in modulus signifying the T_g .(Note: due to the extreme stiffness of the composites materials an amplitude of 7 μ m had to be used)

5.3.2 Scanning Electron Microscopy (SEM)

The composites were evaluated using SEM by cutting 3 mm (length) by 2 mm (width) by 1 mm (thickness) samples from the composite material using a wet saw. The

samples were embedded in a commercial epoxy and cured overnight. The embedded epoxy samples were sanded until the cross-sectional surface of the composite was reached then the surface of the sample was polished and sputter coated with gold. The cross-sectional surface of the sample was then viewed at 50X and 5,000X magnifications to establish the void-free nature of the composites and to confirm good fiber wet-out and resin distribution occurred during the composite fabrication process.

5.3.3 Melt Rheometry

Using a Brookfield rheometer model DV-III the steady shear viscosity at 170 °C and 190 °C of ~12 g of the novolac/BPh (85:15 wt:wt) resin was measured versus time. (Note: Spindle #27 at 15 rpm was used for these measurements)

5.3.4 Cone Calorimetry

The cone calorimetry composite samples were 6” in length by 6” wide and 0.25” thick. The composites were heated in a horizontal orientation in a cone calorimeter at 75 kW/m² incident heat flux. Char yields, smoke toxicity, peak heat release rates, total heat released, and times to ignition were measured.

5.4 Results and Discussion

The novolac/BPh (85:15 wt:wt) resin was selected to be used for fabrication of composites because it consumes a minimal amount of biphenoxyphthalonitrile and once cured generates a network with good toughness, a high T_g and excellent thermo-oxidative stability.²⁰⁹ However one of the basic requirements for high performance resins is that these materials must have good processability. Therefore it was of great interest to evaluate the melt processability of the novolac/BPh (85:15 wt:wt) resin. At 170 °C and

190 °C the steady shear viscosity was measured as a function of time and compared to a novolac/biphenol A diepoxide (65:35 wt:wt) resin which has been previously demonstrated in our labs to have good processability, toughness, and thermo-oxidative stability.^{210, 211, 212, 213} At 170 °C the viscosity is quite high, however, as the biphenoxyphtalonitrile dissolves into the novolac the viscosity decreases substantially to ~ 7 MPa (Figure 5.2). After reaching this minimum in viscosity, the network begins to cure causing the viscosity to increase drastically. The same observation was made at 190 °C however the initial and final viscosities were considerably lower. At both temperatures the overall processing window was only ~10 minutes. Considering the melt prepregger utilized in this study requires a processing window of ~1.5 h to coat enough carbon fiber tows for the fabrication of cross-ply and unidirectional composites a new processing technique had to be developed for novolac/BPh resins.

A melt/powder prepregging process was developed for the novolac/BPh (85:15 wt:wt) resins where initially the novolac was heated to ~200 °C in the resin pot to acquire good wet-out of the carbon fiber tows. Once enough tows were coated with novolac they were cut into 7 or 10 6" X 6" plies. 7 plies were used to fabricate 0/90 ° cross-directional composites and 10 plies were used for unidirectional composites. Once the desired

²¹⁰ C. S. Tyberg, P. Shih, K. N. Verghese, A. C. Loos, J. J. Lesko, J. S. Riffle, "Latent Nucleophilic Initiators for Melt Processing Phenolic-Epoxy Matrix Composites," *Polymer*, **41**, 2000, 9033.

²¹¹ C. S. Tyberg, K. Bergeron, M. Sankarapandian, P. Shih, A. C. Loos, D. A. Dillard, J. E. McGrath, J. S. Riffle, U. Sorathia, "Structure-Property Relationships of Void-Free Phenolic-Epoxy Matrix Materials," *Polymer*, **41**, 2000, 5053.

²¹² C. S. Tyberg, M. Sankarapandian, K. Bears, P. Shih, A. C. Loos, D. Dillard, J. E. McGrath, J. S. Riffle, U. Sorathia, "Tough, Void-Free, Flame Retardant Phenolic Matrix Materials," *Construction and Building Materials*, **13**, 1999, 343.

²¹³ C. S. Tyberg, P. Shih, K. N. E. Verghese, A. C. Loos, J. J. Lesko, J. S. Riffle, "Latent Nucleophilic Initiators for Melt Processing Phenolic-Epoxy Matrix Composites," *Polymer*, **41**, 2000, 9111.

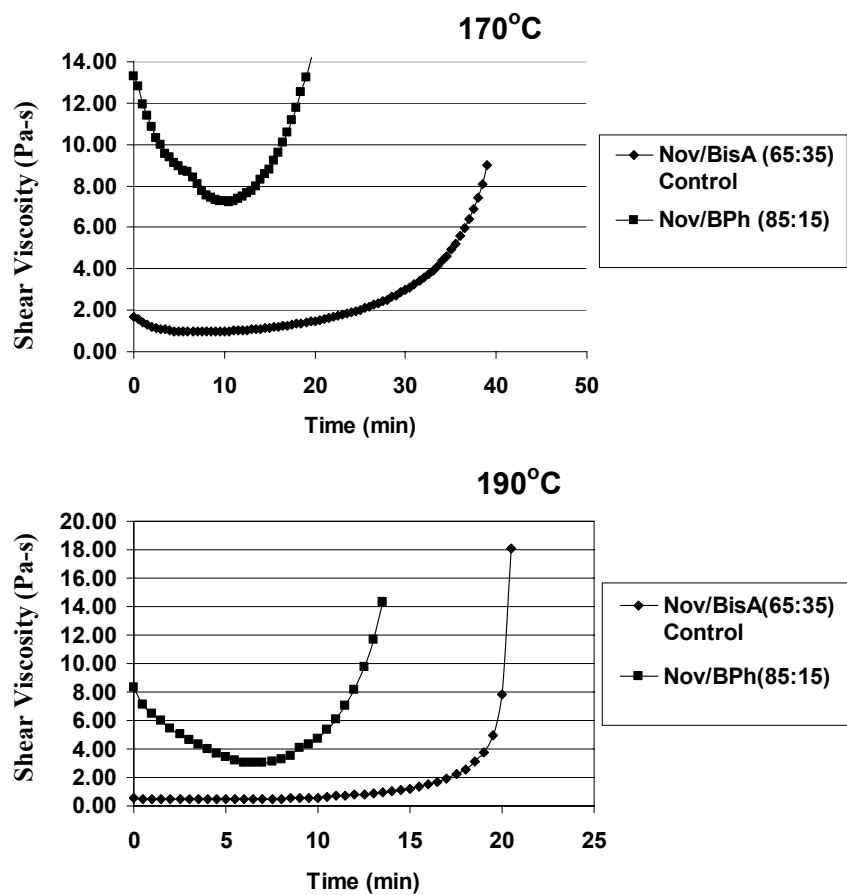


Figure 5.2: Shear viscosity versus time at 170 °C and 190 °C for novolac/BPh (85:15 wt:wt) and novolac/biphenol A diepoxide (65:35 wt:wt) resins

number of plies were cut each ply was placed into a 6" X 6" mold and evenly coated with a predetermined amount of powdered biphenoxyphthalonitrile such that the weight ratio between novolac and BPh was maintained at 85:15. Using a temperature controlled vacuum press, the mold was heated to 200 °C under touch pressure ~50 lbs then the pressure was slowly ramped to 10 tons. Once the final pressure was achieved, the composite was cured for 1.5 h at 200 °C and 1.5 h at 240 °C. Upon completion of the curing cycle the composite was allowed to slow cool to room temperature and the composite was removed from the mold.

Dynamic mechanical analysis was used to evaluate the level of curing that occurred in the composite. The T_g of the matrix material in the composite was compared to the T_g of a neat novolac/BPh(85:15 wt:wt) network material. The results showed that the matrix component of the novolac/BPh (85:15 wt:wt) composite was cured to a lesser extent as compared to the neat novolac/BPh (85:15 wt:wt) network because the T_g of neat network T_g was ~ 20 °C higher than the matrix component in the composite (Figure 5.3) This suggest that the biphenoxyphthalonitrile may not have completely diffused into the novolac during the curing cycle used for the composite. Currently an improved curing cycle for the novolac/biphenoxyphthalonitrile composites is being investigated.

Scanning electron microscopy was utilized to evaluate the wet-out of novolac/BPh (85:15 wt:wt) resin on the carbon fibers and to determine whether the composites were void-free. An analysis of a polished cross-section of the composite demonstrates that the resins did wet-out the fibers due to an absence of cavitation near the surface of the fibers. The lack of voids which would appear as large dark craters within

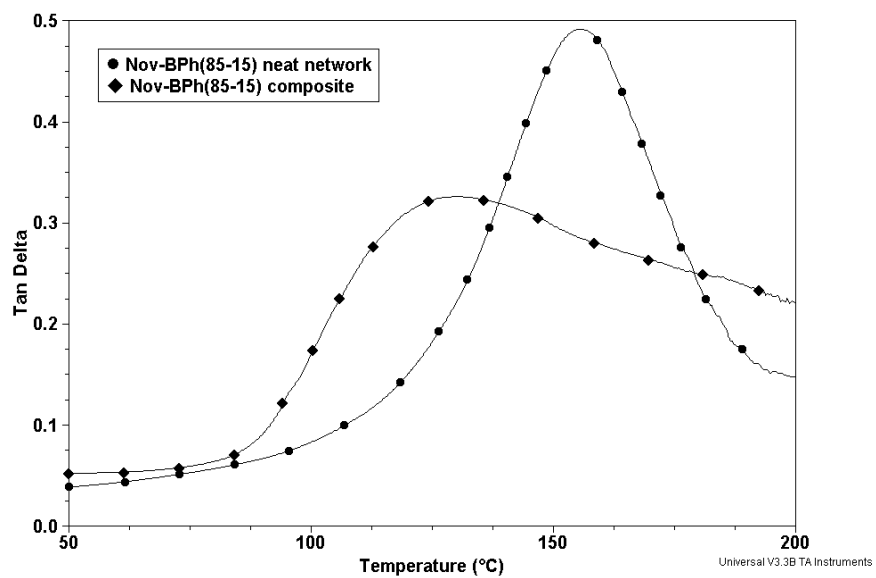


Figure 5.3: DMA at 1 Hz analysis of a novolac/BPh (85:15 wt:wt) neat network and a novolac/BPh (85:15 wt:wt) carbon fiber reinforced composite

the network demonstrated that the composites are indeed void free (Figure 5.4). SEM and DMA analysis both suggested that the melt/powder prepregging process and cure cycle for the novolac/BPh (85:15 wt:wt) resin were both adequate for producing high cured, void-free carbon fiber reinforced composites.

Cone calorimetry at a 75 kW/m^2 heat flux was used to evaluate the thermo-oxidative stability of the novolac/BPh (85:15 wt:wt) composite relative to a novolac/bisphenol A diepoxide(65:35 wt:wt) composite. The results demonstrated that the novolac/BPh composite has improved thermo-oxidative stability in terms of peak heat release rate (Table 5.1). In the event of a fire, the lower peak heat release of the novolac/BPh (85:15 wt:wt) composite suggests that a flame would spread at a considerably slower rate when in contact with the phthalonitrile cured composite. The high char yields for both composites are due to the carbon fiber within the composites.

5.5 Conclusions

It has been demonstrated that novolac/BPh (85:15 wt:wt) composites can be processed into carbon fiber reinforced composite utilizing a new melt/powder prepregging approach. This approach generates a void-less composite with excellent thermo-oxidative stability. In the future an improved curing cycle will be developed and long term mechanical properties at elevated temperatures will be completed on this composite in order to fully evaluate its high performance capabilities.

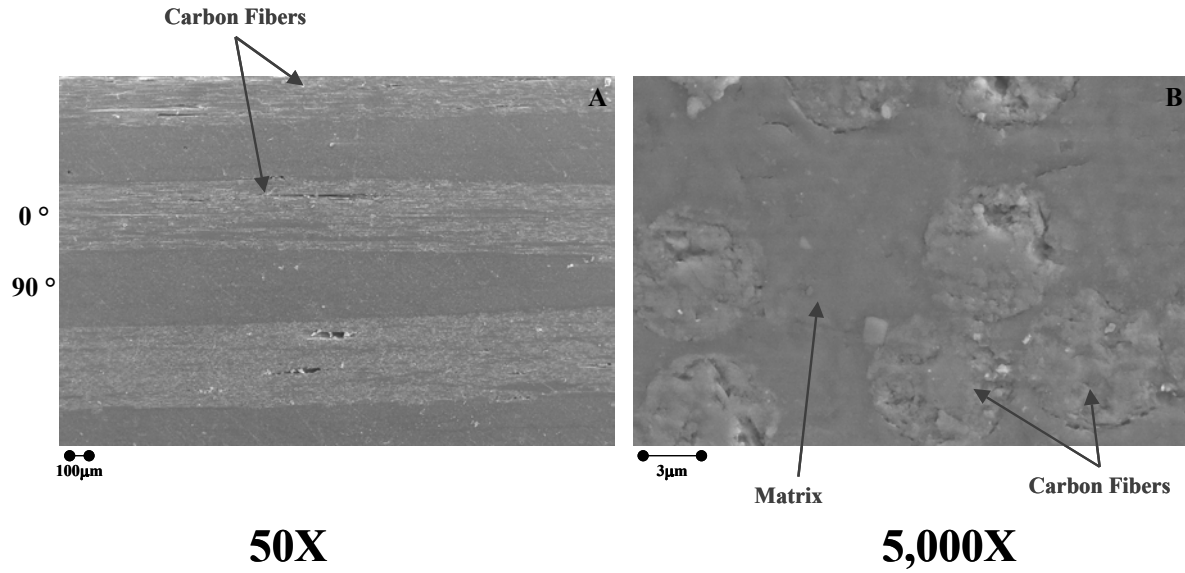


Figure 5.4: A) SEM of a cross-section of a novolac/BPh (85:15) cross ply (0/ 90 °) composite at 50X magnification B) SEM of the 90 ° layer of the cross-ply composite at 5,000X magnification

Table 5.1: Cone calorimetry testing results at a heat flux of 75 kW/m² for novolac/BPh (85:15 wt%:wt%) and novolac/bisphenol A diepoxide composites

Composite	Time to Ignition (s)	Total Heat Release (MJ/m²)	Peak Heat Release Rate (kW/m²)	CO/CO₂ (kg/kg)	% Char Yield
Novolac/BisA Epoxy (65:35)	40	28	216	0.083	70
Novolac/BPh (85:15)	33	29	166	0.072	70

Chapter 6: Synthesis and Characterization of Vinyl Ester/Phthalonitrile Networks and Styrene/Vinyl Phthalonitrile Copolymers

6.1 Introduction

Due to their excellent mechanical and adhesive properties, vinyl ester oligomers diluted with styrene are important matrix resins for thermoset polymer matrix composites. The room temperature processability of the vinyl ester – styrene mixtures coupled with tailorable free radical cure schedules, low cost and excellent mechanical properties make them prime candidates for composites in transportation, infrastructure and marine applications.²¹⁴ However substantial improvements in the flame resistance of these materials must be achieved before these materials can be used in high performance composite applications. The flame performance of current non-halogenated vinyl ester networks in terms of peak heat release is too high for use as structural materials aboard naval vessels or submarines.

Due to its desirable mechanical properties and processability, polystyrene has become a large volume commodity material (~2 billion pounds annually in the U.S.) with a number of current applications.²¹⁵ It is free radically polymerized commercially using suspension and continuous solution processes to a number average molecular weight between 50,000 – 150,000 g/mole.²¹⁶ Due to its relatively low T_g , polystyrene can readily be processed via injection molding into a variety of products for use in domestic and medical applications. However, similar to vinyl ester networks, one of the greatest

²¹⁴ A. Rosario, Ph.D. Thesis, VA Tech, **2002**.

²¹⁵ G. Odian, "Principles of Polymerization," 3rd ed., John Wiley & Sons, Inc., New York, **1991**.

²¹⁶ H. F. Mark, N. M. Bikales, C. G. Overberger, G. Menges, J. I. Kroschwitz (Eds.), "Encyclopedia of Polymer Science and Engineering," Wiley, New York, **1988**.

limiting factors for polystyrene in terms of higher performance applications has been its flammability.

Current technology for enhancing the flame resistance of polystyrene as well as vinyl ester networks involves bromination. Naval and private sector composite manufacturers currently use brominated vinyl ester resins for a variety of applications. Of the 60 million lbs. of vinyl ester sold in the North American market in 2000, 10% (6 million lbs) were flame retardant with an annual growth rate of 4%.²¹⁷ Brominated polystyrene has also been shown to have improved flame resistance relative to pure polystyrene and currently these brominated materials have a number of commercial applications.^{218, 219, 220} Brominated polystyrene and vinyl ester resins have substantially improved flame retardance over analogous non-halogenated materials in terms of reduced peak heat release rates. However these materials generate high levels of toxic smoke during burning, which includes carbon monoxide and corrosive vapors (relative to non-halogenated resins).^{221, 222} The high toxicity of the smoke generated upon burning the brominated resins is undesirable for applications where the material will be enclosed such as aboard naval vessels. Therefore it has been of significant interest to improve the flame resistance of these materials without increasing smoke toxicity.

²¹⁷ R. Martens, Market Manager for CR/FR Composites Inc. Research Triangle Park, N.C. Personal Communications, **2001**.

²¹⁸ K. Pielichowski, A. Puszynski, J. Pielichowski, "Thermal Analysis of Selectively Brominated Polystyrene," *Polymer*, **26**, 1994, 822.

²¹⁹ I. C. McNeill, M. Coskun, "Structure and Stability of Halogenated Polymers. Part 4. Chain-Brominated Polystyrene," *Polymer Degradation and Stability*, **25**, 1989, 1.

²²⁰ I. C. McNeill, M. Coskun, "Structure and Stability of Halogenated Polymers. Part 3. Ring-Brominated Polystyrene," *Polymer Degradation and Stability*, **23**, 1989, 175.

²²¹ M. J. Scudamore, P. J. Briggs, F. H. Prager, "Cone Calorimetry-A Review of Tests Carried Out on Plastics for the Association of Plastic Manufacturers in Europe," *Fire and Materials*, **15**, 1991, 65.

²²² V. Babrauskas, "Smoke and Gas-Evolution Rate Measurements on Fire-Retarded Plastics with the Cone Calorimeter," *Fire Safety Journal*, **14**, 1989, 135.

Improving the flame resistance of commodity materials such as polystyrene and vinyl ester networks has involved the use of fillers such as aluminum trihydrate, antimony oxide, organophosphates, and aluminosilicate nanocomposites. Aluminum trihydrate ($\text{Al}(\text{OH})_3$) is a crystalline material and, when heated to temperatures of 220 °C or greater, decomposes to alumina and water.²²³ The mechanism for flame retardation is that the alumina trihydrate acts as a heat sink absorbing energy through the decomposition reaction. Also the moisture released during this process serves to dilute the gas phase composition which reduces combustion.²²⁴ The greatest hindrance to using aluminum trihydrate as a flame-retardant additive is that it requires high loading levels, ~40 to 60 wt %, to impart significant flame retardance.²²⁵ This increases the viscosity of most polymeric resins to levels that are not processable.

Antimony oxide is a mineral powder and, when used by itself, does not generally improve the flame resistance of organic polymers. However, when this compound is used in combination with an organic chloride, a synergistic effect occurs. The antimony oxide (3 to 1 molar ratio of chlorine relative to each mole of antimony) actually improves the flame resistance of the organo halide.²²³

The antimony oxide/organo halide combinations impart flame resistance by altering the chemistry in the gas phase during thermal degradation. Upon heating, the organic chloride decomposes generating either a chloro acid or chlorine which reacts with antimony oxide to generate antimony halide or antimony oxyhalide.^{223, 224, 225} It has been suggested that these compounds impart flame resistance via three mechanisms. One, a

²²³ H. S. Katz, J. V. Milewski (Eds.), "Handbook of Fillers and Reinforcements for Plastics," Van Nostrand Reinhold Company, New York, **1978**.

²²⁴ P. F. Rankin, "Plastic Additive Handbook," Hanser Publications Inc., Cincinnati, **2001**.

²²⁵ J. Stepek, H. Daoust, "Additives for Plastics," Springer-Verlag Inc., New York, **1983**

reaction between the antimony trihalide and the polymer produces char that serves as a flame protective barrier. Two, the antimony trihalide generates an inert atmosphere and inhibits combustion, and three, it serves as a hydrogen radical scavenger. The combination of these three flame-retarding mechanisms ultimately serves to suppress combustion.^{223, 224, 225}

The addition of organo halides can plasticize polymeric materials. Certain physical properties such as glass transition temperatures and tensile strength are often reduced. It should also be noted that antimony oxide/organic halide flame-retardant combinations can generate high levels of toxic smoke upon burning. The reduction of mechanical properties and increase in smoke toxicity are unattractive features of antimony oxide/organo chloride combinations which limit their utility in high performance applications.

Organic phosphates are usually liquid flame-retardants that can improve the flame resistance of polar polymers. It has been proposed that organic phosphates improve flame resistance of polymers by decomposing into non-volatile acids. These acids promote the formation of char which can act as a flame insulator and mass transport barrier. The mass transport barrier properties of the char retard the escape of volatile decomposition products.^{223, 225, 226}

The greatest disadvantage to utilizing organic phosphates is that high concentrations are required to afford significant improvements in flame retardance. Incorporating high levels of phosphate esters into network materials or linear polymers plasticizes these materials, and this reduces their glass transition temperatures and some

²²⁶ R. P. Levek, "Additives for Plastics," Academic Press Inc., New York, **1978**.

mechanical properties. Also, organic phosphates are hydrolytically unstable due to their reactive ester bonds. Over time upon exposure to water, phosphate esters will lose effectiveness as flame retardants due to hydrolytic cleavage.

Recently, several studies have demonstrated that inexpensive, naturally-occurring aluminosilicate materials, such as smectic clays, can substantially improve the flame retardant properties of polystyrene and vinyl ester networks, while increasing some mechanical properties.²²⁷ Typically these nanocomposite materials are prepared by first replacing the sodium cations in the aluminosilicates with more organophilic cations such as ammonium or phosphonium salts containing alkyl chains which are at least 14 or 16 carbons in length.²²⁸ These material modifications allow for introducing organic polymers through blending or bulk polymerizations.

It has been suggested that these nanocomposite materials exist as either intercalated clay sheets, where the aluminosilicate layers have not lost registry, or exfoliated forms where the aluminosilicate layers are delaminated.²²⁹ From previous investigations there is some evidence to suggest the intercalated materials have the best flammability properties.²³⁰ An intercalated vinyl ester nanocomposite was observed to have a 40% reduction in peak heat release rate (35 kW m⁻² incident heat flux) which is comparable to reductions observed for brominated vinyl ester resins. A mechanism was proposed to explain the flame retardance effects of aluminosilicate materials. It suggests the aluminosilicate material concentrates at the surface of the polymer during the

²²⁷ M. Alexandre, P. Dubois, "Polymer-Layered Silicate Nanocomposites: Preparation, Properties and Uses of a New Class of Materials," *Material Science and Engineering*, **R28**, 2000, 1.

²²⁸ A. R. Horrocks, D. Price (Eds.), "Fire Retardant Materials," Woodhead Publishing, Cambridge, **2001**.

²²⁹ J. Wang, J. Du, J. Zhu, C. A. Wilkie, "An XPS Study of the Thermal degradation and Flame Retardant Mechanism of Polystyrene-Clay Nanocomposites," *Polymer Degradation and Stability*, **77**, 2002, 249.

degradation process where it functions as a barrier to mass transport from the underlying polymer and a barrier to the flame.²³¹

Aluminosilicate materials have been demonstrated to improve the flame resistance of polymers and networks at relatively low concentrations. However, as in the case of linear polymers, adding clay to the vinyl ester resins drives the viscosity of these materials far in excess of 1000 cP. This prohibits these materials from being processed using VARTM (vacuum assisted resin transfer and molding) technology. The VARTM processing method is typically used to prepare large composite parts and has been selected by the U.S. Navy for fabricating fiber reinforced composite materials.²¹⁴

Development of non-halogenated, flame-retardant additives and/or monomers to improve the flame performance of vinyl esters to a level equal to, or superior to, the current naval standard Derakane 510A (a partially brominated vinyl ester – a Dow product) are of great interest. It is also important, however, to maintain processability and mechanical properties. Thus, the objective of this research was to develop a vinyl functional monomer with the following attributes (Figure 6.1):

1. High solubility in vinyl ester resins without increasing viscosity well beyond that required for VARTM composite processing.
2. Free radically curable into vinyl ester networks and copolymerizable with other vinyl monomers (i.e. styrene) without sacrificing the mechanical properties or T_g of the resultant network or polymer.

²³⁰ S. Al-Malaika, A. Golovoy, C. A. Wilkie (Eds.), "Chemistry and Technology of Polymer Additives," Blackwell-Scientific, **1999**.

²³¹ T. J. Pinnavaia, G. W. Beall (Eds.), "Polymer-Clay Nanocomposites," John Wiley and Sons, New York, **2000**.

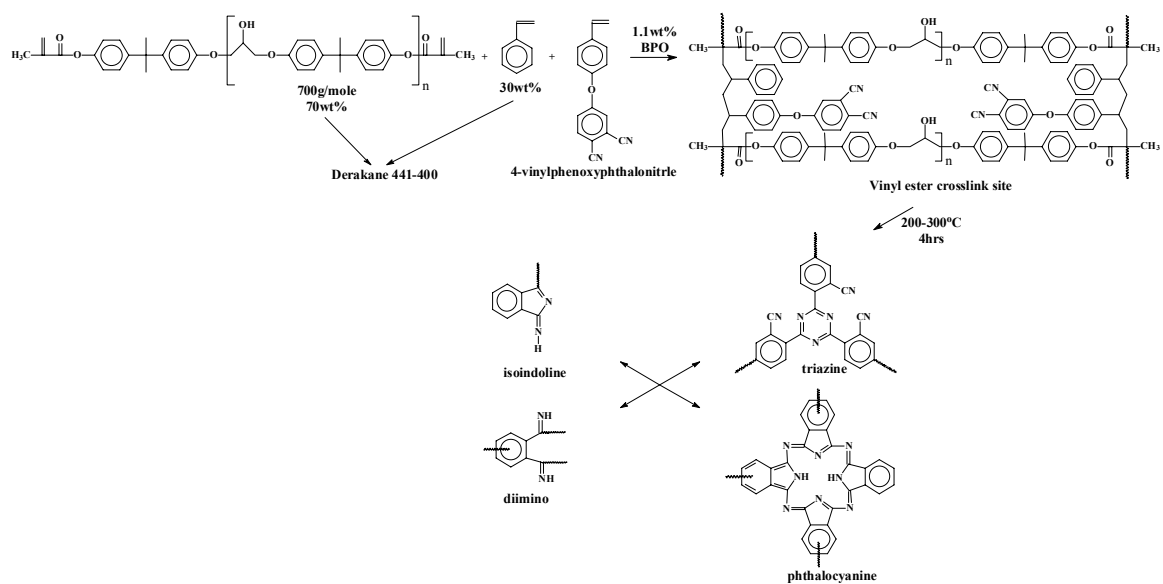


Figure 6.1: Free radical synthesis of the vinyl ester/styrene/4-vinylphenoxyphthalonitrile networks and the formation of heterocyclic crosslinks within the network via post-curing between 200-300 °C for 4 h

3. Improves the flammability performance, due to heterocyclic crosslink formation at elevated temperatures, of vinyl ester networks and styrene to a level that is equivalent or superior to their brominated counterparts.

6.2 Experimental

6.2.1 Materials

4-acetoxystyrene was generously provided by ChemFirst Incorporated and used as received. Hydrochloric acid (38%) (HCl), sodium hydroxide (NaOH), potassium carbonate (K_2CO_3), N-methylpyrrolidone (NMP) and benzoyl peroxide (BPO) were purchased from Aldrich and used as received. 4-Nitrophthalonitrile was synthesized according to the procedure described in Chapter 3. Derakne 441-400 and 510A were kindly provided by the Dow Chemical Co. and used as received. Styrene and chlorobenzene were purchased from Aldrich, stirred over calcium hydride for 24 h, and distilled at 40 °C under vacuum onto activated molecular sieves. Both were kept in a sealed round bottom flask under argon until used (styrene was kept refrigerated). 2,2'-Azobisisobutyronitrile (AIBN) was purchased from Aldrich and refrigerated until used.

6.2.2 Synthesis of 4-Vinylphenoxyphthalonitrile (VinylPh)

An aqueous basic solution was prepared by dissolving 35.2 g (0.628 mol) KOH in 500 mL of deionized water. The solution was charged to a 1000-mL, two-neck, round bottom flask and then cooled to 0-10 °C with an ice bath. 4-Acetoxystyrene (50 mL, 0.327 mol) was added to the cold, rapidly agitating solution, and the hydrolysis reaction was carried out for 4 h at 0-10 °C. After reaction completion, aqueous hydrochloric acid (38% HCl, 30 mL, 0.015 mol) was added with rapid stirring. 4-Vinylphenol (33.9 g,

0.283 mol) precipitated and the intermediate was collected via vacuum filtration and dried for 8-12 h (yield: 86%). The 4-vinylphenol was stored in a sealed amber bottle in a freezer until used.

4-Vinylphenol (5.0 g, 0.042 mol), potassium carbonate (K_2CO_3) (13.821 g, 0.100 mol), 4-nitrophthalonitrile (7.570 g, 0.0438 mol), and ~30 mL of N-methylpyrrolidone (NMP) were charged to a one-neck, 250-mL, round bottom flask. This produced a solution of 4-vinylphenol in NMP with the heterogeneous K_2CO_3 slurried in the mixture. The mixture was rapidly stirred for 24 h at $\approx 25^\circ C$. The 4-vinylphenoxyphthalonitrile product was precipitated by slowly adding the reaction mixture to rapidly stirring (stirred with a blender) water at $\approx 25^\circ C$. The precipitation mixture was agitated for ~10 min in a blender and then 4-vinylphenoxyphthalonitrile was collected and dried via vacuum filtration. The 4-vinylphenoxyphthalonitrile was extracted in water for 8-12 h to remove residual NMP. The 4-vinylphenoxyphthalonitrile (8.58 g, 0.035 mol) was collected by vacuum filtration and allowed to air dry overnight (yield: 84%). The 4-vinylphenoxyphthalonitrile was kept in a sealed amber bottle and stored in a freezer until used. The structure was verified via 1H NMR: 5.3 (dd, 1H), 5.8 (dd, 1H), 6.85 (dd, 1H), 7.15 (m, 2H), 7.4 (dd, 1H), 7.6 (m, 2H), 7.8 (dd, 1H), 8.1 (dd, 1H).

6.2.3 Synthesis of Vinyl Ester/Styrene/4-Vinylphenoxyphthalonitrile Networks

An exemplary synthesis of a vinyl ester/styrene/4-vinylphenoxyphthalonitrile network containing 30 wt % of 4-vinylphenoxyphthalonitrile is provided. 4-Vinylphenoxyphthalonitrile (21 g, 0.0854 mol) and Derakane 441-400 (49 g) (Note: Derakane 441-400 is a Dow Chemical product containing ≈ 70 wt % of an ≈ 700 g mol $^{-1}$ vinyl ester oligomer based on bisphenol-A and epichlorohydrin capped with methacrylate

functional groups, and ≈ 30 wt % styrene) were weighed into a 125-mL Erlenmeyer flask. The vinyl ester/4-vinylphenoxyphthalonitrile resin was heated at ~ 65 °C for about 30 min while rapidly stirring to form a reddish-brown opaque mixture. (It should be noted that resins containing 10 and 20 wt % 4-vinylphenoxyphthalonitrile formed reddish-brown transparent mixtures.) Benzoyl peroxide (0.77 g, 0.003 mol) was dissolved into the resin mixture over ~ 10 min at room temperature. The resin mixture was degassed, then slowly poured into a polysiloxane mold. The resin was cured by heating at 90 °C for 2.5 h, 120 °C for 8 h, and then at 200 °C for 1 h. This heating cycle cured the resin in a free radical reaction. The thermoset network was heated between 200-260 °C for ≈ 4 h to form heterocyclic structures from reaction of the phthalonitrile groups. The crosslink density was a function of the post-curing temperature where the material became more crosslinked as the post-curing temperature was increased.

6.2.4 Synthesis of Styrene/4-Vinylphenoxyphthalonitrile Copolymers

An exemplary synthesis of a copolymer comprised of 75 mole % styrene and 25 mole % of 4-vinylphenoxyphthalonitrile is provided. Other compositions were prepared in a similar manner. Styrene (1.342 g, 1.48 mL, 0.0129 mol) and 4-vinylphenoxyphthalonitrile (1.058 g, 0.004 mol) were dissolved in chlorobenzene (11 mL) and the solution was filtered using a 10-mL disposable syringe equipped with a 0.02 μm (Nylon with GMF) filter to remove any residual salts in the 4-vinylphenoxyphthalonitrile. The solution was transferred to a one-neck, 100-mL, round bottom flask and purged with argon for one hour. AIBN (0.0120 g, 7.0×10^{-5} mol, 0.5 wt % relative to the total weight of monomer) was dissolved in ~ 0.5 mL chlorobenzene and this solution was added to the solution containing the two monomers. The reaction mixture was purged with argon for

approximately 15 min. Using an oil bath, the solution was heated to 75 °C and the free radical copolymerization was allowed to proceed for 24 h at this temperature. The copolymer was precipitated by adding the reaction solution to rapidly stirring (stirred with a blender) methanol and collected via vacuum filtration. The copolymer was dried overnight for 8-12 h under vacuum at 60 °C.

The copolymers were crosslinked using two different curing cycles: 4 h at 220 °C or 4 h at 240 °C. This resulted in a portion of the phthalonitrile groups pendent along the copolymer backbone forming heterocyclic crosslinks.

6.3 Measurements

6.3.1 Dynamic Mechanical Analysis (DMA)

A TA dynamic mechanical analyzer model Q800 equipped with a three-point-bend clamp was used to determine the T_g 's of vinyl ester-styrene-4-vinylphenoxyphthalonitrile networks. The sample dimensions were ~3 mm in thickness, ~6 mm in width, and ~20 mm in length. At a frequency of 1Hz and an amplitude setting of 20 μ m, the samples were heated from 25 °C to 220 °C at 5 °C min⁻¹ with the abrupt loss in modulus signifying the T_g .

6.3.2 Differential Scanning Calorimetry (DSC)

A TA Q1000 model DSC was used to determine the glass transition temperatures (T_g) (approximately 3 to 5 mg) of the styrene-4-vinylphenoxyphthalonitrile copolymers. The samples were heated over a temperature range of 25 to 180 °C at 5 °C min⁻¹, then quenched to 25 °C and heated a second time over the same temperature range at the same rate. The second heating cycle was used to determine the T_g of the copolymer.

6.3.3 Thermogravimetric Analysis (TGA) and Cone Calorimetry

A TA Q0500 TGA was used to evaluate the thermo-oxidative stability of approximately 8 to 10 mg of the copolymers and networks in air. The samples were analyzed in platinum pans from 25 to 800 °C at 10 °C min⁻¹. The temperature at which 5% weight loss occurred was recorded for each sample under atmospheric conditions. Cone calorimetry was completed as described in section 4.3.7.

6.3.4 Gel Permeation Chromatography (GPC)

GPC was performed using a Water 2690 chromatograph equipped with a Viscotek laser refractometer and online differential viscometric detector (Viscotek 100) coupled in series with narrow molecular weight polystyrene standards. The mobile phase was chloroform and the measurements were completed using a flow rate 1.0 mL min⁻¹ at 25 °C.

6.3.5 Proton Nuclear Magnetic Resonance (¹H NMR)

¹H NMR spectra were collected at 80 °C on a Varian Unity 400 MHz instrument operating at a frequency of 399.954 MHz. A 22° pulse angle was used with an acquisition time of 3.7 s and a recycle delay of 1 s. d₆-Dimethylsulfoxide (d₆-DMSO) was used as the NMR solvent for analysis of 4-vinylphenoxyphthalonitrile and 4-vinylphenol. d-Chloroform (d-CDCl₃) was used as the NMR solvent during the styrene/4-vinylphenoxyphthalonitrile synthesis and for the styrene/4-vinylphenoxyphthalonitrile copolymers.

6.3.6 Fourier Transform Infrared Spectroscopy (FTIR) Monitoring of the Conversion of Styrenic, Methacrylate, and Nitrile Groups in Vinyl Ester/Styrene/4-Vinylphenoxyphthalonitrile Resins

FTIR spectra were collected using a Nicolet Impact Model 400 instrument equipped with a controlled temperature cell (Model HT-32 heated demountable cell used with an Omega 9000-A temperature controller). One drop of the vinyl ester/styrene/-4-vinylphenoxyphthalonitrile mixture was placed between two NaCl plates, which were then placed in the FTIR. To cure the networks free radically, the plates were heated to 90 °C for 2.5 h and 120 °C for 8 h. During this cure cycle the heights of the infrared absorbancies at 943 cm^{-1} and 910 cm^{-1} , corresponding to the methacrylate and styrenic group double bonds respectively, were monitored quantitatively and used to calculate reaction conversion. A small background absorbance assigned to the vinyl ester backbone overlapped the absorbance at 943 cm^{-1} (about 20 percent of the initial absorbance at 943 cm^{-1}). Therefore, all spectra were subtracted by a spectrum of the fully cured resin.

, the samples were heated an additional 4 h at 220 °C or 260 °C to cure the nitrile groups and the heights of nitrile stretch (2200 cm^{-1}) were monitored over time and used to calculate reaction conversion. No background subtraction was employed on these spectra because all of the nitrile groups could not be converted without thermally degrading the network. Thus a spectrum with all of the nitrile groups reacted could not be obtained.

Corrections for any changes in sample thickness during the free radical or nitrile cures were made by normalizing the spectra to the 830 cm^{-1} absorbance assigned to the vinyl ester poly(hydroxyether) backbone. Reaction conversion (“a” in equation 6.1) was

$$a = 1 - \frac{A_t}{A_o} \quad \text{Equation 6.1}$$

determined from the change of the normalized absorbance after subtraction of the background (Note: background subtraction was not used for monitoring the conversion of the nitrile groups) where A_o and A_t were the normalized absorbances before the reaction and at reaction time t .

6.3.7 Melt Rheometry

Steady shear viscosities between 25 and 60 °C of approximately 12 g of a vinyl ester-styrene/4-vinylphenoxyphthalonitrile resin mixture were measured at 15 rpm using a Brookfield rheometer model DV-III. After each temperature increase the sample was given ~5 minutes to thermally equilibrate before the shear viscosity was recorded. (Note: Spindle #27 at 15 rpm was used for these measurements)

6.4 Results and Discussion

6.4.1 Synthesis of 4-Vinylphenoxyphthalonitrile

A two step synthetic scheme was used to synthesize 4-vinylphenoxyphthalonitrile in good yield (Figure 6.2). The first step involved hydrolyzing the acetate group of 4-acetoxystyrene (**1**) with an aqueous, 10 wt % potassium hydroxide solution. Initially, the basic aqueous solution was cooled in an ice bath, then the required amount of 4-acetoxystyrene was added with rapid mixing, to form a heterogeneous solution. However, after ≈ 3 hours at ≈ 0 °C, the reaction became a homogeneous transparent yellow solution. The reaction was continued for another hour to ensure completion, and

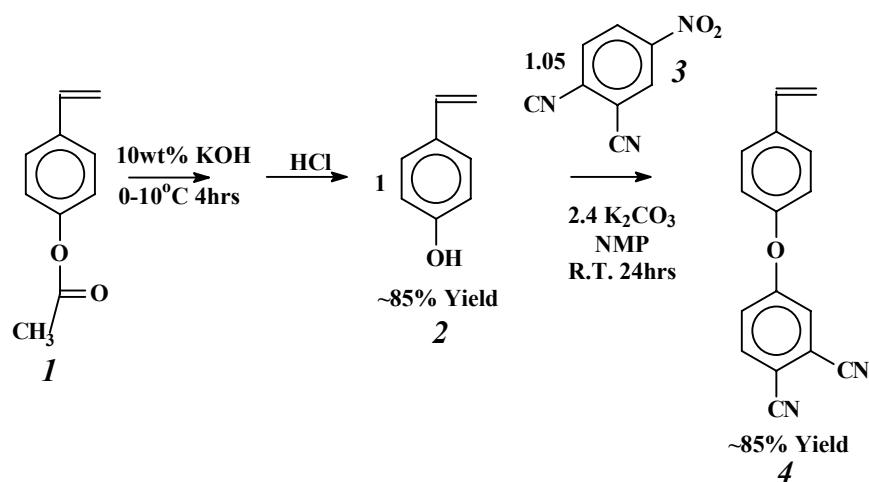


Figure 6.2: Two step synthetic scheme for the synthesis of 4-vinylphenoxyphthalonitrile

then HCl was added while rapidly stirring. Upon adding the acid, 4-vinylphenol (**2**) precipitated out of solution and was collected via vacuum filtration, air dried overnight, and then characterized using ^1H NMR (yield $\sim 85\%$) (Figure 6.3).

The second step in the reaction scheme was a nucleophilic aromatic displacement reaction between 4-vinylphenol and 4-nitrophthalonitrile. 4-Vinylphenol (**2**) was reacted with 4-nitrophthalonitrile (**3**) (5 mole % excess) at room temperature with NMP as the solvent and potassium carbonate serving as the weak base. The reaction was carried out for 24 hours, and after completion, 4-vinylphenoxyphthalonitrile was precipitated by adding the reaction solution to rapidly stirring (stirred with a blender) room temperature water. The brownish-beige 4-vinylphenoxyphthalonitrile was collected via vacuum filtration and then stirred for ~ 24 hours in room temperature water to remove residual salts and NMP. After extraction, the compound turned a light beige and was collected and dried via vacuum filtration (yield $\sim 85\%$). Characterization via ^1H NMR demonstrated that the desired 4-vinylphenoxyphthalonitrile product was indeed synthesized (Figure 6.4).

6.4.2 Synthesis and Characterization of Vinyl Ester/Styrene/4-Vinylphenoxyphthalonitrile Networks

The free radical curing reactions of the vinyl ester/styrene/4-vinylphenoxyphthalonitrile resins was studied with FTIR by monitoring the disappearance of the vinyl stretches at 900 and 950 cm^{-1} . No new vinyl stretches were present in the FTIR spectra relative to the control vinyl ester material (Figure 6.5). This demonstrated that the vinyl stretches of styrene and 4-vinylphenoxyphthalonitrile overlapped. Therefore

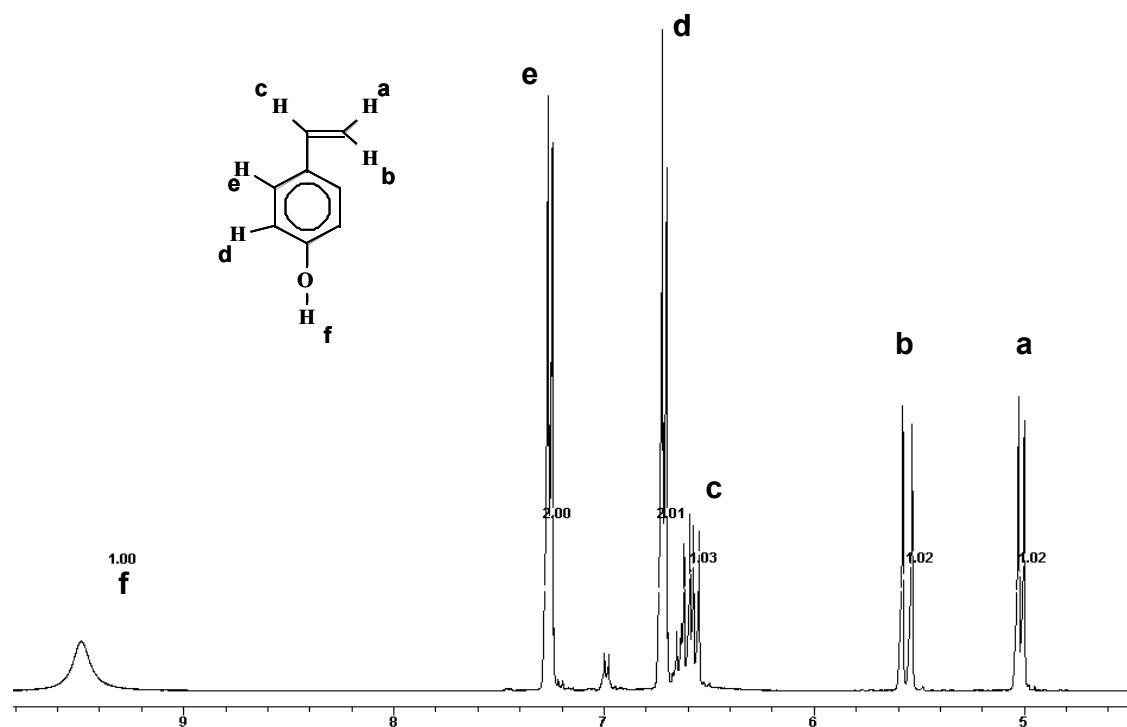


Figure 6.3: ^1H NMR of 4-vinylphenol

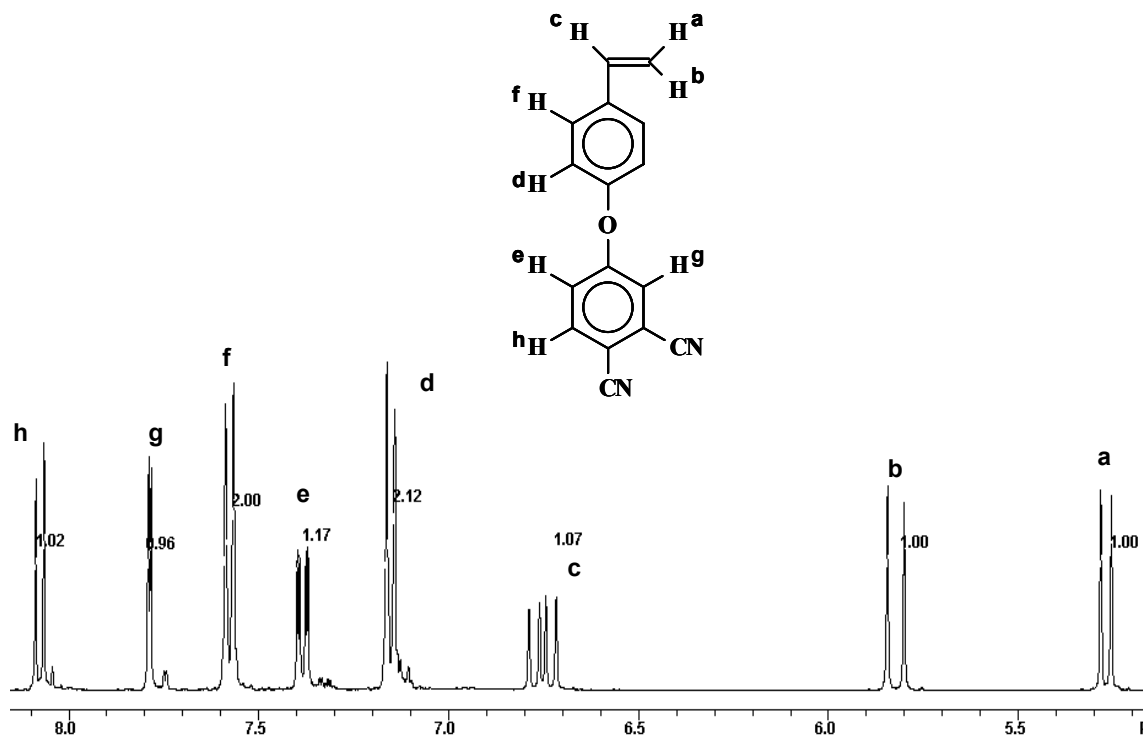


Figure 6.4: ^1H NMR of 4-vinylphenoxyphthalonitrile

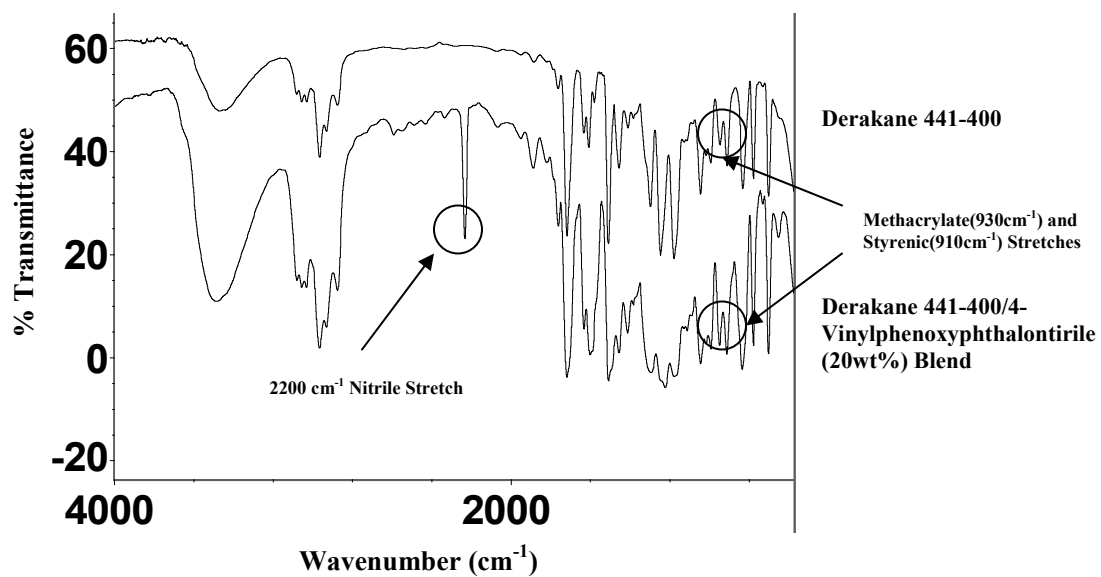


Figure 6.5: FTIR spectra of Derakane 441-400 resin and a blend of 80 wt % Derakane 441-400 with 20 wt % 4-vinylphenoxyphthalonitrile

when monitoring the cure of the Derakane 441-400/4-vinylphenoxyphthalonitrile resins, the vinyl stretch at 910 cm^{-1} was indicative of both the vinyl groups of styrene and 4-vinylphenoxyphthalonitrile.

The free radical curing of Derakane 441-400 and three different Derakane 441-400/4-vinylphenoxyphthalonitrile (VinylPh) resin mixtures containing 20, 30 and 40 weight % 4-vinylphenoxyphthalonitrile were quantitatively monitored using FTIR. Each resin contained 1.1 weight % of benzoyl peroxide and the FTIR spectra were collected from one drop of the resin placed between two NaCl plates and heated to the appropriate temperature. The plates were heated for 2.5 hours at $90\text{ }^{\circ}\text{C}$, 3 hours at $120\text{ }^{\circ}\text{C}$, and 1.5 hours at $220\text{ }^{\circ}\text{C}$ using a temperature controlled cell. The heights of the methacrylate absorbance at 930 cm^{-1} and the styrenic peak at 910 cm^{-1} were monitored versus time and temperature. Corrections for any changes in sample thickness during the cure were made by normalizing the spectra to the 830 cm^{-1} absorbance assigned to the poly(hydroxyether) backbone.

The FTIR data indicated that increasing the weight % of 4-vinylphenoxyphthalonitrile does not affect the overall conversion of the styrenic groups. The control material without any phthalonitrile monomer, and the resins containing 20, 30 and 40 wt % 4-vinylphenoxyphthalonitrile all had similar cure profiles. The FTIR indicated that all of these networks had $\sim 90\%$ conversion of the styrenic groups after reacting for 2.5 hours at $90\text{ }^{\circ}\text{C}$ and ~ 2 hours at $120\text{ }^{\circ}\text{C}$ (Figure 6.6). This observation demonstrated that 4-vinylphenoxyphthalonitrile was curing into the networks and had similar reactivity to styrene. However, $\sim 85\%$ of the methacrylate groups in the control material had

Curing Conditions: 1.1wt% BPO 2.5hrs 90 °C, 3hrs 120 °C, and 1.5hrs 220 °C

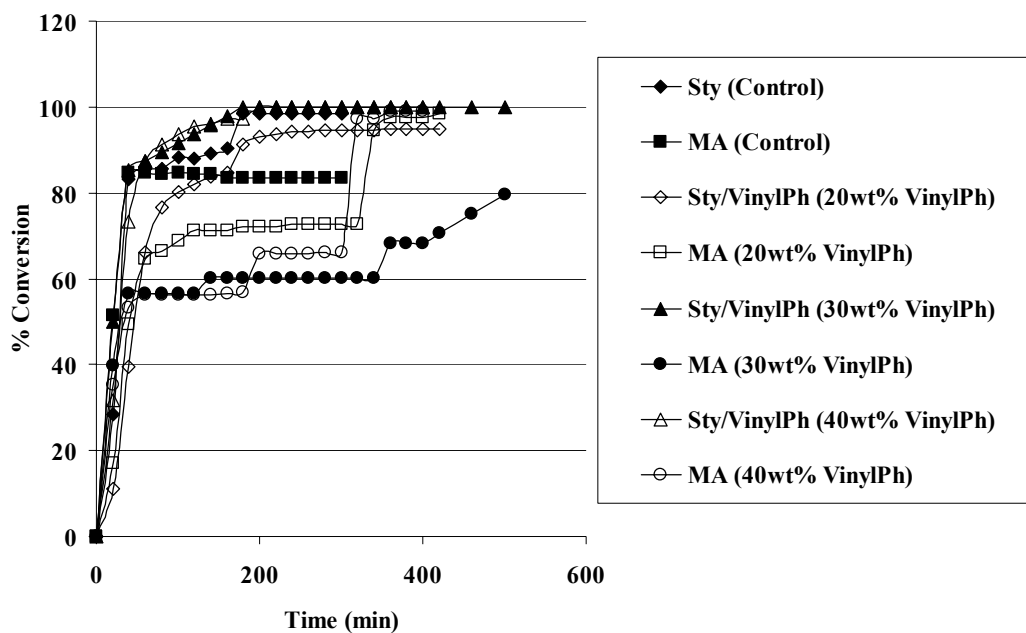


Figure 6.6: Conversion of methacrylate and styrenic groups with Derakane 441-400 and Derakane 441-400/4-vinylphenoxyphthalonitrile resins mixtures versus time

reacted after curing for 2.5 hours at 90 °C, whereas methacrylate conversion in the resins containing 20, 30, and 40 weight % of 4-vinylphenoxyphthalonitrile were between 60 and 70% after curing under similar conditions. The control and the 20 and 40 weight % 4-vinylphenoxyphthalonitrile resin mixtures reached greater than 90% conversion of the methacrylate groups in less than an hour after the temperature was increased to 220 °C. The reason for the approximately 15-20% reduction in conversion of the methacrylate groups upon adding 20-40 weight % 4-vinylphenoxyphthalonitrile remains under investigation.

The Derakane 441-400/VinylPh networks were also post-cured for either 4 hours at 220 °C or 4 hours at 260 °C to determine if the phthalonitrile groups would increase the crosslink density of the networks through the formation of heterocyclic crosslinks. FTIR was used to monitor the disappearance of the nitrile stretch at 2200 cm^{-1} with each spectrum being normalized relative to the absorbance at 830 cm^{-1} (associated with the poly(hydroxyether) backbone). Background subtraction was not utilized for these spectra because curing all of the nitrile groups to obtain the spectrum of a fully reacted network would have required elevated temperatures such that the network would have degraded thermo-oxidatively.

FTIR results demonstrated that the phthalonitrile groups reacted during the post-cures (Figure 6.7). All of the networks exhibited 10-15% conversion of the nitrile groups when post-cured for 4 hours for 220 °C. The fractional conversion of the nitrile groups in the network containing 20 wt % VinylPh only increased slightly (to 20%) when the post-curing temperature was increased to 260 °C. However, in the networks containing 30

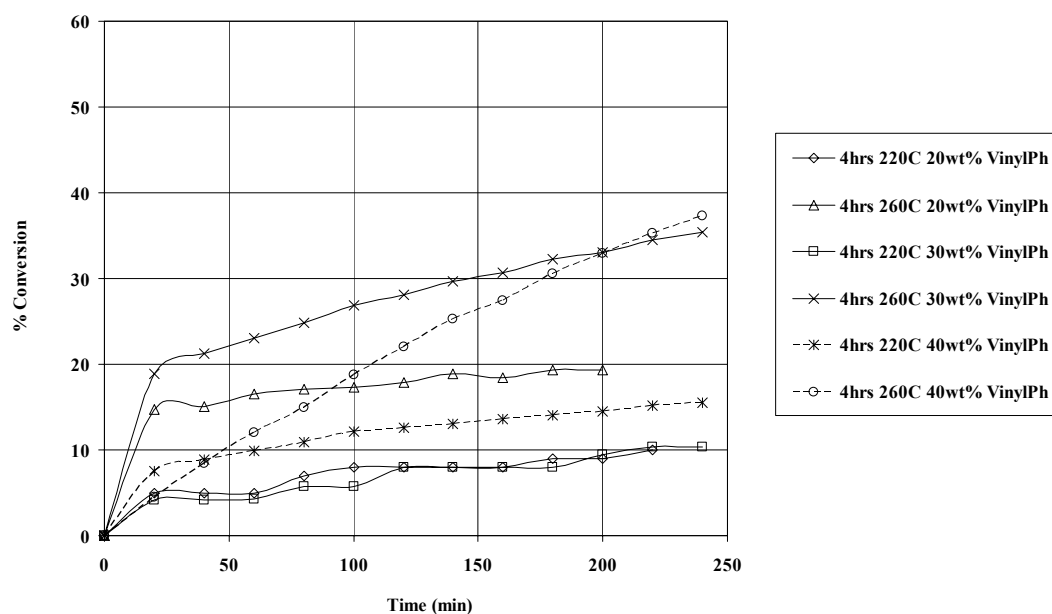


Figure 6.7: Conversion of nitrile groups versus time for Derakane 441-400/4-vinylphenoxyphthalonitrile networks containing 20, 30, and 40 weight% of the vinyl phthalonitrile monomer

and 40 wt % VinylPh, the % conversion increased to ~35%. Overall, the FTIR data indicated that the nitrile groups crosslinked within the first hour at either 220 or 260 °C, and higher post-curing temperatures further increased the conversion of the nitrile groups.

DMA was used to evaluate effects of increasing the concentration of 4-vinylphenoxyphthalonitrile as well as the post-curing temperature on T_g 's and rubbery moduli of Derakane 441-400/VinylPh networks. For networks that were not post-cured, it was anticipated that increasing the weight % of 4-vinylphenoxyphthalonitrile (a difunctional vinyl monomer) in the network would reduce the crosslink density, and result in lower T_g 's and/or rubber moduli relative to the pure Derakane 441-400 network. By contrast, it was expected that the post-cured networks containing the phthalonitrile monomer would have higher T_g 's and/or rubbery moduli relative to the pure Derakane 441-400 networks due to higher crosslink densities.

DMA evaluations demonstrated that networks cured with 1.1 wt % BPO for 2.5 hours at 90 °C, 8 hours at 120 °C, then 1 hour at 200 °C, had lower T_g 's and rubbery moduli as the 4-vinylphenoxyphthalonitrile was increased up to 30 weight % (Figure 6.8). Thus, as expected, increasing concentrations of 4-vinylphenoxyphthalonitrile probably reduced the crosslink densities in the Derakane 441-400/VinylPh networks relative to the control.

DMA also clearly showed the expected increases in T_g 's and rubbery moduli as the concentrations of 4-vinylphenoxyphthalonitrile in the networks and the post-curing temperatures were increased (Figure 6.9). For example, the network containing 40 wt % 4-vinylphenoxyphthalonitrile that was post-cured for 4 hours 260 °C had a T_g of ~180 °C

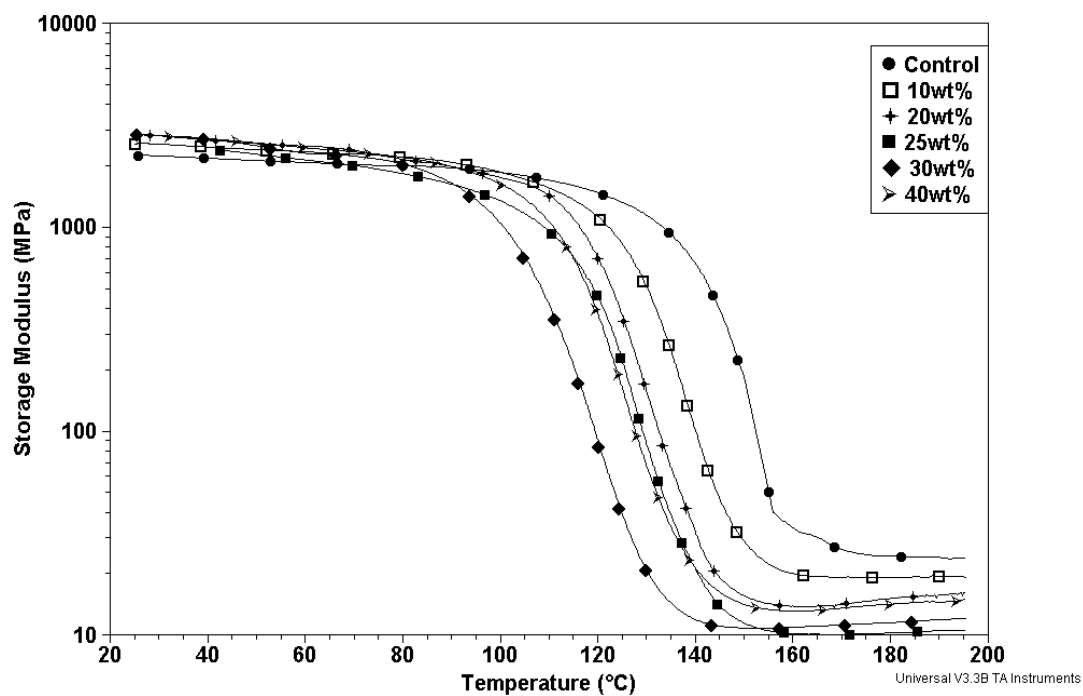


Figure 6.8: DMA analyses of Derakane 441-400/VinylPh networks as a function of the wt % 4-vinylphenoxyphthalonitrile

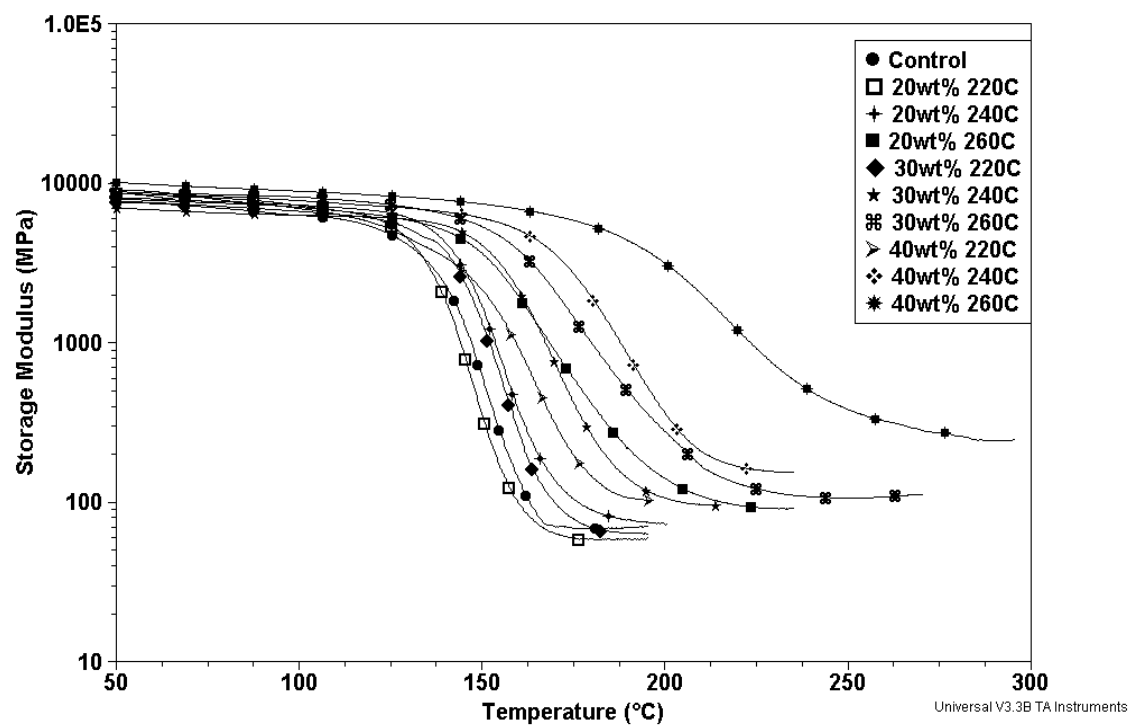


Figure 6.9: DMA analyses of Derakane/4-VinylPh networks that had been post-cured for 4 hours at 220 °C, 240 °C, or 260 °C

(~50 °C above the control), and this network also had a rubbery modulus considerably higher than the control. These results demonstrated that increasing the post-curing temperature and the weight % of 4-vinylphenoxyphthalonitrile increased the crosslink densities. This was attributed to reactions of the phthalonitriles to form higher concentrations of heterocyclic crosslinks.

Thermo-oxidative stabilities of the Derakane/VinylPh networks were evaluated in air with TGA and cone calorimetry. TGA was used to evaluate the weight loss profiles of the networks as the concentrations of 4-vinylphenoxyphthalonitrile and the post-curing temperatures were increased. This demonstrated that increasing concentrations of 4-vinylphenoxyphthalonitrile led to significantly higher char yields between 400 and 600 °C (Figure 6.10). Incorporation of only 10 wt % 4-vinylphenoxyphthalonitrile increased the char yield over this temperature range by ~15%. The network material containing 40 wt % 4-vinylphenoxyphthalonitrile had ~2.5 times greater char yield than the control. These results are significant because char formation is one mechanism by which materials may form a protective coating that may aid in reducing burning rates. Low peak heat release rates in a cone calorimetry experiment are often indicative of materials with good thermo-oxidative performance.

Effects of post-cure conditions on the thermo-oxidative performance of the Derakane 441-400/VinylPh networks were also evaluated by TGA. The results from this study suggested that post-curing the networks for 4 hours at 220, 240, or 260 °C did not improve their stabilities. For example, the network containing 40 wt % of 4-vinylphenoxyphthalonitrile had the same weight loss profile whether the material was post-cured or not (Figure 6.11).

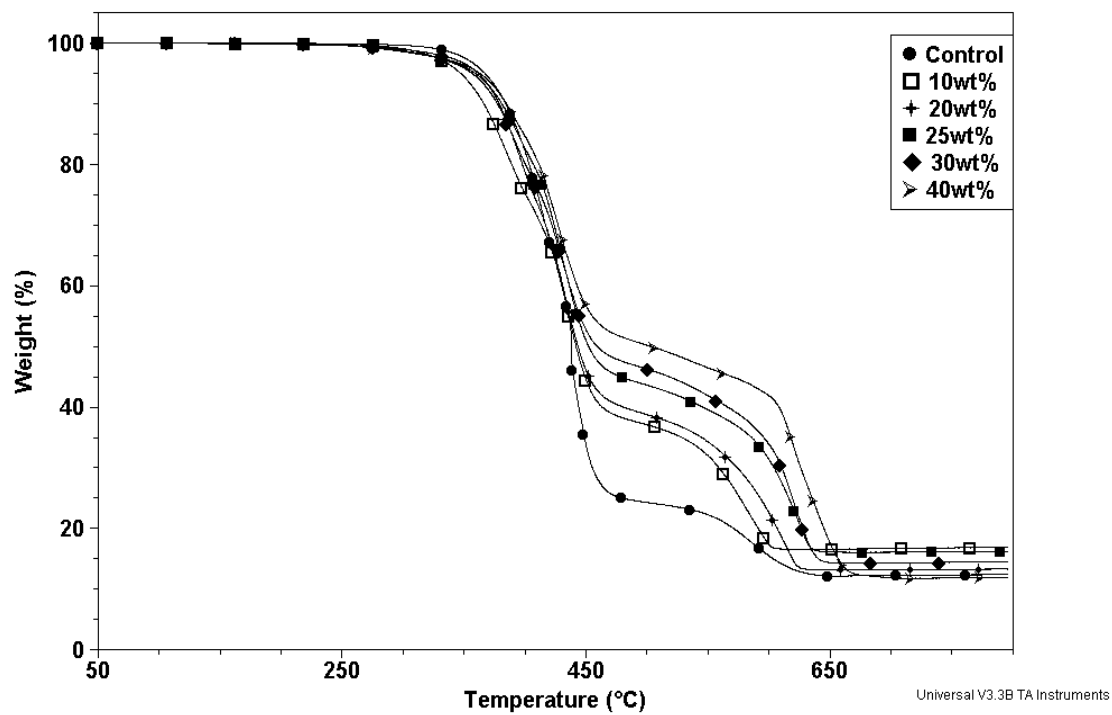


Figure 6.10: TGA analyses of Derakane 441-400/VinylPh networks in air

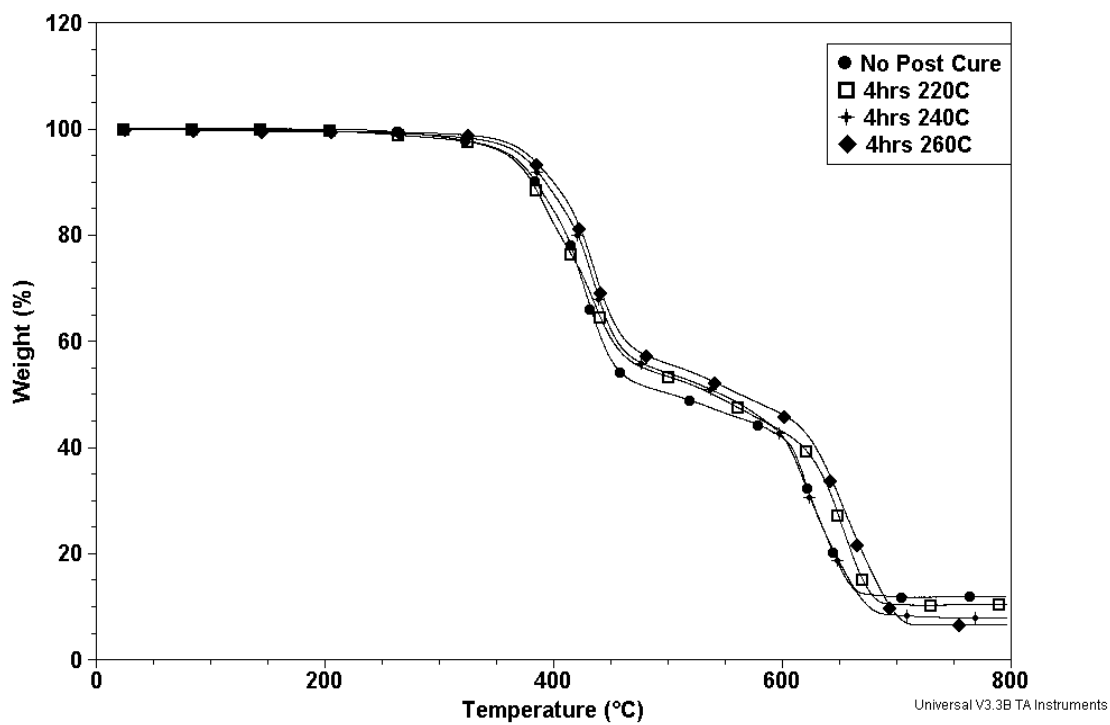


Figure 6.11: TGA analyses of Derakane 441-400/VinylPh (40 wt %) networks in air after post-curing for 4 hours at 220 °C, 240 °C or 260 °C

This finding suggested that the phthalonitrile groups formed heterocyclic crosslinks as the material was heated between 200 and 500 °C before the material began to thermo-oxidatively degrade. The increased crosslink densities enhanced the thermo-oxidative performance of the materials, as evidenced by higher char yields over the 400 to 600 °C temperature range. This observation was significant because this suggests that the Derakane 441-400/VinylPh may have good thermo-oxidative resistance without the post-cure steps.

Cone calorimetry was utilized to evaluate the flame properties of a Derakane 441-400/VinylPh (30 wt %) network relative to Derakane 441-400 (standard resin) and Derakane 510A-40 (brominated resin) networks. The incident heat flux for these measurements was 50 kW•m⁻². The results demonstrated that incorporating 30 wt % of 4-vinylphenoxyphthalonitrile into the Derakane 441-400 resin substantially improved the thermo-oxidative stability of the cured network in terms of peak heat release rate, char yield, and time to ignition (Table 6.1). The peak heat release rate was decreased by ~50%, the time to ignition increased by approximately 10 s, and the char yield increased by ~10%. The flame properties of the Derakane 441-400/VinylPh (30 wt %) networks was further increased by post-curing the network for 4 hours at 240 °C. After post-curing, the peak heat release rate further decreased to ~350 kW•m⁻² which is an approximate 70% reduction relative to the neat network material. The char yield also increased to ~20% and the time to ignition increased an additional 10 seconds. It is interesting to point out that the smoke toxicity levels of the networks co-reacted with the new phthalonitrile monomer (both post-cured and non-post-cured networks) were much

Table 6.1: Cone calorimetry data at an incident heat flux of 50 kW m⁻² for the vinyl ester control (Derakane 441-400), the brominated vinyl ester (Derakane 510A-40), and Derakane 441-400/VinylPh (30 wt %) networks.

Network Material	Time to Ignition (s)	Peak Heat Release Rate (kW/m²)	Total Heat Released (MJ/m²)	Smoke toxicity CO/CO₂ (kg/kg)	% Char Yield
Derakane 441-400 (Control)	30	921	162	0.06	0
Derakane 510A-40	44	193	57	0.13	0
Derakane 441-400/VinylPh (30wt%)	48	489	121	0.03	13
Derakane 441-400/VinylPh (30wt%) (Post-Cured 4 h 240 °C)	60	347	126	0.03	20

lower than for the brominated vinyl ester network. This finding suggests that vinyl ester/VinylPh networks may be suitable alternatives to brominated vinyl ester networks as materials to be used in enclosed spaces.

An important aspect to consider when developing a new flame-retardant monomer is its impact on viscosity after dissolution in the resin (e.g., Derakane 441-400). The resin viscosity should remain below ≈ 1000 cP to be processable into fiber reinforced composites using VARTM technology. Steady shear viscosities of the resin mixture containing 30 wt % 4-vinylphenoxyphthalonitrile were measured from 25-60 °C. The room temperature viscosity of the resin was ~ 1900 cP (somewhat high for VARTM processing). However, when the mixture was heated only ~ 10 °C, the viscosity decreased to ~ 750 cP (easily processable by VARTM) (Figure 6.12). This demonstrated that with only slight heating, the Derakane 441-400/VinylPh resins should be processable by these methods into fiber reinforced composites.

6.4.3 Synthesis and Characterization of Styrene/4-Vinylphenoxyphthalonitrile Copolymers

It was of significant interest to determine whether 4-vinylphenoxyphthalonitrile would free radically copolymerize with styrene at high styrene to 4-vinylphenoxyphthalonitrile molar ratios (75:25 and 90:10) (Figure 6.13). The copolymers were synthesized using 0.5 wt % AIBN as the initiator and chlorobenzene as the solvent, at a reaction temperature of 75 °C for 24 hours. Conversion of the vinyl groups of styrene and 4-vinylphenoxyphthalonitrile versus time were monitored using ^1H NMR. Proton “b” of 4-vinylphenoxyphthalonitrile and proton “a” of styrene were

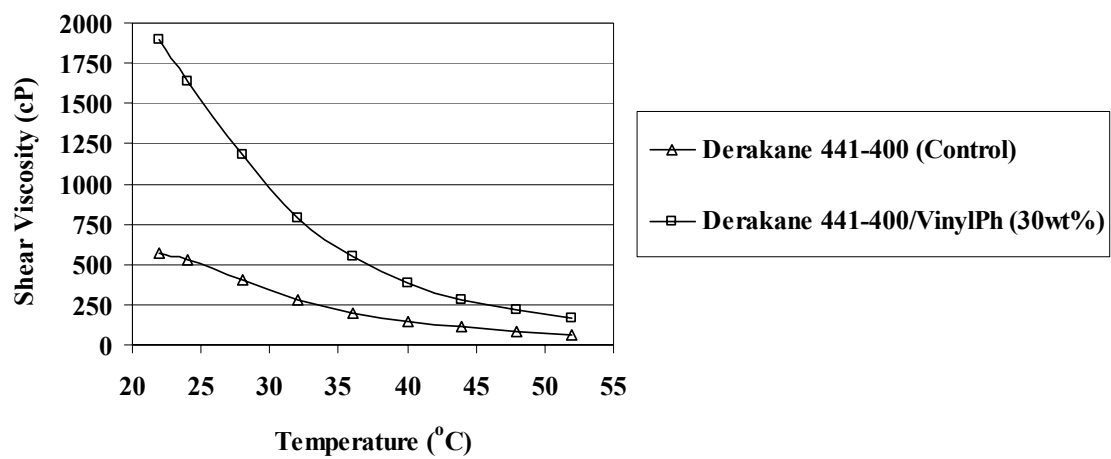


Figure 6.12: Shear viscosity versus temperature for the vinyl ester control (Derakane 441-400) and Derakane 441-400/VinylPh (30 wt %) resins

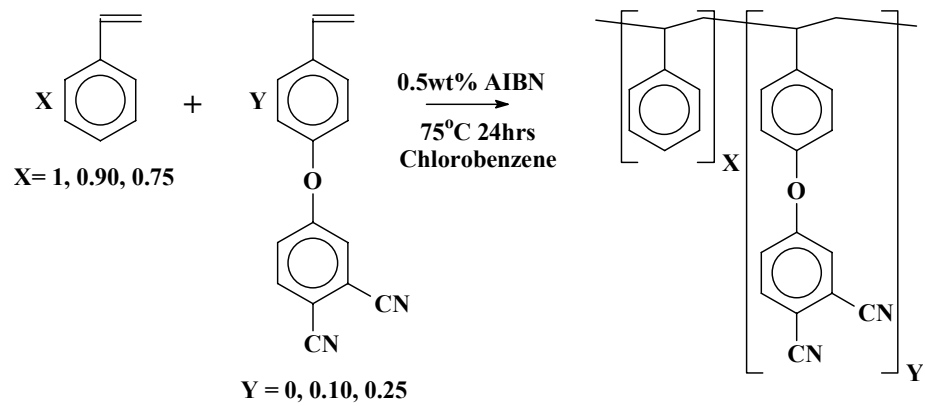


Figure 6.13: Synthesis of styrene/4-vinylphenoxyphthalonitrile random copolymers

normalized in each spectrum relative to proton “c” of 4-vinylphenoxyphthalonitrile (Note: The other two vinyl protons of styrene and 4-vinylphenoxyphthalonitrile at 5.9 ppm and 6.8 ppm overlapped) (Figure 6.14). The “c” proton was used to normalize each spectrum because its concentration in solution did not change over time. The ^1H NMR study indicated that random copolymers of styrene and the vinylphthalonitrile monomer (low mole fractions of phthalonitrile) can be prepared by the method employed. The total conversion of the vinyl groups, including both styrene and 4-vinylphenoxyphthalonitrile, was approximately 60%.

^1H NMR was also used to evaluate the compositions of the 75:25 and 90:10 mol:mol phthalonitrile:styrene copolymers. The fraction of proton “h” to the aromatic protons “a-g” corresponding to the monomer charge ratio in the copolymers was compared to the experimental ratios derived from the ^1H NMR spectra (Figure 6.15). The experimental ratio was higher than the monomer charge ratio in both copolymers. One recommendation for continuing work is to quantify the reactivity ratios of this monomer combination.

GPC indicated that reasonably high molecular weight copolymers were obtained and that their molecular weights and molecular weight distributions were similar to a homopolystyrene prepared under similar conditions (Table 6.2).

DSC was used to evaluate any effects on T_g 's of incorporating 10 and 25 mole % of 4-vinylphenoxyphthalonitrile into the copolymer. DSC was also utilized to determine whether or not crosslinking occurred when the copolymers were cured for 4 hours at 220 °C or 240 °C. The results from the DSC study showed that the (90:10) and (75:25)

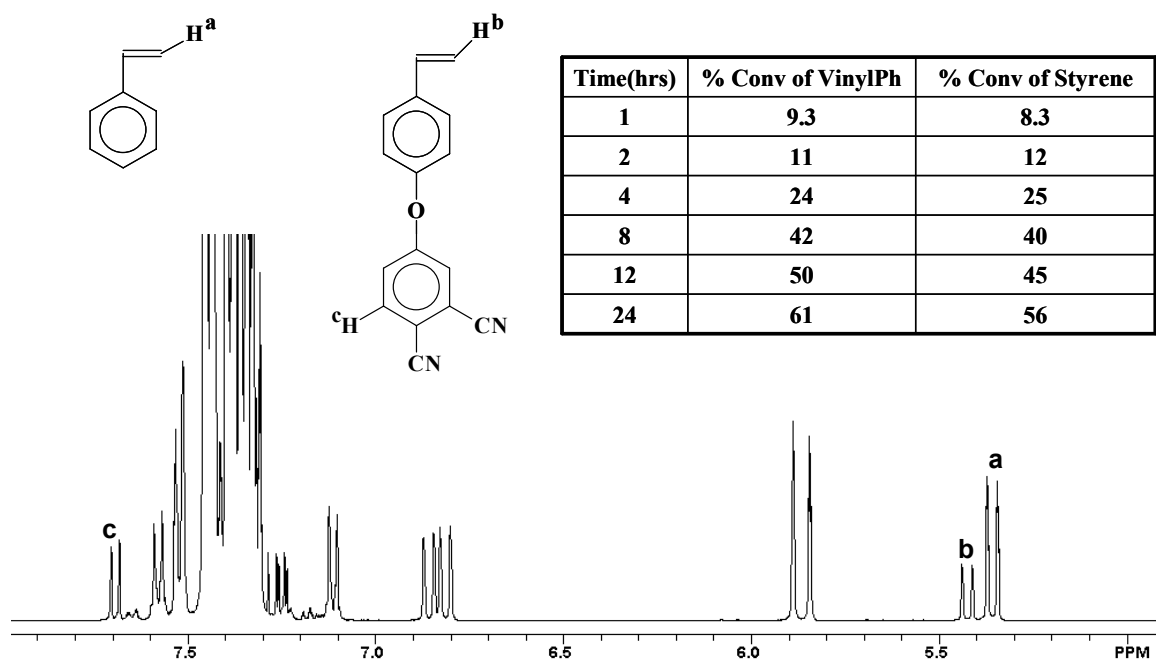


Figure 6.14: 1H NMR monitoring the conversion of styrene versus time for the (75:25 mol:mol) styrene/VinylPh copolymer

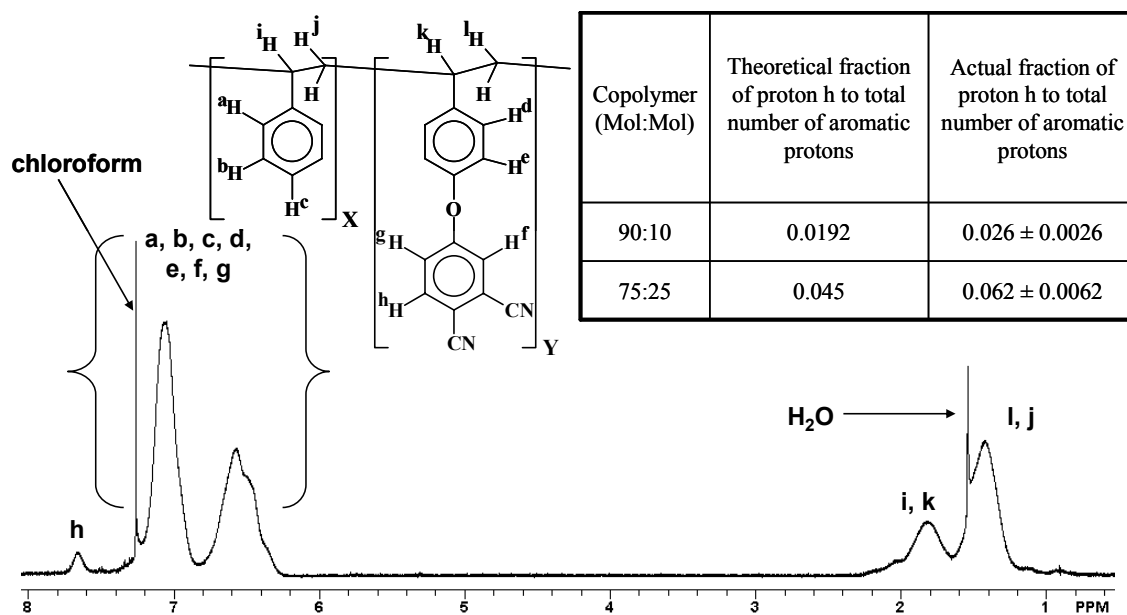


Figure 6.15: ^1H NMR of styrene/VinylPh (90:10) and (75:25) copolymers

Table 6.2: GPC analysis of polystyrene, a styrene/VinylPh (90:10) copolymer and a styrene/VinylPh (75:25) copolymer in chloroform

Copolymer (Molar Ratio of Styrene to VinylPh)	Mn (g/mole)	Mw (g/mole)	PDI
Polystyrene	21,200	35,500	1.67
Styrene -VinylPh (90:10) Copolymer	27,000	43,900	1.63
Styrene -VinylPh (75:25) Copolymer	30,000	47,000	1.57

copolymers had T_g 's approximately 10 °C higher than the control (polystyrene) (Figure 6.16). The slight increase in T_g 's may be due to the bulky, polar phthalonitrile groups pendent to the chain, hindering rotation about the polymer backbone.

The T_g 's of the (90:10) and (75:25) copolymers after curing for 4 h at 220 °C or 240 °C increased, which suggested the phthalonitrile groups crosslinked during the cure cycle (Figures 6.17 and 6.18). After curing the (90:10) copolymer for 4 hours at 220 °C or 240 °C the T_g increased by ~10 °C. The slight increase in crosslink density was most likely due to the low concentration of phthalonitrile groups only lightly crosslinking the material. The (75:25) copolymer T_g increased approximately 14 °C after curing for 4 hours at 220 °C and, after curing for 4 hours at 240 °C, the T_g increased ~20 °C relative to the uncured copolymer. The greater increase in T_g for the two curing cycles relative to the 90:10 copolymer indicated that the higher concentration of phthalonitrile groups along the copolymer backbone resulted in a network with higher crosslink density. The increased crosslink density caused the cured (75:25) copolymer to be more rigid, thus elevating its T_g to higher temperatures.

TGA was utilized to evaluate the thermo-oxidative stability of the uncured and cured (90:10) and (75:25) copolymers relative to polystyrene. The results showed that the two copolymers had improved thermal stability relative to polystyrene. Both copolymers had higher thermal degradation temperatures (the onset of weight loss was ~70 °C higher in air) and they also had increased char yields between 400-600 °C (Figure 6.19). The 75:25 copolymer had approximately three times the char yield of polystyrene over the 400-600 °C temperature range.

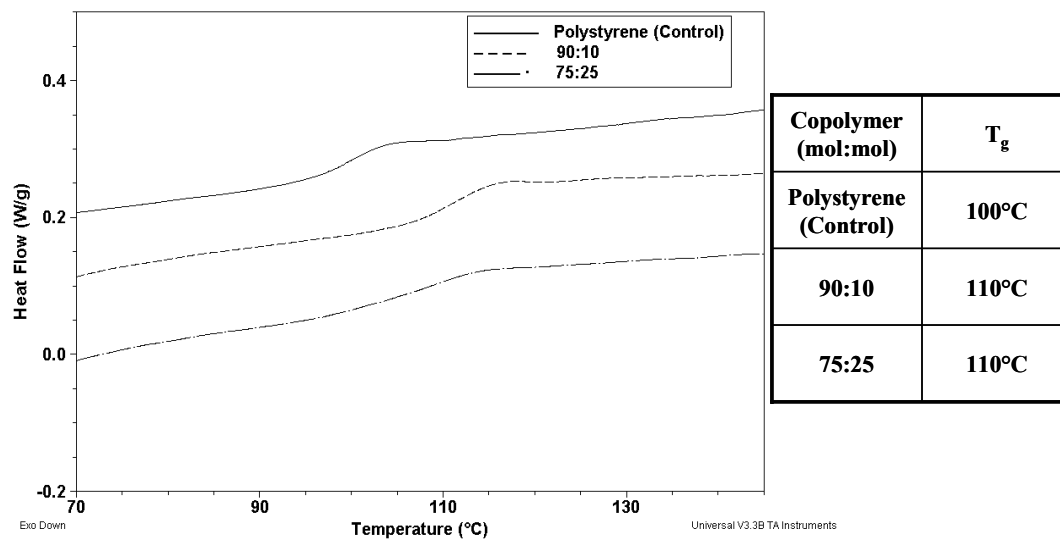


Figure 6.16: DSC analysis of styrene/VinylPh (90:10) and (75:25) copolymers versus polystyrene

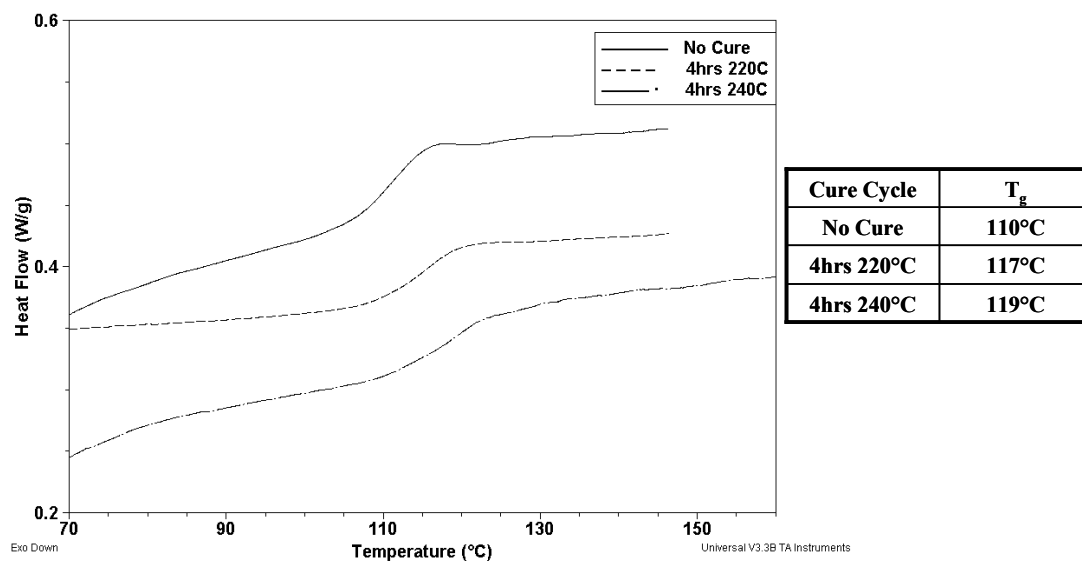


Figure 6.17: DSC analysis of the styrene/VinylPh (90:10)copolymer cured for either 4 hours at 220 °C or 4 hours at 240 °C

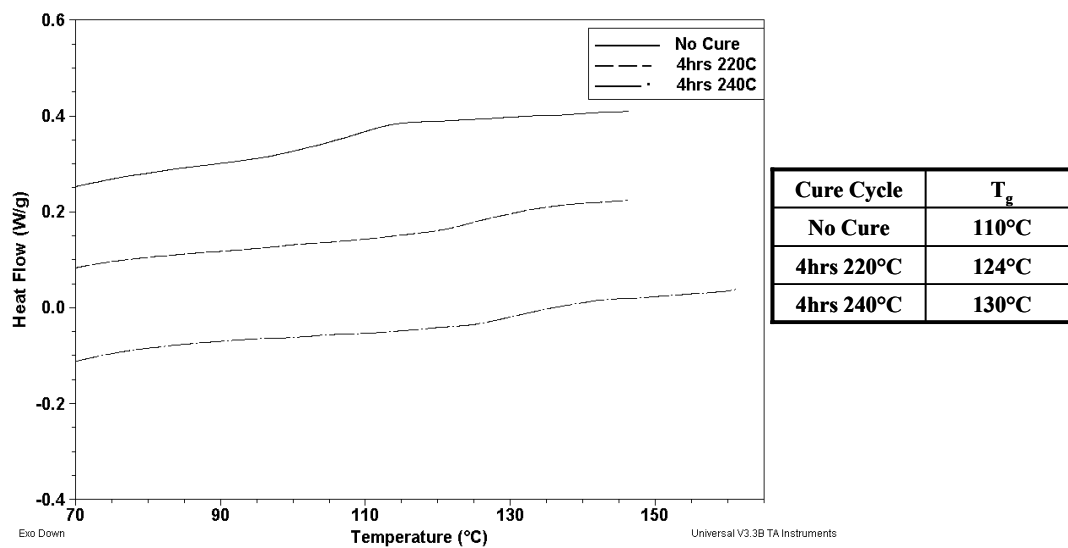


Figure 6.18: DSC analysis of the styrene/VinylPh (75:25) copolymer cured for 4 hours at 220 °C or 4 hours at 240 °C

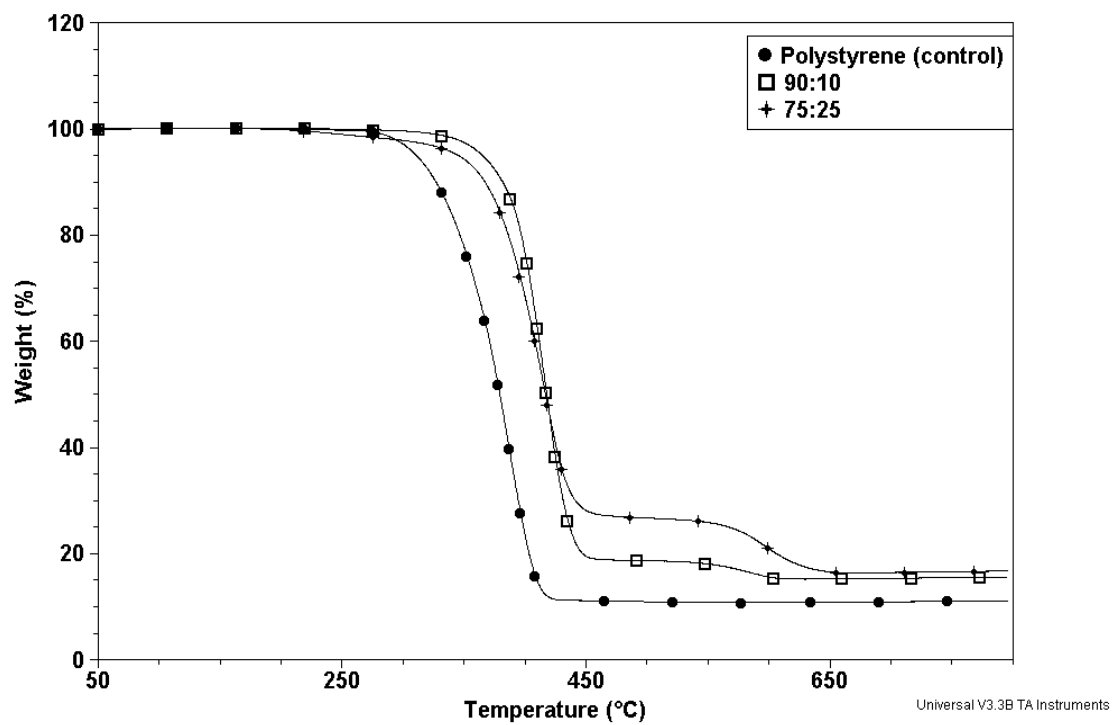


Figure 6.19: TGA analysis in air of styrene/VinylPh (90:10) and (75:25) copolymers

No difference in thermo-oxidative stability was observed after curing the (90:10) copolymer using two different cure cycles (4 hours at 220 or 240 °C). By contrast, upon curing the (75:25) copolymer, a substantial difference in thermo-oxidative stability was observed. The char yield between 400 and 600 °C doubled when the copolymer was cured for 4 hours at 240 °C (Figure 6.20). Overall the TGA study demonstrated that higher densities of heterocyclic crosslinks improved the thermo-oxidative stabilities of (75:25) styrene/phthalonitrile copolymers. Also the incorporation of low mole fractions of 4-vinylphenoxyphthalonitrile into polystyrene as a comonomer significantly enhanced the thermal performance of these materials.

6.5 Conclusions

A two-step synthetic scheme was developed which generated a new non-halogenated, flame-retardant monomer, 4-vinylphenoxyphthalonitrile, in good yield. It was demonstrated that this monomer could be free radically copolymerized into vinyl ester/styrene networks and that it substantially improved the flame performance of cured Derakane 441-400 networks in terms of peak heat release rate, time to ignition, and char yield. The 4-vinylphenoxyphthalonitrile comonomer increased the network T_g 's over the control vinyl esters (Derakane 441-400) as much as 50 °C depending on the concentration of 4-vinylphenoxyphthlaonitrile in the network, and the post-curing conditions. Up to 30 wt % of 4-vinylphenoxyphthalonitrile was soluble in the Derakane 441-400 resin. With slight heating to ~32 °C the resin mixture had a steady shear viscosity under 1000 cPs, which suggests that it may be processable by VARTM methods. ^1H NMR demonstrated that 4-vinylphenoxyphthalonitrile could be free radically copolymerized with styrene (at up to at least 0.25 mole fraction

vinylphenoxyphthalonitrile). The random copolymers had reasonably high molecular weights. The 75:25 and 90:10 styrene:vinylphenoxyphthalonitrile copolymers could be cured into crosslinked networks with significantly higher T_g 's relative to polystyrene. Moreover, the cured 75:25 copolymers had significantly improved flame properties (quadruple the char yield relative to polystyrene) in the temperature range of 400-600 °C.

In summary, 4-vinylphenoxyphthalonitrile is a non-halogenated vinyl ester/styrene soluble monomer. At relatively low concentrations, this monomer substantially improves the flame retardance of Derakane 441-400 networks and polystyrene via char formation. In contrast to certain flame-retarding additives that plasticize the matrix, this monomer elevates the T_g 's of polystyrene and vinyl ester/styrene networks. Also 4-vinylphenoxyphthalonitrile can be readily dissolved into Derakane 441-400 and with slight heating, the resin viscosities remain sufficiently low to be processable by VARTM technologies.

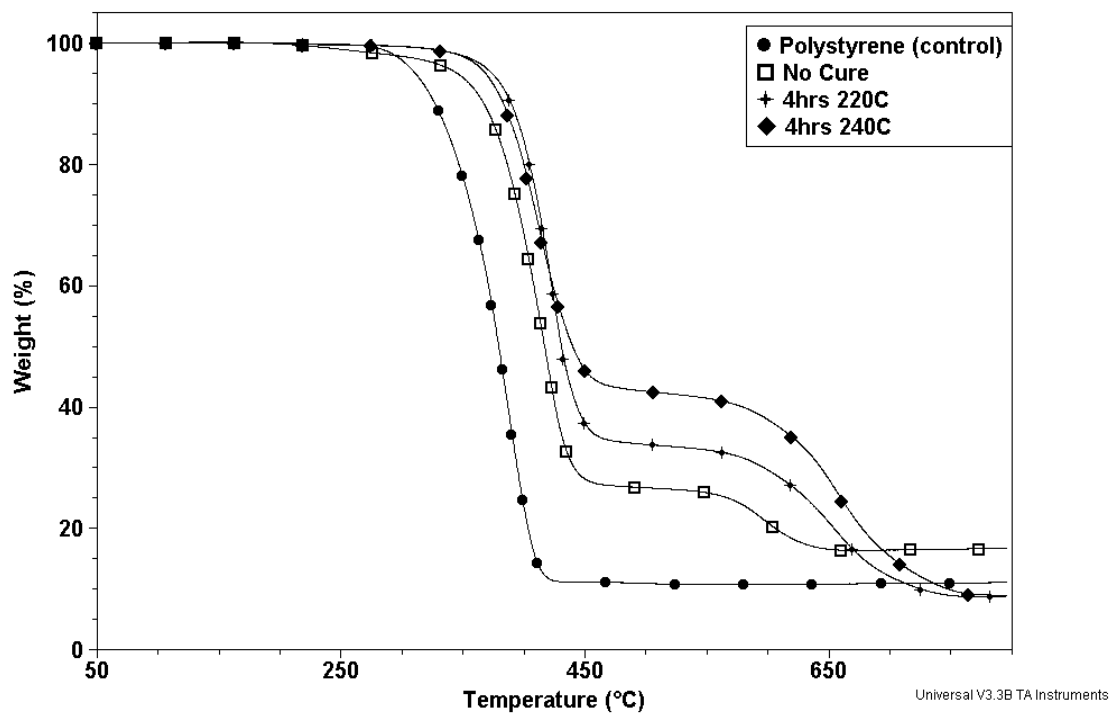


Figure 6.20: TGA analysis in air of the styrene/VinylPh (75:25) copolymer uncured, cured for 4 hours at 220 °C, and cured for 4 hours at 240 °C

Chapter 7: Novel Proton Conducting Disulfonated Poly(Arylene Ether) Copolymers Containing Aromatic Nitriles

7.1 Introduction

The development of polymer electrolyte membrane fuel cells as alternative energy sources has been ongoing continuously since the 1960's.²³² Initially these devices were developed for specialized applications such as electrical power sources aboard spacecraft and submarines. However, the current vision is that polymeric electrolyte membrane fuel cells can be implemented in many applications such as power sources for vehicles (i.e. cars, trucks, and locomotives), stationary power, and portable electronic devices. The conditions inside a fuel cell are harsh and include chemically active noble metal catalysts, highly acidic environments, fuels such as hydrogen or methanol, and its partial oxidation products, oxidants such as oxygen, reactive radicals at electrodes, and operating temperatures in excess of 100 °C.²³² Polymers containing perfluorosulfonic acid groups such as Nafion[®] have been used as separation membranes and these materials now represent the industrial standard. Such materials have demonstrated good performance at moderate temperatures (less than ~90 °C), relatively high humidities, and with hydrogen gas as the fuel.²³³

There is significant interest in using fuels other than hydrogen, such as methanol, methane, or gasoline. These fuels usually contain trace concentrations of gases such as carbon monoxide which poison and reduce efficiencies of platinum fuel cell catalysts.²³⁴

²³² J. A. Kerres, "Development of Ionomer Membranes for Fuel Cells," *Journal of Membrane Science*, **185**, 2001, 3.

²³³ K. D. Kreuer, "On the Development of Proton Conducting Polymer Membranes for Hydrogen and Methanol Fuel Cells," *Journal of Membrane Science*, **185**, 2001, 29.

²³⁴ R. Ianniello, V. M. Schmidt, U. Stimming, J. Stumper, A. Wallen, "CO Adsorption and Oxidation on Pt-Ru Alloys-Dependence on Substrate Composition," *Electrochimica Acta*, **39**, 1994, 1863.

At elevated temperatures (greater than ~100 °C), carbon monoxide poisoning of platinum catalysts is less of a hindrance and cathode kinetics can be enhanced. However, limited application temperatures and undesirably high methanol permeabilities of Nafion[®] membranes limits their scope of applicability.

The need for alternatives to copolymers containing perfluorosulfonic acid groups has led to development of a number of aromatic sulfonated polymers as membrane candidates. Poly(arylene ether sulfone)s are of considerable interest because these materials are well-known for their excellent thermal and mechanical properties as well as their resistance to oxidation and stability under acidic conditions.^{235, 236, 237, 238}

Over the last 30 years, chemically modifying poly(arylene ether sulfone)s through sulfonation has been of great interest. Some of the early work in this area reported by Noshay and Robeson included electrophilic aromatic sulfonation of a commercial poly(arylene ether sulfone) (prepared with bisphenol A and dichlorodiphenylsulfone) under mild conditions.²³⁹ Sulfonation occurred at the activated ortho positions relative to the ether oxygen on the bisphenol A rings with a 2:1 complex of SO₃ and triethylphosphate (Figure 7.1).²⁴⁰ This sulfonation procedure minimized undesirable side reactions such as branching and crosslinking. The sulfonated polymers were evaluated as

²³⁵ L. M. Robeson, A. G. Farnham, J. E. McGrath, in D.J. Meier (Ed.), *Dynamic mechanical characteristics of polysulfone and other polyarylethers*, Vol. 4, Gordon and Breach, 1978, p. 405.

²³⁶ R. J. Cotter, "Engineering Plastics: A Handbook of Polyarylethers," Gordon and Breach, London, **1995**.

²³⁷ J. J. Dumais, A. L. Cholli, L. W. Jelinski, J. L. Hedrick, J. E. McGrath, "Molecular Basis of the β -Transition in Poly(Arylene Ether Sulfone)s," *Macromolecules*, **19**, 1986, 1884.

²³⁸ S. Wang, J. E. McGrath, in M. Rogers, T.E. Long (Eds.), *Step Polymerization*, Vol. Wiley, New York, 2002.

²³⁹ A. Noshay, L. M. Robeson, "Sulfonated Polysulfone," *Journal of Applied Polymer Science*, **20**, 1976, 1885.

²⁴⁰ B. C. Johnson, I. Yilgor, C. Tran, M. Iqbal, J. P. Wightman, D. R. Lloyd, J. E. McGrath, "Synthesis and Characterization of Sulfonated Poly(Arylene Ether Sulfone)s," *Journal of Polymer Science: Part A: Polymer Chemistry*, **22**, 1984, 721.

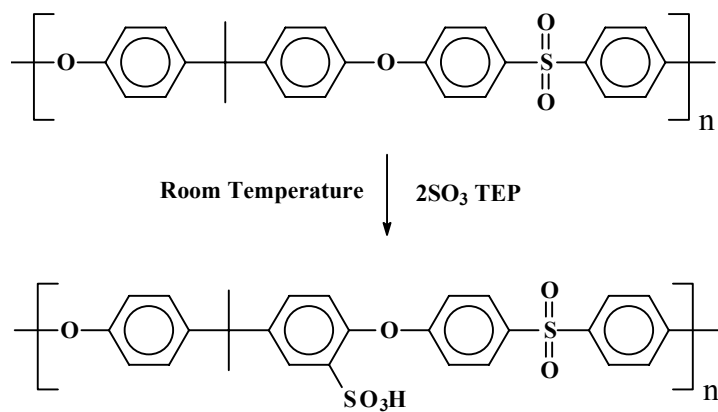


Figure 7.1: Post-sulfonation of a poly(arylene ether sulfone)²⁴⁰

materials for desalinization membranes for water purification.^{241, 242} However, these materials would have limited utility as fuel cell membranes because the sulfonation procedure only incorporated one sulfonic acid group on the polymer repeat unit. Location of the substituents on the bisphenol component of the repeat units, together with the limited number of sulfonic acid groups along the polymer chain, did not afford sufficient acidity for proton conducting fuel cell membranes.

We have recently investigated syntheses and characterization of wholly aromatic poly(arylene ether sulfone)s with two sulfonic acid groups on the rings adjacent (meta) to the sulfonyl groups.^{243, 244, 245} The syntheses require that the aromatic sulfone-activated aryl halide monomer be disulfonated, then the disulfonated monomer (in the salt form) can be copolymerized directly to form the copolymer shown in Figure 7.2.^{243, 244} This approach is advantageous in that the acidity is increased due to the electron withdrawing sulfonyl substituents located on the same rings as the sulfonic acids, and these copolymers also have two sulfonic acid groups per repeat unit, randomly distributed throughout the chains.²⁴⁶ Some of the earliest research on the synthesis of deactivated-ring sulfonation included sulfonating 4,4'-dichlorodiphenylsulfone with fuming

²⁴¹ M. A. Dinno, Y. Kang, D. R. Lloyd, J. E. McGrath, J. P. Wightman, in K.L. Mittal (Ed.), *Physiochemical Aspects of Polymer Surfaces*, Vol. 1, Plenum Press, New York, 1983, p. 347.

²⁴² D. R. Lloyd, L. E. Gerlowski, C. D. Sutherland, J. P. Wightman, J. E. McGrath, M. Iqbal, Y. Kang, "Poly(Aryl Ether) Membranes for Reverse Osmosis," *ACS Symposium Series*, **152**, 1981, 327.

²⁴³ F. Wang, M. Hickner, Y. S. Kim, T. A. Zawodzinski, J. E. McGrath, "Direct Polymerization of Sulfonated Poly(Arylene Ether Sulfone) Random (Statistical) Copolymers: Candidates for New Proton Exchange Membranes," *Journal of Membrane Science*, **197**, 2002, 231.

²⁴⁴ M. A. Hickner, F. Wang, Y. S. Kim, B. Pivovar, T. A. Zawodzinski, J. E. McGrath, "Chemistry-Morphology-Property Relationships of Novel Proton Exchange Membranes for Direct Methanol Fuel Cells," *Fuel Chemistry Division Preprints*, **46**, 2001.

²⁴⁵ Y. S. Kim, M. Hickner, L. Dong, B. Pivovar, J. E. McGrath, "Methanol Permeability of Sulfonated Poly(Arylene Ether Sulfone) Copolymers: Effect of Morphology," *Submitted to Journal of Membrane Science*, 2003.

²⁴⁶ L. M. Robeson, M. Matzner, US Patent 4,380,598 (1983).

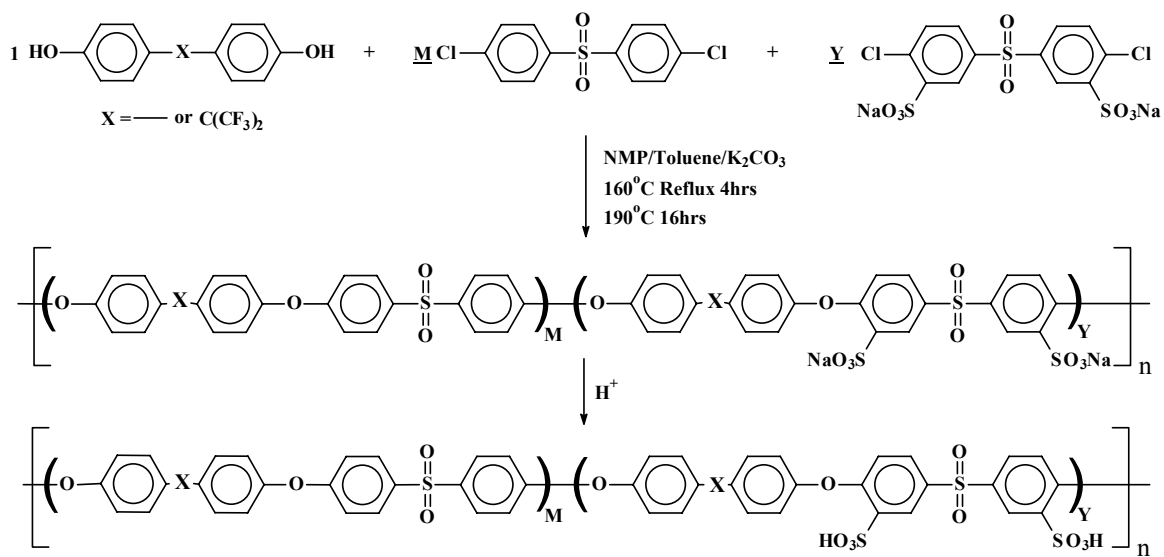


Figure 7.2: Synthesis of disulfonated poly(arylene ether sulfone)s and disulfonated hexafluoroisopropylidene poly(arylene ether sulfone)s

sulfuric acid.²⁴⁷ The earlier procedure was modified to synthesize disulfonated 4,4'-dichlorodiphenylsulfone in this work. The directly copolymerized, disulfonated poly(arylene ether sulfone)s described in figure 7.2 had substantially lower methanol permeability, lower electro-osmotic drag, and comparable proton conductivities compared to Nafion 117[®].

This chapter describes the synthesis and characterization of a series of high molecular weight, nitrile-functional, disulfonated poly(arylene ether sulfone)s by the direct copolymerization of disulfonated aromatic dihalides, 2,6-dichlorobenzonitrile, and hexafluoroisopropylidene diphenol (hexafluorobisphenol A). Nitrile-activated aryl halide monomers are viable alternatives to sulfone and ketone electron withdrawing systems for polymerizations via nucleophilic aromatic substitution. Membranes cast from these materials are promising in that good proton conductivities at similar ionic concentrations (i.e. similar ion exchange capacities) relative to other disulfonated poly(arylene ether sulfone)s studied have been demonstrated. The inclusion of the fluorinated comonomer in these copolymers also results in polymers with less equilibrium water absorption compared to previously studied disulfonated poly(arylene ether sulfone)s.

7.2 Experimental

7.2.1. Materials

4,4'-Dichlorodiphenylsulfone (DCDPS) was generously provided by Solvay Advanced Polymers. The 4,4'-(hexafluoroisopropylidene)diphenol (hexafluorobisphenol

²⁴⁷ M. Ueda, H. Toyota, T. Ouchi, J. Sugiyama, K. Yonetake, T. Masuko, T. Teramoto, "Synthesis and Characterization of Aromatic Poly(Ether Sulfone)s Containing Pendant Sodium Sulfonate Groups," *Journal of Polymer Science: Part A: Polymer Chemistry*, **31**, 1993, 853.

A) (HFBA) was kindly provided by Ciba-Geigy, and used as received. DCDPS was recrystallized from methanol and dried under vacuum at 80 °C for 12 h. The 2,6-dichlorobenzonitrile (Aldrich) was recrystallized from methanol, then sublimed before use. Methanol, isopropanol, dimethylformamide, toluene, fuming sulfuric acid (30 wt% SO₃), potassium carbonate, and calcium hydride were purchased from Aldrich and used as received. N-Methylpyrrolidinone (NMP) (Aldrich) was purified by stirring overnight over calcium hydride, then distilled at ~80 °C under vacuum and collected over activated molecular sieves.

7.2.2 Synthesis of 3,3'-Disulfonate-4,4'-dichlorodiphenylsulfone (SDCDPS)

4,4'-Dichlorodiphenylsulfone (12.5 g, 0.0437 mol) was dissolved in fuming sulfuric acid containing 30 wt% SO₃ (25 mL) and reacted for 6 h at 110 °C. The acidic solution was slowly added to ice water saturated with sodium chloride to precipitate the sulfonated monomer. The sulfonated monomer was recrystallized from a 15 wt% solution of 3:1 wt:wt isopropanol:water at 55 °C. It was then stirred overnight at room temperature in a fresh 15 wt% solution (3:1 wt:wt isopropanol:water) and collected via vacuum filtration. The monomer was dried overnight in a vacuum oven at 140 °C and stored under ambient conditions until used. The yield of the crude monomer was ~ 82% and purification reduced the yield to 65%. Further studies on optimizing this process will be reported in detail in a subsequent publication.²⁴⁸

²⁴⁸ M. Sankir, V. A. Bhanu, H. Ghassemi, K. B. Wiles, M. L. Hill, W. Harrison, M. J. Sumner, T. E. Glass, J. S. Riffle, J. E. McGrath, "Systematic Study of the Synthesis and Characterization of 3,3'-Sulfonylbis(6-Chlorobenzene Sulfonic Acid) Disodium Salt Monomer for Proton-Conducting Polymeric Membranes in Fuel Cell Applications," *Polymer Preprints*, **44**, 2003, 1079.

7.2.3 Synthesis of Poly(Arylene Ether) Copolymers Containing Disulfonated Repeat Units

An exemplary synthesis for a copolymer containing 30% of disulfonated repeat units and 70% of non-sulfonated, nitrile-functional repeat units is provided.^{249, 250, 251, 252} 4,4'-(Hexafluoroisopropylidene)diphenol and potassium carbonate were dried in a vacuum oven overnight at ~60 °C just prior to weighing. 2,6-Dichlorobenzonitrile was dried under vacuum overnight at room temperature (instead of 60 °C) to avoid sublimation. 3,3'-Disulfonate-4,4'-dichlorodiphenylsulfone was not further dried. 4,4'-(Hexafluoroisopropylidene)diphenol (8.0000g, 0.0238 mol), 2,6-dichlorobenzonitrile (2.8647 g, 0.0166 mol), 3,3'-disulfonate-4,4'-dichlorodiphenylsulfone (3.6209 g, 0.0071 mol) (Note: As determined by TGA, the 3wt% moisture in this monomer was accounted for in this calculation), and potassium carbonate (3.7812 g, 0.0274 mol) were charged to 3-neck round bottom flask equipped with a vacuum tight mechanical stirrer, Dean-Stark trap, and reflux condenser. Under constant stirring, ~20 mL of dry NMP and ~10 mL of toluene were added via syringe to form a pinkish-white hazy mixture. Under nitrogen purge, the reaction mixture was refluxed for 4 h using an oil bath heated to ~155 °C. After refluxing, the toluene-water Dean-Stark trap was drained and the mixture was heated to ~200 °C. Over approximately 20 min, toluene was collected in the Dean-Stark trap and the reaction was held at 200 °C for 20 h. Following the reaction, the highly

²⁴⁹ J. L. Hedrick, D. K. Mohanty, B. C. Johnson, R. Viswanathan, J. A. Hinkley, J. E. McGrath, "Radiation Resistant Amorphous-All Aromatic Poly(Arylene Ether Sulfone)s: Synthesis, Characterization, and Mechanical Properties," *Journal of Polymer Science: Part A: Polymer Chemistry*, **23**, 1986, 287.

²⁵⁰ R. N. Johnson, A. G. Farnham, R. A. Clendinning, W. F. Hale, C. N. Merriam, "Poly(Aryl Ethers) by Nucleophilic Aromatic Substitution I. Synthesis and Properties," *Journal of Polymer Science: Part A: Polymer Chemistry*, **5**, 1967, 2375.

²⁵¹ C. Genies, R. Mercier, B. Sillion, N. Cornet, G. Gebel, M. Pineri, "Soluble Sulfonated Naphthalenic Polyimides as Materials for Proton Exchange Membranes," *Polymer*, **42**, 2001, 359.

viscous mixture was diluted with ~20 mL DMAc while still hot. The hot copolymer solution was precipitated by slowly pouring the polymer solution into ~500 mL of rapidly stirring isopropanol (in a blender). It was vacuum filtered and dried at 60 °C in a vacuum oven for ~12 h. A series of analogous copolymers were prepared with systematically varied fractions of disulfonated repeat units in a similar fashion by altering the relative concentrations of comonomers.

7.2.4 Membrane Preparation

Approximately 1 g of the copolymer in the sodium salt form was dissolved in ~7 mL of dimethylformamide and the solution was cast directly onto a glass plate positioned on a leveled hot plate. The glass plate was heated at 80 °C for ~12 h until most of the solvent was removed. The film was removed from the glass plate and immersed in a 0.5M solution of aqueous sulfuric acid. The solution was heated to reflux and the film was acidified in the refluxing solution over ~2 h. The film was subsequently treated with refluxing deionized water for ~2 h. This acidification procedure has been referred to as “Method 2” in earlier papers.²⁵³ The acidified films were dried in a vacuum oven overnight at 60 °C.

²⁵² R. Viswanathan, B. C. Johnson, J. E. McGrath, "Synthesis, Kinetic Observation, and Characterizations of Poly(Arylene Ether Sulfone)s Prepared by Potassium Carbonate DMAC Process," *Polymer*, **25**, 1984, 1827.

²⁵³ Y. S. Kim, F. Wang, M. Hickner, S. McCartney, Y. T. Hong, W. Harrison, T. A. Zawodzinski, J. E. McGrath, "Effect of Acidification Treatment and Morphological Stability of Sulfonated Poly(Arylene Ether Sulfone) Copolymer Proton Exchange Membranes for Fuel Cell Use Above 100°C," *Journal of Polymer Science: Part B: Polymer Physics*, **in press**, 2003.

7.3 Measurements

7.3.1 Proton Nuclear Magnetic Resonance (^1H NMR).

^1H NMR spectra were collected at 80 °C on a Varian Unity 400 MHz instrument operating at a frequency of 399.954 MHz to analyze the SDCDPS monomer. A 22 ° pulse angle was used with an acquisition time of 3.7 s and a recycle delay of 1 s. d_6 -Dimethylsulfoxide (d_6 -DMSO) was used as the NMR solvent. In order to determine the copolymer compositions, the same instrument and solvent were used except the ^1H NMR data was collected at 25 °C.

7.3.2 Differential Scanning Calorimetry (DSC) and Thermogravimetric Analysis (TGA)

A TA Q1000 model DSC was used to determine the glass transition temperatures (T_g) (approximately 3 to 5 mg) of the disulfonated polymer films. The films were heated over a temperature range of 100 to 300 °C at 5 °C min⁻¹, then quenched to 100 °C and heated a second time over the same temperature range at the same rate. The second heating cycle was used to determine the T_g of the copolymer. A TA Q0500 TGA was used to evaluate the thermo-oxidative stability of approximately 8 to 10 mg of the copolymers in air. The samples were heated to 150 °C and held at this temperature for 30 min to remove any residual water or solvent remaining in the copolymer film. The samples were cooled to room temperature and then heated to 900 °C at 10 °C min⁻¹. The temperature at which 5% weight loss occurred was recorded for each material.

7.3.3 Intrinsic Viscosities

Approximately 20 mg of a copolymer was dissolved in 20 mL of NMP and filtered. Intrinsic viscosities of the samples were measured in NMP at 25 °C using an Ubbelohde viscometer.

7.3.4 Gel Permeation Chromatography (GPC)

GPC was performed using a Waters chromatograph equipped with a Waters 2414 refractive index detector calibrated with polystyrene standards and a Waters 1515 HPLC pump. The mobile phase was a 0.05 molar solution of lithium bromide in NMP. The data was collected using Waters Styragel HT 4, 5, and 6 columns using a 1.0 mL/min flow rate at 60 °C.

7.3.5 Water Absorption.

After acidification, the membranes were vacuum dried overnight at 60 °C, weighed (dry weight), then immersed in deionized water for several days. During the first 24 hours of soaking, the weight of the films (wet weight) was measured several times. After the first 24 h, the films were measured every 24 h. The weighing procedure involved removing the films from the deionized water, quickly patting them dry, and then remeasuring their weight. After weighing the films, they were re-submersed in deionized water. The water uptake of the films was recorded as a weight percent calculated from equation 1:

$$\text{Water uptake} = [(W_{\text{wet}} - W_{\text{dry}}) / W_{\text{dry}}] \times 100 \quad \text{Equation 1}$$

where W_{wet} and W_{dry} were the wet and dry weights, respectively.²⁵⁴

7.3.6 Atomic Force Microscopy

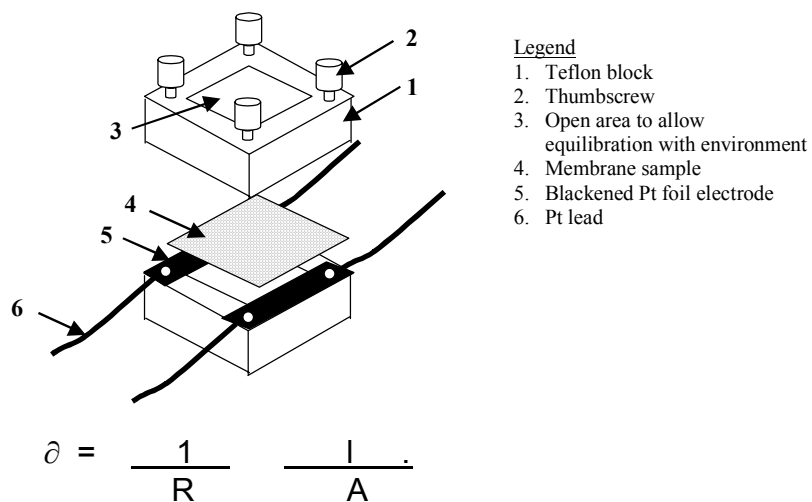
The films were embedded in an epoxy (Epo-fix manufactured by Struers Inc.), cured for 12 h at room temperature, and a cross-section of each film was microtomed under liquid nitrogen. The microtomed samples were kept under vacuum at room temperature for ~6 h, then imaged immediately under a relative humidity of ~40%. The samples were imaged in the tapping mode using a Digital Instruments Dimension 3000 instrument equipped with a micro-fabricated cantilever with a force constant of 40 N m⁻¹.

7.3.7 Conductivity

A Hewlett-Packard 4129A LF impedance/gain phase analyzer was used to measure the resistance of each film in the acid form over a frequency range of 10 Hz to 1 MHz under fully hydrated conditions. The resistance of each film was measured at ~25 °C using the conductivity cell shown in Figure 7.3. The film geometry in the conductivity cell was such that the film resistance dominated the response of the system. The resistance of the film was recorded when the imaginary resistance was at a minimum. The detailed procedure has been reported previously.²⁴³

Using the same analyzer, the resistance of some films was measured as a function of relative humidity. (Note: The resistance of the film was recorded when the imaginary resistance reached a minimum.) The films were placed in a conductivity cell and the cell was stored in an ESPEC SH-240 temperature and humidity controlled oven. The resistance of the films was measured at 50, 75, 85, and 95% relative humidity at 80 °C. Upon changing the humidity level in the oven and before any resistance measurements

²⁵⁴ T. A. Zawodzinski, T. E. Springer, J. Davey, R. Jestel, C. Lopez, J. Valerio, S. Gottesfeld, "A Cooperative Study of Water Uptake by and Transport Through Ionomeric Fuel Cell Membranes," *Journal of the Electrochemical Society*, **140**, 1993, 1981.



Where σ = conductivity (S/cm)
 R = resistance (ohms)
 l = length between electrodes (cm)
 A = cross-sectional area of film (cm²)

Figure 7.3: Conductivity cell with labeled components

were completed, the films were held for ~8 h to ensure that the moisture levels inside the films were in equilibrium with the environment.

The proton conductivity of the nitrile-functional copolymer with 35 % of the repeat units disulfonated was measured as a function of temperature. The membrane was placed in the conductivity cell, then suspended above deionized water in a Parr pressure reactor (Figure 7.4.). The sample was heated to various temperatures ranging from 60 to 120 °C in the Parr reactor at 100% humidity under pressure. Upon reaching a particular temperature, the membrane was equilibrated for several hours with the environment, then the proton conductivity was measured using the Hewlett-Packard impedance analyzer.

7.3.8 Methanol Permeability

Methanol permeabilities of the acidified copolymer films were characterized by conducting diffusivity measurements in a membrane-separated diffusion cell.²⁴⁵ A copolymer membrane was placed between two compartments: one filled with deionized water and the other filled with a 2M methanol/water solution. The temperature of the diffusion cell was maintained at 25 °C with a water bath and both compartments were stirred continuously during the experiments. Methanol permeabilities of the films were quantified using a differential refractometer and recirculating pump to measure the rate of change of the methanol concentration in the water-filled compartment. The diffusivities of the membranes were calculated from equation 2 below:

$$DH = \left(\frac{l}{At} \right) \left(\frac{V_a x V_b}{V_a + V_b} \right) \ln \left(\frac{C_a^o - C_b^o}{C_a - C_b} \right) \quad \text{Equation 2}$$

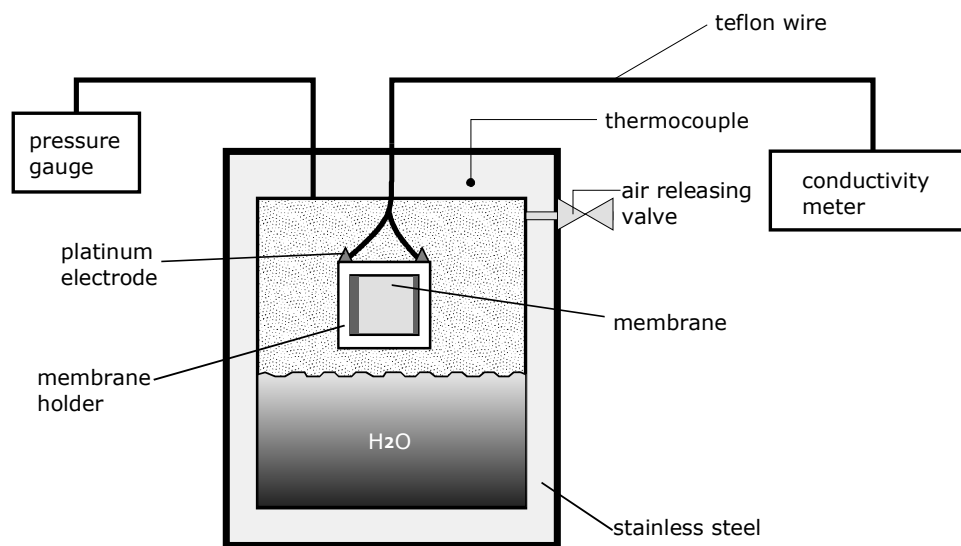


Figure 7.4: Parr reactor assembly for high temperature fuel cell measurements

where D was the diffusivity (cm^2/s), H was the partition coefficient, l the film thickness (cm), A was the cross-sectional area (cm^2), t was time (s), V was the cell volume (mL), C was the methanol concentration (wt%), subscript a noted the water cell, subscript b noted the water/methanol mixture cell, and the superscript o noted the initial conditions. Details concerning these calculations have been reported previously.²⁵⁵

7.4 Results and Discussion

7.4.1 Synthesis of the Disulfonated Monomer (3,3'-Disulfonate-4,4'-Dichlorodiphenylsulfone), and Copolymers Containing Nitrile Moieties

3,3'-Disulfonate-4,4'-dichlorodiphenylsulfone was synthesized by electrophilic aromatic sulfonation of 4,4'-dichlorodiphenylsulfone in fuming sulfuric acid at 110 °C for 6 h. Due to the ortho-para directing effects of chlorine substituents and the meta directing effect of the sulfonyl group on the benzene rings of 4,4'-dichlorodiphenylsulfone, the 3 positions (ortho relative to chlorine) were sulfonated. ^1H NMR confirmed that substitution occurred in the 3 and 3' positions due to the chemical shift (8.4 ppm) of proton c (Figure 7.5). The chemical shift of a proton on the aromatic carbon between the positions substituted with a chlorine and a sulfonate group was expected to be smaller due to less deshielding relative to the expected shift for substitution in the 2 position (meta relative to chlorine).

The crude reaction product could be isolated by adding the highly acidic reaction solution slowly into ice water saturated with sodium chloride.

²⁵⁵ E. L. Cussler, "Diffusion Mass Transfers in Fluid Systems, 2nd Ed.," Cambridge University, New York, 1997.

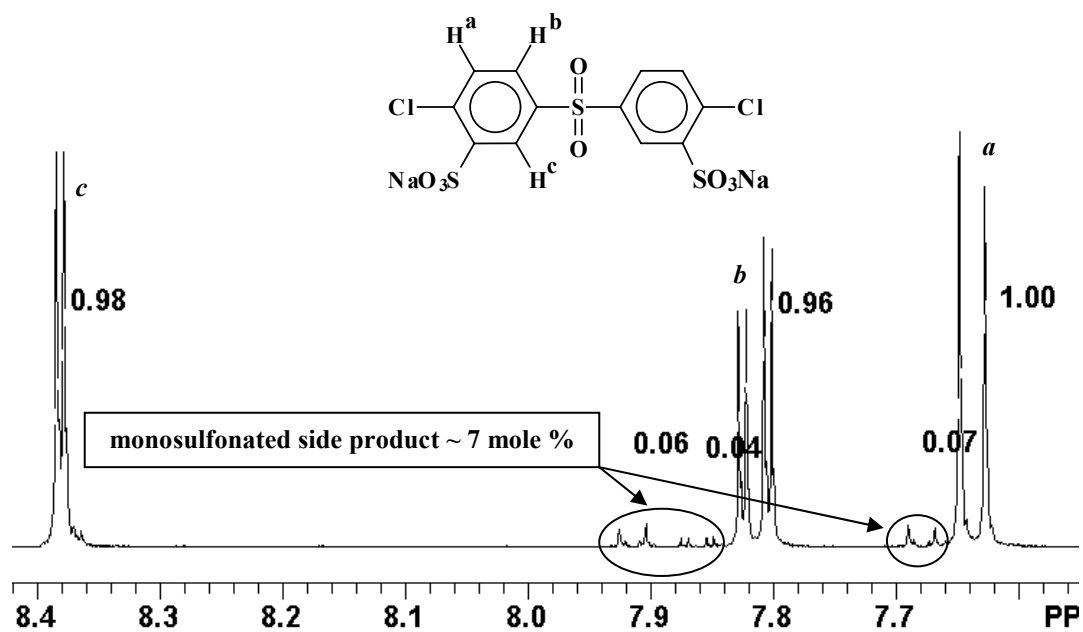


Figure 7.5: 1H NMR at 80 °C of SDCDPS after recrystallization

small amounts of the monosulfonated product remained at this stage (observed at 7.91, 7.86, and 7.68 ppm in Figure 7.5). The crude monomer was purified by first recrystallizing it from a 15% solids solution in 3:1 (wt:wt) isopropanol:water. The crystallized monomer was subsequently extracted for approximately 12 hours at room temperature in a fresh isopropanol:water (3:1 wt:wt) mixture, then dried overnight under vacuum at 140 °C. After this purification procedure, the yield of the desired product was ~65%. After 12 hours of extraction, ¹H NMR showed that the monosulfonated side-product was removed (Figure 7.6). The disulfonated monomer was dried under vacuum for ~12 hours at 140 °C, but TGA demonstrated that small amounts of moisture (~3-5 wt%) remained even after this drying process.

Syntheses of linear high molecular weight polymers via step growth polymerizations require monomer charges to be highly accurate in terms of molar stoichiometries. Therefore, the residual moisture content in the disulfonated monomer was determined via TGA so that the weight of any remaining moisture could be accurately included in the monomer weights. Knowledge of the concentration of water in the disulfonated monomer enabled accurate monomer ratios to be charged to the reaction solutions.

To evaluate the propensity of the monomer to absorb moisture under ambient conditions, it was equilibrated for 7 days and moisture contents were monitored by TGA. Monomer samples were heated to approximately 200 °C, well below the degradation temperature of the compound, and held isothermally for approximately six hours while the weight loss was monitored. The TGA data indicated that the sulfonated monomer

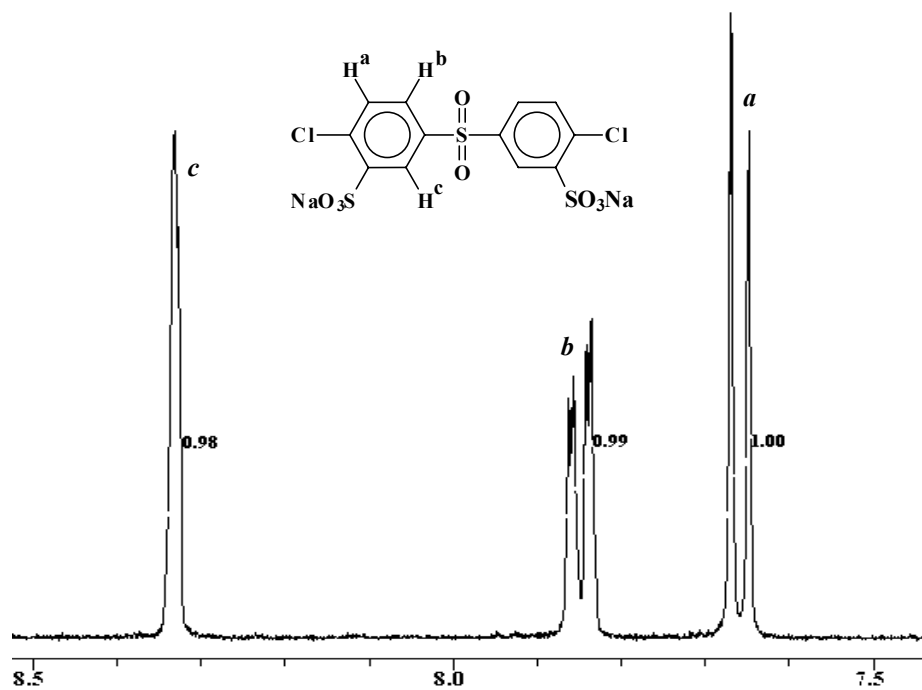


Figure 7.6: ^1H NMR of SDCDPS after stirring for 12 hours in a 3:1 wt:wt isopropanol:water solution

contained approximately 3.17 % water by weight. Interestingly, this concentration remained constant over the seven-day period (Figure 7.7). Most of the water was lost during the first 30 minutes at 200 °C. The slight changes observed in weight loss for the different curves were within experimental error. Also the consistency in the weight loss data over the seven-day timeframe suggested the sulfonated monomer was not particularly hygroscopic under ambient conditions. It is important to note that if the disulfonated monomer was impure, it typically exhibited inconsistent weight losses in the isothermal TGA experiments. The reasons for this are unclear.

A series of copolymers were prepared by nucleophilic aromatic substitution from 4, 4'-hexafluorobisphenol A as the diphenol and mixtures of 2,6-dichlorobenzonitrile and the disulfonated monomer, 3,3'-disulfonate-4,4'-dichlorodiphenylsulfone (SDCDPS), as the activated dihalides (Figure 7.8). The mole fractions of the disulfonated dihalide ranged from 0.05-0.55. All of the copolymers were prepared in NMP-toluene solvent mixtures utilizing potassium carbonate as a weak base to form the required phenolate nucleophile. The reactions were refluxed for four hours at 155 °C, then the toluene and any water were distilled from the mixtures at 197 °C with the aid of a Dean Stark trap to ensure dry polymerization systems. The copolymerizations were maintained for 20 hours at 197 °C. It should be noted that the disulfonated monomer reacted slowly relative to its unsulfonated counterpart, 4,4'-dichlorodiphenylsulfone. It is reasoned that this trend toward lower reactivity with substitution at the ring positions ortho to the leaving groups

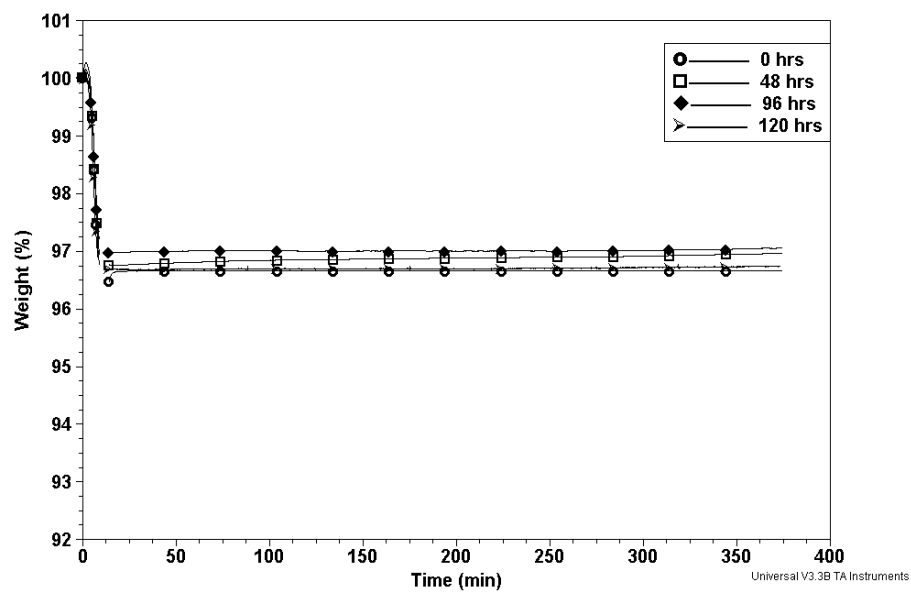


Figure 7.7: Isothermal (200 °C) TGA measurements on moisture content in SDCDPS versus time exposed to the atmosphere

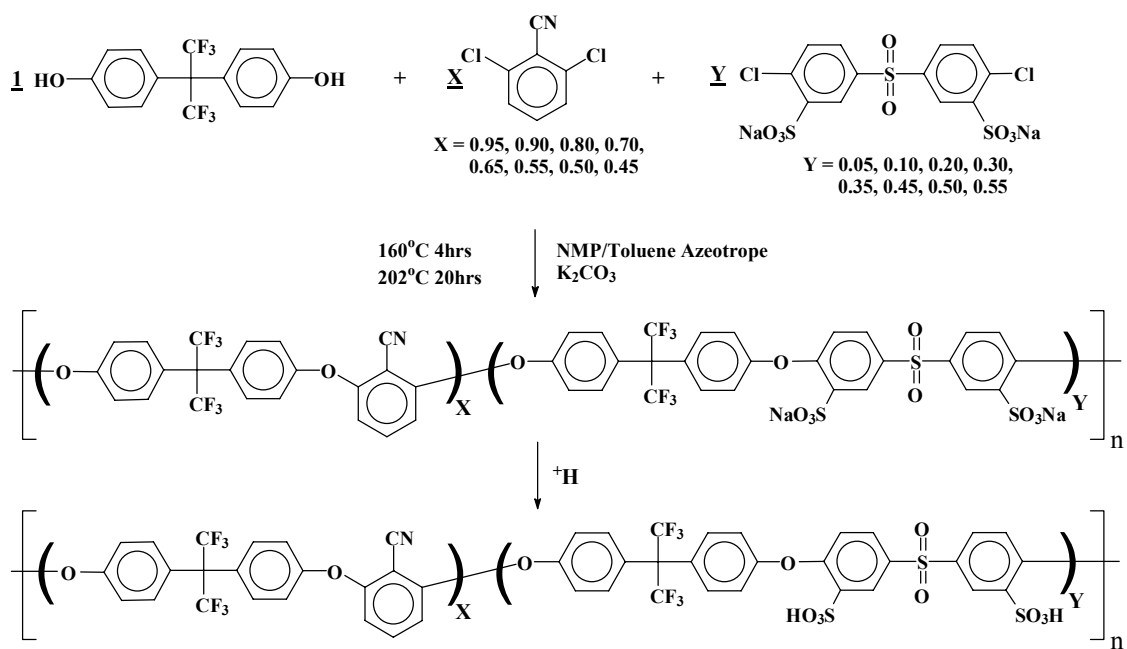


Figure 7.8: Synthesis of disulfonated hexafluoroisopropylidene poly(arylene ether nitrile)s

was primarily a steric effect. Highly viscous solutions containing ~50wt% copolymer formed toward the ends of the reactions.

Proton NMR confirmed that the polymer compositions after purification were consistent with the charged compositions (Figure 7.9 and Table 7.1). Concentrations of disulfonated units along the polymer chains were determined by ratioing the integrals corresponding to the aromatic protons meta to the nitrile groups to the aromatic protons ortho to the sulfone and sulfonate groups (proton a – meta to the nitrile group, proton i – ortho to the sulfone and sulfonate groups in Figure 7.9). The ^1H NMR data indicated that SDCDPS was quantitatively incorporated into the backbones of most of the copolymers in the series because the integral ratios were within experimental error of the charged compositions.

Relative molecular weights were analyzed with intrinsic viscosity measurements, average molecular weights, and polydispersities were measured using GPC with a 0.05M lithium bromide NMP solution as the mobile phase. One series of copolymers was synthesized with the moisture content in SDCDPS included in the charged monomer weights. By contrast, another series was prepared without including the moisture weight in the monomer charges. Intrinsic viscosities were $\sim 1.0 \text{ dL g}^{-1}$ (NMP, 25 °C) or above for all of the materials wherein the moisture weight was accounted for, suggesting that high molecular weights were obtained in these cases (Table 7.2). The weight average molecular weights by GPC (calibrated against polystyrene standards) were substantially higher ($\sim 50,000 - 70,000 \text{ g mole}^{-1}$) for the series of copolymers where moisture in the SDCDPS was accounted for stoichiometrically during synthesis (Table 7.2).

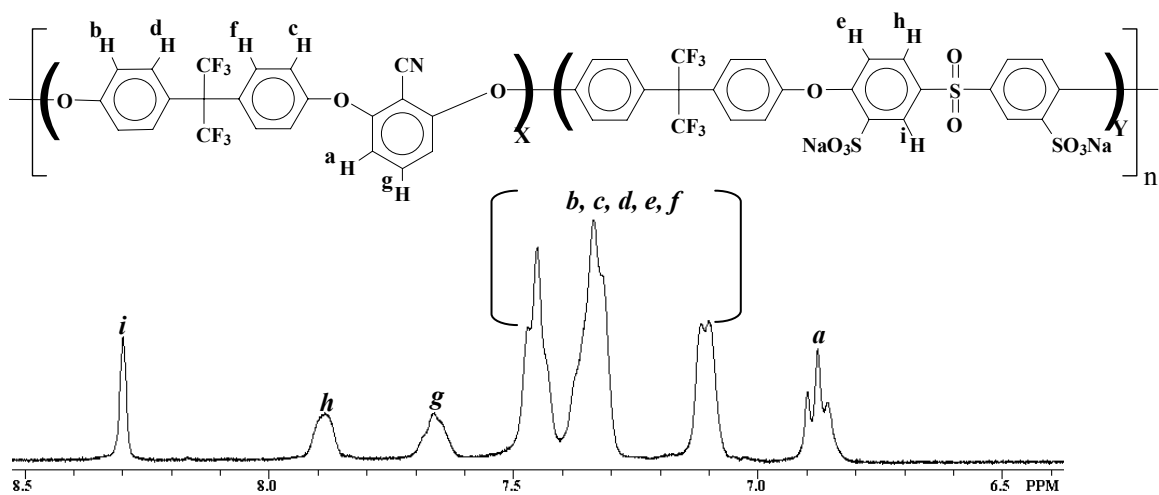


Figure 7.9: ^1H NMR of disulfonated hexafluoroisopropylidene poly(arylene ether nitrile) copolymers

Table 7.1: Theoretical versus experimental ^1H NMR integration ratios of protons “a” to “i” for disulfonated hexafluoroisopropylidene poly(arylene ether nitrile) copolymers containing 5 up to 50 mole % disulfonation

Copolymer	Theoretical ratio of proton a to i	Experimental ratio of proton a to i from ^1H NMR
95:5	0.95:0.05	$0.95 \pm 0.03 : 0.07 \pm 0.03$
90:10	0.90:0.10	$0.90 \pm 0.03 : 0.07 \pm 0.03$
80:20	0.80:0.20	$0.80 \pm 0.03 : 0.20 \pm 0.03$
70:30	0.70:0.30	$0.70 \pm 0.03 : 0.30 \pm 0.03$
65:35	0.65:0.35	$0.65 \pm 0.03 : 0.35 \pm 0.03$
55:45	0.55:0.45	$0.55 \pm 0.03 : 0.35 \pm 0.03$
50:50	0.50:0.50	$0.50 \pm 0.03 : 0.46 \pm 0.03$

Table 7.2: Intrinsic viscosity (NMP, 25 °C) and weight average molecular weights of disulfonated hexafluoroisopropylidene poly(arylene ether nitrile) copolymers containing 20, 30, 35, and 50 mole % disulfonation

Weight % of water in SDCDPS accounted for stoichiometrically	Copolymer	Intrinsic Viscosity (dL/g)	M _w (g/mole)	PDI
Yes	80:20	1.76	141,000	3.2
No	80:20	0.90	91,000	2.7
Yes	70:30	1.44	142,000	3.5
No	70:30	0.93	106,000	3.1
Yes	65:35	1.84	146,000	3.4
No	65:35	0.81	76,000	2.8
Yes	50:50	0.98	95,000	2.9
No	50:50	0.73	57,000	2.6

These high molecular weight copolymers formed tough ductile films.

7.4.2. Thermal Properties of the Disulfonated Copolymers

Pendent sulfonate groups along a polymer chain elevate glass transition temperatures for at least two reasons. The sulfonate groups associate and increase intermolecular interactions, thereby reducing mobility. Secondly, these pendent groups are large and bulky. Both the ionic associative effect and the bulkiness of the sulfonate groups hinder rotation about the polymer chain. Glass transition temperatures of the copolymers were evaluated using DSC by heating the samples from 25 °C to 300 °C at 5 °C min⁻¹. The glass transition temperatures of the acidified copolymers increased substantially as the mole fraction of disulfonation was increased (Figure 7.10). The T_g 's increased from 169 °C for the control (no sulfonation) to 258 °C for the copolymer containing 35 mole % disulfonated repeat units. Increasing the mole fraction of the disulfonated units beyond 0.35 caused little increase in the glass transition temperatures. The acidified copolymers containing higher fractions of disulfonated units were heated to 400 °C to determine whether a second transition could be detected due to a hydrophilic phase. A secondary transition was not detected up to 350 °C and heating beyond this temperature caused some degradation. This was consistent with thermal properties of other disulfonated poly(arylene ether)s.

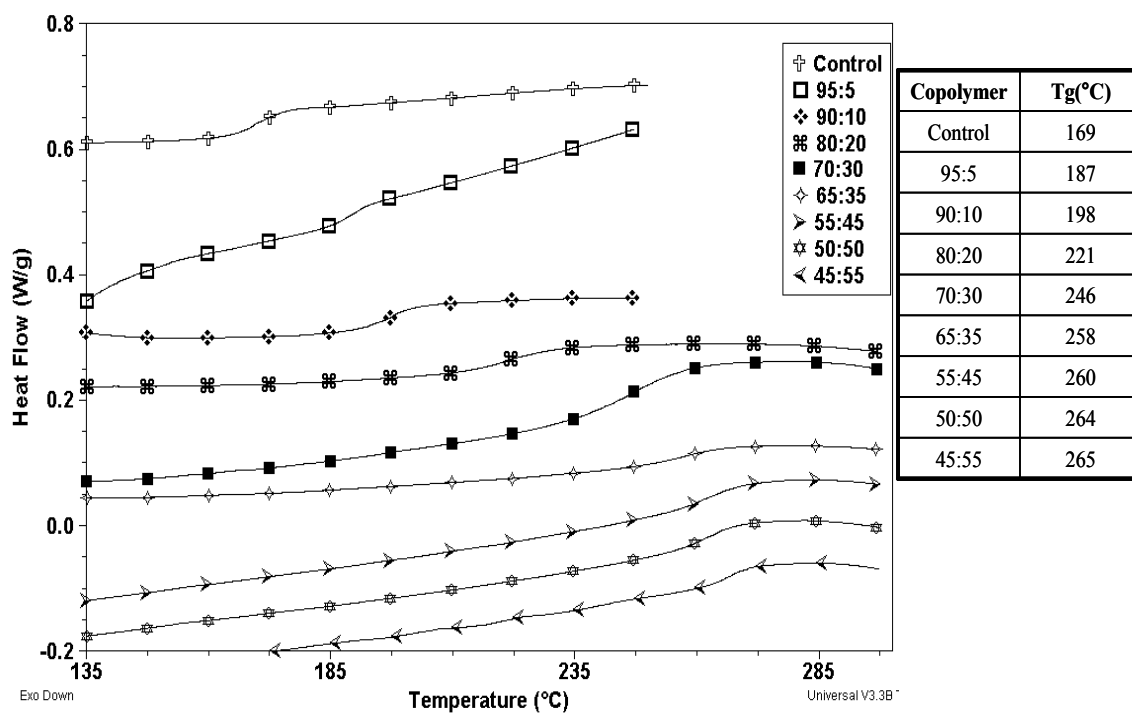


Figure 7.10: Glass transition temperatures of disulfonated hexafluoroisopropylidene poly(arylene ether nitrile) copolymers (in the acidified form) containing 5 up to 55 mole % disulfonation

Previous DSC studies on disulfonated poly(arylene ether sulfone) salts and the corresponding acidified polymers also did not detect two T_g 's.^{240, 256}

The mass losses with temperature of the acidified copolymer films were examined by TGA to determine the temperature range wherein the sulfonic acid groups cleaved from the polymer chain. Copolymer films were heated to 150 °C and held at this temperature for 30 minutes to remove any residual moisture. They were then cooled to room temperature and heated to 900 °C at 10 °C min⁻¹. The temperatures where 5% weight loss was observed and the percentages of char remaining were considered an evaluation of thermal stability. All of the disulfonated copolymers exhibited good thermal stability up to ~350 °C where weight loss was observed. The mass loss at this temperature increased as the level of disulfonation along the copolymer chain was increased (Figure 7.11). This observation was consistent with previous measurements from our labs on other disulfonated poly(arylene ether)s.²⁴³ The final weight loss temperatures were observed at ~500 °C and this was attributed to degradation of the polymer chains. All of the copolymers had char yields at 900 °C between ~15 and 35%, but these did not correlate with the concentrations of sulfonate groups.

²⁵⁶ J. F. O'Gara, D. J. Williams, W. J. Macknight, F. E. Karasz, "Random Homogeneous Sodium Sulfonate Polysulfone Ionomers: Preparation, Characterization, and Blend Studies," *Journal of Polymer Science: Part B: Polymer Physics*, **25**, 1987, 1519.

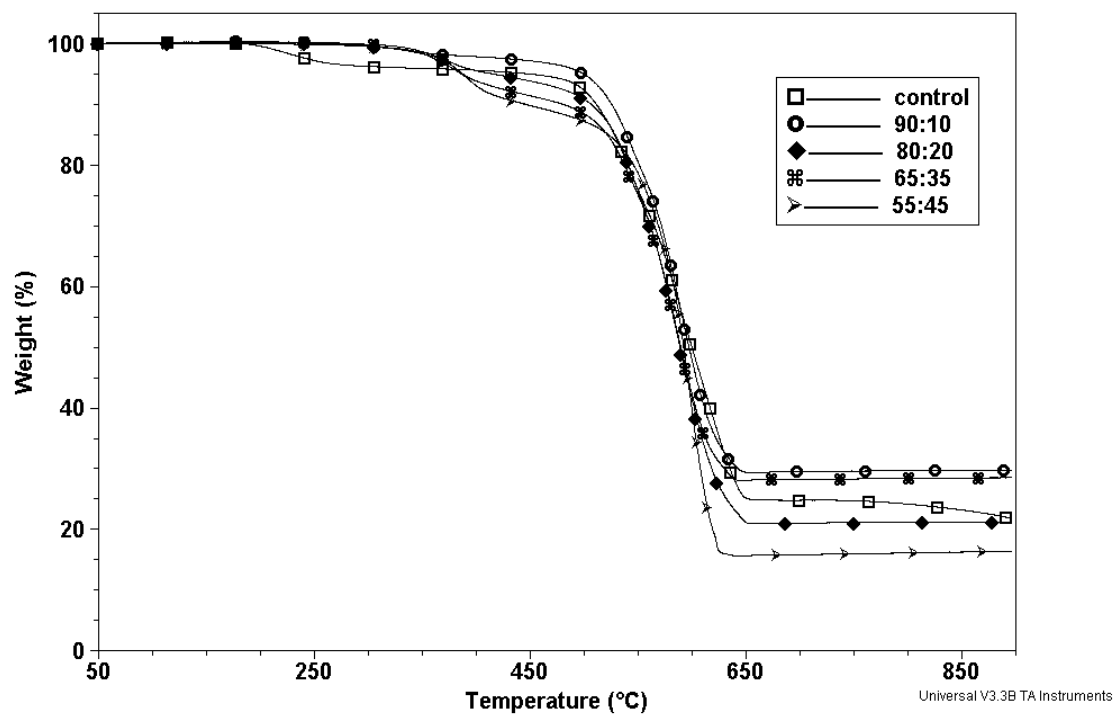


Figure 7.11: TGA curves in air at $10\text{ }^{\circ}\text{C min}^{-1}$ of disulfonated hexafluoroisopropylidene poly(arylene ether nitrile) copolymers containing 0, 10, 20, 35, and 45 mole % disulfonation

7.4.3 Water Uptake, Methanol Permeability, and Morphology

Small-angle X-ray investigations of the morphology of Nafion[®], a perfluorosulfonic acid copolymer, have demonstrated that this polymer is phase separated.²⁵⁷ One phase consisted of hydrophilic domains wherein polar sulfonic acid groups were aggregated. The other region was comprised of hydrophobic portions of the polymer aggregated in clusters. The hydrophilic domains in these sulfonated copolymers were primarily responsible for water absorption via hydrogen bonding. Typically, the equilibrium water absorption of disulfonated poly(arylene ether sulfone)s, acidified using “Method 2” conditions, is linear up to about 0.40 mole fraction of disulfonated units. Beyond this level of disulfonation, water uptake increases drastically, signifying a change in phase morphology.^{243, 245}

For comparisons, water absorption of the nitrile-functional copolymers was measured (Figure 7.12). Upon submersion in deionized water, the copolymer membranes with ≥ 0.1 mole fraction of disulfonated units reached the equilibrium in water uptake within the first hour (Figure 7.12). Water absorption increased linearly up to 0.35 mole fraction of the units disulfonated. Beyond this level of disulfonation, the water uptake increased drastically and the copolymer containing 0.55 mole fraction of disulfonated units absorbed ~300% water by weight. The ionic concentrations were expressed in terms of ion exchange capacities (IEC's in meq g⁻¹) so that these copolymers could be compared to disulfonated copolymers previously studied (Table 7.3)

²⁵⁷ T. D. Gieke, G. E. Munn, F. C. Wilson, "The Morphology in Nafion Perfluorinated Membrane Products, as Determined by Wide-and Small-Angle X-Ray Studies," *Journal of Polymer Science: Part B: Polymer Physics*, **19**, 1981, 1687.

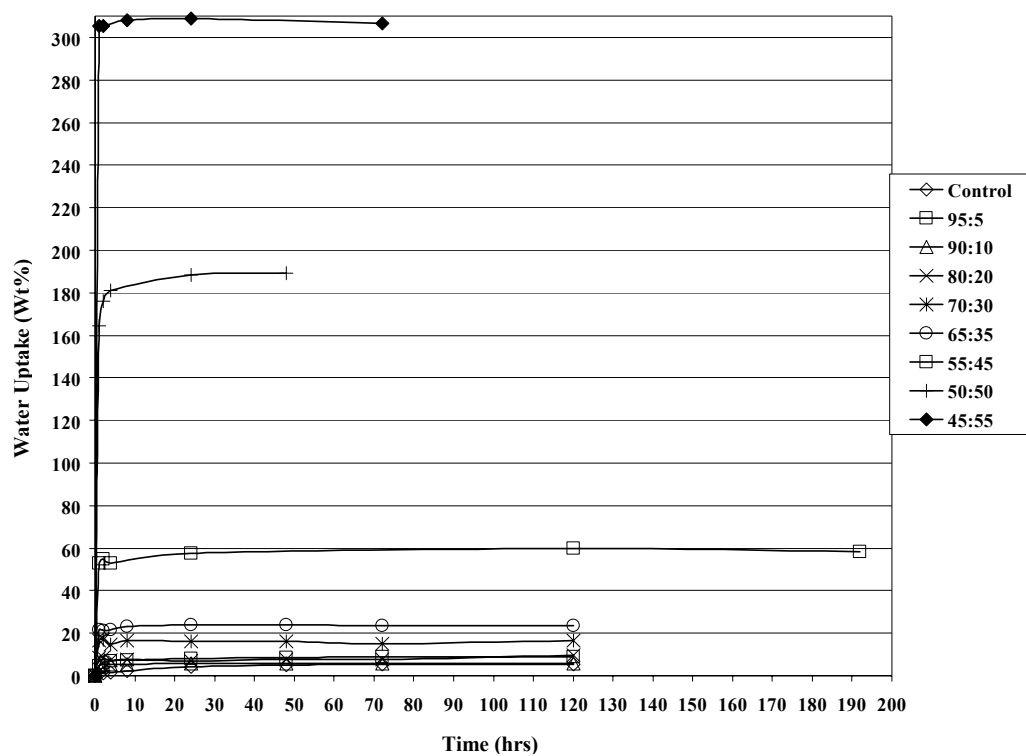


Figure 7.12: Water uptake (wt%) versus time for disulfonated hexafluoroisopropylidene poly(arylene ether nitrile) copolymers containing 0 up to 55 mole % disulfonation

Table 7.3: Water uptake (wt%) and calculated IEC values for Nafion 117[®] and three different disulfonated poly(arylene ether)s at 20, 30, and 35 mole % disulfonation

Mole % Disulfonation	Copolymer	Water Uptake (wt%)	IEC (meq/g)
20	*Disulfonated PAES	17	0.92
	**Disulfonated-6F-PAES	15	0.69
	***Disulfonated-6F-PAE-CN	7	0.82
30	*Disulfonated PAES	31	1.34
	**Disulfonated-6F-PAES	23	1.00
	***Disulfonated-6F-PAE-CN	16	1.16
35	*Disulfonated PAES	44	1.53
	**Disulfonated-6F-PAES	38	1.15
	***Disulfonated-6F-PAE-CN	24	1.32
-	Nafion 117 [®]	37	0.91

* disulfonated poly(arylene ether sulfone)

** disulfonated hexafluoroisopropylidene poly(arylene ether sulfone)

*** disulfonated hexafluoroisopropylidene poly(arylene ether nitrile)

In comparison to disulfonated poly(arylene ether sulfone)s prepared with biphenol or hexafluoroisopropylidene diphenol previously analyzed in our labs, as well as to Nafion 117[®], the nitrile-functional copolymers with 20, 30, and 35 mole percent of the units disulfonated had lower equilibrium water absorption. Moreover, at equivalent IEC values, the nitrile functional copolymers absorbed considerably less moisture (Table 7.3). These aspects will require significant investigation to be better understood.

The phase morphology of the nitrile functional poly(arylene ether) with 0.35 of the repeat units disulfonated was investigated with AFM in the tapping mode. This copolymer had a two-phase morphology as demonstrated by the dark and light regions (Figure 7.13). The dark regions in the image depict the softer hydrophilic regions containing the water, while the light regions correspond to the harder hydrophobic regions (Figure 7.13). The dark regions were continuous and approximately 4-10 nm in width. The lighter regions were also continuous but ranged from about 25–40 nm. The nitrile-functional copolymer morphology (“B” in figure 7.13) was considerably different from a disulfonated poly(arylene ether sulfone) prepared from biphenol, dichlorodiphenylsulfone and SDCDPS with 40% of the units disulfonated (“A” in figure 7.13). The disulfonated poly(arylene ether sulfone) (“A” in figure 7.13) had a more segregated morphology with many of the hydrophilic domains in clusters with less connectivity.

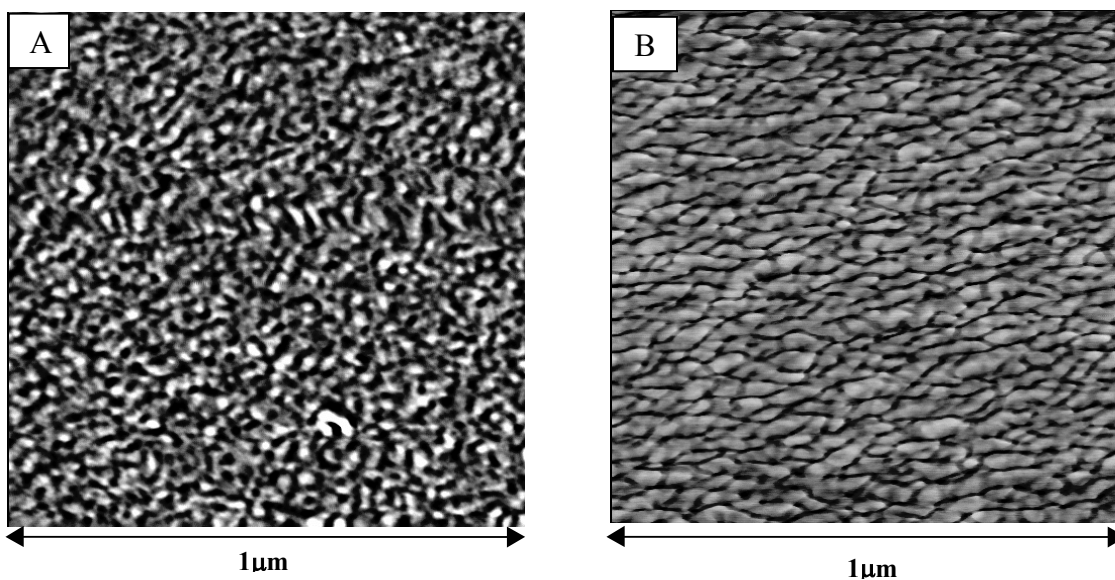


Figure 7.13: AFM images using a scan size of 1 μm for: A) disulfonated biphenol poly(arylene ether sulfone) at 40 mole % disulfonation, B) disulfonated hexafluoroisopropylidene poly(arylene ether nitrile) at 35 mole % disulfonation

Previous work has demonstrated that transforming from segregated to continuous morphologies of the hydrophilic domains in perfluorosulfonic acid copolymers and in disulfonated poly(arylene ether sulfone)s correlated with large increases in equilibrium water uptake.^{243, 245, 258} Percolation of the hydrated hydrophilic regions into continuous structures occurred in the poly (arylene ether nitrile) copolymers with $\geq 35\%$ of the units disulfonated. The continuous morphologies of the hydrated hydrophilic phases in the disulfonated poly(arylene ether)s containing the nitrile groups may help to explain the nonlinear increase in water uptake above 35 mole % disulfonation (Figure 7.14).

Achieving low methanol permeation through a membrane is important for copolymer membrane performance in direct methanol fuel cells. Recent work in our labs has demonstrated that disulfonated poly(arylene ether sulfone)s have considerably lower methanol permeabilities and comparable proton conductivities when compared to Nafion 117[®].²⁴⁵ It has also been shown that methanol permeability and water uptake in disulfonated poly(arylene ether sulfone)s are correlated.²⁴⁵ As the fraction of disulfonated units is increased, both the equilibrium water uptake and the methanol permeability increase.

²⁵⁸ G. Gebel, R. B. Moore, "Small-Angle Scattering Study of Short Pendant Chain Perfluorosulfonated Ionomer Membranes," *Macromolecules*, **33**, 2000, 4850.

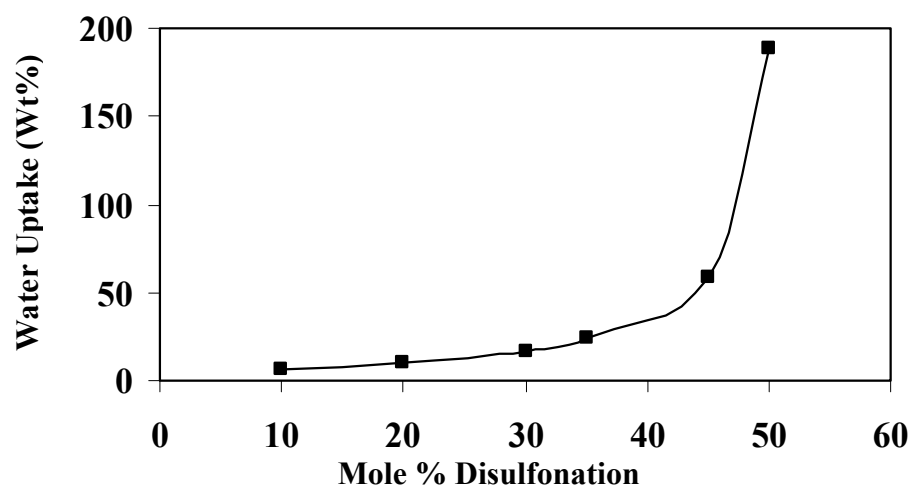


Figure 7.14: Water uptake (wt%) versus mole % disulfonation for disulfonated hexafluoroisopropylidene poly(arylene ether nitrile) copolymers

Methanol permeabilities of disulfonated poly(arylene ether sulfone) copolymers with different chemical structures and Nafion 117[®] were compared at 25 °C (Table 7.4).^{259, 260, 261} The three disulfonated copolymers were selected because they had similar equilibrium water absorption, IEC's, and proton conductivities. Methanol permeabilities through the disulfonated copolymer containing the nitrile groups were higher than through the other disulfonated poly(arylene ether sulfone)s, but were considerably lower than Nafion 117[®] (Table 7.4).

7.4.4 Conductivity

Proton conductivities of the series of disulfonated copolymers containing nitrile groups were measured as a function of mole fraction of units disulfonated, relative humidity, and temperature. The experiments were conducted in a conductivity cell submersed in deionized water (Figure 7.4). Proton conductivities increased linearly from 0.0005 S cm⁻¹ to ~ 0.10 S cm⁻¹ as a function of the concentrations of disulfonated units at 25 °C (Figure 7.15). Conductivity of the copolymer containing 0.45 mole fraction of the disulfonated repeat units was 0.10 S cm⁻¹, comparable to Nafion 117[®].

To compare acidities of the disulfonated nitrile-functional copolymers relative to two other disulfonated copolymers, proton conductivities between 10 and 35 mole %

²⁵⁹ B. S. Pivovar, Y. Wang, E. L. Cussler, "Pervaporation Membranes in Direct Methanol Fuel Cells," *Journal of Membrane Science*, **154**, 1999, 155.

²⁶⁰ X. M. Ren, "Methanol Cross-Over in Direct Methanol Fuel Cells," *Electrochemical Society Proceedings*, **PV95-23**, 1995, 284.

²⁶¹ X. M. Ren, W. Henderson, S. Gottesfeld, "Electro-Osmotic Drag of Water in Ionomeric Membranes. New Measurements Employing a Direct Methanol Fuel Cell," *Journal of the Electrochemical Society*, **144**, 1997, L267.

Table 7.4: Methanol permeability values at 25 °C for Nafion 117[®] and three different disulfonated poly(arylene ether) copolymers

Copolymer-(mole % Disulfonation)	IEC (meq/g)	Methanol Permeability x 10⁻⁸ (cm²/s)
*Disulfonated-PAES-(35 mole % Disulfonation)	1.53	55
**Disulfonated-6F-PAES-(40 mole % Disulfonation)	1.30	62
***Disulfonated-6F-PAE-CN-(35 mole % Disulfonation)	1.32	87
Nafion 117 [®]	0.91	167

* disulfonated poly(arylene ether sulfone)

** disulfonated hexafluoroisopropylidene poly(arylene ether sulfone)

*** disulfonated hexafluoroisopropylidene poly(arylene ether nitrile)

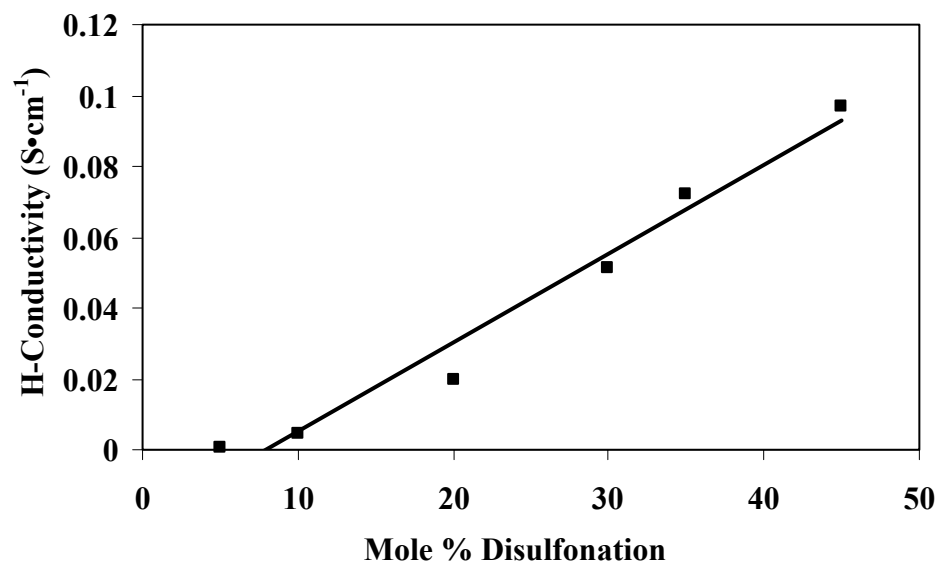


Figure 7.15: Proton conductivity versus mole % disulfonation for disulfonated hexafluoroisopropylidene poly(arylene ether nitrile) copolymers

sulfonation were plotted as a function of IEC values (Figure 7.16). The two other copolymers in the comparison were disulfonated poly(arylene ether sulfone)s and hexafluoroisopropylidene disulfonated poly(arylene ether sulfone)s. The curves demonstrate that between IEC's of ~ 0.8 and 1.6 meq g^{-1} the disulfonated nitrile-functional copolymers have comparable proton conductivities relative to the other two copolymers. This is interesting since these materials appear to have lower equilibrium moisture uptake as compared to the other materials.

Proton conductivities of the nitrile-functional copolymer containing 35 mole % disulfonated units was evaluated as a function of temperature at 100% humidity in a Parr pressure reactor. As temperature was increased, proton conductivities increased to 0.11 S cm^{-1} at $\sim 110^\circ\text{C}$. Further increases in temperature caused excessive swelling of the membranes and proton conductivities could not be accurately measured (Figure 7.17). This temperature versus conductivity behavior is similar to that of other disulfonated poly(arylene ether sulfone)s. However, the upper temperature where conductivity could be measured before excessive swelling occurred was slightly lower for the nitrile-functional copolymers. The study demonstrated that proton conductivities of the disulfonated nitrile functional copolymer membranes could be elevated to high levels by controlling temperature.

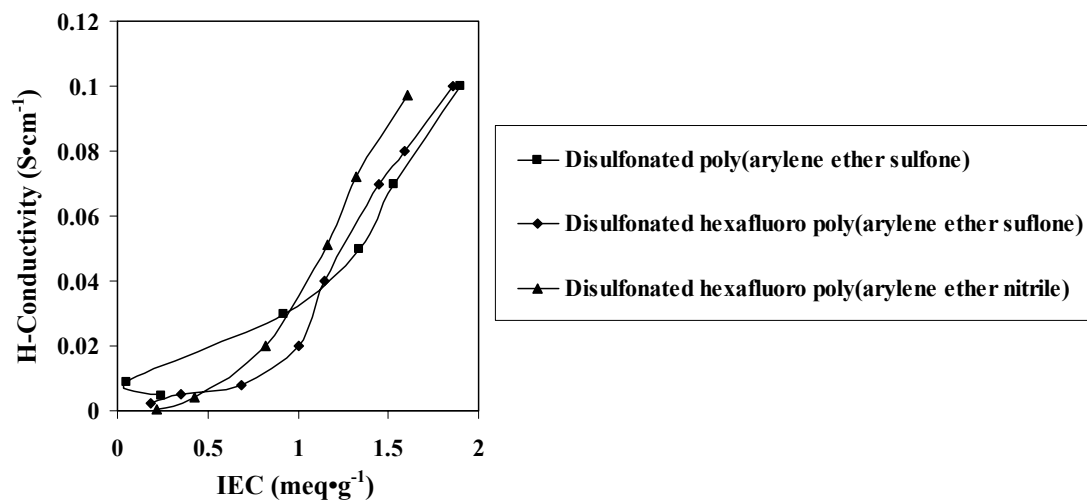


Figure 7.16: Proton conductivity versus calculated IEC values for three different disulfonated poly(arylene ether) copolymers

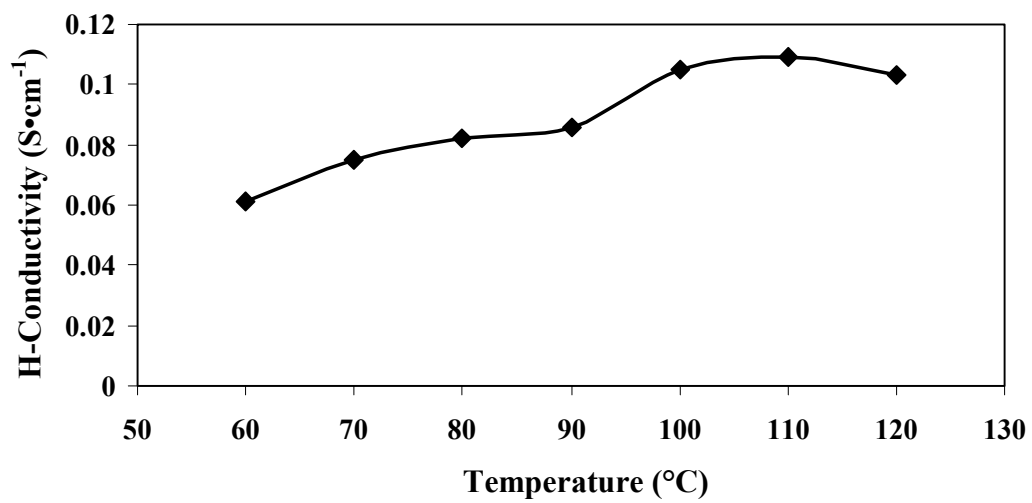


Figure 7.17: Proton conductivity versus temperature for the 35 mole % - disulfonated hexafluoroisopropylidene poly(arylene ether nitrile) copolymer

It is of great interest to determine the performance of a membrane as a relative humidity is reduced. Proton conductivities of four disulfonated nitrile-functional copolymers (20, 30, 35, and 45 mole % disulfonation) were studied at different humidity levels using a humidity/temperature controlled oven at 80 °C. As expected, proton conductivities increased slightly as the relative humidity was increased from 50 to 85% in all four of the copolymers (Figure 7.18). However, proton conductivities through membranes of copolymers with 30, 35, and 45 mole % disulfonated units increased drastically when the relative humidity was elevated from 85 to 95%. Such dramatic increases in proton conductivities suggest that these copolymers may reorganize into different morphologies when exposed to such high humidities. The morphological behavior of these copolymers versus relative humidity is currently under further investigation.

7.5 Conclusions

A series of high molecular weight, disulfonated, nitrile-functional copolymers containing as much as 45 mole % disulfonation were synthesized and characterized. For comparable IEC values ranging from ~0.8 and 1.6 meq g⁻¹, these copolymers absorbed ~15% less water, but had comparable proton conductivities relative to previously investigated sulfonated poly(arylene ether sulfone)s. AFM phase imaging suggested that the morphology of the nitrile-functional copolymer with 35 mole % disulfonated units had a co-continuous morphology. As expected, the proton conductivities for the 35 mole % disulfonated copolymer were substantially improved with increasing temperature.

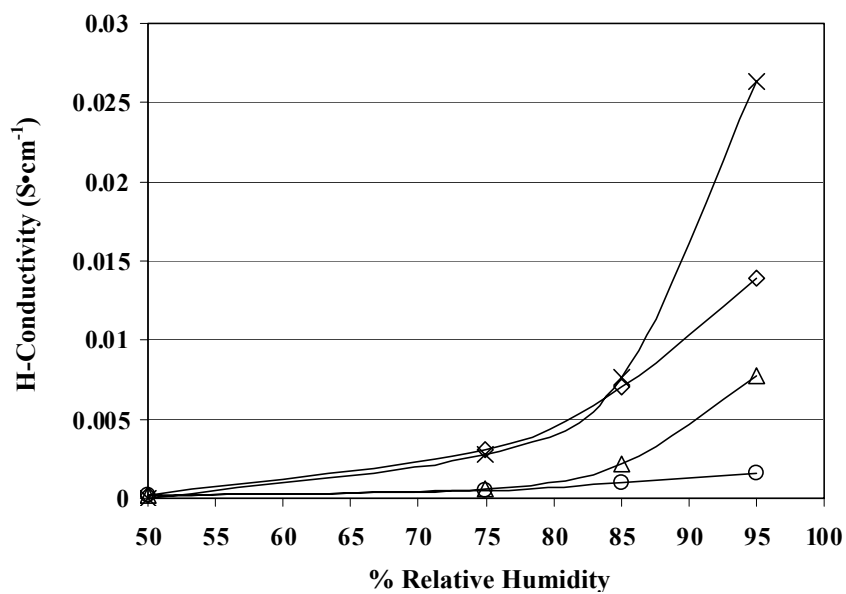


Figure 7.18: Proton conductivity versus % relative humidity for the 20, 30, 35, and 45 mole % - disulfonated hexafluoroisopropylidene poly(arylene ether nitrile) copolymers

Chapter 8: Summary and Conclusions

A new inexpensive synthetic scheme which requires minimal workup has been developed for the production of biphenoxypthalonitrile in good yield. Using 15 – 20 weight percent of this reagent it has been demonstrated that phenolic novolac oligomers can be readily crosslinked into tough, high T_g , flame resistant thermosets. A new melt/powder prepregging process has been developed for processing these networks into void-less carbon fiber reinforced composites with excellent thermo-oxidative resistance.

The synthesis of a nonhalogenated vinyl ester soluble monomer which substantially improves the flame resistance and increases the T_g of vinyl ester networks and polystyrene copolymers has been achieved. A two step synthetic scheme has been successfully developed which generates 4-vinylphenoxypthalonitrile in good yield. This monomer is readily soluble in vinyl ester resins at high weight percents (as much as ~40 wt%) and with slight heating complex viscosity measurements have suggested that the resin mixture is VARTM processable.

It has been demonstrated this monomer can be free radically copolymerized into vinyl ester/styrene networks and copolymerized with styrene. The copolymerization of this monomer into vinyl ester networks substantially improved the flame performance of these networks between the temperature range of 400 to 600 °C. After copolymerizing this monomer with styrene at 25 mole % a similar improvement in flame retardance was observed. The T_g of the vinyl ester network was shown to be a function of the 4-vinylphenoxypthalonitrile content in the networks and post-curing temperature. The T_g of the network increased as the post-curing temperature and 4-vinylphenoxypthalonitrile content increased.

The synthesis of a new low water uptake high conductivity membrane has been completed. A series of high molecular weight nitrile functional sulfonated poly(arylene ether) copolymers containing as much as 55 mole % sulfonation was synthesized. These copolymers were cast into tough ductile films with high T_g 's. These films exhibited lower water uptake and slightly higher proton conductivity over an equivalent IEC range relative to analogous sulfonated poly(arylene ether sulfone)s. As expected, the proton conductivities for the 35 mole % sulfonated copolymer were substantially improved with increasing temperature.

Finally, AFM phase imaging demonstrated that the morphology for the copolymer with 35 mole % sulfonation was substantially different from previously investigated sulfonated poly(arylene ether sulfone)s. It was shown that this sulfonated nitrile functional copolymer had a co-continuous morphology similar to that of Nafion 117.

Chapter 9: Suggested Research

9.1 Phenolic/Biphenoxyphthalonitrile Matrix Materials

It has been illustrated that a 700 g/mole novolac oligomer can be highly crosslinked with low weight percents (15-25 wt%) of biphenoxyphthalonitrile. The novolac/BPh networks were shown to have good toughness, excellent thermo-oxidative resistance, and high T_g 's. Due to their high performance characteristics there is significant interest in processing these materials into fiber reinforced composites for naval applications via VARTM technology. However the uncured novolac/BPh resins have complex viscosities that are far too high for VARTM processing.

One approach to addressing the processability issue will be to dissolve biphenoxyphthalonitrile into lower molecular weight novolac oligomers (~250-400 g/mole). The lower molecular weight oligomers would potentially serve to lower the viscosity of the overall resin to a point where VARTM processing would be possible. Also, the networks containing the lower molecular novolac oligomers will be evaluated in terms of physical and thermo-oxidative properties to ensure that these materials retained the high performance characteristics of the former networks.

9.2 Fabrication of Vinyl Ester/4-Vinylphenoxyphthalonitrile Fiber Reinforced Composites

Considering that vinyl ester/4-vinylphenoxyphthalonitrile networks have improved thermo-oxidative resistance relative to neat vinyl ester networks, it is envisioned that these materials will potentially serve as replacements for brominated vinyl ester resins. It has been shown that these materials with slight heating have low enough viscosities for VARTM processing. The next logical step in this project is to demonstrate

the feasibility of processing these materials via VARTM technology into fiber reinforced composites. Once these composites are fabricated they will be evaluated in terms of mechanical and thermo-oxidative properties relative to brominated vinyl ester composites.

9.3 Free Radical Synthesis of 4-Vinylphenoxyphthalonitrile Copolymers

^1H NMR has demonstrated that 4-vinylphenoxyphthalonitrile has similar reactivity relative to styrene. Preliminary results demonstrate that copolymers of styrene containing low mole % of 4-vinylphenoxyphthalonitrile have improved thermo-oxidative resistance relative to polystyrene. Also, it has been shown that after curing for 4 h at 240 °C the T_g of these copolymers substantially increases. Therefore, the next step is to synthesize copolymers of 4-vinylphenoxyphthalonitrile and other vinyl monomers such as methacrylates and acrylates. Using ^1H NMR the reactivity of 4-vinylphenoxyphthalonitrile relative to these copolymers will be evaluated. Also, the thermo-oxidative properties and T_g values of these copolymers will be determined relative to the neat polymer.

9.4 Further Evaluation of Sulfonated Poly(Arylene Ether Nitrile) Proton Conducting Membranes

A nitrile functional sulfonated poly(arylene ether) membrane has been developed which has comparable conductivity and lower water uptake relative to analogous sulfonated poly(arylene ether sulfone)s. These membranes have a co-continuous morphology and lower methanol permeability relative to Nafion 117. Due to the low methanol permeability characteristics, there is significant interest in using these membranes as proton conductors for direct methanol fuel cells. Therefore intensive

evaluation of the methanol permeability of these membranes under various time and temperature conditions will be completed. Finally, the feasibility of scaling up the synthesis of the sulfonated poly(arylene ether nitrile) copolymers will be completed.

Vita

Michael Sumner was born on June 6, 1975 in Richmond, Virginia. He grew up and attended school in Hopewell, VA where he graduated from Hopewell High School in June of 1993. In August of 1993, he entered Virginia Tech as a Chemistry major. He was graduated Magna Cum Laude in May of 1997 and upon graduation he accepted a position with Carpenter Company of Richmond, Virginia. During his two years at Carpenter Company he helped to develop new viscoelastic polyurethane foam technologies. In August of 1999 he began graduate school at Virginia Tech and his research under the advisement of Dr. Judy Riffle. In May of 2003, Michael will be the first person in his family to earn a doctoral degree. Upon graduation he will assume a research position at Ashland Chemical Company in Dublin, Ohio.